NASA CR-168115 **EDR 11283**

ADVANCED PROPFAN ENGINE TECHNOLOGY (APET) **DEFINITION STUDY,** SINGLE AND COUNTER-ROTATION GEARBOX/PITCH CHANGE MECHANISM **DESIGN** E OVERRIDE

by R. D. ANDERSON

ALLISON GAS TURBINE DIVISION

General Motors Corporation

N87-28554

Unclas

PREPARED

for

NATIONAL AERONAUTICS AND SPACE ADMINISTRATION



NASA LEWIS RESEARCH CENTER CONTRACT NAS3-23046

NASA-CR-168115) ECHANISM DE ND

FOREWORD

The propulsion system definition study reported herein was performed under the technical direction of Gerald A. Kraft, Advanced Turboprop Project Office, NASA Lewis Research Center. The Allison Gas Turbine Division of General Motors Corporation conducted the study. The Allison program manager was R. Daryel Anderson.

The Allison Engineering Staff developed the engine designs, prepared the gearbox preliminary design, and performed the mission analyses to evaluate the potential fuel savings. This study was performed with inputs from Allison's technical areas of advanced design, compressor aerodynamics, turbine aerodynamics, combustion, heat transfer, stress and weight analysis, performance analysis, engine controls, noise, emission and computer-aided drafting. The principal Allison engineering personnel performing this study were as follows:

- Tasks I–VI: J. A. Korn and D. V. Staton
- Tasks VII-X: J. D. Black
- Tasks XI-IV: N. E. Anderson and R. W. Cedoz

The Hamilton Standard Division of the United Technologies Corporation provided recommendations concerning the propfan aerodynamic performance, weight, costs, and design considerations used in the propulsion system integration and evaluation tasks. Hamilton Standard also performed the conceptual design of both the single-rotation and counter-rotation pitch controls and mechanisms and prepared the technology plans for these elements of the propulsion system. Douglas Aircraft Company provided assistance through review of the Task IV reference airplane.

PRECEDING PAGE BEANK NOT FILMED

TABLE OF CONTENTS

Section	า	Title	Page
1	Summary		. 1
11	•		
Ш	Executive Su	ummary	. 4
	Task I.	Selection of Evaluation Procedures and Assumptions	. 4
	Task II.	Engine Configuration and Cycle Evaluation	. 7
	Task III.	Propulsion System Integration	. 10
	Task IV.	Engine/Aircraft Evaluation	. 12
	Task V.	Advanced Propfan Engine Technology Plan	. 14
	Task VII.	Preliminary Design of the Single-Rotation Propfan Reduction Gearbox	. 16
	Task VIII.	Conceptual Design of the Single-Rotation Pitch Control and Mechanism	. 20
	Task IX.	Research and Technology Plan for the Single-Rotation Gearbox and Pitch Control and	
		Mechanism	21
	Task XI.	Preliminary Design of the Counter-Rotation Propfan Reduction Gearbox	26
	Task XII.	Conceptual Design of the Counter-Rotation Pitch Control and Mechanism	31
	Task XIII.	Counter-Rotation Gearbox Research and Technology Plan	. 33
IV			-
	References		28
	Appendix A.	Selection of Evaluation Procedures and Assumptions	A-1
	Appendix B.	Engine Configuration and Cycle Evaluation	B-1
	Appendix C.	Propulsion System Integration	C-1
	Appendix D.	Engine/Aircraft Evaluation	D-1
		Advanced Propfan Engine Technology Plan	
	Appendix F.	Preliminary Design of the Single-Rotation Propfan Reduction Gearbox	F-1
	Appendix G.	Conceptual Design of the Single-Rotation Pitch Control and Mechanism	G-1
	Appendix H.	Single-Rotation Gearbox Technology Plan	H-1
	Appendix I.	Preliminary Design of the Counter-Rotation Propfan Reduction Gearbox	1-1
	Appendix J.	Conceptual Design of the Counter-Rotation Pitch Control and Mechanism	J-1
	Appendix K.	Counter-Rotation Gearbox Technology Plan	K-1
	Appendix L.	List of Abbreviations	L-1
	Appendix M.	Distribution List	M-1

PRECEDING PAGE BLANK NOT FILMED

LIST OF ILLUSTRATIONS

Figure	Title	Page
1	Domestic-local service stage length preference	5
2	Reference aircraft	5
3	Design mission profile	6
4	Reference turboprop engine used to develop sensitivities	8
5	Configurations selected for further evaluation	9
6	PD436–10 engine general arrangement for axial/centrifugal compressor	10
7	PD436–11 engine general arrangement for axial/axial compressor	11
8	Installation drawing for engine PD436–10	11
9	Installation drawing for engine PD436–12	12
10	Aircraft/engine results	13
11	Economic results	13
12	Compressor efficiency correlation	15
13	APET turbine technology levels compared with EEE	16
14	Offset and in–line candidate gearbox arrangements	
15	Dual compound idler gear arrangement	18
16	Preliminary design drawings of the state-of-the-art and advanced technology gearboxes	19
17	Pitch change system	
18	Tapered roller bearing and helical gearing	28
19	Single row spherical bearing and high contact ratio spur gear	
20	Counter-rotation gearbox cross section	
21	Planet gear arrangement	
22	Counter-rotation gearbox side view	
23	Counter-rotation gearbox power loss breakdown	
24	Rotary hydraulic pitch control concept	32

LIST OF TABLES

Table	Title	Page
1	Guide to appendixes	. 4
· II	Cost method sources	. 4
Ш	Reference airplane wing parameters	. 6
IV	Emission standards adopted for APET	. 7
V	Engine installation factors	
VI	Reference turbofan engine performance	. 8
VII	Candidate engine configurations	. 8
VIII	Final screening results	
IX	Design specifications of APET turboprop engines	. 9
X	Engine/aircraft ground rules and assumptions summary	
ΧI	Criteria for the two technology levels	
XII	Gearbox physical dimensions	. 19
XIII	Bearing types used in both the current and advanced designs	. 19
XIV	Gearbox power loss and efficiency	
XV	Power system concept ranking	. 20
XVI	Motor control system ranking	. 20
XVII	Weighting categories	
VIII	Weighted decision analysis	
XIX	Planet form selection	. 28

I. SUMMARY

The Advanced Propfan Engine Technology Definition Study was performed to define two candidate turboprop propulsion systems for commercial airliners of the 1990s. This study focused on identifying the engine cycles that would result in the most favorable fuel consumption for a 120 passenger advanced technology airplane operating at 0.72 Mach at 32,000 ft altitude. Several engine configurations were considered, and conceptual designs of two engine configurations were defined for the following purposes:

- to provide general arrangements of advanced-technology high-pressure-ratio engines having dual-axial and axial-plus-centrifugal compressor stages in the 10,000 hp takeoff power class
- to provide installed engine performance and physical descriptions for use in projecting airline operating cost and to access the potential fuel savings for propfan powered aircraft relative to turbofan aircraft of the same technology level
- to provide a development plan for the key technology required for the candidate engines and drive systems and for their critical components.

The recommended engines for the commercial airliner of the 1990s are both 32.5:1 overall pressure ratio, three-spool, free turbine designs. Of the two compressor types considered—the all-axial and axial-plus-centrifugal stage—both are good candidates for the 10,000 shp takeoff size propfan application. Representative installation requirements of contoured, aerodynamically favored nacelles indicate that the offset gearbox arrangements have an advantage for the over-the-wing propulsion systems.

In the performance of this study, various engine configurations and cycles were evaluated. The final engine designs were integrated with other elements of the propfan propulsion system. A mission simulation study of the two resulting candidate turboprop engines and a reference turbofan engine was performed to determine the benefits of the propfan-powered aircraft.

The results of the aircraft/engine evaluation indicate that the single-rotation propfan-powered aircraft has a significantly lower fuel consumption than the turbofan-powered aircraft. This fuel savings is as much as 18.6% for the alternate 300 nmi mission. On an economic basis, the comparison shows up to 9.7% lower direct operating cost (DOC) for the propfan. The DOC advantage is primarily caused by less fuel burned and lower propulsion system maintenance cost.

Following the propulsion system study, additional tasks were added to the APET program to accomplish the prelimi-

nary design of the propfan reduction gearbox and conceptual design of a pitch control and mechanism. The objective of this design activity was to define in more detail these components for both single (SR) and counter-rotation (CR) as they would apply to production propfan airplane of the 1990s. In the case of the SR gearbox, the dual compound idler gear arrangement was selected for the SR gearbox preliminary design to take advantage of the accessibility to the propfan drive shaft and simplify packaging of the accessories and engine with a contoured nacelle. Hamilton Standard's linear hydraulic pitch change system was the preferred SR configuration for the offset gearbox because of better maintainability. The SR pitch change featured electrical power integral with the propfan, a digital control system, capacitor signal transfer, modular design, and minimal impact on the offset gearbox. Estimated pitch control slew rates, blade angles, and torque are provided along with predictions of improved reliability, maintenance cost, acquisition cost, and weight. Allison's SR gearbox design is fully compatible with specific needs of the pitch change system. Oil and a highspeed drive are provided for the hydraulics and heat rejection of the pitch change. A signal transfer module is mounted at the front of the gearbox, and bearings and shafting are designed to accommodate propfan loads.

The differential planetary gearing arrangement was selected as the favored configuration for the counter-rotating propfan system. This is an inline design that is very compact, 22 in. diameter by 24 in. long. It is also light weight, 548 lb; efficient, 99.2% at cruise; and long life, 30,000 hr MTBUR. Helical gears were used because of their lower surface temperature and greater bending strength compared to high contact ratio spur gears. The helical planet gears were mounted on tapered roller bearings, which were favored over single row special bearings because of lower raceway stress. Hamilton Standard evaluated several CR pitch change concepts before deciding on a rotary system. It is adaptable to diagnostic and static checkout, adaptable to emergency feather, lighter weight than other concepts and has advantages in locating the electronic control for both blade rows in a common unit on the axis of rotation. The modular pitch change change system simplifies the interface with the gearbox, improves gearbox reliability and reduces maintenance cost. The MTBUR is 2600 hr for the pitch change system.

The technology features assumed in the Advanced Propfan Engine Technology (APET) study are, in many cases, beyond the state of the art of propulsion system and engine design. For example, the engine inlet operates in a skewed (3-D) flow-field environment characterized by high transonic Mach numbers, significant total pressure gradients, and thick boundary layers.

These flow-field conditions and the dynamic interaction of the propfan, inlet, gearbox, and compressor require considerable investigation. The development of a low maintenance, main reduction gearbox to drive the propfan is critical to acceptance of propfan-powered aircraft by the airlines. The research and development of the high-pressure-ratio compressors required for fuel economy requires more than simply scaling the Energy Efficient Engine (EEE) power sections. New levels of aerodynamic and mechanical performance are required in both the compressor and turbine. The control systems of future propfan-powered aircraft must use the integrated control system concept to achieve optimum propulsion system performance and a high degree of safety and reliability.

To realize the full potential of a turboprop propulsion system requires improvements in the state of the art in several areas. These are summarized as follows:

 Engine Inlet. A joint airframe/engine company project is needed to develop inlets and ducts for the propulsion systems described herein.

- Gearbox. A major gearbox technology project is needed to develop long life low maintenance gearboxes that would be suitable for commercial airline service.
- Pitch Change. Development programs are needed for a high-pressure pump, rotating electronic control module and capacitor signal transfer.
- Compressor. An aerodynamic technology program is needed to achieve high polytropic efficiency in the moderate flow size, APET compressor. The problems to be overcome are the low specific speed of the centrifugal compressor required to avoid high borestress and the small latter stage blade heights of the high-pressure (HP) axial compressor.
- Turbines. Further development of small flow turbines is needed with particular emphasis on reducing cooling air and secondary flow losses.
- Controls. A joint project to develop an integrated control system for the propfan and engine is required.

II. INTRODUCTION

Since establishment of the Aircraft Energy Efficiency (ACEE) program in 1975, NASA has moved forward with the development of propfan propulsion system technology. Early in the program the potential to achieve the predicted propfan efficiency was demonstrated in wind tunnel tests of 2 ft diameter propfan models. This work was continued with flight tests of the structural and noise characterization and has progressed to the design of a series of large-scale propfans in the 9 ft diameter size for wind tunnel and flight testing of structural integrity and noise properties. With this technology base established, NASA initiated the APET Program early in 1982 with study contracts awarded to three engine manufacturers: Allison, General Electric (Ref 1), and Pratt & Whitney (Ref 2). The purpose of these studies is to define engine configurations and advanced technology requirements so that attention can be given to developing the key components and resolving the enginerelated issues so that the technology will be ready for commercial airline service in the early 1990s. The APET study objectives will be accomplished by a systematic evaluation process that will consider the major design configuration options relative to the engine, gearbox, inlet, mounting system, and inlet/propeller/nacelle interactions. The Allison evaluation consists of the following 14 tasks:

- Task I. Selection of evaluation procedures and assumptions required in Tasks II through V.
- Task II. Engine configuration and cycle evaluation of four turboprop engine configurations.
- Task III. Propulsion system integration of two turboprop engine configurations.
- Task IV. Engine/aircraft evaluation of two turboprop propulsion systems and a reference turbofan propulsion system.
- Task V. Preparation of an advanced propfan engine technology plan.
- Task VI. Reporting.
- Task VII. Preliminary design of a single-rotation propfan reduction gearbox.
- Task VIII. Conceptual design of a single-rotation pitch control and mechanism.
- Task IX. Research and a technology plan for a single-rotation gearbox and pitch control mechanism.
- Task X. Reporting for Task VII–IX.

- Task XI. Preliminary design of a counter-rotation propfan reduction gearbox.
- Task XII. Conceptual design of a counter-rotation pitch control and mechanism.
- Task XIII. Research and technology plan for a counter-rotation gearbox and pitch control mechanism.
- Task XIV. Reporting for Tasks XI-XIII.

Tasks I and II represent the cycle optimization phase of the study. Engine cycle conditions, the engine configuration, and the predicted engine performance provided a basis for the study. The procedures used to decide the engine type and operating temperature/pressure ratio involved a detailed trade study of the benefits of high cycle temperature and pressure to achieve low specific fuel consumption. It also considered the penalties associated with these advanced technology designs. Task III involved the conceptual designs of two 10,000 shp engines and the installation of these engines with the other propulsion system components. Engine designs were based on Allison's view of the aerodynamic component performance level and the state-of-the-art mechanical features that would exist by 1990. It was assumed that NASA's APET hardware program would be initiated in 1984, thereby allowing five to six years of intensive engine research and development in the 1980s. An important part of the APET study was the mission analysis modeling of an advanced technology airplane to identify the relative importance of advanced technology engine features and to show the payoff should the assumed performance be realized. The results of this analysis are the basis for the technology plan produced in Task V. This plan will provide guidance and direction for the APET hardware program.

The completed Task II propulsion system designs are the basis for computer card decks and performance data packages which are available on request to airframe companies and others involved in evaluating propfan-powered aircraft.

Tasks VII through X were added to the program to provide a more in-depth look at two components of the single rotation system that require new technology: the gearbox and pitch change system.

Tasks XI through XIV were added to the program to focus on the counter-rotation gearbox and pitch change system.

III. EXECUTIVE SUMMARY

This section summarizes the technical work of the APET study. Each of the study elements is discussed in detail in an appendix as shown in Table I.

Table I. Guide to appendixes.

	<u>Task</u>	Appendix
1	Procedures and Assumptions	Α
11	Engine Configurations and Cycles	В
111	Propulsion System Integration	С
IV	Engine/Aircraft Evaluation	D
V	Engine Technology Plan	E
VII	Single-Rotation Propfan Gearbox	F
VIII	Single-Rotation Pitch Control and Mechanism	G
IX	Single-Rotation Research and Technology Plan	Н
ΧI	Counter-Rotation Propfan Gearbox	1
XII	Counter-Rotation Pitch Control and Mechanism	J
XIII	Counter-Rotation Research and Technology Plan	K

The APET study provided a systematic evaluation of candidate turboprop engine configurations best suited to a medium-range commercial airliner mission. A base level of evaluation procedures and assumptions is required to develop trade factors and propulsion system performance trends. These elements form the basis for selecting the power section configuration and cycle conditions for fuel economy and low direct operating cost.

The engine cycles selected were expanded into preliminary designs of two engine configurations. Both power sections were three-spool designs with dual-spool compressors and free power turbines operating at 32.5:1 overall design pressure ratio and 2500 °F maximum temperature. The primary output of the preliminary design effort is engine descriptive information in the form of general arrangement drawings and steady-state performance over the range of altitudes and speeds from sea level to 35,000 ft. Performance data are provided in a computer program on tape and in tabular form for representative flight conditions and power settings.

As a part of this study the engines were installed and flown using an advanced commercial airliner computer model and operating on a 1000 nmi design mission and a 300 nmi alternate mission. Estimates of fuel burned and direct operating cost were measured against a comparable technology advanced-technology turbofan-powered aircraft. The results showed that for the 300 nmi alternate mission the direct operating cost of the turboprop-powered aircraft would be 9.7% less than for the turbofan. Fuel burned was 18.6% less for the turboprop system. All results were obtained with single-rotation propfans mounted on each wing.

TASK I. SELECTION OF EVALUATION PROCEDURES AND ASSUMPTIONS

The key evaluation procedures and assumptions used in the study are summarized below and discussed in detail in Appendix A.

Fuel Price

The fuel price used in the APET study is \$1.50/gal in 1981 dollars. This price was arrived at by applying 3.0% real growth and 8.0% inflation rate over the period 1980 to 1993. This resulted in a price of \$3.80/gal in 1993 dollars which is equivalent to \$1.50/gal in 1981 dollars.

Direct Operating Cost (DOC)

Estimates of DOC contain elements of both acquisition cost and operating cost. The source of cost methods and the economic "ground rules" are presented in Table II.

Table II.
Cost method sources.

Cost Item	Source of cost method
Insurance Airframe maintenance Depreciation Flight crew cost	Boeing DOC formulas for Domestic Trunk and Local Service (1979) updated to 1981 economics
Aircraft acquisition cost	Data correlation of aircraft empty weight-minus-engine weight versus cost
Propfan engine cost	Allison material index factor method applied to component finished weight
Turbofan engine cost	Data correlation of \$/pound of thrust versus price as determined from published data for nine, modern turbofan engines
Propfan cost	Hamilton Standard data contained in NASA CR-165813 (Ref 5)
Engine maintenance cost	1967 ATA formulation method with constants updated to account for advanced technology and economic year
Propfan maintenance cost	Hamilton Standard report SP04A82 (Ref 6)
Fuel cost	\$1.50/U.S. gallon, ±\$0.50: per NASA study manager

Aircraft utilization 3000 hr/year (about 8 hr per day)
Insurance rate 0.5% of acquisition cost per year
Depreciation schedule 15 years to 10% residual value
Spares Airframe—6% of its acquisition cost Engine—30% of its acquisition cost

Maintenance burden 220%

Labor rate \$13.75/hr

The aircraft operating scenario presumes that the aircraft will not be operated the majority of the time on its design mission. This fact is born out by CAB statistics for all classes of commercial aircraft. Therefore, it was necessary for the APET study to estimate a realistic service use or revenue mission for the airplane so that reasonable DOC values would be compared. The basis for selection of the revenue mission was a compilation of stage lengths, by distance groups, for domestic local service airliners obtained by the Civil Aeronautics Board (CAB Form 41) during calendar year 1980. The relationship of percent departures versus stage length group is shown in Figure 1. Note that the vast majority of departures occurred in the 200-300 nmi range. A revenue mission length, for the comparison of system DOCs, was therefore

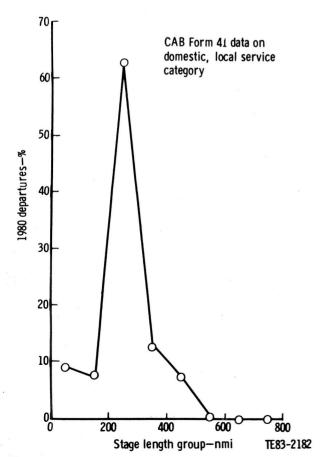


Figure 1. Domestic-local service stage length preference.

selected at 300 nmi. For the revenue mission, the cruise Mach number and fuel reserves were held to the design values and the aircraft was launched at its design gross weight; cruise altitude was optimized for minimum DOC.

Reference Aircraft

While Allison is not in the business of designing airplanes, computer models for typical advanced development applications are maintained and updated for studies involving propulsion system evaluation.

The type and size aircraft selected for evaluating the candidate APET engines was based on consideration of the commercial transport market and aircraft technologies consistent with a 1992 initial operation. This stipulated an upper size of 120 passengers to preclude competition with new 150 passenger aircraft going into service prior to 1992. A payload consisting of 120 passengers plus 4000 lb of cargo was selected for the APET airplane.

The aircraft configuration was held to conventional standards, which provided a large data base from which to scale weights and sizes and a consistency of configuration between fan and prop aircraft. It was kept in mind that the objective of the study was to evaluate propulsion systems—not design new aircraft. The reference aircraft is shown in Figure 2. It is a low-wing design featuring twin, wing-mounted engines and a "T" tail. The structural features and wing parameters (see Table III) were selected under aircraft company consultation and are based on technology timing for a 1992 initial service date. It is assumed that this airplane will have a supercritical wing, advanced aluminum and composite materials, and active controls. The cabin arrangement seats six abreast (all economy) with a single, center aisle.

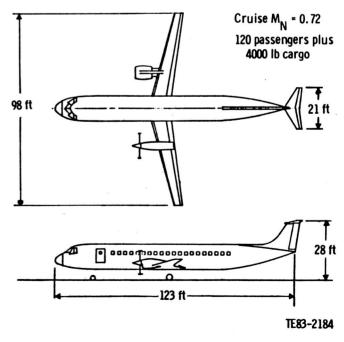


Figure 2. Reference aircraft.

Table III. Reference airplane wing parameters.

Wing loading	123 lb/ft ²
Aspect ratio	12.0
Sweep at quarter chord	13.5 deg
Average thickness ratio	14%
Taper ratio	0.40

Consideration of acoustic treatment weight penalty for the propfan was estimated from a correlation of data from NASA CR-166138, with sound pressure level determined by estimates contained in Hamilton Standard Report SPO4A80. No penalty for propfan-induced wing scrubbing or swirl drag was included. No wing/nacelle interference drag was considered. These assumptions were consistent with NASA direction.

Design Mission

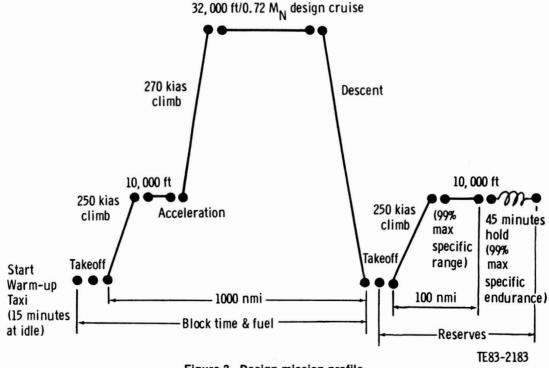
A design range of 1000 nmi was selected. The design mission determines the amount of fuel capacity of the aircraft. Therefore, it was important that the mission requirement be consistent with the vehicle's revenue capacity, i.e., 120 passengers. This size aircraft falls into the area of short-haul at the lower end of the domestic local service category. Current aircraft of this size (BAC1-11, DC9-30, Boeing 737) have design ranges of 1500 nmi or greater and do not fit the short-haul trends that have become prominent since deregulation occurred. The design mission profile shown in Figure 3 was

made consistent with ATC procedures, aircraft capability, and reserves definition sufficient for the short-haul transportation concept. The cruise Mach number was selected in consultation with an aircraft company, and the cruise altitude was a compromise (had to be above 30,000 ft for traffic/weather considerations) to provide a good comparison between the turbofan and propfan engines.

Engine Trade Factors

Part of the Engine/Aircraft Evaluation (Task IV) will be to develop trade factors indicating the sensitivity of system performance and economics to various propulsion system-affected parameters. Since the revenue mission requirements are fixed, the system performance dependent variable will be amount of fuel burned and the cost dependent variable will be DOC. The sensitivities of fuel burned and DOC defined in Task IV were as follows:

- the sensitivity of fuel burned as a function of
 - propfan efficiency
 - thrust specific fuel consumption
 - · engine plus gearbox weight
 - propfan weight
 - nacelle drag
 - acoustic treatment weight
 - aircraft drag
- the sensitivity of DOC as a function of
 - propfan efficiency
 - thrust specific fuel consumption



- engine plus gearbox weight
- propfan weight
- engine plus gearbox cost
- engine plus gearbox maintenance cost
- propfan cost
- propfan maintenance cost
- acoustic treatment weight
- nacelle drag
- aircraft drag
- aircraft cost

Emissions

Currently, there are no gaseous exhaust emissions standards for turboprop or propfan engines. Therefore, for use in this program as design requirements, Allison has developed gas generator equivalent emissions indexes (grams of pollutant per kilograms of fuel). These are based on the ICAO 1986 standards for turbofans. These emissions indexes (Els) are shown in Table A-XVI in Appendix A.

The turboprop smoke standard developed in a joint USAF and Allison program defines the threshold of smoke visibility for large turboprop engines and has subsequently been adopted by the EPA as a standard.

The APET engines used in this study all incorporate combustion technology sufficient to meet the standards given in Table IV.

Table IV. Emissions standards adopted for APET.

Pollutant	1986 ICAO TF/TJ standards— g/kN	Gas-generator equivalent— (G/kg)/hr		
HC	19.6	5		
CO	118	29.5		
NO _x	$40 + 2 (R_c)$	$11 + 0.55 (R_c)$		
Smoke	40 + 2 (R _c) 83.6 (F _n) ^{-0.274}	11 + 0.55 (R _c) 187 (kW) ^{-0.168}		

Engine Sizing

Point-performance requirements were defined to size the engine to the aircraft. For transport aircraft, safety-of-flight and field performance standards are the basis for engine sizings. The following engine sizing points were stipulated:

- takeoff field length of 5500 ft over a 35-ft obstacle, at sea level on a 86°F day, with takeoff power
- 300 ft/min rate-of-climb at M_N 0.72, 32,000 ft, max cruise power and takeoff gross weight, all engines
- 3. 100 ft/min rate-of-climb at 15,000 ft, max climb power and takeoff gross weight, on one engine

Engine Installation

Propulsion system installation factors are presented in Table V. The propfan used is a single-rotation, 10 blade

Table V.
Engine installation factors.

	Turbofan	Propfan
Inlet recovery (PT2/PT0)	1.00	1.00
Customer power extraction—shp/engine	100	100
Customer bleed extraction	none	none
Gearbox power loss—%	N/A	1.0

design with a tip speed of 800 ft/sec. The power loading at the initial cruise point is 32 shp/D². Efficiency estimates were taken from Hamilton Standard (HS) report SPO7A82 (Ref 1). Weight estimates were taken from HS report SPO6A82 (Ref 2).

Reference Turboprop Engine

A 15,000 shp reference turboprop engine (PD436-1) was used to develop sensitivity factors of fuel burned and DOC. As shown in Figure 4, the propeller drive gearbox is an offset-down type. The physical size of the engine is also shown in Figure 4.

The technology level of this 81.3 lb/sec corrected flow engine was assumed to be the same as the reference EEE core. That is to say, the component efficiencies, cooling airflow rates, and assumed losses in the cycle for the 15,000 shp turboprop engine are the same as for the considerably larger flow size EEE core.

Engine PD436-1 is a dual-spool configuration with an axial flow, single spool compressor driven by a two-stage axial flow, high-pressure turbine. The cycle of 25.0:1 overall pressure ratio and 2200°F turbine inlet temperature produces 7544 shp at 0.303 brake specific fuel consumption. The maximum temperature of 2500°F at takeoff requires 6.9% chargeable cooling air.

Reference Turbofan Engine

A 20,000 lb thrust class reference turbofan engine was defined in preliminary design detail for use in the mission analysis comparison of the turboprop- and turbofan-powered aircraft.

At the cruise condition, the reference turbofan engine has an overall pressure ratio of 34.0:1, has a 6.0 bypass ratio, and develops 4800 lb thrust at 2200°F rotor inlet temperature. The cruise thrust specific fuel consumption is 0.518. These data and the component performance levels are summarized in Table VI.

TASK II. ENGINE CONFIGURATION AND CYCLE EVALUATION

The procedures and assumptions identified in Task I were used to select the engine configurations and the cycle conditions for Task III. The selection criteria were chosen to place priority on the fuel burned and direct operating cost of the reference turboprop airplane. Therefore, engine specific fuel consumption, reliability, and ease of maintenance were key parameters. Study guidelines dictated the use of

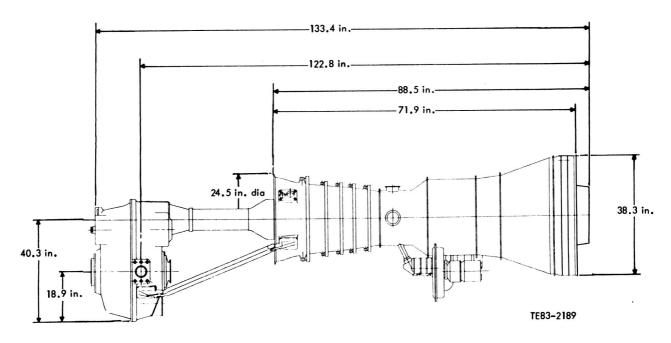


Figure 4. Reference turboprop engine used for developing sensitivities.

Table VI.
Reference turbofan engine performance.

	Takeoff, sea level static 86°Fday	Design point- 36,089 ft/ 0.72 M _N
Thrust—Ib	20,000	4,800
Turbine inlet temperature—°F	2,500	2,200
Specific fuel consumption	0.324	0.518
Corrected flow—lb/sec	696	804
Core flow—lb/sec corr	55.0	64.3
Overall pressure ratio	26.4	34:1
Fan pressure ratio	2.53	1.65
Bypass ratio	7.8	7.4
Compressor pressure ratio	17.2	20.6
Fan efficiency—%		88.0
Compressor efficiency—%		86.2
HP turbine efficiency—%		90.5
LP turbine efficiency—%		91.0
Chargeable cooling air and		
leakage—%		6.9
Mixer effectiveness—%		83.0

advanced technology components for the production date of the early 1990s. It was anticipated that new engines in commercial service in the 1990s would have component performance representing improvements over the EEE engines. This improved component performance would be (1) EEE technology in the smaller size APET turboprop engines of 9000 shp to 15,000 shp and (2) new designs and manufacturing methods directed toward solving the problems associated with smaller size, high pressure engines.

The seven candidate engine cycles and configurations shown in Table VII for turboprop-powered commercial airliners were evaluated to arrive at the best engine arrangement and most favorable match of fuel efficiency and direct operating cost. The four engine configurations shown in Figure 5 were selected for further evaluation and optimization of overall pressure ratio and cycle temperature by applying factors to account for size, cost, and weight.

Table VII.
Candidate engine configurations.

Engine configuration	Compressor-turbine type	of spools
1.	Single-spool axial compressor plus power turbine	2
2.	Single-spool axial/centrifugal compressor plus power turbine	2
3.	Dual-spool axial compressor plus power turbine	3
4.	Dual-spool axial/centrifugal compressor plus power turbine	3
5.	Single-spool dual-centrifugal plus power turbine	2
6.	Dual-spool dual-centrifugal compressor plus power turbine	3
7.	LP axial plus single-spool axial compressor plus power turbine	2

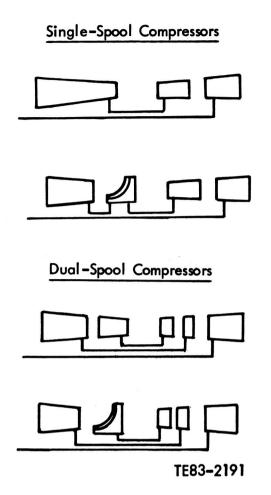


Figure 5. Configurations selected for further evaluation.

The results of these mission analyses, shown in Table VIII, favor the dual-spool compressors for fuel efficiency. The two configurations recommended for additional preliminary design work are the two three-spool engines with axial/axial and axial/centrifugal dual-spool compressors. The favored cycle conditions are 38:1 overall pressure ratio and 2400°F turbine temperature.

The mechanical design features of the HP axial and centrifugal compressors were evaluated early in the preliminary design. The required scaling from the 15,000 shp reference PD436-1B turboprop to the 10,000 shp APET size reduced the compressor polytropic efficiency from 91 % to 90%. The minimum specific fuel consumption for this case occurs at 32.5:1 overall pressure ratio. Therefore the design point of the turboprop engines was selected at 32.5:1. The turbine inlet temperature selected was 2200°F. The engine preliminary design point is summarized in Table IX.

Table IX.

Design specifications of APET turboprop engines.

	Engine PD436-10	Engine PD436-11
Size—shp	10,000	10,000
Overall pressure ratio	32.5:1	32.5:1
Turbine temperature		
Cruise—°F	2200	2200
Takeoff—°F	2500	2500
Compressor	Axial/centrifugal	Axial/axial
Turbine	HP/LP/power	HP/LP/power

Table VIII.
Final screening results.

	Cruise condition — 32,000 ft/0.72 M _N		Thrust sfc at	Fuel burned		Direct operating cost	
	Pressure ratio	Turbine temp	midpoint cruise	300 nmi	1000 nmi	300 nmi	1000 nmi
Single-spool axial compressor	25.0	2200	0.476	2580 (+7.1%)	6580 (+7.0%)	4.62 (+0.7%)	3.44 (+0.9%)
Single-spool axial/centrifugal compressor	25.0	2200	0.480	2610 (+8.3%)	6660 (+8.3%)	4.68 (+2.0%)	3.49 (+2.3%)
Dual-spool axial/axial compressor	38.0	2400	0.451	2410 (Base)	6150 (Base)	4.59 (Base)	3.41 (Base)
Dual-spool axial/centrifugal compressor	38.0	2400	0.455	2440 (+1.2%)	6220 (+1.1%)	4.62 (+0.7%)	3.46 (+1.5%)

The engine general arrangement for the axial/centrifugal compressor is shown in Figure 6, and the arrangement for the axial/axial compressor is shown in Figure 7. These engines are both three-spool configurations with individual HP and LP turbines and a free power turbine.

TASK III. PROPULSION SYSTEM INTEGRATION

The propulsion system integration effort utilized the two power sections shown in Figures 6 and 7. Both are three-spool configurations designed for 32.5:1 overall pressure ratio. The primary difference in the two engines is the type of HP compressor, axial or centrifugal. These two selected configurations are combined with the other propulsion system components and accessories and installed in a nacelle to arrive at representative propulsion systems.

Installation drawings are shown in Figures 8 and 9 for offset and inline gearboxes. The axial/centrifugal compressor power section with an offset gearbox allows for nacelle contouring to achieve the preferred aerodynamic shape for the over-the-wing mounted propulsion system. A top-mounted, single-scoop inlet is ducted to the compressor face transitioning from the scoop to the full annular shape required

for uniform air distribution. This arrangement has a bottomlocated aircraft-mounted accessories drive system (AMADS) gearbox, engine accessory gearbox, and air/oil cooler. Engine mounts are located on the gearbox housing and power turbine case. The axial/axial compressor power section with the offset gearbox is installed the same way. The only differences are locations of the rear mount and the design of the engine accessory gearbox. Installation of the inline gearbox dictates a different arrangement. With the in-line gearbox, the engine inlet is forced to be further from the engine centerline. The radial flow path becomes greater and a bifurcated inlet is preferred. The air/oil cooler location is moved to the top location and the pitch change and AMADS components are relocated. Engine mounts remain in approximately the same locations. This arrangement applies to both engine configurations with the in-line gearbox.

Engines PD436-10 and PD436-11 with offset gearboxes were selected for further evaluation in the engine-aircraft studies of Task IV. These engines are also available in the form of a performance computer code and data package.

The computer code is available on tape with a user's manual, Allison EDR 11321 (Ref 3). It contains the steady-

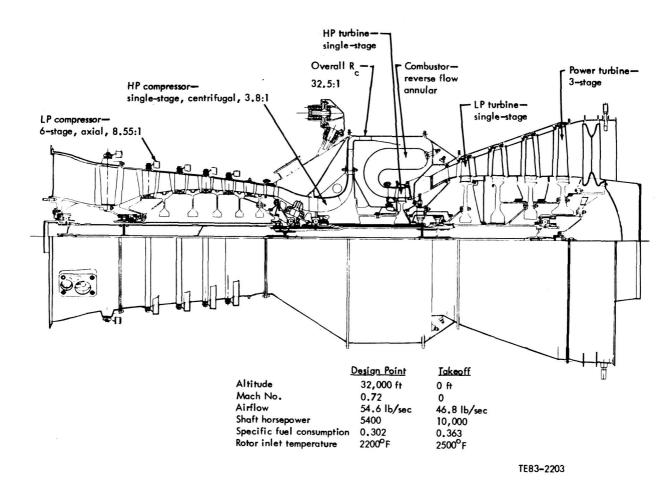


Figure 6. PD436-10 engine general arrangement for axial/centrifugal compressor.

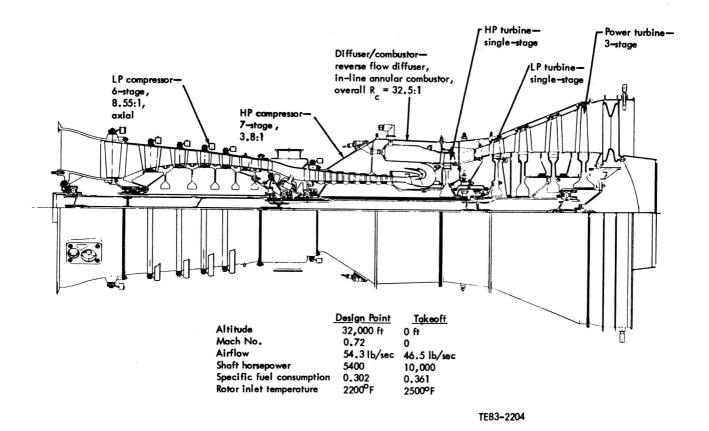


Figure 7. PD436-11 engine general arrangement for axial/axial compressor.

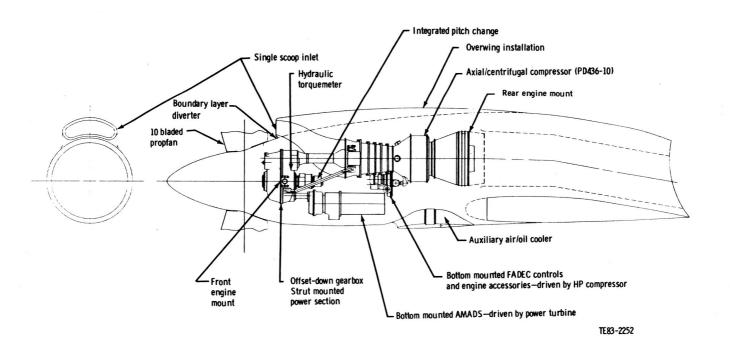


Figure 8. Installation drawing for engine PD436-10.

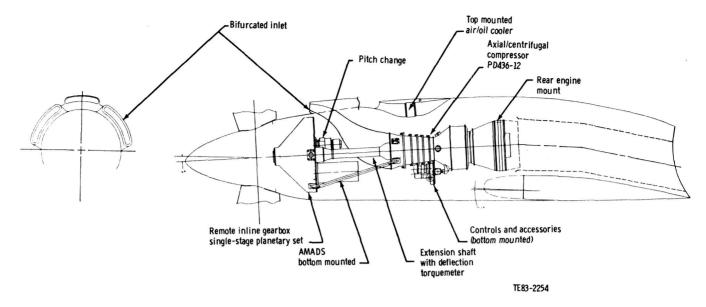


Figure 9. Installation drawing for engine PD436-12.

state engine parameters required for airplane company use in evaluating uninstalled performance. For quick reference, a range of data points is tabulated and presented with engine description and scaling procedures in Allison EDR 11375A (Ref 4).

TASK IV. ENGINE/AIRCRAFT EVALUATION

The objective of the engine/aircraft evaluation was to conduct a mission performance and economic analysis for the reference turbofan and the candidate turboprop engines in a commercial transport system.

Characteristics of the engines to be evaluated and their nacelle arrangements are presented in Table X. These engines were installed in the aircraft and sized to the appropriate point performance requirement. The turbofan engine was sized at the takeoff condition, and the propfans were both sized at the initial cruise point, 300 ft/minute rate-of-climb condition.

The aircraft/engine combinations were then scaled to carry sufficient fuel for the design mission plus reserves. Finally, the sized aircraft were flown in the 300 mile revenue mission to determine fuel burned, DOC, and sensitivities of these parameters to engine design features. The minimum DOC cruise altitude for all engines in the revenue mission was 30.000 ft.

Based on a block fuel comparison for the three engines, as shown in Figure 10, there is a significant fuel savings for both turboprop propulsion systems over the turbofan.

Direct operating costs (DOC), in terms of cents per seatnautical-mile, are compared in Figure 11. This figure depicts the impact of fuel-burned savings of the turboprop-powered aircraft on DOC over the turbofan-powered aircraft. Note that the slight advantage of the axial/axial turboprop in fuel burned has widened in this comparison. This reflects the lower power section cost of the axial/axial engine compared with the axial/centrifugal engine. The propfan-powered aircraft

Table X.
Engine/aircraft ground rules and assumptions summary.

	Study engines			
	Reference	Selected propfan engines		
	engine	PD436-10	PD436-11	
General description	2-spool mixed flow turbofan	3-spool axial LP and centrifugal HP	3-spool axial LP and axial HP	
Gearbox	NA*	Offset down	Offset down	
Inlet	Conventional	Single scoop—top mtg	Single scoop—top mtg	
Nacelle	Strut mtg underwing	Overwing	Overwing	
Design condition	Cruise	Cruise	Cruise	
Design BPR	7.4	NA	NA	
Design R _{coa}	36:1	32.5:1	32.5:1	
Design RIT—°F	2200	2200	2200	
Maximum RIT—°F	2500	2500	2500	

^{*}Not applicable

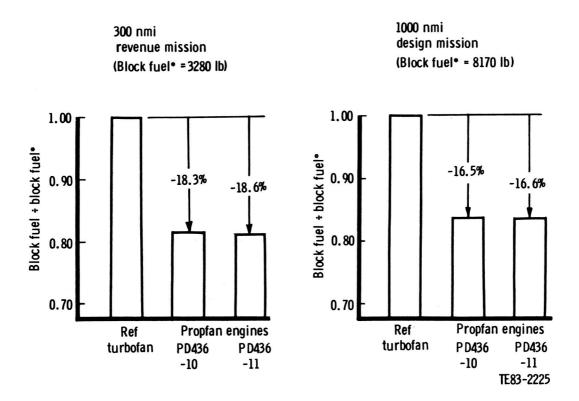


Figure 10. Aircraft/engine results.

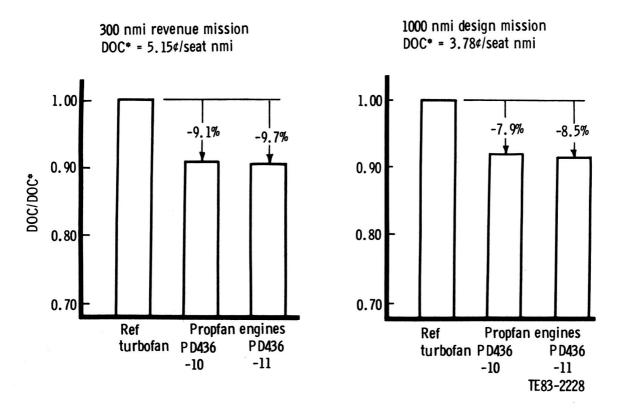


Figure 11. Economic results.

enjoy an 8%-10% DOC reduction compared with the turbofan-powered aircraft.

The aircraft used in this study meets the FAR Pt 36 Stage III airport/community noise constraints. The propfan engine requires no engine or inlet sound treatment whereas inlet treatment was required by the turbofan. No current emission standards exist for turboprop or propfan engines. Therefore, Allison has developed a gas-generator equivalent emission index calibrated to the fuel consumption and based on the ICAO 1986 agreed standard for turbofans and turbojets. The APET engines used in this study all incorporate combustion technology sufficient to meet these standards.

Trade studies were performed to estimate the effect of independent variables on fuel burn and DOC for the 300 nmi revenue mission. Propfan efficiency, engine specific fuel consumption, and aircraft drag are identified as major fuel burn "drivers." They affect fuel consumed on a nearly one-to-one basis. The remaining independent variables had sensitivities of one-tenth or less.

Additional variables were evaluated to examine DOC sensitivity. The sensitivity of the propfan aircraft DOC to a 10% change to a range of variables was estimated. The same three variables that drove fuel burn are again prominent here. However, the additional variables of aircraft cost, engine plus gearbox cost, and engine plus gearbox maintenance cost also have an effect greater than 1% DOC. The important propulsion parameters are as follows: propfan efficiency, engine specific fuel consumption, engine plus gearbox cost, and engine plus gearbox maintenance cost. The propfan cost, acoustic panel weight, and other weight items have a small effect on the operating cost of the aircraft.

TASK V. ADVANCED PROPFAN ENGINE TECHNOLOGY PLAN

The technology definition plan was developed to identify those components requiring more extensive development than would be encountered in a normal development program. The resulting six key technology components are as follows:

- engine inlet
- gearbox
- LP compressor
- HP compressor
- turbines
- controls

Engine Inlet

High speed propfan inlets operate in flow field environments that demand careful design integration for good performance stability. The inlet is characterized by high transonic Mach number flow, skewed (3-D) flow field, significant total pressure gradients, thick boundary layers, and blade passage effects from the propfan. The performance of the inlet duct is measured by the inlet recovery and the degree of compressor stability achieved. Design procedures must deal with internal diffusion, external spillage, and overall drag at the inlet and diffusion urning, prop/duct proximity, gearbox envelope, and shafting in the duct area.

A joint Allison/airframer/NASA program to complement current APET inlet studies should be initiated. This program would be interactive with the Allison/NASA APET advanced gearbox preliminary design study proposed as additional work in the current contract. This program would extend the existing subscale propfan/inlet wind tunnel data base to further evaluate a baseline and alternate inlet design.

The benefits of the propfan inlet program are summarized as follows:

- high performance inlet duct designs for acceptable engine stability over a broad range of power setting, angle of attack, and cross winds
- duct designs for high installed thrust minus drag from high inlet pressure recovery and reduced inletchargeable drags
- sensitivity of key inlet performance variables to gearbox and shafting optimization for minimum weight, frontal area, cost, and reliability
- steady-state and dynamic pressure mapping of inlet duct exit plane, and duct wall pressure distributions for future correlations and analytical modeling

Particular emphasis is directed to the importance of having a good definition of the inlet flow field and stability limits and the impact of design variables on installed engine/nacelle performance. An additional benefit of this effort could also be the associated impact of nacelle cooling flow rate on engine performance through case cooling and related tip clearance control versus possible spillage drag or frontal area drag.

Gearbox

The advancement of gearbox technology in the 10,000 shp class is needed because the gearbox configuration has a major impact on inlet/nacelle integration and, therefore, on installed performance. The efforts of industry in the field of compact, lightweight, high horsepower reduction gearboxes has been almost nonexistent for the past 15 to 20 years. This lack of technology has been in the mechanical design and manufacturing disciplines and also in the configuration of the overall package and internal gear train.

The proposed program plan for generating gearbox technology is to be initiated with a preliminary design study of the gearbox configuration and related propfan pitch change mechanism. The configuration studies should be closely integrated with the proposed propfan inlet study program because of the major interrelated impact of two components. The studies would also include the investigation of various reduction schemes. Maintenance cost, weight, reliability, heat rejection and/or power absorption. Out of these studies will evolve an identification of needs to advance gearbox technol-

ogy to the levels of other current gas turbine components. These potential needs would involve materials, manufacturing techniques, bearings, and housing structures.

The gearbox technology program will result in significant benefits to the overall NASA APET objectives. It will produce a gearbox commensurate in technology with gas turbine and airframe technology of the 1990s. Of equal importance is the fact that the gearbox configuration will be integrated with the inlet and nacelle configuration to ensure optimum installed propulsion system performance.

Low Pressure Compressor

The key technology components of the APET advanced technology power sections are the compressors. Fuel savings and DOC results indicated in this study are based on assumed efficiencies that have not yet been demonstrated in the 10,000 shp class engines. Verification of these assumptions must be accomplished if the turboprop engine advantages are to be fully realized.

Figure 12 illustrates a correlation of compressor polytropic efficiency with compressor exit corrected flow. A current technology band is shown as well as the EEE and APET goals. These data illustrate that the APET goals represent about the same extension of efficiency as the EEE program. The demonstrated performance of the EEE programs is also shown illustrating good advancement toward goals.

The program plan is based on using an existing Allison component rig in the 30 lb/sec flow class as a baseline. It is a six-stage low aspect ratio component rig that has undergone

initial baseline testing with conventionally designed blading. This program would use that rig as a vehicle to investigate the potential of velocity controlled blading (velocities selected to pass the correct flow in all stages) to increase both the efficiency and loading of the compressor. Goals would be to achieve the 90% polytropic efficiency in a usable compressor in terms of surge margin and flow stability.

High Pressure Compressors

The major problem of the centrifugal compressor is the low specific speed (64) brought on by high borestress. The major problem of the axial compressor is the small latter stage blade heights. The prime objective of the proposed program is to evaluate the best-effort centrifugal compressor compared with the best-effort axial compressor. This evaluation would be in terms of design point and off-design efficiency, surge margin, and stability.

With the compressor work accomplished as outlined herein, the state of the art of high pressure compressor design will be advanced to the levels assumed in the APET study. It is anticipated that the level of technology developed in the NASA-sponsored EEE programs will be demonstrated in the smaller size APET engines. The primary benefit will be to apply the EEE compressor research and development accomplishments to a turboprop engine. Although additional tasks are involved, particularly in the centrifugal configuration, many of the advances in compressor design and manufacturing made in EEE are applicable and must be applied to the APET engines.

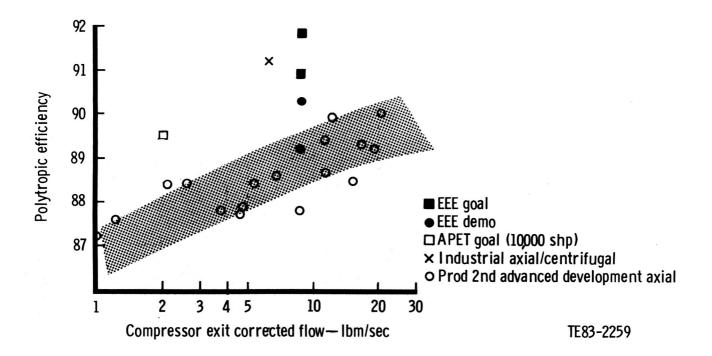


Figure 12. Compressor efficiency correlation.

Turbine Development

Much effort has been devoted toward improving efficiency of small air-cooled gasifier turbines, but very little work has been directed toward one of the prime sources of loss in any turbine, which is the loss associated with endwall secondary flows. Therefore, the objective of this proposed program is to increase stage aerodynamic performance and/or reduce endwall cooling requirements through the control of secondary flows.

The vane inlet endwall boundary layer and associated velocity profile strongly influence the formation and magnitude of the secondary flows on the vane endwalls. These secondary flows are in the form of vortex flows, which aggravate the vane endwall heat transfer, produce loss within the vane passage, and also have a detrimental effect on the downstream rotor performance.

Figure 13 illustrates a summary of turbine overall polytropic efficiency for an overall expansion ratio of approximately 6. For comparison, the combined HP/LP turbines and the power turbine are illustrated. These efficiency levels are equally aggressive to EEE performance goals. This work is applicable to both cooled and uncooled turbines, but prime emphasis will fall on uncooled stages.

Control System

The major problem with many current gas turbine turboprop and turboshaft propulsion systems is the division of management between prop or rotor and the engine. Systems are designed independent of each other, and although coordinated, they seldom achieve optimum performance, reliability, and cost effectiveness.

A joint venture into a combined or integrated control system is a prime requirement of the program. This work would include computer simulation of the engine and the propfan from which to investigate control modes. From these studies an overall system architecture and component interface can be defined. The recommended program would be performed by the engine and propfan companies to define the integrated system concept. It would involve the design and procurement of hardware for demonstration testing using an integrated "BREADBOARD" system. The major benefit of this program will be an individual control system definition for the propfan and the engine so that they work in harmony, which will potentially enhance performance in terms of response, failure modes, and overall performance.

TASK VII. PRELIMINARY DESIGN OF THE SINGLE-ROTATION PROPFAN REDUCTION GEARBOX

A preliminary design study was performed to define a single-rotation, 10,000 shp class, advanced technology propfan gearbox for the APET mission. The design compared two levels of technology: a state-of-the-art gearbox that could be manufactured with existing technology and an advanced gearbox that requires implementation of the technology plan programs defined in Appendix H. The advanced technology gearbox is the design forecast for production propfan aircraft of the 1990s. The current tech-

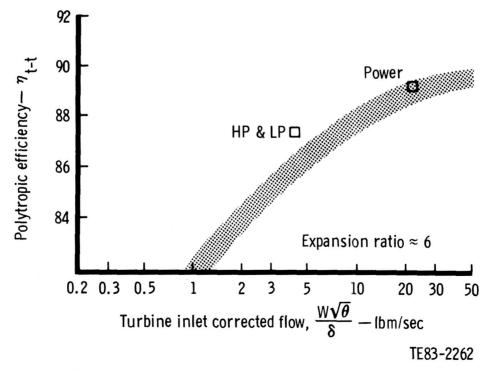


Figure 13. APET turbine technology levels compared with EEE.

nology design served as a baseline against which the extra benefits of advanced technology could be evaluated. The gearbox preliminary design study was conducted in four phases:

- a trade study to select the bearing and gearing configuration
- 2. gearbox preliminary design of current and advanced technology versions of the selected configuration
- comparison of the two gearbox designs to determine the benefits of advanced technology features
- preparation of a research and technology plan for verification of technology assumptions in the advanced design

Trade Study

A configuration selection procedure was performed to arrive at the favored gearing and bearing arrangement for the preliminary design phase. This evaluation considered both in-line and offset input-to-output shafting as indicated by the star and dual compound idler gearing types shown in Figure 14.

The procedure involved a weighted-decision analysis to rank the candidate configurations relative to nine parameters:

- reliability
- efficiency
- maintenance cost
- acquisition cost
- propfan pitch change compatibility
- weight
- technical risk
- ease of scaling
- spatial envelope

Reliability and efficiency, the most important criteria, were essentially the same for the candidates. The remaining seven parameters favored the dual compound idler system. However, due to the closeness of the results, five additional criteria were used in the evaluation:

- adaptability of the configuration to over- and under-wing mounting
- impact on inlet duct efficiency
- impact on reliability and maintainability of gearbox and airframe accessory drives
- impact on torquemeter design
- adaptability to an aerodynamically contoured nacelle

The dual compound idler offset configuration received higher ratings for these installation criteria. It is also better suited for use with a hydraulic torquemeter. This capability offers a 20-lb weight saving over the phase detector type torquemeter required for the star planetary configuration. The overall rating of the dual compound idler offset gearbox was greater, and it was selected for the design phase.

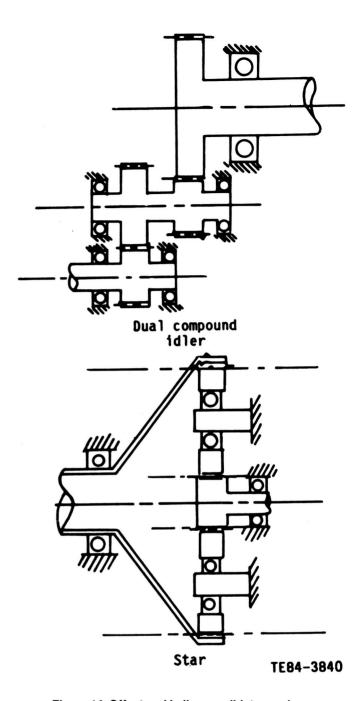


Figure 14. Offset and in-line candidate gearbox arrangements.

Design Criteria

The two versions of the gearbox required that design allowables be established that were consistent with the assumptions of state-of-the-art technology in one case and advanced technology in the other case. Design allowables are summarized in Table XI.

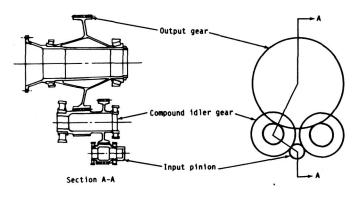
Gearbox Preliminary Design

The dual compound idler gear arrangement selected for the preliminary design is composed of a single input

Table XI.

Criteria for the two technology levels.

	State-of-the-art (1980s)	Advanced technology (1990s)
Gear teeth		
Lewis bending stress limit—lb/in.2	40,000	50,000
Hertzian contact stress limit—lb/in.2	160,000	200,000
Pitch-line velocity—ft/min	25,000	25,000
Surface finish—microinches		
(arithmetic average)	10	6
Bearings		
life factor	10	30
B ₁₀ set life—hr	18,000	18,000
Finish—microinches		
(arithmetic average)	6	3
Allowable temperature rise— °F	60	90
Flash temperature index	370	440
Gearbox efficiency—%	98.8	99.3



TE84-3841

Figure 15. Dual compound idler gear arrangement.

pinion, two idler gears, and an output gear, as shown in Figure 15. The idlers are compound gears consisting of two gears per idler. Power is applied to the input pinion gear, split through the idlers, and recombined in the output gear.

Features of this type of gearbox are summarized as follows:

- load sharing—equalizes loads on each idler and provides for torquemeter readout
- modularity—provides external accessibility
- prop load isolation—minimizes gear misalignment
- tapered bearings—reduce part count
- fine filtration—reduces bearing denting

Preliminary design drawings of the current and advanced technology gearboxes are shown in Figure 16.

Both designs have the same gear train configuration. However, design differences result in the advanced gear-box being smaller and lighter (640 lb vs 800 lb) and having a lower acquisition cost. The frontal area is reduced 17%,

and the offset between the engine and propfan centerlines is reduced 7%. Physical dimensions are compared in Table XII.

The gearbox preliminary design included provisions for accessories required by the propfan pitch change system, such as an oil pump and high-speed drive, a propfan brake, an airframe accessory drive, a gearbox oil pump, and an oil filter. Details of these interfaces with the gearbox are discussed in Appendix F. The gearing used in the input side of the gearbox (pinion-to-idlers) is spur gears. The output side (idler-to-output) used helical gears with a 5-deg helix angle. Improved stress allowables and high contact ratio spur gears show significant payoff in the advanced design. The advanced spur gears have a 20% smaller pitch diameter and are 33% smaller on a volume basis. The advanced helical gears have a 9% smaller pitch diameter and are 27% smaller on a volume basis.

The same type of bearings are used in both designs, as indicated in Table XIII. However, the materials and manufacturing techniques are quite different.

Bearing materials in the advanced technology gear-box have improved fatigue strength, corrosion resistance, fracture toughness, microdamage tolerance, and wear/skid resistance over today's VIM/VAR M50 steel. Candidate materials are powder metals such as MRC 2001 and low-carbon wrought steels such as CBS 600. Future bearings will be manufactured by processes such as hot isostatic pressing and advanced contour induction hardening. Finishes will be ultrasmooth.

Heat generation and power loss estimates for the two designs are summarized in Table XIV.

At the 0.72 Mach number/32,000-ft cruise condition, the total loss of the advanced gearbox is estimated to be 61.4 hp, which is an efficiency of 98.82%. This compares to 64.1 hp and 98.77% for the current technology design.

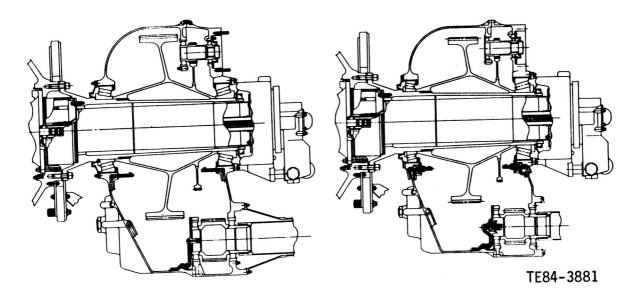


Figure 16. Preliminary design drawings of the state-of-the-art and advanced technology gearboxes.

Table XII.

Gearbox physical dimensions.

Dimension	Current technology	Advanced technology
Frontal area—in. ²	900.0	745.1
Height—in.	34.31	31.62
Length—in.	24.38	23.22
Width		
Between mounts—in.	28.44	26.75
Maximum—in.	32.06	26.75
Centerline offset (engine-propeller)—in.	15.375	14.375

Table XIII.

Bearing types used in both the current and advanced designs.

Bearing	Туре	
Pinion front	Cylindrical roller	
Pinion rear	Cylindrical roller	
Idler front	Cylindrical roller	
Idler rear	Cylindrical roller	
Idler thrust	Ball	
Output front	Tapered roller	
Output rear	Tapered roller	

Table XIV.
Gearbox power loss and efficiency.

	Current technology		Advanced technology	
	Cruise	Takeoff power	Cruise	Takeoff power
Gears—hp	40.80	73.57	40.31	79.22
Bearings-hp	14.68	19.80	14.33	19.12
Oil pumps—hp	8.60	8.60	6.80	6.80
Total loss—hp	64.08	101.97	61.44	105.14
Gearbox efficiency—%	98.77	98.98	98.82	98.95

The advanced gearbox also incorporates power saving features not included in the power loss and efficiency estimates. For example, it has a modulated oil flow at the cruise condition to reduce churning/windage losses. Also, gear sliding losses should be lower than predicted for the advanced gears due to the lower frictional forces demonstrated for ion implantation of the tooth flanks.

The acquisition cost of the advanced gearbox in production is estimated to be \$165,000 for the 10,000-shp size as compared with \$220,000 for the current technology design. These are 1984 dollars, and the reduction is attributed to the use of powder metal gears and bearings, near net shape manufacturing processing, and the reduced size and weight of the assembly.

Likewise, maintenance cost for the advanced design is less—\$1.08/engine flight hour compared with \$1.31.

An inherent assumption of the design comparison is that both designs have the same design MTBR of 30,000 hr. Additional detail of the designs is given in Appendix F.

TASK VIII. CONCEPTUAL DESIGN OF THE SINGLE-ROTATION PITCH CONTROL AND MECHANISM

A conceptual design study was performed by Hamilton Standard to define a single-rotation pitch control and mechanism for the 10,000-shp class advanced technology propfan propulsion system of Task III. This study was conducted concurrently with the gearbox preliminary design of Task VII. The pitch change design is a flight weight configuration integrated with the advanced technology gearbox. The advanced technology issues requiring technology verification are defined, and a plan is described in Appendix H to accomplish the technology advancements needed in the areas of electronic controls, capacitative signal transfer, and hydraulics to fully realize the benefits of propfan propulsion.

The conceptual design was conducted in four phases:

- a trade study to select the optimum concept
- 2. conceptual design of an advanced technology pitch change mechanism and control
- estimates of reliability and cost factors for the conceptual design
- 4. identification of advanced technology issues

Trade Study

Current technology in propeller pitch change systems generally incorporates a linear hydromechanical actuator with a metering valve and a mechanical pitch lock, which are mounted in the rotating propfan assembly. Mechanical, hydraulic, and electrical inputs are required to traverse the boundary from the gearbox to the rotating components. This is presently accomplished in the following manner:

- mechanically (Rotary motion to position the pitch lock and metering valve uses differential gearing or a bearing-mounted ball screw.)
- hydraulically (High pressure oil is transmitted to the metering valve and actuator through a lowclearance oil transfer bearing and transfer tubes.)
- electrically (Electrical power for de-icing is transmitted to the propfan by contact brushes running on a rotating slip ring assembly.)

The advanced technology trade study considered the pitch change system as two parts—a power system and a control system.

A thorough analysis of power system concepts resulted in the seven candidates ranked in Table XV. These rankings and the considerations discussed in Appendix G resulted in the selection of the linear hydraulic power system for the conceptual design.

Table XV.
Power system concept ranking.

Ranking	Power system concept		
1	Hydraulic piston actuator		
2	Ball screw, hydraulic motor		
3	Ball screw, electric motor		
4	Ball screw, differential gears, hydraulic motor		
5	Ball screw, magnetic coupling		
6	Bal screw, differential gears, electric motor		
7	Ball screw, traction drive		

Likewise, after considering the advanced technology possibilities applied to the pitch change control, the control system rankings shown in Table XVI were determined.

The favored concept incorporates a fractional horsepower direct current electric servomotor to position a metering valve to provide high-pressure oil to a linear piston. The servomotor and its electronic controller are installed in the rotating propfan.

In summary, the trade study showed that a linear hydraulic actuator is preferred. It should have a power supply rotating with the propfan to eliminate the need for transmitting power across the rotating interface. It should use a capacitor concept to transfer control signals across the rotating interface.

Table XVI.

Motor control system ranking.

Ranking	Control system concept		
1	Electric servomotor, metering valve, hydraulic piston		
2	Electric servomotor, metering valve, hydraulic motor		
3	Electric servomotor, gears, metering valve		
4	Electric motor (magnetic coupling)		
5	Electric motor		

Conceptual Design

A modular pitch change approach was followed using the linear hydraulic actuator, rotating power supply, and capacitor signal transfer components recommended in the trade study. Three designs were considered early on. However, with the selection of an offset gearbox configuration in Task VII, the pitch change design focused on making maximum use of the advantage of the offset relative to accessibility. This resulted in locating a hydraulic power module as a separate unit on the rear of the gearbox housing. The power system for the pitch change mechanism is more accessible and more easily maintained when mounted on the gearbox. The general arrangement including this and other features such as the generator drive, generator, signal transfer module, actuator, pitch lock screw, and electronic control module is shown in Figure 17.

Three features of this system have been identified as requiring technology development and test verification before finalizing the design. These three areas are the (1) rotating electronic control module, (2) capacitor signal transfer module, and (3) high-pressure hydraulic power module attached to the rear of the gearbox.

Results of a weight analysis conducted on the advanced pitch change system when compared with the state-of-the-art design applied in the earlier APET tasks show that the advanced system is lighter. The net result is a 4% reduction in propfan weight.

The reliability of the advanced pitch change system is estimated to be significantly improved over the state-of-the-art design. The "chargeable" mean time between all maintenance actions for the advanced system is 8,900 hr. This represents an improvement of 102% over the 4,400 hr for the baseline system.

Maintenance was assumed to on-condition, which is in line with present-day experience. Considering scheduled inspections, unscheduled line repairs, and unscheduled removals, the total maintenance cost for the advanced system was estimated to be \$2.51 per flight hour. This represents a 15% decrease from the baseline state-of-the-art system.

Acquisition cost of the advanced system is estimated to be 7% less than the baseline.

Details of the advanced technology pitch change system design are presented in Appendix G.

TASK IX. RESEARCH AND TECHNOLOGY PLAN FOR THE SINGLE-ROTATION GEARBOX AND PITCH CONTROL AND MECHANISM

The technology definition plan described in this section was prepared to identify those components of the single-rotation gearbox and pitch change system requiring more extensive development than would be encountered in a normal development program. Components identified for special attention are listed as follows:

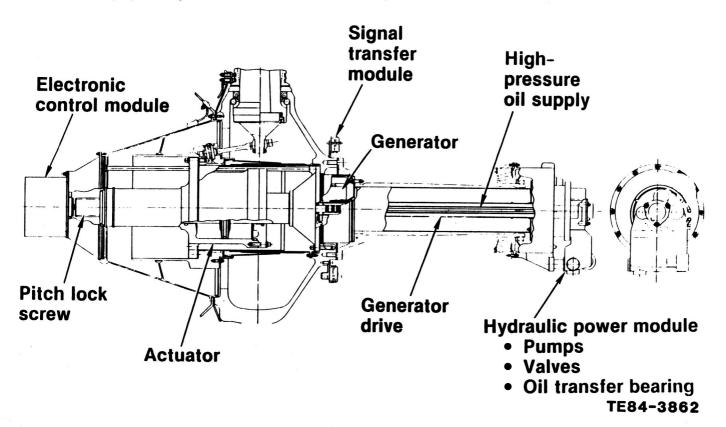


Figure 17. Pitch change system.

- gearbox components
 - gear and bearing material
 - gear and bearing manufacturing processes
 - high contact ratio gearing
 - tapered roller bearing
 - lubrication system
 - housing
- pitch change system
 - capacitor signal transfer system
 - high-pressure rotating hydraulic power module
 - rotating electronic control

Gearbox

The following is a summary of recommendations for the gearbox taken from the detailed technology plans of Appendix H.

Gear and Bearing Material

AMS 6265 (AISI 9310) steel has been used to meet gearing material requirements for the majority of Allison's gearbox designs. New gear materials will be needed if technology is to be advanced in future gearboxes. Materials such as Vasco X2, Pyrowear 53, and CBS 600 have demonstrated some advantages over AMS 6265 in component testing. The major focus in many of these materials has been in the area of improved hot hardness for oil-off capability. Some of these materials have also demonstrated life improvements in limited testing. Greater improvements are needed to meet the goals that have been established in this study for the advanced technology gearbox.

The following requirements offer the greatest potential for gear materials:

- high hot hardness
- increased allowable stresses/improved fatigue

Both powder metal steel and wrought low-carbon steels will be evaluated in this program.

Traditional aircraft bearing materials primarily consist of intermediate carbon (0.5%-1.0%) through hardening type steels. VIM/VAR M50 (AMS 6491) steel fits this classification and has been used in a major portion of gearbox bearing applications. M50 has demonstrated properties, such as fatigue strength, which are far superior to other types of properties. Corrosion resistance and low fracture toughness have been a problem for this type of steel.

The low-fracture toughness properties are primarily due to the through-hardened condition of these steels. The low fracture toughness leads to race fractures, which are catastrophic type failures. The race fracture is initiated by spalling or pitting. Only a relatively small spall or pit is needed to reach a critical crack size for this material. Upon reaching the critical crack size, race fracture progresses rapidly. Intermediate-carbon-level steels with better fracture toughness properties obtained through improved manufacturing processing or chemistry changes are needed.

Corrosion has also been a significant problem for these bearing materials. In a number of gearbox bearing locations, corrosion has been the primary problem. Therefore, more corrosion resistance is needed in advanced bearing materials.

Various steels that are corrosion resistant or have good fracture toughness have been examined. While these materials demonstrated excellent results in the corrosion and/or fracture toughness areas, they exhibited deficiencies in areas such as fatigue (spall) strength. Thus, compromises in material properties are required in the selection of current bearing materials. It is desirable to develop a bearing material that avoids these compromises for future gear-boxes.

The bearing material properties that will provide the greatest improvements for the advanced technology gearbox are as follows:

- improved fatigue strength
- improved corrosion resistance
- improved fracture toughness
- equivalent hot hardness

As with gear materials, powder metal steels have the potential of meeting all these requirements without compromises. The powder would be processed as outlined for gears by the following:

- VIM/VAR melting
- rapid solidification
- pulverizing to 200-270 mesh powder

Gear and Bearing Manufacturing Processes

A number of benefits can be realized through improved gear and bearing manufacturing techniques. The techniques being proposed consist of the following:

- hot isostatic pressing—gears and bearings
- hot forging to near net shape—gears
- advanced contour induction hardening—gears and bearings
- ultrasmooth surface finishing—gears and bearings
- ion implantation—gears

The hot isostatic press process provides powder metal preforms that are 100% dense and that are closer to final part shape than is obtainable with conventional wrought processing. Density of 100% is required to ensure optimum fatigue strength. Providing a near net shape preform thus eliminates a number of machining steps that would be required in conventional wrought processing. These reduced steps provide cost reductions.

Hot forging to near net shape provides both gear cost savings and potential gear performance improvements. The cost savings result from the elimination of processing steps such as hobbing. At the current technology level, the forged parts would require grinding and honing of gear teeth to provide aircraft-quality gears. However, with tech-

nology improvements it may be possible to eliminate some or all of these finishing steps. Cost savings are also realized through better use of the raw material.

The gear performance improvements are a result of the ideal forging flow patterns that this process produces. Current forged gears are processed from forged blanks. When the teeth are hobbed, the flow lines are severed and the resulting flow pattern is not the optimum desired. With hot forging, the teeth are forged to net shape and the resulting flow lines are parallel to the free surfaces, which is the most desirable orientation. This improved flow pattern should result in fatigue life improvements.

The advanced induction hardening process offers a number of gear and bearing improvements. These improvements include:

- better fracture toughness for intermediate carbon steels
- cost savings
- better surface durability (spall) life due to better residual compressive stresses
- less part distortion

Traditional aircraft gear materials are composed of low carbon type steels. Intermediate carbon steels (0.5%-1.0%) have been avoided due to their low fracture toughness properties. The low fracture toughness is primarily a result of the through-hardened condition of these steels. The fracture toughness could be greatly improved if the core could be left at a lower hardness level while the case was fully hardened. Lasers and electron beam heat treatment methods have focused on this goal in recent work. Allison has developed a contour induction hardening technique that also meets these goals while avoiding the difficulties that have been encountered in the laser and electron beam methods, such as special atmospheres for lasers, beam directing/raster pattern development complexities, high capital costs, and high reflectivity associated with beam heating.

Bearings will also benefit from the contour induction hardening process by eliminating the race cracking problems that have occurred in some gearbox applications. As stated previously, the race cracking is caused by low fracture toughness properties. Case hardening these steels with the induction hardening technique will improve fracture toughness and eliminate this problem.

Improved surface finishes offer potential for life improvements. Better finishes improve the lubrication film thickness to surface asperity height relationship. This relationship is normally expressed as the ratio of the film thickness to the composite surface finish and is known as the lambda ratio. Testing has shown that improvements in the lambda ratio result in an improvement in fatigue life in the lambda ratio regime, which applies to the components in this study.

Ion implantation techniques offer gear efficiency improvement potential. Implantation of Ta + and Mo + ions

into AISI 9310 has demonstrated a 30% reduction in the coefficient of friction in tests run in a no-lubrication environment.

The following program is recommended to develop processes for application to gear and bearing fabrication.

Material selection. The first step in this program will be material selection. AMS 6265 (AISI 9310) and M50 will be used as a baseline for comparison purposes. Five other materials will also be selected and tested. These materials will consist of three intermediate-carbon-level (0.5%-1.0%) steels and two low-carbon-level steels (0.1%-0.2%).

Hot isostatic press. The objective of this phase will be to develop a hot isostatic press process for manufacturing of powder metal gear and bearing preforms and test specimens. The preforms and specimens will be hot isostatic pressed to 100% density. The test specimens will be taken from a hot isostatic pressed ingot. A ceramic container will be developed to provide the desired consolidated preform shape for the hardware items. An inert gas will be used to develop consolidation pressures in the vicinity of 15,000 lb/in.². Dwell times of approximately 4 hr with a peak cycle temperature of approximately 1900 °F-2075 °F will be used. The hot isostatic press equipment needed for this work is available outside of Allison. Use of this equipment will be pursued on a subcontract basis.

Hot forging to near net shape. The objective of this phase is to develop a hot forging process that provides parts requiring minimal finishing processes. Powder metal preforms and/or wrought blanks would be required for this phase. Dies will be developed for test specimens and for full-scale hardware. This phase will require effort in finding an adequate die lubricant and determining the optimum forging parameters to ensure proper die fill and part ejection.

The forging equipment needed for this program is available from outside sources. Use of this equipment will be pursued on a subcontract basis. Dies will also be fabricated outside Allison.

Advanced contour induction hardening. The objective of this phase is to develop a contour induction hardening technique that provides a uniformly hardened case and low part distortion in intermediate-carbon-level steels. Allison has the induction hardening equipment needed for this program.

Fabricated test gears and test bearing components will be induction hardened. The case hardness gradient in the root and profiles of the gears and the races and roller/balls of the bearings will be examined. The process parameters, primarily the heating levels and heating dwell times, will be varied to determine the optimum settings. Full-scale and test gear and bearing hardware will be heat treated and tested following the process cycle development phase.

Ultrasmooth surface finishing. The objective of this phase is to develop a cost-effective finishing process that provides parts with surface finishes that are 40%-50% bet-

ter than finishes produced on current production gears and bearings. Current production gears are being produced with finishes of 0.000025 in. peak-to-valley (approximately 10μ in arithmetic average [AA]). The goal would be to produce gears with finishes of 0.000015 in. peak-to-valley (approximately 6μ in AA). Current gear finishing practice is a three-part process. Gears are normally full-form ground by a single grinding wheel. The grinding process is followed by shot peening the roots and profiles twice. Finally, the profiles are honed by a fine grit hone.

The program will consist of modifying one parameter at a time in the current manufacturing process. Surface finish will be measured after each process step to determine the benefits of each process change. Gears and bearings will be fabricated, tested, and compared with the current baseline to quantify benefits.

lon implantation. The objective of this phase will be to ion implant gear teeth and verify efficiency and scoring/scuffing improvements. Erdco test gears will be fabricated and implanted with ions such as Ta + and Mo + . The Erdco test head will be insulated, and oil flow and oil temperature rise will be measured to determine the efficiency improvements.

Gear testing. These processes will be evaluated through a testing program. Test gears will be fabricated using the materials and manufacturing processes discussed. These gears will be evaluated in the following tests:

- efficiency test—modified Erdco rig
- scuff test—Erdco rig
- spall life test—Erdco rig
- single-tooth bending test—shaker rig

Bearing testing. The bearing manufacturing processes will be evaluated through a testing program. Test balls and rolling contact specimens will be fabricated using the materials and manufacturing processes discussed. The test specimens will be evaluated in the spall life test, which involves three ball tester balls and rolling contact tester rolls.

High contact ratio gearing. The objective of this program is to design, develop, test, and evaluate high contact ratio spur and helical gear sets.

Design will be performed using finite element methods. This approach provides the best method for defining tooth deflections, stresses, and the optimum profile modifications required. Both nonbuttress and buttress designs will be analyzed.

Test gears and full-scale gears will be fabricated using the beneficial processes developed in the manufacturing process program. If the process program is not funded, conventional forge, hob, shot peen, grind, and hone techniques will be used. A tooth surface treatment program will be pursued if not undertaken in the manufacturing process program.

Spalling fatigue tests of the following designs will be conducted. A single-tooth bending test will also be conducted to quantify the benefits of the buttress design over the conventional approach.

The best spur and helical designs from the test programs will be selected and developed for full-scale hardware tests. Tests will be conducted on a back-to-back gearbox rig. The gears will be strain gaged in the roots to determine bending stresses, load distribution, and compressive stresses when subjected to gearbox operating conditions.

Tapered Roller Bearing

Tapered roller bearings provide the most compact design for applications such as prop shafts. In these applications both thrust and radial loads must be reacted. The conventional approach has been to use two cylindrical roller bearings with one ball bearing. The cylindrical roller bearings provide most of the needed capacity. They cannot carry the thrust load; therefore, a ball bearing is needed to react the thrust. Tapered roller bearings can carry both radial and thrust loads and also have the high capacity inherent in roller bearings. Therefore, only two bearings are needed in these applications. Reducing envelope requirements and part count results in improvements in size, weight, and reliability/set life.

Improving the oil-off capability of tapered roller bearings will make this type of bearing more viable for use in future gearboxes. Being able to use tapered roller bearings in place of the conventional ball and cylindrical roller bearing arrangement for thrust and radial load environment provides the following benefits:

- reduced size
- reduced weight
- increased bearing reliability/set life

Tapered roller bearing ribs will be ion implanted with two types of ions. Powder metal ribs using the optimum parameters from the Timken program will also be fabricated.

These bearings will be oil-off tested in a bearing rig under rated loading conditions.

Lubrication System

A modulated oil system will be investigated to verify and quantify the expected gearbox efficiency benefits.

The program will be started with the design of a modulated orifice for rig testing. Two modulated orifices will be fabricated for rig testing. The rig will be composed primarily of a pressure-regulating pump, the modulated orifice, and a variable-oil-pressure source to simulate torquemeter pressure.

The effects of varying torquemeter pressure and system oil pressure will be evaluated during rig testing. This

testing will be used to evaluate jet velocity, jet length-todiameter ratio, jet quality, and jet targeting.

Following successful rig testing, hardware will be designed and fabricated for testing in a back-to-back gear-box. The gearbox will be tested with both a conventional lubrication (baseline) system and a modulated system. Increasing gearbox temperatures and increasing the temperature rise across the gearbox will be investigated.

This program will be initiated by an oil cooler sizing study. Oil coolers will be designed for various temperature levels, temperature drop levels, and flow rates that would be expected for a typical mission. The cooler system will consist of in-line fuel/oil and air/oil coolers. The study will be directed toward reducing the air/oil cooler size and associated drag and weight penalties. Cooler size, weight, and drag will be determined for each temperature setting.

A back-to-back gearbox rig will be used for high-temperature testing. Gearbox component materials that can withstand the higher temperatures will be used. Gearbox inlet and outlet temperatures will be varied during operation at various speed and power settings. Heat generation and gearbox efficiency will be measured to determine any gearbox benefits.

Allison will work with an oil company to develop a gearbox oil that provides the following:

- satisfactory performance over a temperature range of -40°F to 600°F
- adequate load carrying ability with respect to scuffing and spalling over this temperature range
- improved friction characteristics in comparison with MIL-L-23699
- equivalent properties to MIL-L-23699 with respect to other requirements

Five oils will be subjected to evaluated tests. These tests will consist of:

- scuff testing-Erdco rig
- heat generation and efficiency measurements modified Erdco rig
- spall testing—Erdco rig and rolling contact tester
- other tests outlined in MIL-L-23699 specification

These oils will also be treated in a back-to-back gearbox. The gearbox will be operated at various gearbox oil-in and oil-out temperatures and flow rates. Gearbox heat generation and efficiency will be determined for each one of these test points.

A 3-micron filter system that will clean itself will be developed. Two system types will be designed. One filter system will be a continuous cleaning type. The second system will be a periodic cleaning type.

The designs will be fabricated and tested on an oil rig. The rig will be a closed-loop system composed of an oil pump, a self-cleaning filter, valves, a heater/temperature controller, and an oil tank. The tank will be capable of adding contaminants at a controlled rate.

The rig will be operated at various oil temperatures, flow rates, and pressures. Contaminants will be added to the system at each of the test points. The pressure drop across the filter will be measured and used to evaluate the success of each of the self-cleaning designs.

Housing Plan

A composite housing material that provides the following areas of improvement with respect to aluminum and magnesium will be investigated:

- stiffness-to-weight ratio
- strength-to-weight ratio
- creep resistance
- noise damping
- corrosion resistance
- thermal expansion more compatible with the steel gearbox components

The key areas that will be addressed in the composite materials program are the following:

- improving moisture protection—resin matrix
- improving fabrication techniques—metal matrix composite (MMC) and resin matrix
- improving fracture toughness—MMC and resin matrix
- improving design analysis techniques

The development program will be conducted as follows:

- material selection
- resin matrix moisture protection
- test specimen development and testing
- full-scale housing fabrication
- full-scale housing tests

The specimen testing will be followed by a full-scale housing development phase. This phase will be directed toward developing less complex fabrication techniques to reduce cost for full-scale housings. This cost reduction effort will focus on development of automated fabrication techniques.

A preform design and development effort will be undertaken for the resin matrix composite. This effort will be directed toward development of a low-cost preform that will provide a finished housing demonstrating the expected weight, stiffness, and strength benefits. The resin matrix housings will be fabricated by the compression molding technique discussed earlier.

An MMC housing fabrication study will also be undertaken. This study will be aimed at identifying the optimum MMC housing fabrication technique. The optimum technique is one in which all the expected benefits are demonstrated. Front and rear housings of each type of composite will be fabricated.

These housings will undergo a number of tests. A static deflection test will be conducted first. This test will be used to verify the expected stiffness benefits. Thermal

testing will be conducted to determine thermal expansion. These housings will be submitted to 150 hr of back-to-back gearbox endurance testing to evaluate the effects of an actual gearbox environment. During the endurance test, noise levels and oil heat rejection will be measured and compared with baseline magnesium or aluminum housings. Bore locations will be measured following endurance testing to evaluate creep effects. Test specimens will also be taken from each housing. These specimens will be subjected to strength testing.

Pitch Control and Mechanism

The conceptual design of a pitch change system developed under the SRP APET Add-On contract specifies advanced technology features that will require technology programs to establish their acceptability for future production development programs. These technology features are a capacitor signal transfer, a high-pressure rotating hydraulic power module, and a rotating electronic control module.

Capacitor Signal Transfer

There are two major areas of concern with regard to the capacitor signal transfer concept. The first is susceptibility to electromagnetic interference and vulnerability to lightning strike interference. The second is ensuring that the capacitor does not emit electromagnetic interference.

The program includes the design, fabrication, and testing of a shielded capacitor system. This system will be adaptable to an existing turboprop barrel. It includes a breadboard transmitter/receiver, and it will be subjected to an electromagnetic interference survey test for susceptibility and emission. If necessary, additional shielding systems should be designed, fabricated, and tested.

Lightning transient tests are needed to determine if the capacitor ring can withstand high-voltage transients without damage or signal quality degradation. This program will result in a control signal transfer technique that is adaptable to both current and future turboprop systems and eliminates the need for brushes and slip rings.

High-Pressure Rotating Hydraulic Power Module

A system has been devised for changing pitch on future turboprops with high-pressure hydraulic supply components. For in-line gearbox systems, the components would be mounted on the rotating portion of the system. This eliminates the need for a transfer bearing and permits removal of hydraulic pitch change hardware from the gearbox. For offset gearbox configurations, the option exists to mount the hydraulic supply components on the stationary side of the system. A concept has been developed whereby this can be achieved with a reliable, small-diameter transfer bearing and without impacting the gearbox. The use of

high-pressure hydraulics results in reduced size and weight of these components for optimized installation and maintenance. The objective of the pitch change technology program for offset gearbox configurations is to establish an acceptable gear pump that will operate at 4,750 lb/in.² with an operating life design goal of 30,000 hr.

The recommended approach is to design and build a gear pump sized for the requirements of a potential propfan system. Testing to determine torque characteristics, leakage, endurance, and susceptibility to cavitation will be conducted.

This program will establish the feasibility of a 4,750 lb/ in.² gear pump and define hardware suitable for development on advanced pitch change systems.

Rotating Electronics

The objective of this technology program is to determine both the operational characteristics and the reliability of the electronic controller (the interfacing electronics package for signal conditioning, feedback signals, and control of the electrohydraulic servomotor) when mounted and operating in a rotating field. Electronic circuits operating in a high-level "g" field such as the hub of a propeller are the technology issue.

It is first necessary to establish the environmental requirements. Concepts for the structural packaging of the electronics for survival in this environment will be developed and a breadboard differential input digital data transmitter/receiver circuit constructed for dynamic test evaluation. These tests include both whirl and vibration over the total frequency spectrum anticipated for propfanmounted hardware. This program will establish the feasibility of a rotating electronic control and define hardware suitable for development on advanced pitch change systems.

TASK XI. PRELIMINARY DESIGN OF COUNTER-ROTATION PROPFAN GEARBOX

A preliminary design study was performed to define a counter-rotation (CR), 10,000-shp class, advanced technology propfan gearbox for the APET mission. This design incorporates the requirements for a tractor arrangement of wing-mounted CR propfan propulsion system. The advanced technology propfan pitch change system reported in Task XII was integrated with the gearbox to determine the interface requirements and establish the overall envelope.

The gearbox preliminary design study consisted of the following phases:

- a configuration selection procedure to establish the design concept
- gear and bearing type selection based primarily on long life and efficiency considerations

- design of the general arrangement including the main gear train, accessory gearing, mounts and lubrication system
- design analysis to estimate bearing life, gear stresses, heat rejection to the oil and surroundings, and integrity of the supporting structure
- 5. propfan interface requirements
- modifications required for converting this tractor gearbox arrangement to a pusher configuration

The details of the CR gearbox design are described in Appendix I. A brief summary of highlights from this Appendix follows.

CR Gearbox Configuration Selection

Six candidate configurations were evaluated for the counter-rotating gearbox. The best configuration for preliminary design was determined through a series of competitions between the candidate configurations: differential planetary, compound planetary, split path parallel offset, triple com-

Table XVII. Weighting factors.

Reliability	All gearbox configurations defined equal. Part life will be designed for 30,000 hr MTBR in each case.
Efficiency	Differential planetary is slightly more efficient than compound planetary because of the compound ring gear tare losses. The parallel offset has only external meshes so it is the least efficient.
Maintenance	This was determined by major part count with planet bearings being more time consuming to replace than shaft bearings.
Acquisition cost	Estimations of production cost based on weight.
Pitch control	High and low pressure oil glands and a high speed power shaft.
Weight	Estimates of production weight based on steel gears and bearings and aluminum housings.
Technical risk	Number of technical risk items in each gearbox. Example, tapered planet bearings.
Ease of scaling	Increase in frontal area with a doubling of horsepower.
Spacial envelope	All three configurations have close to the same length; therefore, this rating is based on frontal area.
Propeller shafts	Number of brakes required to stop all shafts.

pound idler, differential epicyclic and split path planetary concepts.

The gearbox candidate configurations were first compared by a count of the major parts with the result being the elimination of the split path planetary concept. The second comparison involved the initial sizing of gears and bearings for five configurations, which resulted in the elimination of the differential epicyclic gear set. Based on a forced decision analysis of the five candidate configurations, the differential and compound planetaries were chosen for further analysis. The three planetaries were subjected to a weighted decision analysis that compared the 10 categories listed in Table XVII. Based on this comparison, shown in Table XVIII, the differential planetary gear set was selected for the preliminary design study.

CR Gearbox Gear and Bearing Type Selection

The selection of gear type refers to helical, spur, or high contact ratio spur gears. Bearing types considered were spherical or tapered roller bearings. The tapered roller bearing mounted with a helical gear for a planet system is shown in Figure 18. Tapered rollers with the tapers facing outward are required for helical gears to resist the overturning moment caused by the thrust loads at the meshes.

The single row spherical bearing is more desirable with a high contact ratio spur gear for the planet system shown schematically in Figure 19. The spherical seat allows the spur gears to locate and reduce misalignment errors.

Table XIX lists the significant comparisons between the two candidate planet forms. The candidates are practically equal but the tapered roller bearings show a greater potential for life improvement because of their lower raceway contact stress. Therefore, the preliminary design was based on a helical gear with tapered roller planet bearings in a differential planetary configuration.

Table XVIII.
Weighted decision analysis.

Category (weight factor)	Compound planetary	Differential planetary	Offset parallel
Reliability (18)	18	18	18
Efficiency (17)	16.8	17	16.7
Maintenance (13)	8.2	9.6	13
Initial cost (12)	11.5	12	9
Pitch control (12)	12	12	12
Weight (11)	10.5	11	7.3
Technical risk (6)	4.5	4.8	6
Ease of scaling (5)	5	5	4.4
Spacial envelope (4)	4	4	1.5
Propeller brakes (2)	2	1	2
	92.5	94.4	89.9

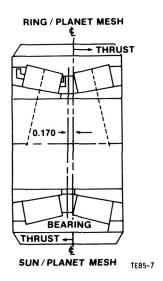


Figure 18. Tapered roller bearing and helical gearing.

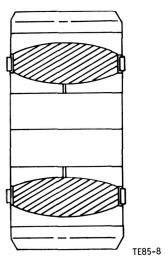


Figure 19. Single row spherical bearing and high contact ratio spur gear.

Table XIX. Planet form selection.

	Single row spherical bearings with high contact ratio spur gears	Tapered roller bearings with helical gears
Gear contact stress — lb/in.2	153,400	168,300
Gear bending stress — lb/in.2	30,600	25,500
Sliding velocity — ft/min	5,374	3,042
Temperature index rise — °F	43	64
Bearing life — hr	68,900	117,000
Raceway stress — lb/in.2	233,000	136,000

CR Gearbox General Arrangement

A general arrangement of the advanced technology CR propfan gearbox is shown in Figure 20. The gearbox main power gear train is a differential planetary gear set with four planet gears. The sun gear is driven by the input shaft, the outer output shaft is driven by the ring gear, and the inner output shaft is driven by the planet gear carrier.

Cross section of a planet gear arrangement is shown in Figure 21. The planet bearings are tapered roller bearings mounted in the indirect method that provides maximum stiffness. The ring gear floats radially with two involute splines providing the flexibility. These splines transmit thrust loads through captured snap rings.

The input shaft bearing is a steep angle tapered roller bearing. Only one bearing is located on the shaft since the other end of the shaft floats allowing the sun gear to locate itself among the planets. The steep angle, which provides a high thrust capacity bearing, supports the thrust from the helical gear.

The planet carrier is a combined shaft and structure that supports four planets equally spaced around the sun gear. The carrier also has a series of oil channels and jets that direct the fresh oil flow through the gearbox.

The planet carrier is supported by a cylindrical roller bearing and a split inner ball bearing. The front carrier is a cylindrical roller bearing with under the race lubrication.

The rear carrier bearing is a split inner ring ball bearing with under the ball lubrication supplying oil directly to the balls.

The sun gear is mounted to the input shaft on a helical spline. This helical spline transmits the thrust from the sun gear to the input shaft and keeps axial contact between the two on the thrust shoulder. Reverse thrust is held by snap rings. The spline is crowned and lubricated to provide flexibility to the sun gear.

The oil pump is a modular unit base on Gerotor type pumps. There are four separate pumps in the pump unit: two scavenge pumps, one high pressure lubrication pump and one low pressure lubrication pump. Each pump will be capable of scavenging all of the gearbox and propfan oil.

The airframe to gearbox mount points are located in the front section of the gearbox near the prop shaft bearings to reduce the effect of propfan loads on the housing. These

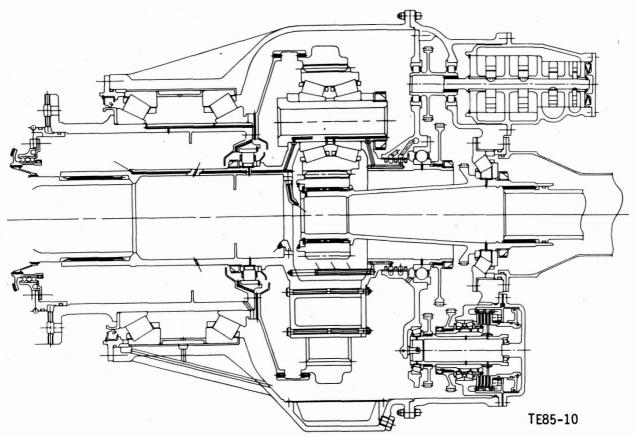


Figure 20. Counter-rotation gearbox cross section.

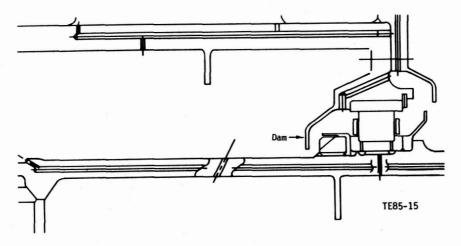


Figure 21. Planet gear arrangement.

mount points are displayed in Figure 22. Additional mount points toward the input end of the gearbox are provided for gearbox-to-engine brackets. Locating these mounts in this manner improves reliability by reducing the probability of oil leakage.

Counter-rotation Gearbox Design Results

The three power levels used in the design of the gearbox were 10,000 hp takeoff, 5,227 hp initial cruise, and 5,980 hp

cubic mean power. The 10,000 hp takeoff rating was used to size all gears.

The gears will be manufactured from an advanced gear steel such as MCR 2001 powder metal and wrought low carbon steels such as CBS 600. These steels would be VIM VAR melted, and the powders would be rapidly solidified to provide high cleanliness and fine grain structures.

The helical gears result in a low bending stress. Low bending stress results from the axial load sharing between

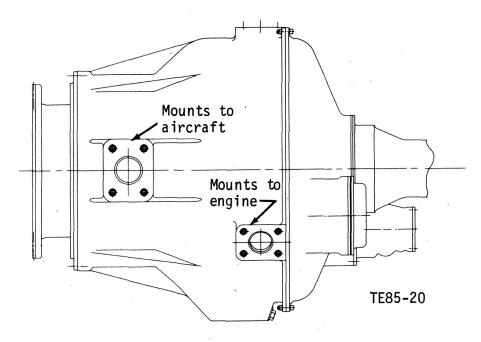


Figure 22. Counter-rotation gearbox side view.

adjacent gear teeth created by the face overlap of gear teeth. A face overlap greater than one ensures that there are always two teeth or more in contact.

The bearings for the advanced CR gearbox would be manufactured from an advanced bearing steel providing improvements in fatigue strength, corrosion resistance, fracture toughness, micro-damage tolerance, and wear/skid resistance over VIM VAR M50.

There are 13 bearings in the advanced CR gearbox. Eleven of these bearings are tapered roller bearings that have good properties for gearboxes because of their high capacity, thrust carrying ability and stability in close mount situations. There is also one cylindrical roller bearing and one split inner ring ball bearing.

Two major components in a planetary gear set structure are the external housing and the planet carrier. The external housing is made from cast aluminum, which provides better corrosion resistance than current magnesium housings. The planet carrier is designed as a steel framework. Steel provides excellent stiffness and creep resistance for good alignment of the gear teeth. It also provides good fatigue strength and wear resistance for the integral shaft and spline portions.

Interface requirements between the gearbox and the propfan have been kept to a minimum. This simplicity improves the maintainability of both the propfan and the gearbox.

The propfan assembly is mounted to the gearbox by a curvic coupling that is directly connected to the gearbox outer output shaft. The inner output shaft drives a quill shaft through an involute spline. Fresh oil is supplied to the propfan

at the inside of the outer output shaft. Centrifugal action causes the oil to flow into the rear propfan spinner where it is scavenged by pumps. The heated, used oil is returned to the inside of the inner shaft. The gearbox returns this oil to the sump where it is cooled and filtered.

Control signals are transferred to the propfan by a capacitive coupling system. Provisions were made to attach the stationary component to the gearbox housing.

Gearbox weight and acquisition price were estimated to be 548 lb and \$149,500*. The maintenance cost for the gearbox was estimated at \$1.01* per engine flight hour.

The CR gearbox was analyzed for power loss to determine both gearbox performance and cooling requirements. Considered in these calculations were gear power loss, tapered roller bearing power loss, and oil pump loss.

The results of the CR gearbox power loss analysis are shown in Figure 23. Efficiency of this gearbox arrangement is relatively high, 99.18% at cruise and 99.24% at full power.

The CR gearbox lubrication system must provide an adequate supply of clean, cooled lubricant to both the gearbox and the propfan pitch-change mechanism. The system also must be designed to minimize parasitic losses such as oil churning, windage and oil pump power requirements. To accomplish these objectives, oil flow paths were selected to provide once through lubrication to all heat generating components. Extensive use was made of shaft rotation to centrifuge oil back to the housing sump and to eliminate entrained air at the same time.

The CR gearbox lubrication system will be independent of the engine oil supply system. This will allow the use of

^{*1984} year dollars

modern, high capacity gearbox oils such as Aeroshell 555 or Exxon Turbo Oil 25.

Changes to the CR gearbox for a pusher application are needed in three areas: bearings, structure, and lubrication. The gearing system does not have to be changed since the helical forces are in the proper direction without changing the hand of the helix.

Two bearing sets need to be changed for the pusher gearbox. The offset in the planet bearing centerline, allowing the equivalent radial load to be equal, needs to be at the opposite side from the tractor planet application. The planet could be designed with no offset for flexibility, but bearing life would be sacrificed. The input shaft bearing must support thrust forces in the opposite direction from the tractor design. The input shaft tapered roller bearing could be designed with the taper in the opposite direction. A crossed roller bearing could be designed as the input shaft bearing. This would give the flexibility of either application with the reduction of life not critical to the overall system life. The prop shaft bearings and the carrier bearings do not have to be changed.

The structure should be redesigned for a pusher application. The aircraft framework will not be able to reach through the engine exhaust to get to the mounts at the small end of the gearbox. A more likely structure will have three or more struts connecting the cover of the gearbox to the aircraft frame. The engine will then be mounted to the aircraft and not to the gearbox. The drive shaft to the gearbox from the engine will have to work through a flexible coupling to accommodate the increase in misalignment.

Lubricating jets for the sun gear in the planet carrier require adjustment. The sun gear is loaded on the opposite

side. The jets need to cool this side. The oil pump will rotate in the opposite direction and will need to accommodate this. All other lubrication uses centrifugal force so modifications are not needed.

TASK XII. COUNTER-ROTATION PITCH CHANGE CONTROL AND MECHANISM

A conceptual design study was conducted under Task XII to provide an advanced flight weight pitch change control and mechanism design that is compatible with the in-line gearbox designed in Task XI. Prior to the conceptual design, a Hamilton Standard funded conceptual trade study was conducted to select the concepts for further design effort under the APET contract. The selected concepts incorporated rotary and linear hydraulic actuators with hydraulic and electrical power generated within the propfan assembly. A digital electronic control and a rotary capacitor signal transfer assembly were also incorporated in the propfan. Modular design of all pitch control components was used to reduce maintenance cost.

The concept drawings, descriptions of operation, and estimates of acquisition cost, reliability (MTBUR) and maintenance cost of the propfan pitch control are presented in this report. Blade angles, twisting moments and slew rates are provided for key operating conditions. The qualitative changes to the pitch control system required by a pusher instead of a tractor propfan installation are also provided.

Trade Studies

Prior to the APET single rotation propfan (SR) pitch control study, Hamilton Standard conducted company-funded

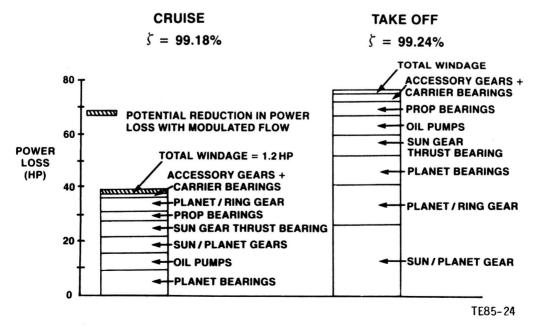


Figure 23. Counter-rotation gearbox power loss breakdown.

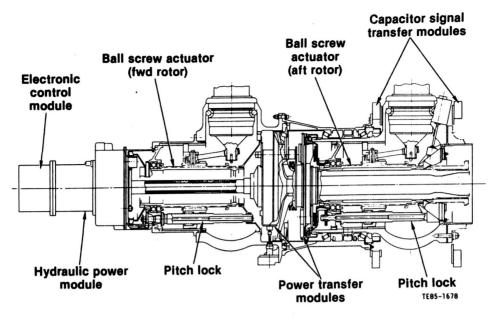


Figure 24. Rotary hydraulic pitch control concept.

pitch control trade studies to select the advanced technology concepts that were subsequently used for the APET SR propfan and counter-rotation (CR) propfan studies. The primary criterion was that the pitch control system be adaptable to any gearbox configuration with minimal impact on the gearbox design. The pitch control was divided into two parts; a power system and a control system. A comprehensive matrix of the most viable concepts was prepared for each system and each matrix was evaluated separately as described for the single-rotation gearbox in Appendix G.

Conceptual Design of Selected Concepts

The primary design objectives for the APET pitch control conceptual designs were to minimize impact on the gear-box and to maximize accessibility and maintainability. These objectives were attained by implementing a modular pitch control design, which is contained within the rotating propfan assembly. This simplifies the interface with the gearbox; improves gearbox reliability and maintenance cost; and reduces pitch change maintenance cost by providing accessible, easily maintainable modules.

This APET conceptual design study was conducted to refine the rotary and linear pitch control concepts selected from the trade studies. The study also evaluated the configurations to choose the best one for a counter-rotating propfan in a tractor installation. Three concepts were studied: rotary hydraulic, "non-modular" linear hydraulic, and rotary/linear.

Evaluation of the rotary hydraulic concept was continued, and a new non-modular linear hydraulic concept was generated for comparison. The non-modular concept incorporates a power module and electronic control mounted in each hub to reduce parts count at the possible expense of maintainability.

A variation of the rotary concept called rotary/linear was also studied. This concept incorporates a linear actuator in the forward hub of the rotor system with the objective of reducing the total number of parts.

The counter-rotating propfan is flange-mounted to the gearbox output shaft through curvic face splines at the rear face of the aft hub. This flange reacts all CR propfan mounting loads and drives the aft rotor. The forward rotor is driven by the planet carrier of the gearbox output through a splined quill shaft.

Each blade is retained in the hub with a single row angular contact ball bearing. Additional support for static blade pitch operation is provided by an external blade clamp. Blade retention bearings are lubricated by a fixed amount of oil in the hub. A lip seal at the blade root prevents external leakage. A sectional assembly drawing of the CR propfan with rotary hydraulic pitch control is shown in Figure 24. Blade trunnion arms splined to the inboard end of the blades are used to rotate the blades about the pitch axis. Links with spherical rod—end bearings connect the trunnion arms to a ball screw nut assembly in each rotor that translates to change blade pitch. Each ball screw is straddle—mounted on hub—mounted support bearings.

The ball screws are driven by a hydraulic power module that consists of drive gearing, hydraulic motors, 4-way metering valves (beta control), mechanical in place pitchlocks, pumps, oil sumps, pressure regulating and relief valves, and a generator. A bolted flange is used to mount the power module on the CR propfan forward hub-mounted housing. Blade pitch is changed toward high or low pitch by the ball screws that are rotated by drive gearing in response to pressurized oil applied to the high or low pitch side of hydraulic drive motors. An irreversible acme screw and nut acts as a pitch lock in each rotor. The pitch lock nuts are integral with the ball nuts. A small axial gap is maintained between the end of the pitch lock screw and the hub-mounted actuator bulkhead during operation. This prevents the blade pitch from decreasing by more than one degree toward low pitch if hydraulic power is inadvertently lost anywhere in the blade operating range.

The pitch lock screw is driven by a small bi-directional dc servomotor to control pitch upon command from the electronic control module. Each rotational position represents a discrete blade angle setting in the operating range. This position is measured by an RVDT that is geared to the servomotor and fed back to both the electronic control module and the nacelle-mounted EEC.

The three concepts were rated by the same evaluation parameters used in the trade studies. Rating scores for the three concepts were close but the linear concept rated slightly higher than the rotary concepts based on cost and technical risk. The rotary and rotary/linear concepts rated the same, but the rotary is favored because of the commonality of the fore and aft actuators. Common actuators reduce development cost and logistic cost of replacement parts.

The rotary concept shown in Figure 24 was selected instead of the linear concept on the basis of the following additional considerations:

- Location of the electronic control and hydraulic power module on the forward end of the propfan facilitates providing power for static check-out and mounting instrumentation for diagnostics.
- The ball screw actuator is more adaptable to utilization of propfan rotational energy to mechanically feather the blades if normal power is lost.
- Lower system pressure can be used with the rotary concept, with minimal weight penalty, since it is significantly less weight sensitive to pressure level than the linear piston concept.

TASK XIII. RESEARCH AND TECHNOLOGY PLAN FOR TASKS XI AND XII

The technology definition plan described in this section was prepared to identify those components of the counter-

rotation gearbox and pitch change system requiring more extensive development than would be encountered in a normal development program. Components identified for special attention are discussed as follows.

Counter-Rotation Gearbox Technology Plan

Preliminary analysis of the counter-rotating (CR) gearbox identifies areas of research that could have impact on the gearbox design. Two technology items, tapered roller planet bearings and steep-angle single row tapered roller thrust bearings with bidirectional load capability, are required to achieve the level of performance predicted for the CR gearbox. The technologies listed below would enhance the design but are not required for the gearbox defined as a result of Task XI.

- 1. Double helical gearing
- 2. Single row spherical planet bearings
- 3. Fluid film planet bearings
- Lubrication system methods to allow 30 min of gearbox operation without oil
- 5. Stainless steel housing
- Long life flexible splines for the gearbox/prop interface

All areas of research detailed in Appendix H are applicable to the CR gearbox as well.

Required Design Technologies

Tapered Roller Planet Bearings

Background. The tapered roller bearing was selected for the planet bearing in this study because of its high capacity and ability to react to the overturning moment created by the helical gears. Although tapered roller bearings have been operated at the speeds required in this design, a development effort would be required to ensure satisfactory operation in a planet bearing environment. The planet bearing requires opposite rotation of the inner and outer races in a high "g" field created by rotation of the planet carrier. There is no experimental data available for this application.

Recommended Program. A subcontract would be arranged with a bearing manufacturer who would perform analyses according to specifications provided by Allison. Inhouse computer studies would augment work being done at the bearing supplier. At the completion of the design, fabrication of the planet bearings would begin. Testing of the bearings would best be accomplished in the CR gearbox since at present there is no test rig available to test this bearing under the gearbox loads. If time and funds are available, a planet bearing test rig would be constructed to simulate planet bearing operation. Parametric tests would determine operating temperatures, heat generation, and integrity of design.

Steep Angle, Single Row Tapered Roller Thrust Bearings With Bidirectional Load Capability

Background. Tapered roller bearings can carry large thrust loads yet require a minimum amount of space. In situa-

tions where thrust load can reverse direction, two tapered roller bearings are required. The CR gearbox input shaft bearing must carry a significant thrust load, normally, in one direction only. Under some conditions, the thrust can reverse direction but the magnitude of the reversed load is low. Preliminary design of this bearing indicates that it is possible to use only one tapered roller bearing with an additional thrust rib to handle the reverse thrust loading. It has not been proved, however, that this bearing will function in practice since under maximum thrust in the normal direction, the roller retaining rib must operate at maximum allowable bending stress levels. The concept of using a cup rib to absorb the light reversed thrust is also unproven. Cylindrical roller bearings are currently being designed to carry moderate thrust loads; the same technology should apply to this bearing.

Recommended Program. To verify the bearing performance, it would be subjected to conditions that simulate its actual operating environment. A similar test will soon be conducted at Timken for an Allison engine application. Since Timken can readily perform this type of test, a subcontract would be arranged so that the CR gearbox sun gear thrust bearing design would be optimized to both Allison's and Timken's satisfaction and then fabricated and tested at Timken. The tests would determine operating temperatures, power loss and integrity of the design.

Counter-Rotation Pitch Control and Mechanism Technology Plan

The conceptual design of a pitch change mechanism developed under the counter-rotation APET Add-On contract identified advanced technology features that will require technology programs to establish their acceptability for future production development programs. These technology features are a capacitor signal transfer, a high pressure rotating hydraulic power module, and a rotating electronic control module.

Capacitor Signal Transfer

There are two major areas of concern with regard to the capacitor signal transfer concept. First, is the susceptibility to electromagnetic interference (EMI), and vulnerability to lightning strike interference. Second, the concern is to ensure that the capacitor does not emit electromagnetic interference.

The program will include the design, fabrication and testing of a shielded capacitor system. This system, which will be adaptable to an existing propeller barrel, will include a breadboard transmitter/receiver and will be subjected to an EMI survey test for susceptibility and emission. If necessary, additional shielding systems will be concepted, fabricated and tested.

Lightning transient tests will be conducted to determine if the capacitor ring can withstand high voltage transients without damage. This program will result in a control signal transfer technique that is adaptable to both current and future turboprop systems and eliminate the need for brushes and slip rings.

High Pressure Hydraulic Power Module

A system has been devised for changing pitch on future turboprops with high pressure hydraulic supply components. For in-line gearbox systems, the components would be mounted on the rotating portion of the system. This eliminates the need for a transfer bearing and permits removal of hydraulic pitch change hardware from the gearbox. For offset gearbox configurations, the option exists to mount the hydraulic supply components on the stationary side of the system. A concept has been developed whereby this can be achieved with a reliable, small diameter transfer bearing and without impacting the gearbox. The use of high pressure hydraulics results in reduced size and weight of these components for optimized installation and maintenance. The objective of the pitch change technology program for in-line gearbox configurations is to establish an acceptable gear pump and gear motor that will operate at 4750 lb/in.2 in a rotating environment, with an operating life design goal of 30,000 hr.

The recommended approach is to design and build both a gear pump and gear motor sized for the requirements of a potential propfan system. Testing to determine torque characteristics, leakage, endurance and susceptibility to cavitation will be conducted. Gear motor testing will also include measurement of break out $\Delta\!P$ and assessment of low speed characteristics due to the requirements for low friction.

This program will establish the feasibility of a 4750 lb/in.² gear pump and gear motor, and will define hardware which is suitable for development on advanced pitch change systems.

Rotating Electronics

The objective of this technology program will be to determine both the operational characteristics and the survivability of the electronic controller (the interfacing electronics package for signal conditioning, feedback signals, and control of the electro-hydraulic servomotor), when mounted and operating in a rotating field. Concerns have been expressed regarding the ability of the electronic circuits to operate and survive in a high level "g" field.

It is first necessary to establish the environmental requirements. Concepts for the structural packaging of the electronics for survival in this environment will be developed and a breadboard differential input digital data transmitter/receiver circuit will be constructed for dynamic test evaluation. These tests will include both whirl tests and vibration tests over the total frequency spectrum anticipated for

propfan mounted hardware. This program will establish the feasibility of a rotating electronic control and will define hard-

ware that is suitable for development for advanced pitch change systems.

IV. CONCLUSIONS

This study was conducted to provide identification of candidiate engines applicable to early 1990s aircraft utilizing the propfan and to formulate an engine readiness plan for critical engine technologies. These objectives were accomplished and conclusions regarding the study results are as follows:

- 1. Engine Design. The engine cycle pressure ratio is the dominant factor for saving fuel. It should be as high as practical. For engines of 10,000 shp, values of 30:1 to 35:1 are recommended. Engines of 15,000 shp or larger should have higher goals of 35:1 to 40:1. Maximum turbine inlet temperatures of 2500°F are adequate to achieve the fuel savings potential of the high pressure ratios without imposing overriding operational and cost penalties. Three-spool engines with
- dual-spool compressors plus a free power turbine are recommended.
- 2. Key Technologies Issues. Five engine components require research and development attention to prepare for engine readiness: inlet, compressors, turbines, gearbox, and controls. The compressors, turbines, and gearbox development are the responsibility of the engine company. The inlet and controls are joint responsibilities of the engine, propfan, and airframe companies. Because of the high risk relative to both technology and return-on-investment, government sponsorship of this component development is needed. Without the component research and development, it is unlikely that the propfan will power aircraft in the early 1990s.

REFERENCES

- D. F. Sargisson, "Advanced Propfan Engine Technology (APET) Final Report," General Electric Company, NASA CR-168113, November 1983.
- C. N. Reynolds, "Advanced Prop-fan Engine Technology Definition Study Final Report," Pratt & Whitney, United Technologies Corporation, PWA5869-26, February 1983.
- J. C. Muehlbauer et al, "Turboprop Cargo Aircraft Systems Study," Lockheed-Georgia Company, NASA CR-165813, November 1981.
- 4. "Propfan Data Package: Maintenance," Hamilton Standard, United Technologies, SP04A82, May 1982.

- "Propfan Data Package: Performance, Near-Field Noise, Far-Field Noise," Hamilton Standard, United Technologies, SP07A82, May 1982.
- 6. "Propfan Data Package: Weights," Hamilton Standard, United Technologies, SP06A82, May 1982.
- R. E. Herrold, "Instructions for Use of a Program, in the Form of an Object Deck of Digital Computer Cards to Calculate Steady-State Performance of the Allison Model PD436-10 and PD436-11 Turboprop Engines," EDR 11321, 15 February 1983.
- 8. "Data Package for PD436-10 and -11 Engines," EDR 11375A, 25 March 1983.

APPENDIX A

TASK I. SELECTION OF EVALUATION PROCEDURES AND ASSUMPTIONS

TABLE OF CONTENTS

Title Charles and the second s	Page
Introduction	A-1
Procedures and Assumptions	A-2
Fuel Price	A-2
Mission Analysis Procedure	
Aircraft/Mission Requirements	A-4
Reference Aircraft Characteristics	A-6
Engine Installation Factors	A-7
Direct Operating Cost Model	A-8
Propulsion System Trade Factors	A-12
Environmental Constraints	A-12
Acoustic Assumptions	A-14
Gearbox Configurations	A-17
Reference Turboprop Engine PD436-1	A-17
Reference Turbofan Engine	A-18
References and Bibliography	A-29

LIST OF ILLUSTRATIONS

igure	Title	Page
	APET study fuel price forecast	. A-3
A-2	Mission analysis procedure	
A-3	Domestic-local service stage length preference	. A-5
A-4	APET design mission profile	. A-5
A-5	Reference aircraft layout	. A-6
	Passenger seating arrangement	
A-7	Engine scaling relationships	. A-8
A-8	Propfan nacelle size and weight equations	
A-9	Turbofan nacelle size and weight equations	
A-10	FAR part 36 takeoff noise limits for transport-category aircraft	. A-15
	FAR part 36 sideline noise limits for transport-category aircraft	
	FAR part 36 approach noise limits for transport-category aircraft	
	Reference turboprop engine	
A-14	Reference turbofan engine	A-23

PRECEDING PAGE BLANK NOT FILMED

LIST OF TABLES

Table	Title	Page
A-I	Adjusted Air Force estimates in 1980 dollars	_
A-II	Adjusted Air Force estimates in future year dollars	A-2
A-III	Oil company forecasts of crude-oil demand for the non-Communist world based on annual 2.5 to 3.5% GNP	
	growth	A-3
A-IV	Kearney's data extended to 1995	A-3
A-V	Aircraft/mission requirements	
A-VI	Design mission cruise velocity and altitude selection	A-5
A-VII	Aircraft data sources	A-6
A-VIII	Reference aircraft parameters	
A-IX	Horizontal and vertical tail parameters	
A-X	Reference aircraft weight breakdown	A-7
A-XI	Propulsion system installation factors	
A-XII	Cost methodology for APET cost model	
A-XIII	Turbofan engine cost data	A-11
A-XIV	Direct engine maintenance hours	
A-XV	Engine maintenance man-hour comparisons	
A-XVI	Recommended design standards for APET	A-13
A-XVII	Exhaust emissions standards for aircraft gas turbine engines	
A-XVIII	Comparison of ICAO standards and goals (subsonic turbofan and turbojet)	A-14
A-XIX	Engine noise sources and prediction methods used	A-17
A-XX	Gearbox design criteria	A-17
A-XXI	Turboprop engine PD436-1B weight	A-18
A-XXII	Performance of reference turboprop Engine PD436-1B on standard day	A-19
A-XXIII	Performance of reference turboprop Engine PD43-1B on 86°F day	
A-XXIV	Reference turbofan engine performance summary	A-25
۷XX-۸	Performance of reference turbofan engine on standard day	A-25
	Performance of reference turbofan engine on 86°F day	

INTRODUCTION

Task I of the APET study involved defining the procedures and assumptions to be used in performing the technical work of the contract. The evaluation procedures and assumptions described herein represent the results of Task I as updated to show the actual procedures and assumptions used.

The procedures and assumptions were defined by Allison with NASA inputs in several areas and with assistance from Hamilton Standard and Douglas Aircraft Company. NASA provided guidance relative to fuel price in that the economic evaluation is made at \$1.50/gal and in 1981 year dollars. Other assumptions guided by NASA were those dealing with installation aerodynamics and engine inlet recovery. Also, it was assumed that the level of turbofan cove engine

technology set forth as goals in the Energy Efficient Engine (EEE) program is applicable to the APET turboprop engine in sizes as small as 15,000 hp with no loss of component performance. Thus, the APET engines are EEE-plus technology.

The propfan data used in the analyses were provided by Hamilton Standard, which also reviewed the propfan selected for the propulsion system integration. Douglas Aircraft Company provided guidance relative to the reference airplane, engine installation, and direct operating cost (DOC) results. Both companies were present at the interim oral briefing 20 July 1982 at NASA Lewis Research Center, and adjustments were made in both the propfan data and reference airplane as a result of their inputs.

PROCEDURES AND ASSUMPTIONS

The evaluation procedures and assumptions used in the APET study are described in detail in this section. The procedures and assumptions are first stated, and then supporting information is presented concerning the source used on applicable background requirements.

FUEL PRICE

The fuel price used in the APET study is \$1.50/gal. A description of the basis for selecting this value follows. Considerable effort was directed toward fuel price forecasting following OPEC's 14% increase in December 1978. This increase spread over the first three quarters of 1979, which was the beginning of a period of extremely rapid fuel price increases continuing to the present time.

As reported by Mr. W. Swihart (Ref 1)* of Boeing, the late 1977 forecast of 1987 fuel at 84.5*/gal represented 45.5% of DOC. Similar late 1979 forecasts of 1987 fuel ranged from 161*/gal to 242*/gal, representing 61.2% and 70.3% DOC. Boeing predicted a leveling off of yearly price increases during 1981 that would continue through 1987.

Air Force cost estimates (Ref 2), based on midterm energy supply and demand forecasts for 1985 to 1995, using the middle scenario given for the industrial sector in Annual Report to Congress 1979, Volume 3, DOE/EIA 0173 (79/3) and adjusting the values to 1980 dollars using the Consumer Price Index 152/132.8 in International Financial Statistics, yield the data shown in Table A-I.

Projecting 3.7% real growth in price for 8% inflation from 1980 yields the data shown in Table A-II. Later forecasts, such as the mid-1981 Kearney Report (Ref 3), predict (on the high end of the range) 228*/gal for 1987 fuel assuming 8% inflation and 5% real growth in price. On the low end, Kearney forecasts 203*/gal based on 3% real price growth and 8% inflation.

The 27 January 1982 Wall Street Journal quoted Mr. Tom Meloe, Chief Economist of Texaco, "We aren't looking for any increase in oil demand in the industrialized world for the long term. A tremendous restructuring of the oil-consuming part of the business has occurred." Also reported in this article was scaled back oil demand. Averaging figures supplied by Exxon Corp., Texaco Inc., Standard Oil of California, British Petroleum Co., and Royal Dutch/Shell Co. (see Table A-III) yields a rise from 47 million barrels/day in 1981 to 50.7 million barrels/day in 1985 and to 52.5 million barrels/day in 1990. This is an average demand growth rate of 1.9% between 1981 and 1985 and 0.7%/yr from 1985 to 1990. According to the Journal, oil company officials and independent energy experts are interpreting these demand forecasts to mean more stable oil prices in the 1980s.

A 3.0% real growth of fuel price and 8.0% inflation rate are recommended for the APET study. These factors result in a projected fuel price in 1993 of \$3.81/gal as shown in Table A-IV. Deflating this price to 1981 economics yields approximately \$1.50 per gallon. These values are selected to be consistent with the Boeing trend curves and Kearney's lower

Table A-I.

Adjusted Air Force estimates in 1980 dollars.

Type of fuel	FY 1975	FY 1980	FY 1985	FY 1990	FY 1995	FY 2000
JP-4 1980 \$/gal	0.37	1.04	1.25	1.50	1.80	2.16
JP-5 1980 \$/gal	0.35	1.11	1.33	1.59	1.91	2.29

Table A-II.

Adjusted Air Force estimates in future year dollars.

Type of fuel	FY 1980	FY 1985	FY 1987	FY 1990	FY 1995	FY 2000
JP-4 \$/gal	1.04	1.81	2.26	3.14	5.47	9.51
JP-5 \$/gal	1.11	1.93	2.41	3.36	5.84	10.15

Future price = $(1980 \text{ price}) [1 + (IR + RG)]^N$ where: IR = inflation rate (assumes 8%)

RG =real growth (assumes 3.7%)

N = number years

Future price = 1980 price $(1.117)^N$

^{*}The references in Appendix A are listed at the end of this appendix.

Table A-III.

Oil company forecasts of crude-oil demand for the non-Communist world based on annual 2.5 to 3.5% GNP growth.

(From Wall Street Journal, 27 January 1982)

Company	Future year	Estimate Jan 1982— <u>millions barrels/day</u>	Estimate 1979— millions barrels/day
Texaco	1985	52	64.3
	1990	54-55	71.7
Standard Oil of California	1985	49.3	63.5
	1990	51.3	67.8
British Petroleum	1985	50-51	NA*
	1990	51	51-55
Shell	1985	48	53
	1990	50-52	NA
Exxon	1985	54	56
	1990	55	60

^{*}Not applicable

Table A-IV.

Kearney's Data Extended to 1995.

High Price Calculation

Future Price = Base Price $[1 + (IR + RG)]^N$

Base Price = 109 /gal in 1981

IR = 8% inflation rate

RG = 5% real growth in price

Year	<u>N</u>	Future price—*/gal
1991	10	370
1992	11	418
1993	12	472
1994	13	534
1995	14	603

Lower Side Calculation

ın -	- 070
RC.	- 3%

/0		
Year	<u>N</u>	Future price—*/gal
1991	10	310
1992	11	344
1993	12	381
1994	13	423
1995	14	469

forecast. The lower value of real growth in fuel price is selected as a result of the assumption that increased demands over those foreseen by the current oil company survey will be counterbalanced by alternative energy supplies, thereby maintaining more modest demands of crude oil. These references are shown in Figure A-1.

MISSION ANALYSIS PROCEDURE

The APET cycle selection and candidate engine evaluation required the definition of reference aircraft characteristics, mission requirements, engine installation factors, and an

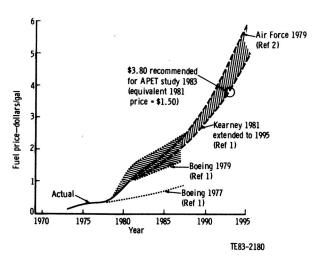


Figure A-1. APET study fuel price forecast.

economic model for use in performance and cost comparisons. The above items were integrated into the mission analysis computer program used in the APET definition study. The logic sequence of this program is illustrated in the block diagram shown in Figure A-2. There are two major steps in this procedure:

- sizing or scaling the airframe/engine combination to meet fixed design mission requirements, i.e., rubberized airframe and engines
- 2. evaluation of the sized airframe/engine in a typical or revenue mission requirement

Input parameters, major calculation functions, and output parameters are generalized in the block diagram. Mission requirements, aircraft, and engine data are used in the engine/airframe sizing calculations to determine the engine/aircraft size combination that will meet the specified mission requirements. The resultant aircraft, mission fuel, and time data, plus input economic criteria, are then used in the cost routine to calculate the required cost parameters.

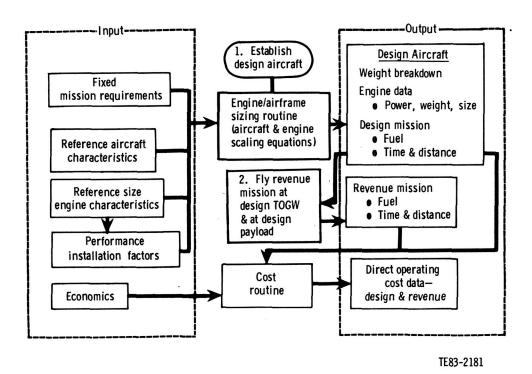


Figure A-2. Mission analysis procedure.

AIRCRAFT/MISSION REQUIREMENTS

The aircraft type and size selected for the APET studies are based on short-haul commercial transport requirements and aircraft technologies consistent with a 1992 in-service date. The aircraft/mission requirements are summarized in Table A-V.

Table A-V.
Aircraft/mission requirements.

	Design mission	Revenue mission
Takeoff gross weight (TOGW)	Design	Design
Payload		
Passengers	120	120
Cargo—lb	4,000	4,000
Range—nmi	1,000	300
Cruise velocity—M _N	0.72	0.72
Cruise altitude—ft	32,000	Selected for
		minimum DOC

An upper size limit of 120 passengers, coach seating only, was selected. A typical cargo capability of 4000 lb was assumed for the aircraft to provide some flexibility with respect to cargo utilization, package delivery, and mail service.

Since the design mission determines the aircraft fuel

load it is important to select mission requirements consistent with the vehicle's revenue capacity, i.e., 120 passengers. This size aircraft falls into the area of short-haul, at the lower end of the domestic local service category. Current aircraft in this approximate passenger size (BAC-111, DC-9-30, and 737-200) have design ranges of 1500 nmi or greater and do not fit the short-haul trends that have become prominent since deregulation occurred. Therefore, Allison selected a shorter design range of 1000 nmi to bias the design toward shorter mission legs and still be long enough to provide operator flexibility.

The APET operating scenario presumes that the aircraft will not be operated the majority of the time on its design mission. This fact is born out by Civil Aeronautics Board (CAB) statistics for all classes of commercial aircraft. Therefore, it was necessary to estimate a realistic service use or revenue mission for the airplane so that reasonable DOC values would be compared. The basis for selection of the revenue mission was a compilation of stage lengths, by distance groups, for domestic local service airliners obtained by the Civil Aeronautics Board (CAB Form 41) during calendar year 1980. The relationship of percent departures versus stage length group is shown in Figure A-3. Note that the vast majority of departures occurred in the 200-300 nmi range. A revenue mission length for the comparison of system direct operating cost was therefore selected at 300 nmi.

The cruise Mach number was selected to be consistent with previous airframe company studies having approxi-

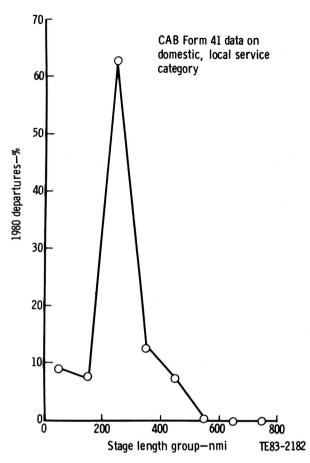


Figure A-3. Domestic-local service stage length preference.

mately the same passenger size and range requirements. Table A-VI is a tabulation of airframe company inputs and reports in the open literature. The cruise altitude selection was based on a 30,000 ft minimum requirement for traffic and weather considerations. The design mission Mach number of 0.72 and altitude of 32,000 ft were selected. For the typical (revenue) mission, the cruise Mach number was the design value of 0.72 and the cruise altitude was optimized to obtain minimum DOC. The aircraft takeoff gross weight (TOGW) for the revenue mission was assumed to be the design gross weight, i.e., design fuel load and passenger/cargo payload.

Table A-VI.

Design mission cruise velocity and altitude selection.

Aircraft company	No. of passengers	Design <u>Mach</u>	Altitude—ft
Α	100	0.7	35,000
В	120	0.72	Best DOC
С	100	0.70	31,000
Allison	120	0.72	32,000

The resultant design mission profile is shown in Figure A-4. This mission is consistent with ATC procedures, aircraft capability, and reserve definition sufficient for the short-haul transport concept.

The engine sizing criteria used in this study were selected to provide the following capabilities:

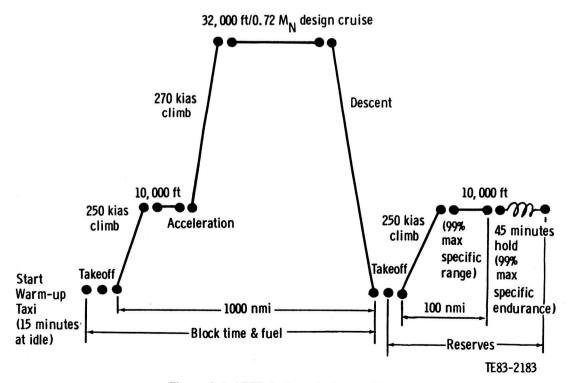


Figure A-4. APET design mission profile.

- 1. takeoff field length of 5500 ft (35 ft obstacle height) at sea level 86°F day, takeoff power and at design **TOGW**
- 2. specified design initial cruise capability of 300 ft/min rate of climb at 0.72 Mach number, 32,000 ft with initial cruise weight and at maximum cruise power
- 3. one engine inoperative (OEI) capability of 100 ft/min rate of climb at 15,000 ft with climb power and at TOGW less 20% of design fuel load

Engine sizing calculation procedures will iteratively select the one requirement out of the three listed that results in the largest engine size.

REFERENCE AIRCRAFT CHARACTERISTICS

The aircraft configuration that was developed to satisfy the previously presented aircraft/mission requirements is a "generic" transport derived from several airframe company turbofan/propfan aircraft studies. The references used in this effort are listed in Table A-VII. The aircraft is intended to be an advanced technology design incorporating features identified as acceptable for design application in 1986 (1992 initial service date). This will provide for the inclusion of a supercritical wing, advanced aluminum material for wing/fuselage, advanced composite materials for empennage, control surfaces, and secondary structures, plus active controls for the wing and tail.

Table A-VII. Aircraft data sources.

Turboprop Cargo Aircraft System Study Twin turboprop

NASA CR-165813 (Ref 6)

 $(0.75 M_N)$ Cargo transport

Advanced Turboprop Program Summary

Twin turboprop $(0.70 M_N)$

(Viewgraph Presentation) Douglas Aircraft Company (Ref 11)

100 passenger aircraft

Parametric Study of Transport Aircraft System Cost and Weight NASA CR-151970

Generalized data 100→120 passenger

Science Applications, Inc./ Douglas Aircraft Co. (Ref 12) aircraft

Lockheed Model No. 188 Specification Report No. 10637

Four engine turboprop $(0.58 M_N)$ 85 passenger aircraft

Lockheed-California Company (Ref 13)

The aircraft was held to a conventional configuration with respect to engine placement and wing and tail arrangement. This provided a large data base from which to scale and/or adjust weights and dimensional data. It was kept in mind that the objective of the study was to evaluate propulsion systems-not to design new and innovative aircraft. A general layout of the reference aircraft with major dimensions

is shown in Figure A-5. It is a low-wing design featuring twin,

wing mounted engines and a "T" tail. For illustration purposes, Figure A-5 shows both propfan and turbofan engine mounting arrangements. However, the reference aircraft was developed with a current technology turboprop study engine coupled with a Hamilton Standard advanced technology propfan propeller.

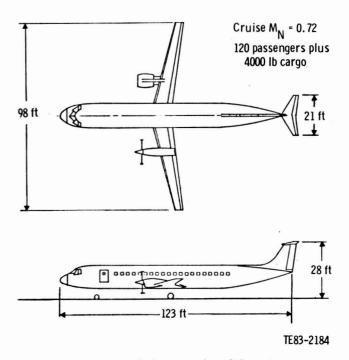


Figure A-5. Reference aircraft layout.

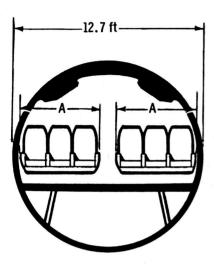
The cabin arrangement seats 120 persons (all economy class), six-abreast, with a single center aisle, as shown in Figure A-6. The seating arrangement was selected to be spacious with respect to current short-to-medium range passenger aircraft. This configuration establishes the fuselage diameter as shown in Figure A-6. Consideration of fuselage acoustic treatment weight penalty for the propfan was estimated from a correlation of acoustic panel weight to sound power level from the Douglas Aircraft Company's NASA CR-166138 (Ref 4) with sound pressure level determined by estimates contained in Hamilton Standard report SPO7A82 (Ref 5).

The design parameters selected for the APET reference aircraft are summarized in Tables A-VIII and A-IX. These values are nominal as obtained with the baseline turboprop engine. Allison has not attempted to design an aircraft; the only purpose was to obtain "generic" aircraft characteristics that would allow preliminary evaluation of engine configurations within the context of the APET study effort. However, these characteristics do compare favorably with current configurations under study by several airframe companies.

The base drag polar, excluding nacelle and pylon drag, was estimated for the reference aircraft. The NASA study manager stipulated no penalty for propfan-induced wing scrubbing or swirl drag and that no wing/nacelle interference Six-abreast configuration with

- 17.9-in, seat width
- 19.0-in, aisle width

Provides 120 passenger seats at 38-in. pitch



Dimension A = 61.7 in.

TE83-2185

Reference: C9B passenger seat arrangement NAVAIR 01-C9BAAA-1

Figure A-6. Passenger seating arrangement.

Table A-VIII. Reference aircraft parameters.

TOGW	98,600 lb
Fuselage Diameter Length L/D ratio	12.7 ft 123.3 ft 9.7
Wing Wing area Aspect ratio Sweep at quarter chord Avg thickness ratio Taper ratio	800 ft ² (W/S = 123 lb/ft ²) 12.0 13.5 deg 14% 0.40
Propulsion (Preliminary Study Engine) Ratings of SLS, std day Prop diameter	8600 shp 11.6 ft

drag should be considered. Likewise, the beneficial effects of swirl recovery by the wing were not accounted for. The resultant base polar was adjusted relative to changes in wing aerodynamic reference area and the fuselage wetted area brought

Table A-IX.

Horizontal and vertical tail parameters.

	Horizontal tail	Vertical tail
Area—ft ²	98	132
Aspect ratio	4.5	1.2
Sweep at c/4—deg	18.5	30
Avg thickness ratio—%	10	10
Taper ratio	0.35	0.80
Lever arm—ft	70	66
Volume coefficient	0.99	0.11

about by propulsion system influences developed in the air-frame/engine sizing procedure. Appropriate nacelle (turbofan or propfan) drag increments were then added to obtain total aircraft drag. The procedure used to determine nacelle drag increments will be presented under the heading "Engine Installation Factors" in this appendix. An evaluation of the aircraft aerodynamic characteristics obtained from the turbofan and propfan mission analysis program is presented in Appendix D under the heading "Aircraft/Engine Results."

In Table A-X a weight breakdown for the reference aircraft is summarized for each major weight grouping in both pounds and as a fraction of the design takeoff gross weight. As with the aircraft design parameters, these values are intended to be representative of an advanced technology short-haul transport aircraft.

Table A-X.
Reference aircraft weight breakdown.

	Weight—lb	Weight fraction (wt/TOGW)
Propulsion group	12,800	0.13
Structures group	25,900	0.26
Fixed equipment	16,400	0.17
Operating items	3,200	0.03
Operating empty weight	58,300	0.59
Payload	28,000	0.28
Fuel	12,300	0.13
TOGW	98,600	1.00

ENGINE INSTALLATION FACTORS

Cycle studies result in engine performance definitions sufficient to compare bare engine performance. However, use of the engines in an aircraft demands power extraction and installation loss definition for proper simulation of the system performance. For the APET study, propulsion system installation factors involved installation of the engines and propeller (propfan) performance. The factors used and/or the source of data for these items is presented in Table A-XI.

Engine weights, i.e., power section plus gearbox weights, were estimated by Allison using material index factors and in-house component weight correlations based on experience. The assumed propfan design parameters selected for this study are shown in Table A-XI. The Hamilton Standard reports used to obtain propeller efficiencies and weight data consistent with the selected propeller design are referenced.

Table A-XI.

Propulsion system installation factors.

Engine installation	Turbofan	Propfan
Inlet recovery (PT2/PT0)	1.00	1.00
Customer power extraction—shp/engine	100	100
Customer bleed extraction	None	None
Gearbox power loss—%	NA	1
Weight	Allison-es	timated

Propeller definition (single rotation propfan)

and controls)

Design parameters

No. blades/tip speed
Power loading—shp/prop dia²

Efficiencies

Hamilton Standard Report
SPO7A82 (Ref 5)
(Computer Deck
F204 A00)

Weight (blades, spinner,
Hamilton Standard Report

In addition to these factors, engine scaling relationships used in the study to adjust from reference size engine dimensions and weight values to the size required to meet design mission requirements are briefly summarized in Figure A-7.

SPO6A82 (Ref 14)

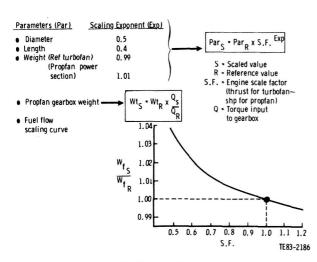


Figure A-7. Engine scaling relationships.

Nacelle size and weight equations used for the propfan engine installations are shown in Figure A-8. The relationship used to estimate propfan nacelle drag increments (ΔC_D) is as follows:

$$\Delta C_{D_{nac}} = \frac{0.067 \times A_F}{S_{wing}}$$
 (Ref 6)
$$\Delta C_{D_{nac}} = \frac{0.0064 \times A_w}{S_{wing}}$$
 $A_f \rightarrow A_w$ modification

where

 A_f = projected frontal area of nacelle—ft² A_w = wetted area of nacelle—ft²

The nacelle size and weight equations used for the reference turbofan engine installation are shown in Figure A-9. The relationships used to determine the turbofan nacelle drag and the estimated drag penalty for the turbofan nacelle pylon are as follows:

$$\Delta C_{D_{nac}} = \frac{C_D \pi \times A_w}{S_{wing}} = \frac{0.0048 \times A_w}{S_{wing}}$$

where

 $C_{D\pi}$ is obtained from plot of $C_{D\pi}$ versus nacelle length to diameter ratios (Ref 4)

 $A_w =$ wetted area of nacelle—ft²

 $\Delta C_{D_{pylon}} = constant (Ref 5) = 0.00012$

DIRECT OPERATING COST MODEL

Operating costs fall into two categories: direct and indirect cost. Indirect costs are dependent upon the particular service the operator is offering, although, in certain particulars, the indirect costs may also be dependent upon and related to the airplane's characteristics. With the exception of maintenance burden, this method deals with only the direct operating costs. These costs are calculated as a cost per airplane nautical mile (C_{am}); however, they can be converted as follows:

cost/seat nmi = $C_{am} \div$ number of passenger seats cost/block hour = $C_{am} \times V_b$ cost/flight hour = $C_{am} \times V_b \times t_b/t_f$

where

$$t_b$$
 = block time—hr
 t_f = flight time = (T_b - T_{gm})—hr
 v_b = block speed—knots

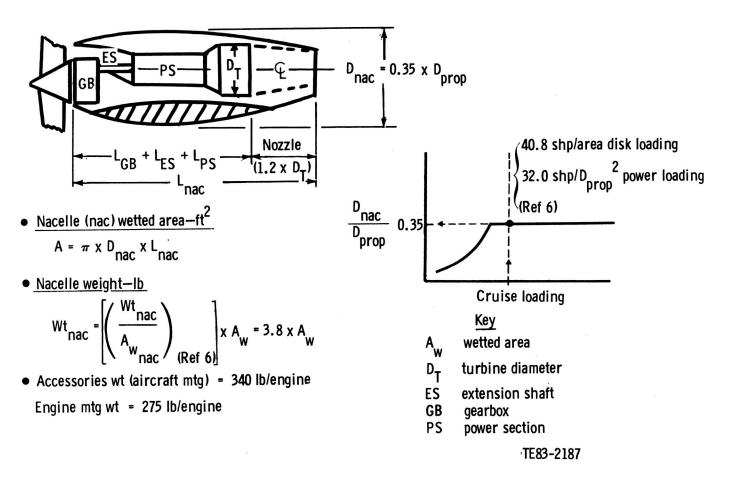


Figure A-8. Propfan nacelle size and weight equations.

For uniformity of computation of block speed, the following formula based upon a zero wind component was used:

$$V_b = D/(T_{am} + T_{cl} + T_d + T_{cr})$$

where

V_b = block speed in knots

D = mission range or stage length in nautical miles

T_{gm} = ground maneuver time in hours including one minute for takeoff

T_{cl} = time to climb including acceleration from takeoff speed to climb speed

T_d = time to descend including deceleration to normal approach speed

T_{cr} = time at cruise altitude

Notes:

 Climb and descent rates were such that 300 ft/min cabin pressurization rate of change was not exceeded. In the transition from cruise to descent the cabin floor angle was not changed by more than 4 deg nose down.

- 2. The true air speed used was the average speed attained during the cruising portion of the flight.
- Zero wind and standard temperature was used for all performance.

Block fuel was computed from the following formula:

$$F_b = F_{am} + F_{cl} + F_{cr} + F_d$$

where

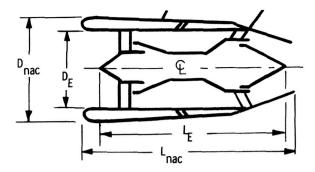
F_b = block fuel in lb

F_{gm} = ground maneuver fuel based on fuel required to taxi at ground idle for the ground maneuver time of 15 minutes plus one minute at takeoff power

F_{cl} = fuel to climb to cruise altitude including that required for acceleration to climb speed

F_{cr} = fuel consumed at cruise

F_d = fuel required to descend including deceleration to normal approach speed



Nacelle wetted area—ft²

$$A_{w} = \pi \times D_{nac} \times L_{nac}$$
where:
$$D_{nac} = D_{E} + 12$$

$$L_{nac} = 1.3 \times L_{E}$$

Nacelle weight—lb

Wt_{nac} =
$$\left[\frac{W_{nac}}{A_{w}} \right]_{nac}$$
 Allison value $x A_{w} = 3.3 \times A_{w}$

- Accessories wt (aircraft mtg) = 360 lb/engine
- •Engine mtg wt = 275 lb/engine

TE83-2188

Figure A-9. Turbofan nacelle size and weight equations.

APET DOC Model

The direct operating cost model used in the APET study is essentially the Boeing Aircraft Company 1979 cost model with factors to adjust from 1979 to 1981 year dollars. Instructions pertaining to this model were transmitted to Allison via 21 April 1982 letter from the APET Contract Manager (Attachment I). The cost methodology and/or economic "ground rules" used in the APET cost model are summarized in Table A-XII.

Note that the propfan propeller original equipment manufacturer (OEM) and maintenance cost were obtained from Hamilton Standard references. Also, the fuel cost for this study was specified by the APET Contract Manager along with a requirement to investigate consequences of $\pm \$0.50$ changes in the nominal fuel cost value.

In addition to the cost items listed in Table A-XII, three cost elements (engine cost, aircraft less engine cost, and direct engine maintenance cost) plus an estimated aircraft utilization rate were developed for the cost model by Allison.

Table A-XII.

Cost methodology for APET cost model.

Cost Item	Source of cost method
Insurance Airframe maintenance Depreciation Flight crew cost	Boeing DOC formulas for Domestic Trunk and Local Service (1979) updated to 1981 economics
Insurance rate	1/2% of aircraft acquisition cost per year*
Spares	Airframe—6% of airframe and nacelle acquisition cost* Engine—30% of engine acquisition cost*
Maintenance burden	220% •
Labor rate	\$13.75/maintenance man-hour*
Depreciation schedule	15 years to 10% residual value*
Propfan OEM cost	Hamilton Standard data contained in NASA CR-165813 (Ref 6)
Propfan maintenance cost	Hamilton Standard Report SPO4A82 (Ref 8)
Fuel cost	\$1.50/U.S. gallon

Propfan Engine Cost

*Boeing cost model

Original equipment manufacturer costs for the propfan engine power section plus gearbox (PS + GB) in this study were developed using the Allison material index factor methods applied to component finished weights. These PS + GB costs were developed for the reference size engine and then scaled to the appropriate size required by the aircraft/engine combination via the following cost scaling equation:

$$Cost_s = Cost_r (SHP_s/SHP_r)^{0.8}$$

where

r = reference engine sizes = scaled engine sizeSHP = SLS, std day rated horsepower

Turbofan Engine Cost

Turbofan engine costs were estimated using a relationship of dollars per pound of thrust (\$/lb) as a function of rated engine thrust. This value was developed from information obtained from the February 1981 issue of Gas Turbine Forecast. The specific data used were for modern, current, high bypass ratio turbofan engines. The engines used and their specific costs are presented in Table A-XIII. These costs do not include thrust reverser. The thrust reversing system was presumed to be included in the airframe (nacelle) costs.

The data in Table A-XIII were plotted, and a least-squares linear fit for the nine data points was determined. The correlation coefficent for the linear regression was 0.986, i.e., a good fit. The relationship relating specific cost to thrust is as follows:

Specific turbofan cost = 98.24 - 1.22 SLS thrust/1000 (\$1981/lb of thrust)

Table A-XIII.
Turbofan engine cost data.

Engine	SLS thrust—Ib	Cost—\$1981/lb thrust
CFM56	22,000	77.27
CF6-6	40,300	43.42
CF6-45B	45,600	40.57
CF6-50	51,800	37.64
CF34	9,275	86.25
JT90-7A	47,670	37.76
JT10	37,000	56.76
RB211-524	49,120	39.70
RB401	5,500	89.09

Aircraft Acquisition Cost

The aircraft less engine cost was obtained by using a dollar per pound constant determined from aircraft company data contained in Refs 4 and 6. The value of this constant was an average of several calculations from each reference:

Aircraft less engine cost (\$1981)

cost per pound

= Aircraft less engine cost (\$1981)

Mfg empty wt less bare engine weight

Aircraft less engine cost per pound = \$178/lb

Aircraft less engine, engine, and propfan propeller costs identified as being OEM costs were increased by a factor of 1.5; Allison assumed a 50% markup from OEM costs to obtain acquisition or list price dollar levels. Therefore, total acquisition cost of the aircraft is as follows:

Total aircraft acquisition cost =
$$\left(\frac{\text{Mfg empty wt}}{\text{less engine wt}}\right)\left(267\frac{\$}{\text{lb}}\right)$$
 + Total engine acquisition cost

where engine acquisition costs are

Propfans =
$$\begin{bmatrix} (PS + GB) + (Propfan propeller) \\ OEM cost \end{bmatrix} 1.5$$

Reference turbofan

Turbofan specific engine cost per pound of thrust

Total engine acquisition cost (Propfan acquisition cost (Propfan or turbofan)

Direct Engine Maintenance

The term "Maintenance" as presented in this section includes labor and material costs for inspection, servicing, and overhaul of the reference turbofan engine and the propfan engines (power section plus gearbox). Propfan propeller maintenance cost was calculated as a separate item using Hamilton Standard methodology outlined in Ref 8. Items included in the propeller maintenance cost are blades, spinner, disk and aft fairing, pitch change actuator, and regulator mechanisms. These estimates are based on well established procedures used for engine maintenance as outlined by the Air Transport Association's (ATA) Standard Methods of Estimating Comparative DOC of Turbine Powered Transport Airplanes (1967).

The 1967 ATA procedures for estimating engine maintenance were derived from CAB data acquired up to that time. However, the APET study deals with airframe/engine systems incorporating technology features intended to significantly improve reliability and specific performance. Therefore, maintenance labor factors were derived from data of recent airplane system studies and used to form a ratio of the results of the 1967 ATA maintenance man-hour relationships with levels anticipated for these advanced systems. The following discussion presents the derivative of these maintenance labor factors.

First, it was necessary to verify that the 1967 ATA equation was representative of the 1967 vintage system. Data from Reference 7 were used and compared with calculations from the ATA procedure as shown in Table A-XIV. Although the ATA calculations are on the high side, they are fairly representative of vintage turboprop engine maintenance labor requirements.

Table A-XIV.

Direct engine maintenance hours.

Engine maintenance		
man-hours/engine flight hour		
Ref 7 data	1967 ATA (calculated)	
0.72	0.76	
0.817-0.884	0.978	

Adjustments to the ATA equations were obtained by examining engine maintenance man-hour (EMMH) per engine flight hour (EFH) values projected for advanced turboprops and turbofans in various studies reported in Ref 4, 6, and 7

Turboprop

Turbofan

and comparing them to values calculated from the ATA relationship, as shown in Table A-XV.

Observing the valves of the estimated/calculated ratio in Table XV shows consistent reduction of EMMH required for advanced technology engines; the average factor for turboprops is 0.530 and for turbofans is 0.514. These factors were used as multipliers to reflect a reduction in engine maintenance labor required for the advanced technology engines. Engine maintenance equations for labor and material are as follows:

Table XV.
Engine maintenance man-hour comparisons.

Reference 4	Turboprop	Turbofan
Engine size	12,328 shp	19,000 lb
EMMH/EFH estimated	0.552	0.468
EMMH/EFH calculated	1.02	1.113
Estimated/calculated ratio	0.541	0.420
Reference 6		
Engine size	20,424 shp	26,500 lb
EMMH/EFH estimated	1.0	0.8
EMMH/EFH calculated	1.263	1.316
Estimated/calculated ratio	0.792	0.608
Reference 7		
Engine size	12,328 shp	-
EMMH/EFH estimated	0.263	-
EMMH/EFH calculated	1.020	-
Estimated/calculated ratio	0.258	-

Labor—Engine (This includes bare engine, engine fuel control, thrust reverser, and exhaust nozzle systems and includes gearbox but not propeller on turboprop engines. Propeller maintenance will be calculated separately using Hamilton Standard report SP04A82 [Ref 8]).

$$C_{am_{EML}} = \frac{K_{FH_e} x t_f + K_{FC_e}}{v_{b x} t_b} x RL$$

where

 K_{FH_e} = EMLF ([0.6 + 0.027 T/10³] N_e) = labor manhours per flight hour (turbofan)

 K_{FH_e} = EMLF ([0.65 + 0.03 T/10³] N_e) = labor manhours per flight hour (turboprop)

 K_{FC_e} = EMLF ([0.3 + 0.03 T/10³] N_e) = labor man-hours per flight cycle (turbofan and turboprop)

= maximum takeoff thrust at sea level, static, standard day conditions (maximum takeoff shaft horsepower at sea level, static, standard day conditions for turboprop)

RL = labor rate per manhour

N_e = number of engines

ELMF = 0.530 for turboprops ELMF = 0.514 for turbofans

Material—Engine (This includes bare engine, engine fuel control, exhaust nozzle systems, and augmentor systems and includes gearbox on turboprop engines.

$$C_{am_{EMM}} = \frac{C_{FH_e} \times t_f + C_{FC_e}}{v_{b} \times t_b}$$

where

 $C_{FH_e} = 2.5 N_e (C_e/10^5) = material cost - $/flight hour$ $C_{FC} = 2.0 N_e (C_e/10^5) = material cost - $/flight cycle$

N_e = number of engines

C_e = cost of one engine (includes gearbox but not propeller on turboprop engines)

Annual Utilization Rate

The mission block time corresponding to previously discussed 300 nmi stage length revenue mission was determined to be approximately 1 hr. Using this 1 hr block time in conjunction with the 1967 ATA relationship of utilization versus block time for subsonic transports yields an annual utilization rate of 3000 hr.

PROPULSION SYSTEM TRADE FACTORS

Propulsion system trade factors were developed early in Task II using reference turboprop engine PD436-1 to show the sensitivity of system performance and economics to various propulsion system-affected parameters. Since the revenue mission requirements are fixed, the system performance dependent variable is fuel burned and the cost dependent variable is DOC. These results are presented and discussed in Appendix B.

ENVIRONMENTAL CONSTRAINTS

The environmental constraints used in the APET study involve the engine exhaust emissions, aircraft fuel venting restriction, and acoustic constraints of Federal Air Regulation (FAR) Part 36 certification requirements. Details of these constraints are presented in the following discussion.

Exhaust Emissions

Currently there are no gaseous exhaust emissions standards for turboprop or propfan engines. Therefore, for use in this program as design requirements, Allison has developed gas generator equivalent emissions indexes (EI) (grams of

pollutant per kilograms of fuel). These are based on the ICAO 1986 standards for turbofans. These Els are shown in Table A-XVI along with the ICAO standards from which they were derived.

The turboprop smoke standard shown in Table A-XVI was developed in a joint USAF and Allison program. It defines the threshold of smoke visibility for large turboprop engines and has subsequently been adopted by the EPA as a smoke standard.

The APET engines used in this study all incorporate combustion technology sufficient to meet the standards given in Table A-XVI.

Table A-XVI.

Recommended design standards for APET.

Pollutant	ICAO TF/TJ standards— g/kN	Gas generator equivalent emission index—g/kg
HC	19.6	5
CO	118	29.5
NO _x	$40 + 2 (R_c)$	$11 + 0.55 (R_c)$
Smoke	$SN = 83.6 (F_N)^{-0.274}$	$SN = 187 (kW)^{-0.168}$
(Threshold of visibility)	Jet	(EPA TP curve)

Analysis of Regulations

As a part of the APET program Allison has made an analysis of the emissions control regulations applicable to turboprop and turbofan commercial engines. This investigation included past, present, and proposed regulatory activity by the United States Environmental Protection Agency and by the United Nation's International Civil Aviation Organization.

In this analysis it was found that there were no gaseous emissions control regulations for turboprops and that the EPA smoke standard was the only exhaust control applicable to turboprops. The EPA turboprop gaseous standards were withdrawn last year before they became effective. However EPA continues to monitor advanced turboprop and propfan programs with the intent to regulate emissions if these engines become a significant portion of the commercial fleet.

ICAO is currently studying exhaust emissions from turboprop-powered aircraft but has not taken regulatory action. Therefore only smoke is controlled from turboprop-powered aircraft, and these EPA rules become effective in January 1984.

The turbofan-turbojet emissions regulations that the EPA originally issued in 1973 have been greatly moderated in the 1982 final rulemaking. The hydrocarbon (HC) emissions standards were relieved and the carbon monoxide (CO) and oxides of nitrogen (NO_x) standards were withdrawn. These reversals in the usual EPA rulemaking practices were based on airport air quality studies, which placed doubt on the

necessity to control emissions from aircraft (general aviation regulations were completely withdrawn), and cost analyses, which showed that it was more cost effective to control pollution from other sources. The EPA and ICAO standard are compared in Table A-XVII.

Table A-XVII.

<u>Exhaust emissions standards</u>
for aircraft gas turbine engines.

	United States (EPA) pollutants controlled	International (ICAO) pollutants controlled
Turbofans and jets (subsonic)	Smoke, 1973-84 HC, 1984 Fuel venting, 1974	Smoke, 1983 HC, CO, NO _x , 1984 (most stringent use as basis for APET)
Turboprops	Smoke, 1984 Fuel venting, 1975	Study 1983-86

The ICAO regulations were written (subsequent to EPA's original rules) to standardize emission control regulations throughout the international aviation community. These standards are based on the current technology of control that can be applied to production engines. While more stringent regulations were proposed for possible future application, they were not incorporated because "problems still existed in the development of the technology to be compatible with the required usage, maintainability, and service life of components." As a result the ICAO turbofan standards are based on current control technology, and the advanced technology forcing goals appear only in the minutes of the Committee on Aircraft Engine Emissions but not in the International Standards adopted by the Council. The ICAO international standards and the Committee goals are compared in Table A-XVIII.

Allison-Recommended Emissions Design Standards for APET

Even though there are no gaseous turboprop emissions standards, Allison recommends that not only smoke but gaseous emissions be controlled from APET engines. We recommend that the emissions design standards meet the following criteria:

- That they be compatible with the APET program requirements which stress improved fuel economy and engine performance. Environmental control is also required but emphasis on technology forcing control of exhaust emissions is not needed.
- 2. That they are applicable throughout the world, meaning that they will meet ICAO Standards.

Table A-XVIII. Comparison of ICAO standards and goals (subsonic turbofan and turbojet).

	Standards	Goals
1.	HC = 19.6 g/kN CO = 118 g/kN NO _x = $(40 + 2 R_c) g/kN$ Smoke = 83.6 $(F_N)^{-0.274}$	HC = 4.35 g/kN CO = 42.0 g/kN NO _x = $(32 + 0.8 \text{ R}_c) \text{ g/kN}$ Smoke = $83.6 (F_N)^{-0.274}$
2.	Recommended by CAEE with International Agreement and Ratification	Recommended in working group but not accepted; no demon- strated technology
3.	Demonstrated technology	Technology forcing
4.	Over-regulation (US controls only HC, smoke, and fuel venting)	Gross over-regulation Cost Weight Energy penalty Potential flight safety

That the design standards be such that the gas generator can be used either as a turboprop or turbofan engine.

To meet all of these criteria, the levels of the ICAO turbofan standards were adopted. To identify these independently from the propulsion mode finally chosen (propeller, propfan, or turbofan) they were translated from thrust specific values, grams per kilonewton, to gas generator related emission indexes (EI) in grams per kilogram of fuel. These are shown in Table A-XVI.

Because of the regulatory lead times now being experienced by EPA and ICAO and because of the deregulation of turboprops. Allison has concluded that the design emissions standards for APET should be based on current EPA and ICAO levels and not on projected technology advances. This conclusion is supported by the growing body of ambient air surveys on the airport environment. These show that the emissions from aircraft engines cannot be related to ambient air quality without considerable uncertainty, and as that uncertainty is being resolved through airport measurements, the impact of all aviation is shown to be much less than originally estimated by the EPA. Partial agreement with these above effects by the EPA is responsible for the withdrawal of emissions standards for all general aviation and auxiliary power units, the gaseous standards for turboprops, and the CO standards for commercial aviation. NO_x standards were withdrawn from commercial aviation for economic reasons.

NASA Program Directive No. 1

NASA Directive No. 1 requested that the ICAO "Research Goals" for emissions be adopted by APET. Allison study findings show that these goals are technology forcing toward emission control and are not reflected in any known emissions standards throughout the world. Further-

more, the units of specific emissions in grams per kilonewton of thrust are not appropriate to APET unless the engine and propeller were to be developed, procured, and evaluated as a single propulsion system such as the fan and gas generator system in a turbofan engine. For these reasons, Allison recommends that the APET Exhaust Emissions Design Standards previously discussed be adopted in lieu of those of NASA's directive.

Fuel Venting Restriction

The requirements relating to discharge of liquid fuel into the atmosphere (Ref 9) will be assumed to apply: "Aircraft shall be so designed and constructed as to prevent the intentional discharge into the atmosphere of liquid fuel from the fuel nozzle/manifolds resulting from the process of engine shutdown following normal flight or ground operations."

Noise

Acoustic environmental constraints for advanced propfan transports will occur in three areas: (1) Federal Air Regulation (FAR) Part 36 certification requirements. (2) interior levels that will gain passenger acceptance, and (3) restrictions imposed by individual airports to control noise at their own localities. In the APET study, engine acoustic design will be guided by the FAR Part 36 requirements. The primary function of FAR Part 36 is to ensure that the best available noise-reduction tehenology is incorporated in new transport aircraft. Because of the "Economically Reasonable and Technically Practical" requirements in Part 36, aircraft certification requirements must follow demonstrated technology. Therefore, despite continued pressure to control airport noise as evidenced by the recent Washington National and Santa Monica actions, the current Part 36 requirements are expected to remain for some time. The most likely noise regulation to be imposed upon a propfan transport in 1990 to 1995 is the current FAR Part 36 takeoff, sideline, and approach limits. These requirements are shown with the measured or estimated certification levels for current turboprop transports in Figures A-10, A-11, and A-12.

ACOUSTIC ASSUMPTIONS

Nacelle

The nacelle acoustic treatment weight penalty is estimated using unit weights of facing sheet and honeycomb material tailored to the propulsion system noise spectrum. Acoustic treatment material weight will be based on inlet duct wetted area.

Gearbox

The gearbox noise level is calculated using DDA data developed in other programs.

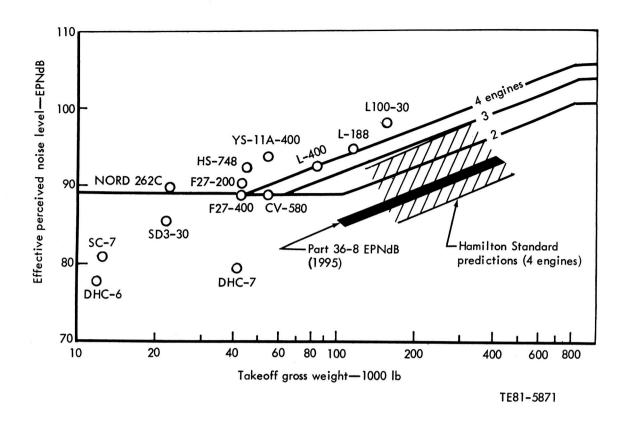


Figure A-10. FAR part 36 takeoff noise limits for transport-category aircraft.

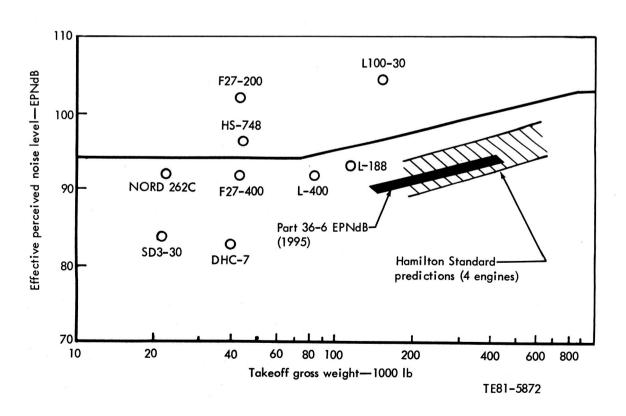


Figure A-11. FAR part 36 sideline noise limits for transport-category aircraft.

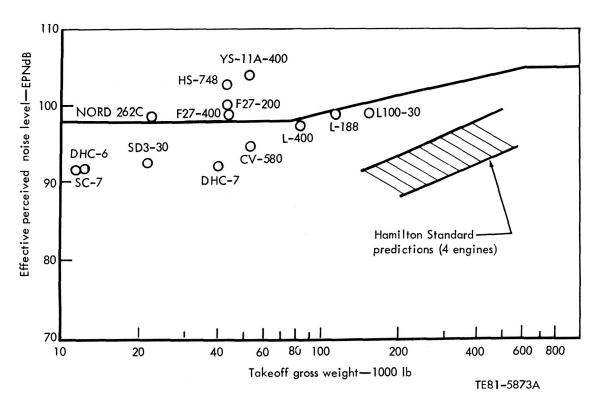


Figure A-12. FAR part 36 approach noise limits for transport-category aircraft.

Propfan

The propfan far field noise is calculated using Hamilton Standard Data Package SP16A77 (Ref 10). Near field noise is calculated using Hamilton Standard Data Package SP07A82 (Ref 5).

Engine

Engine noise is calculated using Allison's computer code OSBD87. Engine generated noise will be considered in the evaluation of the four candidate cycles in Task II. Therefore noise could be a factor in ranking the cycles. A subjective method based on previous noise calculations for components similar to those of the candidate engine cycles will be used. Design methods will be employed to minimize noise where possible so that the best low noise design of each cycle is considered in the rankings. The acoustical performance of the candidate engines will be judged using three criteria: (1) minimal addition to the propfan effective perceived noise (EPN) levels at the FAR Part 36 measurement points, (2) minimum pressure loss due to inlet and/or exhaust duct treatment, and (3) low noise increase due to engine growth.

Turboprop engines radiate compressor noise from the engine inlet, combustor, and turbine; jet noise from the engine exhaust; and case noise from the engine and reduction gearbox. Only compressor, combustor, and turbine gen-

erated noise is considered in judging the candidate engine cycles, because low nozzle exit velocity results in jet noise substantially below combustor noise. Furthermore, based on T56 experience, engine case and gearbox noise will not contribute significantly to total engine noise.

Engine noise generation is determined by the selected engine cycle and by the aerodynamic and mechanical design of the engine components. Since the engine is one part of an acoustic system that must be designed to meet the 1995 certification requirements, the low noise design considerations incorporated in the engine components will be influenced by aircraft performance, notably aircraft takeoff altitude at the 3.5 nmi FAR noise measurement point, by power required on approach, and by the propfan spectrum at the FAR Part 36 measurement points.

Allison's engine noise prediction methods, computer code OSBD87, will be employed to estimate the noise characteristics of the two turboprop engine configurations selected from Task II for further study in Tasks III & IV. The engine noise prediction methods of OSBD87 consider each of the several engine noise sources modeled independently with its own generation, spectral, and directivity description. Each source provides its unique contribution to the engine total noise field for a given operating condition. A listing of engine noise sources and the prediction methods used are shown in Table A-XIX.

Table A-XIX.

Engine noise sources and prediction methods used.

Noise source	Prediction method used
Compressor Combustor Turbine Jet	Allison developed procedure NASA Aircraft Noise Prediction Program Modified Rolls Royce procedure NASA Aircraft Noise Prediction Program

GEARBOX CONFIGURATIONS

The APET study considered a range of gearbox types and power train gear arrangements. Four combinations identified for detailed evaluation are as follows:

- 1. offset configuration with dual compound idler gearing
- 2. offset configuration with spur and planetary gearing
- 3. in-line configuration with split path planetary gearing
- 4. in-line configuration with star gearing

The following design parameters are to be evaluated: number of power train gears, number of power train bearings, weight, cost, prop control access, accessory mounting, and ease of opposite rotation modification. These are discussed further in Appendix C, Propulsion System Integration. The method of gear selection will consider noise, vibration, and fretting of contacting surfaces. Design criteria to be utilized are defined in Table A-XX.

REFERENCE TURBOPROP ENGINE PD436-1

A 15,000 shp reference turboprop engine was defined in preliminary design detail for purposes of developing sensitivity factors of fuel burned and DOC. As shown in Figure A-13, the propeller drive gearbox is an offset-down type. The physi-

Table A-XX. Gearbox design criteria.

Size	10,000 shp
Overall speed ratio	9:1
Design life (MTBR)	30,000 hr
Gear crushing stress	160,000 lb/in.2
Gear bending stress	40,000 lb/in. ²
unidirectional	
Gear bending stress	28,000 lb/in.2
reverse	
Pitch line velocity	25,000 ft/min
Bearing materials and	10
manufacturing life factor	

cal size of the engine is also shown in Figure A-13. The technology level of this engine in reference size, 81.3 lb/sec corrected flow, was assumed to be the same as the reference size EEE core; the component efficiencies, cooling airflow rates, and assumed losses in the cycle of the 15,000 shp turboprop engine are essentially the same as for the EEE core, which has considerably larger flow size. This assumption, in effect, pushes the technology further than EEE for the components that are size sensitive.

PD436-1 is a dual-spool configuration. The compressor is an axial flow, single-spool design driven by a two-stage axial flow, high-pressure turbine. The overall pressure ratio of 25.0:1 at a cruise turbine inlet temperature of 2200°F produces 7544 shp at 0.303 brake specific fuel consumption. The maximum temperature of 2500°F requires 6.9% chargeable cooling air. The weight of the engine is given in Table A-XXI. Scaling relationships are as follows:

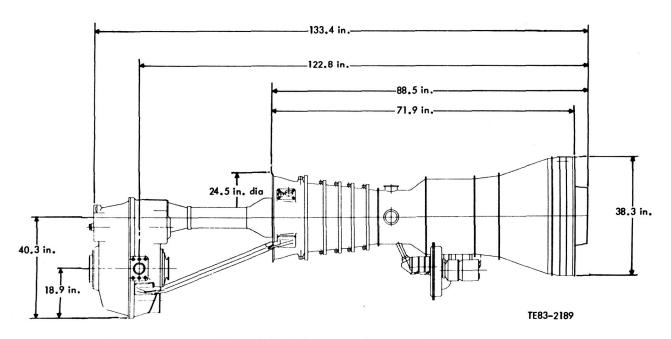


Figure A-13. Reference turboprop engine.

Table A-XXI. Turboprop Engine PD436-1B weight.

Dry weight—lb 1918

Power section

Interconnecting struts and shafts

Torquemeter

Inlet torquemeter fittings and hardware

Compressor air inlet and forward support

Accessory gearbox

Compressor case

Compressor rotor

Diffuser/combustor

HP turbine case

HP turbine rotor

LP turbine case

LP turbine rotor

Rear bearing support

Oil system

Fuel system

Electrical system

Prop control linkage

Reduction gearbox

Total engine weight

 $\frac{1127}{3045}$

1. Power Section (PS) and Gearbox (GB) Dimensions

GB or PS length (scaled) - length (reference) x (S.F.) $^{0.4}$

where: S.F. = scale factor =
$$\frac{\text{shp (scaled)}}{\text{shp (reference)}}$$

GB or PS diameter = diameter (reference) x (S.F.)^{0.5}

2. Power Section and Gearbox Weight

PS wt (scaled) = PS wt (reference)
$$x (S.F.)^{1.01}$$

GB wt (scaled) = GB wt (reference) +
$$\frac{Q \text{ (scaled)}}{Q \text{ (reference)}}$$

where: S.F. = scale factor =
$$\frac{\text{shp (scaled)}}{\text{shp (reference)}}$$

Q = torque output

$$Q = \frac{550 \times shp}{2 \times n}, \text{ ft-lb}$$

$$n = \frac{22 \times 800 \text{ ft/sec}}{2 \times \text{propeller dia}}, \text{ rev/sec}$$

 Engine Brake Specific Fuel Consumption (SFC) and Shaft Horsepower (shp). Engine performance is scalable for purposes of studying other engine sizes. However, component performance will vary, depending upon the magnitude of scale.

Engine shp (scaled) = shp (reference) x 1 -
$$\frac{A}{100}$$
 x S.F.

Engine SFC (scaled) = SFC (reference) x 1 +
$$\frac{B}{100}$$

A = sizing effect on shp

$$A = (27.29 \times S.F.) - (11.90 \times S.F.^2) - 15.39$$

B = sizing effect on SFC

$$B = (7.15 \times S.F.^2) = (17.70 \times S.F.) + 10.54$$

The performance of engine PD436-1B is given in Table A-XXII for standard day conditions and in Table A-XXIII for 86°F day conditions.

REFERENCE TURBOFAN ENGINE

A 20,000 lb thrust class reference turbofan engine was defined in preliminary design detail for use in the mission analysis comparison of the turboprop and turobfan powered aircraft. The turbofan engine is shown in Figure A-14.

At the cruise condition, the reference turbofan engine has an overall pressure ratio of 34.0:1, has a bypass ratio of 6.0, and develops 4800 lb thrust at 2200°F rotor inlet temperature. The cruise thrust specific fuel consumption is 0.518. These data and the component performance levels are summarized in Table A-XXIV.

The performance of the reference turbofan engine is given in Table A-XXV for a range of power/altitude/Mach number conditions on a standard day. Data for an 86°F day are presented in Table A-XXVI.

Table A-XXII.

Performance of reference turboprop engine PD436-1B on standard day.

Alt— ft	Mach No.	Power— shp	Fuel flow— lb/hr	Net thrust —Ib	Turbine temp— °R_	HP turbine speed—%	LP turbine speed—%_	Overall pressure ratio	Corr flow— lb/sec
0	0.0	246	772	123.7	1661	100	71.6	4.70	21.4
0	0.0	2,451	1663	330.7	2011	100	81.7	8.15	33.6
0	0.0	6,128	2817	634.5	2311	100	89.1	11.90	45.6
0	0.0	9,152	3738	894.5	2511	100	92.2	14.45	53.0
0	0.0	10,930	4273	1058.0	2611	100	93.5	15.85	57.0
0	0.0	11,859	4554	1139.8	2660	100	94.1	16.55	58.9
0	0.0	11,865	4561	1140.1	2662	100	94.1	16.55	58.9
0	0.0	14,952	5490	1441.3	2811	100	95.8	18.83	65.1
0	0.0	15,792	5750	1524.7	2850	100	96.3	19.43	66.7
0	0.3	15,575	5619	813.3	2813	100	96.2	18.19	63.5
0	0.4	1,368	1260	-166.1	1861	100	77.7	6.14	26.7
0	0.4	3,386	1912	-111.4	2061	100	83.6	8.33	34.4
0	0.4	6,097	2730	-4.2	2261	100	88.7	10.74	42.3
0	0.4	9,982	3893	204.5	2511	100	92.8	13.66	50.9
0	0.4	11,843	4445	321.0	2611	100	94.2	14.95	54.6
0	0.4	12,827	4744	384.2	2662	100	94.8	15.61	56.4
0	0.4	16,045	5703	616.6	2810	100	96.5	17.71	62.2
0	0.5	1,103	1148	-268.6	1811	100	76.3	5.50	24.5
0	0.5	3,531	1931	-242.1	2061	100	83.5	7.99	33.3
0	0.5	6,449	2791	-156.0	2261	100	88.9	10.43	41.4
0	0.5	10,464	3980	34.5	2511	100	93.2	13.24	49.7
0	0.5	12,371	4542	141.5	2611	100	94.5	14.48	53.3
0	0.5	13,363	4839	200.5	2660	100	95.2	15.10	55.0
0	0.5	16,678	5825	422.4	2810	100	96.9	17.13	60.7
0	0.6 0.6	1,253 3,748	1174	-374.3	1811	100	76.6	5.32	23.9
0	0.6	3,746 7,639	1964 3087	-382.2	2061	100	83.5	7.65	32.2
0	0.6	11,051	4084	-289.7 -145.2	2311 2511	100 100	90.2	10.58	41.9
0	0.6	13,028	4661	-145.2 -43.4	2611	100	93.6 95.0	12.75	48.3
0	0.6	14,048	4964	12.9	2660	100	95.6	13.93 14.53	51.8 53.5
0	0.6	17,487	5975	228.3	2810	100	97.4	16.47	58.9
5,000	0.3	14,440	5078	820.4	2811	100	95.6	19.58	67.2
5,000	0.4	14,869	5160	649.7	2810	100	95.8	19.06	65.8
5,000	0.5	15,436	5270	483.9	2810	100	96.2	18.43	64.2
5,000	0.6	16,137	5404	318.0	2810	100	96.7	17.70	62.3
10,000	0.3	908	862	-40.5	1761	100	75.7	6.56	28.2
10,000	0.3	2,884	1480	45.1	2011	100	83.2	9.78	39.2
10,000	0.3	5,269	2199	184.8	2261	100	88.0	12.78	48.3
10,000	0.3	7,759	2929	356.1	2461	100	90.8	15.55	56.2
10,000	0.3	9,953	3575	524.6	2611	100	92.6	17.82	62.5
10,000	0.3	10,742	3812	588.8	2662	100	93.1	18.61	64.6
10,000	0.4	5,486	2238	74.3	2261	100	88.2	12.48	47.4
10,000	0.4	8,031	2979	229.9	2461	100	91.1	15.16	55.1
10,000	0.4	10,267	3633	390.9	2610	100	92.9	17.36	61.2
10,000	0.4	11,071	3870	452.4	2660	100	93.4	18.12	63.3
10,000 10,000	0.4 0.4	984	876	-111.2	1761	100	75.8	6.42	27.8
10,000	0.4	2,542 13,715	1361	-64.7	1961	100	82.0	8.87	36.3
10,000	0.5	1,086	4656 894	678.0 -185.5	2810 1761	100 100	95.4	20.59	69.9
10,000	`0.5	2,663	1379	-158.1	1961	100	76.0	6.24	27.3
10,000	0.5	5,772	2288	-38.6	2261	100	82.0 88.5	8.54 12.11	35.3 46.4
10,000	0.5	8,382	3042	104.4	2461	100	91.4	14.67	53.8
10,000	0.5	10,680	3710	258.4	2610	100	93.3	16.79	53.6 59.7
10,000	0.5	11,506	3952	317.0	2660	100	93.8	17.53	61.7
10,000	0.5	14,173	4750	531.6	2811	100	95.6	19.85	68.0
10,000	0.6	1,215	915	-265.0	1761	100	76.3	6.04	26.6
10,000	0.6	2,799	1397	-255.8	1961	100	81.9	8.14	33.9
10,000	0.6	6,124	2349	-157.0	2261	100	88.8	11.67	45.2
				0.00	man manada III	12 CD (III		- 1010E10	

Table A-XXII. (cont)

			Fuel	Net	Turbine	HP	LP	Overall	Corr
Alt—	Mach	Power—	flow-	thrust	temp-	turbine	turbine	pressure	flow-
ft	No.	shp	lb/hr	—lb	°R	speed-%	speed-%	ratio	lb/sec
10,000	0.6	8,826	3121	-23.9	2461	100	91.8	14.12	52.3
10,000	0.6	11,193	3805	123.6	2610	100	93.7	16.14	58.0
10,000	0.6	12,044	4053	181.0	2660	100	94.3	16.84	59.9
10,000	0.6	14,797	4867	391.2	2810	100	95.9	19.06	65.9
10,000	0.7	15,537	5009	250.1	2810	100	96.5	18.19	63.6
15,000	0.5	916	738	-151.3	1711	100	75.1	6.39	27.8
15,000	0.5	2,705	1275	-113.0	1961	100	82.5	9.49	38.5
15,000	0.5	5,413	2060	9.1	2261	100	88.1	13.10	49.3
15,000	0.5	7,769	2734	152.5	2460	100	90.8	15.87	57.2
15,000	0.5	9,837	3334		2611	100	92.5	18.16	63.5
				302.7					
15,000	0.5	10,573	3554	361.1	2662	100	93.1	18.95	65.6
15,000	0.5	13,023	4272	577.4	2811	100	95.3	21.56	72.4
15,000	0.6	1,023	755	-218.0	1711	100	75.3	6.17	27.1
15,000	0.6	2,870	1300	-198.8	1961	100	82.6	9.11	37.3
15,000	0.6	5,722	2113	-92.5	2261	100	88.4	12.61	47.9
15,000	0.6	8,155	2804	43.2	2460	100	91.2	15.25	55.5
15,000	0.6	10,290	3419	188.9	2611	100	93.0	17.44	61.6
15,000	0.6	11,039	3637	245.3	2660	100	93.5	18.19	63.6
15,000	0.6	13,514	4371	456.1	2810	100	95.5	20.63	70.0
15,000	0.7	1,152	775	-289.8	1711	100	75.5	5.92	26.3
15,000	0.7	3,049	1325	-289.2	1961	100	82.6	8.65	35.8
15,000	0.7	5,545	2021	-220.5	2211	100	88.0	11.50	44.7
15,000	0.7	8,621	2886	-69.2	2460	100	91.7	14.57	53.6
15,000	0.7	10,063	3297	21.7	2560	100	92.9	15.94	57.5
15,000	0.7	11,605	3743	129.7	2660	100	94.0	17.36	61.4
15,000	0.7	14,135	4491	335.9	2810	100	95.7	19.64	67.5
15,000	0.8	993	705	-356.2	1661	100	74.2	5.20	23.7
15,000	0.8	3,231	1347	-385.6	1961	100	82.5	8.12	34.0
15,000	0.8	5,965	2089	-331.5	2211	100	88.3	10.95	43.2
15,000	0.8	9,169	2980	-186.5	2460	100	92.2	13.85	51.6
15,000	0.8	10,675	3407	-97.3	2561	100	93.5	15.14	55.3
15,000	8.0	12,268	3865	10.1	2660	100	94.6	16.47	59.0
15,000	0.8	14,890	4637	218.9	2810	100	96.3	18.62	64.8
20,000	0.5	11,874	3829	611.2	2810	100	95.0	23.47	77.4
20,000	0.6	12,296	3914	510.2	2810	100	95.2	22.44	74.8
20,000	0.7	12,819	4018	411.8	2810	100	95.4	21.33	71.9
20,000	0.8	13,440	4141	313.9	2810	100	95.6	20.16	68.9
25,000	0.5	840	553	-95.0	1661	100	74.4	7.28	31.0
25,000	0.5	2,468	1029	-40.1	1960	100	82.3	11.29	44.0
25,000	0.5	4,655	1645	82.3	2260	100	86.9	15.46	56.1
25,000	0.5	6,537	2178	221.5	2460	100	89.3	18.73	65.0
25,000	0.5	7,618	2489	315.3	2560	100	90.7	20.54	69.8
25,000	0.5	8,795	2837	426.1	2662	100	92.4	22.47	74.8
25,000	0.5	10,739	3412	634.5	2811	100	95.4	25.64	82.8
25,000	0.6	916	565	-143.7	1661	100	74.5	7.01	30.1
25,000	0.6	2,031	886	-123.1	1860	100	80.5	9.69	39.2
25,000	0.6	4,893	1686	11.3	2260	100	87.3	14.87	54.4
25,000	0.6	6,833	2234	145.4	2461	100	89.7	17.98	63.0
25,000	0.6	7,926	2547	235.6	2560	100	90.9	19.68	67.5
25,000	0.6	9,113	2898	344.7	2661	100	92.5	21.49	72.3
25,000	0.6	11,154	3501	558.2	2811	100	95.1	24.59	80.3
25,000	0.7	1,006	579	-195.2	1661	100	74.7	6.70	29.1
25,000	0.7	2,184	909	-183.7	1861	100	80.7	9.27	37.9
25,000	0.7	5,180	1736	-62.3	2260	100	87.8	14.21	52.6
25,000	0.7	7,193	2300	69.2	2461	100	90.2	17.17	60.8
25,000	0.7	8,312	2622	158.3	2561	100	91.4	18.75	65.1
25,000	0.7	9,524	2975	265.8	2660	100	92.7	20.45	69.6
25,000	0.7	11,569	3584	474.6	2810	100	95.1	23.29	77.0
25,000	0.8	1,112	594	-247.9	1661	100	74.9	6.38	28.1
25,000	0.8	2,326	927	-250.3	1860	100	80.7	8.73	36.2
-,	-500	-,						0.70	30.2

Table A-XXII. (cont)

Alt—	Mach	Power—	Fuel flow—	Net thrust	Turbine temp—	HP turbine	LP turbine	Overall pressure	Corr flow—
ft	No.	shp	lb/hr	—Ib	°R	speed—%	speed—%	ratio	lb/sec
25,000	0.8	4,605	1543	-183.8	2160	100	86.7	12.23	46.9
25,000	0.8	7,612	2375	-9.3	2461	100	90.8	16.29	58.5
25,000	0.8	8,774	2707	78.8	2561	100	91.9	17.79	62.5
25,000	0.8	10,002	3067	185.0	2660	100	93.0	19.34	66.7
25,000	0.8	12,086	3688	395.8	2810	100	95.3	21.98	73.6
30,000	0.5	9,308	2941	606.6	2810	100	97.5	27.38	86.6
30,000	0.6	9,847	3063	570.2	2811	100	96.5	26.64	85.1
30,000	0.7	10,364	3180	523.2	2811	100	95.4	25.54	82.7
30,000	0.8	10,824	3279	466.2	2811	100	95.1	24.12	79.1
32,000	0.72	683	402	-147.8	1561	100	72.4	6.56	28.7
32,000	0.72	2,047	780	-130.7	1860	100	80.7	10.44	41.6
32,000	0.72	3,854	1270	-48.7	2160	100	85.6	14.40	53.2
32,000	0.72	6,276	1946	128.1	2461	100	89.2	19.19	66.3
32,000	0.72	7,250	2224	219.8	2561	100	90.7	21.07	71.2
32,000	0.72	8,275	2530	325.8	2662	100	92.3	23.01	76.3
36,089	0.5	594	355	-52.9	1560	100	72.5	7.98	33.5
36,089	0.5	1,668	663	-9.0	1860	100	79.8	12.33	47.2
36,089	0.5	3,181	1079	86.7	2161	100	84.0	17.11	60.7
36,089	0.5	5,244	1659	270.9	2460	100	88.4	23.04	76.3
36,089	0.5	6,075	1900	362.0	2560	100	90.6	25.38	82.3
36,089	0.5	6,750	2112	441.3	2662	100	94.4	27.19	86.2
36,089	0.5	7,544	2380	540.4	2810	100	99.6	29.14	89.6
36,089	0.6	630	360	-83.5	1560	100	72.4	7.62	32.2
36,089	0.6	1,770	680	-48.0	1860	100	80.1	11.87	45.9
36,089	0.6	3,337	1107	42.5	2161	100	84.5	16.44	58.9
36,089	0.6	5,440	1698	221.3	2461	100	88.6	22.04	73.8
36,089	0.6	6,290	1945	311.0	2561	100	90.3	24.25	79.5
36,089	0.6	7,120	2192	409.1	2661	100	93.3	26.39	84.6
36,089	0.6	8,018	2491	523.5	2810	100	99.0	28.51	88.6
36,089	0.7	681	367	-116.6	1560	100	72.5	7.25	31.1
36,089	0.7	1,895	700	-89.1	1860	100	80.4	11.36	44.4
36,089	0.7	3,517	1138	-4.1	2160	100	84.9	15.69	56.8
36,089	0.7	5,690	1744	174.7	2461	100	88.8	20.99	71.0
36,089	0.7	6,539	1992	262.7	2560	100	90.4	23.02	76.3
36,089	0.7	7,477	2271	371.2	2661	100	92.5	25.25	82.0
36,089	0.7	8,571	2624	515.1	2811	100	98.0	27.74	87.2
36,089	0.72	693	369	-122.6	1561	100	72.6	7.18	30.8
36,089	0.72	1,922	704	-97.8	1860	100	80.5	11.25	44.1
36,089	0.72	3,560	1145	-13.0	2160	100	85.0	15.54	56.4
36,089	0.72	5,746	1755	165.0	2461	100	88.8	20.77	70.4
36,089	0.72	6,595	2003	253.0	2560	100	90.5	22.77	75.6
36,089	0.72	7,544	2287	362.4	2662	100	92.4	24.98	81.3
36,089	0.8	746	377	-151.6	1561	100	72.7	6.88	29.8
36,089	8.0	2,042	723	-133.2	1860	100	80.7	10.82	42.8
36,089	0.8	3,733	1174	-52.0	2160	100	85.4	14.89	54.6
36,089	0.8	5,962	1796	124.5	2461	100	89.0	19.82	68.0
36,089	8.0	6,841	2052	214.7	2561	100	90.6	21.73	73.0
36,089	8.0	7,791	2336	324.7	2661	100	92.3	23.79	78.3
36,089	8.0	9,181	2770	509.1	2811	100	96.7	26.78	85.4

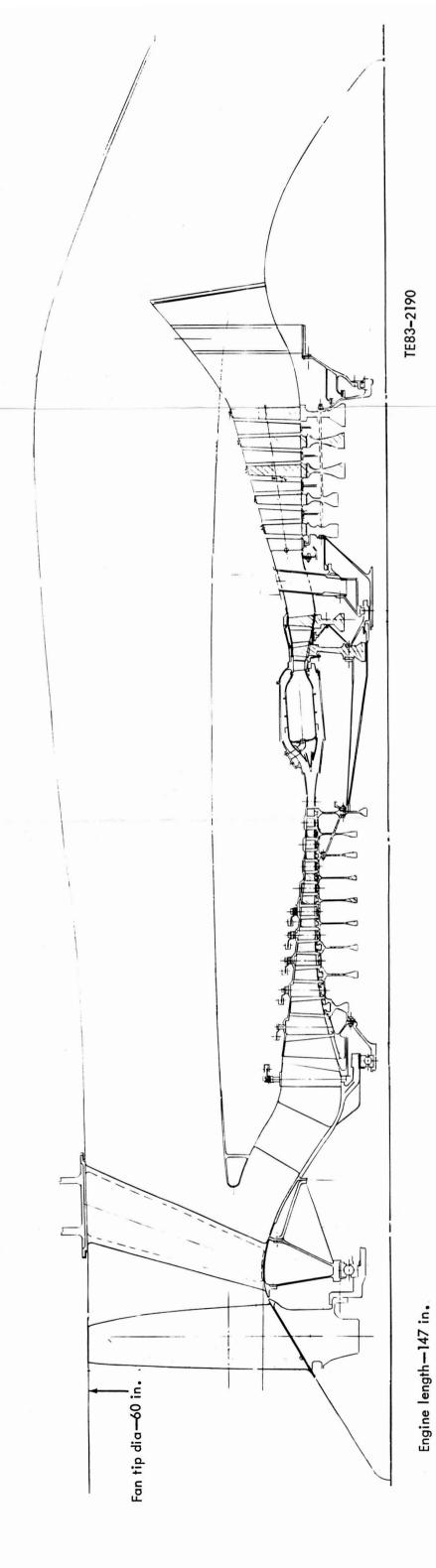


Figure A-14. Reference turbofan engine.

Table A-XXIII. Performance of reference turboprop engine PD436-1B on 86F day.

Alt— ft	Mach No.	Power— shp	Fuel flow— lb/hr	Net thrust —Ib	Turbine temp— °R	HP turbine speed—%	LP turbine speed—%	Overall pressure ratio	Corr flow— lb/sec
0	0.0	15,759	5806	1487.4	2962	100	98.5	19.12	65.93
0	0.1	15,824	5815	1263.2	2961	100	98.5	19.04	65.75
0	0.2	16,038	5855	1053.9	2960	100	98.7	18.82	65.21
0	0.3	16,401	5927	853.2	2960	100	98.9	18.47	64.21

Table A-XXIV. Reference turbofan engine performance summary.

	Takeoff sea level static, 86°F day	Design point, 36,089 ft/0.72 Mach
Thrust—Ib	20,000	4,800
Turbine inlet temperature—°F	2,500	2,200
Specific fuel consumption	0.324	0.518
Corrected flow—lb/sec	696	804
Core flowlb/sec corr	55.0	64.3
Overall pressure ratio	26.4	34:1
Fan pressure ratio	2.53	1.65
Bypass ratio	7.8	7.4
Compressor pressure ratio	17.2	20.6
Fan efficiency—%		88
Compressor efficiency—%		86.2
HP turbine efficiency—%		90.5
LP turbine efficiency—%		91.0
Chargeable cooling air and leakage— %		6.9
Mixer effectiveness—%		83.0
		G .

Table A-XXV. Performance of reference turbofan engine on standard day.

Alt— ft	Mach No.	Thrust—	Fuel flow— lb/hr	Bypass ratio	Turbine temp— °R	HP turbine speed—%	LP turbine speed—%	Overall pressure ratio	Corr flow— lb/sec
0	0.0	903	732	14.62	2342	38.0	60.6	2.89	152.4
0	0.0	4,022	1213	9.60	1829	48.0	81.4	8.29	329.3
0	0.0	8,254	2326	8.94	2142	63.0	90.9	13.63	466.4
0	0.0	12,417	3584	8.55	2418	78.0	95.6	18.34	565.7
0	0.0	15,050	4451	8.27	2569	85.0	97.8	21.32	618.6
0	0.0	16,718	5038	8.09	2660	89.0	99.0	23.23	648.9
0	0.0	16,718	5037	8.09	2660	89.0	99.0	23.23	649.0
0	0.0	19,542	6105	7.78	2810	95.3	101.0	26.56	696.0
0	0.0	19,994	6283	7.73	2833	96.2	101.3	27.10	703.1
0	0.3	14,003	6199	8.10	2810	95.2	101.2	25.45	697.3
0	0.4	1,030	1148	14.00	1810	49.2	79.9	7.12	408.5
0	0.4	2,792	1881	11.29	2010	58.3	88.0	10.70	475.1
0	0.4	5,245	2885	10.18	2260	70.3	93.3	14.39	546.6
0	0.4	7,619	3910	9.44	2460	80.1	96.6	17.74	602.1
0	0.4	9,670	4829	8.95	2610	86.9	98.8	20.53	643.4
0	0.4	10,396	5164	8.79	2660	89.1	99.5	21.50	657.0
0	0.4	12,713	6269	8.33	2810	95.2	101.5	24.62	696.6
0	0.5	874	1309	14.93	1860	52.8	81.8	7.54	456.6

Table A-XXV. (cont)

Alt—	Mach	Thrust— lb	Fuel flow— lb/hr	Bypass ratio	Turbine temp °R	HP turbine speed—%	LP turbine speed—%	Overall pressure ratio	Corr flow— lb/sec
ft	No.		2074	11.98	2060	61.4	89.2	10.88	507.8
0	0.5	2,508 4,908	3147	10.59	2310	72.8	94.3	14.50	569.5
0 0	0.5 0.5	6,722	3957	9.94	2460	80.3	96.8	16.99	609.0
0	0.5	8,648	4888	9.33	2610	86.9	99.0	19.66	645.2
ő	0.5	9,332	5227	9.14	2660	89.0	99.7	20.59	657.0
ő	0.5	11,588	6354	8.61	2810	94.9	101.7	23.60	693.5
Ō	0.6	702	1479	15.82	1910	56.8	83.5	7.80	496.4
0	0.6	2,286	2289	12.66	2110	64.6	90.4	10.95	536.7
0	0.6	4,092	3179	11.28	2310	72.9	94.5	13.72	576.6
0	0.6	6,508	4313	10.24	2510	82.6	97.8	16.95	624.1
0	0.6	7,763	4960	9.76	2610	86.7	99.3	18.67	645.0
0	0.6	8,418	5306	9.54	2660	88.7	100.0	19.56	655.3
0	0.6	10,586	6454	8.93	2810	94.4	102.1	22.42	687.4
5,000	0.3	12,874	5621	7.88	2810	97.0	100.6	27.44	721.3
5,000	0.4	11,756	5686	8.09	2810	96.9	100.8 101.1	26.55 25.47	719.0 714.5
5,000	0.5	10,801	5769	8.33	2810	96.6 96.0	101.4	24.24	707.1
5,000	0.6	9,974 990	5869 756	8.61 12.45	2810 1710	45.8	76.6	7.22	368.0
10,000	0.3 0.3	2,508	1284	10.36	1910	56.2	85.2	11.33	458.3
10,000 10,000	0.3	4,907	2169	9.38	2210	71.7	91.3	16.32	559.0
10,000	0.3	7,494	3181	8.64	2460	84.0	95.2	21.34	641.8
10,000	0.3	8,644	3662	8.35	2560	88.5	96.6	23.56	673.2
10,000	0.3	9,840	4188	8.07	2660	92.7	97.9	25.89	703.0
10,000	0.4	4,274	2192	9.88	2210	72.0	91.4	15.79	570.7
10,000	0.4	6,688	3213	8.95	2460	84.1	95.4	20.63	644.9
10,000	0.4	7,788	3701	8.62	2560	88.5	96.8	22.78	674.0
10,000	0.4	8,944	4236	8.29	2660	92.6	98.1	25.05	702.0
10,000	0.4	948	879	13.23	1760	49.3	79.0	7.92	422.8
10,000	0.4	2,340	1422	10.97	1960	59.2	86.4	11.68	494.6
10,000	0.4	10,846	5142	7.84	2810	98.9	100.2	28.74	743.8
10,000	0.5	885	1011	13.92	1810	53.1	81.1 87.6	8.47 11.88	470.3 524.3
10,000	0.5	2,139	1569 2401	11.54 10.23	2010 2260	62.1 74.7	92.4	15.97	593.8
10,000	0.5 0.5	4,112 5,983	3252	9.33	2460	84.0	95.6	19.75	646.5
10,000 10,000	0.5	7,588	4015	9.33 8.75	2610	90.3	97.7	22.90	685.6
10,000	0.5	8,164	4295	8.57	2660	92.3	98.4	24.02	698.6
10,000	0.5	10,015	5219	8.05	2810	98.3	100.4	27.58	737.0
10,000	0.6	494	1001	15.89	1810	54.8	80.5	7.81	496.7
10,000	0.6	1,697	1587	12.51	2010	63.2	87.7	11.26	540.9
10,000	0.6	3,542	2429	10.83	2260	74.7	92.6	15.14	598.9
10,000	0.6	5,863	3546	9.53	2510	86.0	96.6	19.73	657.4
10,000	0.6	6,374	3804	9.30	2560	87.9	97.4	20.73	668.8
10,000	0.6	7,475	4363	8.87	2660	91.8	98.7	22.83	692.1
10,000	0.6	9,314	5314	8.29	2810	97.6	100.8	26.26	727.5
10,000	0.7	8,734	5432	8.54	2810	96.6	101.2	24.85	715.3
15,000	0.5	709	816	14.09	1760	51.9	79.3	8.38	469.1
15,000	0.5	1,810	1292	11.51	1960 2210	61.4 74.3	86.2 91.0	12.03 16.33	526.9 599.4
15,000	0.5	3,519	1997	10.16 9.03	2460	85.8	94.9	21.37	667.1
15,000	0.5	5,579	2928 3376	9.03 8.64	2560	90.0	96.3	23.65	694.5
15,000 15,000	0.5 0.5	6,539 7,552	3868	8.27	2660	94.0	97.7	26.05	721.0
15,000	0.5	9,269	4711	7.76	2810	100.4	99.9	30.02	762.2
15,000	0.6	669	940	14.58	1810	56.0	81.4	8.85	509.1
15,000	0.6	1,706	1432	12.04	2010	64.4	87.4	12.15	553.5
15,000	0.6	3,440	2195	10.45	2260	76.8	92.1	16.40	617.2
15,000	0.6	5,051	2973	9.41	2460	85.5	95.2	20.31	664.2
15,000	0.6	6,477	3677	8.74	2610	91.5	97.4	23.62	700.8
15,000	0.6	6,992	3937	8.53	2660	93.4	98.1	24.80	713.1
15,000	0.6	8,663	4797	7.96	2810	99.4	100.1	28.57	750.1
15,000	0.7	653	1069	15.15	1860	60.0	83.0	9.10	540.8

Table A-XXV. (cont)

			Fuel		Turbine	HP	LP	Overall	Corr
Alt—	Mach	Thrust—	flow-	Bypass	temp—	turbine	turbine	pressure	flow—
ft	No.	<u>lb</u>	lb/hr	ratio	<u>°R</u>	speed—%	speed—%	ratio	Ib/sec
15,000	0.7	1,665	1590	12.52	2060	67.5	88.6	12.20	575.1
15,000 15,000	0.7 0.7	3,043	2232	11.04	2260 2460	76.9 85.0	92.4 95.6	15.47 19.17	618.7 658.9
15,000	0.7	4,603 5,992	3029 3750	9.81 9.05	2610	90.7	95.6 97.8	22.31	690.7
15,000	0.7	6,506	4018	8.81	2660	92.6	98.5	23.44	701.9
15,000	0.7	8,154	4903	8.18	2810	98.2	100.5	27.03	735.5
15,000	8.0	669	1210	15.59	1910	63.4	84.5	9.23	563.1
15,000	0.8	1,407	1624	13.39	2060	68.2	88.7	11.46	582.6
15,000	0.8	3,090	2469	11.25	2310	78.7	93.5	15.36	626.3
15,000	0.8	4,677	3333	9.92	2510	86.1	96.8	18.97	659.9
15,000 15,000	0.8 0.8	5,601	3840 4115	9.36	2610 2660	89.7 91.5	98.2 98.9	20.97 22.03	678.3 688.3
15,000	0.8	6,101 7,738	5028	9.11 8.44	2810	97.0	101.0	25.42	720.7
20,000	0.5	8,559	4245	7.45	2810	102.7	99.4	32.87	790.4
20,000	0.6	8,022	4320	7.63	2810	101.5	99.6	31.26	775.4
20,000	0.7	7,578	4412	7.84	2810	100.1	99.9	29.54	759.2
20,000	0.8	7,202	4520	8.08	2810	98.7	100.3	27.74	742.3
25,000	0.5	853	692	12.44	1760	54.8	80.2	10.45	501.1
25,000	0.5	1,702	1034	10.85	1960	64.9	85.2	14.05	561.6
25,000	0.5	3,387	1730	9.28	2261	80.5	90.5	20.33	654.5
25,000	0.5	4,753	2342	8.42	2460	89.2	93.5	25.29	713.3
25,000 25,000	0.5 0.5	5,530	2703 3107	8.03 7.66	2560	93.5 98.1	94.9 96.5	28.07 31.08	742.7 773.4
25,000	0.5	6,391 7,822	3806	7.00 7.13	2660 2810	98.1 104.6	96.5 99.1	36.13	819.6
25,000	0.6	626	694	13.75	1760	56.1	80.0	9.80	521.6
25,000	0.6	1,419	1046	11.57	1960	65.2	85.3	13.33	570.7
25,000	0.6	3,051	1756	9.69	2261	80.3	90.7	19.32	653.3
25,000	0.6	4,386	2383	8.69	2460	88.7	93.8	24.07	705.9
25,000	0.6	5,140	2751	8.26	2560	92.7	95.2	26.71	732.5
25,000	0.6	5,981	3164	7.85	2660	97.1	96.7	29.59	760.1
25,000	0.6	7,384	3876	7.30	2810	103.7	99.2	34.37	804.1
25,000	0.7	435	693	15.35	1760	57.6	79.5	9.06	540.5
25,000	0.7	1,193	1064	12.37	1960	65.8	85.5	12.58	579.6
25,000 25,000	0.7 0.7	2,764 4,067	1788 2432	10.13 8.99	2260 2460	79.9 87.9	91.1 94.2	18.23 22.75	649.3 695.4
25,000	0.7	4,831	2814	8.50	2560	91.8	95.6	25.30	720.1
25,000	0.7	5,639	3233	8.07	2660	95.9	97.1	27.98	745.0
25,000	0.7	7,009	3959	7.50	2810	102.4	99.4	32.47	786.8
25,000	0.8	659	895	14.53	1860	63.0	83.1	10.26	571.8
25,000	0.8	1,463	1303	12.20	2060	70.7	87.8	13.45	604.0
25,000	0.8	2,549	1833	10.58	2261	79.5	91.5	17.17	643.9
25,000	0.8	3,810	2491	9.30	2460	86.9	94.6	21.39	682.6
25,000 25,000	0.8	4,561	2884	8.77	2560	90.7	96.1	23.79	705.6
25,000	0.8 0.8	5,353 6,667	3315 4050	8.32 7.73	2660 2810	94.6 100.8	97.5 99.7	26.31 30.43	729.2 767.5
30,000	0.5	6,966	3367	6.82	2810	106.1	98.8	39.55	844.7
30,000	0.6	6,683	3448	6.97	2810	105.3	98.9	37.83	832.9
30,000	0.7	6,413	3533	7.16	2810	104.4	99.0	35.82	817.0
30,000	0.8	6,139	3617	7.39	2810	103.2	99.2	33.57	797.2
32,000	0.72	494	600	14.30	1760	59.1	79.5	10.25	557.8
32,000	0.72	1,147	901	11.86	1960	68.1	84.7	13.91	600.7
32,000 32,000	0.72 0.72	2,473 3,618	1517 2072	9.60 8.48	2261 2460	81.7 89.8	90.1	20.36	672.1
32,000	0.72	4,264	2399	8.01	2560	94.1	93.2 94.7	25.60 28.53	723.2 750.2
32,000	0.72	4,967	2763	7.61	2660	98.5	96.3	31.66	779.6
36,089	0.5	475	403	13.11	1660	51.2	75.2	9.95	494.1
36,089	0.5	1,476	778	10.25	1960	69.2	83.4	16.72	606.4
36,089	0.5	2,759	1309	8.60	2260	84.0	88.6	24.62	706.5
36,089	0.5	3,852	1787	7.71	2460	93.6	91.9	31.08	774.4
36,089	0.5	4,482	2074	7.31	2560	98.3	93.7	34.79	8.808

Table A-XXV. (cont)

			Fuel	_	Turbine	HP	LP	Overall	Corr
Alt— ft	Mach No.	Thrust— lb	flow— lb/hr	Bypass ratio	temp— °R	turbine speed—%	turbine speed—%	pressure ratio	flow— lb/sec
36,089	0.5	5,090	2379	6.93	2660	102.2	95.6	38.56	838.8
36,089	0.5	5,675	2804	6.43	2810	105.7	98.3	43.26	855.3
36,089	0.6	644	530	12.55	1760	58.2	79.1	11.77	548.7
36,089	0.6	1,302	791	10.80	1960	69.4	83.7	15.92	611.5
36,089	0.6	2,541	1332	8.88	2261	83.6	88.9	23.44	700.1
36,089	0.6	3,607	1821	7.90	2460	92.6	92.1	29.61	761.0
36,089	0.6	4,230	2114	7.47	2560	97.4	93.9	33.14	794.1
36,089	0.6	4,866	2434	7.09	2660	101.5	95.7	36.85	826.2
36,089	0.6	5,594	2904	6.58	2810	106.1	98.4	41.83	853.0
36,089	0.7	527	539	13.54	1760	59.4	79.1	11.11	563.0
36,089	0.7	1,155	807	11.38	1960	69.6	84.0	15.07	614.4
36,089	0.7	2,351	1359	9.19	2260	82.9	89.3	22.16	690.0
36,089	0.7	3,405	1862	8.11	2460	91.5	92.5	28.04	746.0
36,089	0.7	4,004	2159	7.67	2560	96.1	94.1	31.31	776.9
36,089	0.7	4,645	2490	7.28	2660	100.6	95.9	34.84	808.9
36,089	0.7	5,543	3015	6.77	2810	106.2	98.6	40.13	848.0
36,089	0.72	506	541	13.75	1760	59.6	79.1	10.97	565.4
36,089	0.72	1,128	810	11.50	1960	69.6	84.0	14.89	614.5
36,089	0.72	2,319	1365	9.25	2260	82.7	89.4	21.90	687.7
36,089	0.72	3,368	1871	8.16	2460	91.2	92.5	27.70	742.8
36,089	0.72	3,963	2169	7.72	2560	95.8	94.1	30.93	773.4
36,089	0.72	4,604	2501	7.33	2660	100.4	95.9	34.42	805.2
36,089	0.8	431	549	14.60	1760	60.4	79.1	10.40	573.1
36,089	0.8	1,030	826	11.96	1960	69.4	84.3	14.19	613.6
36,089	0.8	2,203	1394	9.50	2260	82.0	89.8	20.86	678.0
36,089	0.8	3,233	1909	8.36	2460	90.3	92.9	26.36	730.3
36,089	0.8	3,813	2212	7.90	2560	94.7	94.4	29.41	758.7
36,089	0.8	4,445	2551	7.50	2660	99.3	96.1	32.69	789.5
36,089	8.0	5,427	3116	6.97	2810	105.3	98.8	37.95	833.9

Table A-XXVI.

Performance of reference turbofan engine on 86°F day.

Alt— ft	Mach No.	Thrust—	Fuel flow— lb/hr	Bypass ratio	Turbine temp— ^R	HP turbine speed—%	LP turbine speed—%	Overall pressure ratio	Corr flow— lb/sec
0	0.0	19,905	6451	7.74	2960	98.5	103.8	26.95	701.1
0	0.1	17,688	6462	7.78	2960	98.4	103.8	26.82	701.3
0	0.2	15,847	6494	7.89	2960	98.4	103.9	26.43	701.7
0	0.3	14,319	6551	8.05	2960	98.4	104.1	25.82	701.9

REFERENCES AND BIBLIOGRAPHY

REFERENCES

- 1. John W. Swihart and Jack I. Minnick, "A Fresh Look at Aviation Fuel Prices," AIAA Journal, March 1980.
- 2. Air Force Energy Plan, Air Force Energy Office (LEYSF), January 1981.
- "The Aero Gas Turbine Industry: Today and the Future," Kearney: Management Consultants, November 1981.
- "A Study to Define the Research and Technology Requirements for Advanced Turbo/Propfan Transport Aircraft," Douglas Aircraft Company, NASA CR-166138, February 1981.
- "Propfan Data Package: Performance, Near-Field Noise, Far-Field Noise," Hamilton Standard, United Technologies, SP07A82, May 1982.
- J. C. Muehlbauer et al, "Turboprop Cargo Aircraft Systems Study," Lockheed-Georgia Company, NASA CR-165813, November 1981.
- "Study of Turboprop Systems Reliability and Maintenance Costs," NASA CR-135192, June 1978.
- "Propfan Data Package: Maintenance," Hamilton Standard, United Technologies, SP04A82, May 1982.
- International Standards and Recommended Practices, Annex 16 to the convention of International Civil Aviation, Volume II, Aircraft Engine Emissions, 1981.
- 10. "Propfan Far-Field Noise Prediction," Hamilton Standard, United Technologies, SP16A77, 31 October 1977.
- 11. "Advanced Turboprop Program Summary," viewgraph presentation, Douglas Aircraft Company, May 1982.
- "Parametric Study of Transport Aircraft System Cost and Weight, Science Applications Incorporated/Douglas Aircraft Company," NASA CR-151970, April 1977.
- "Lockheed Model No. 188 Specification," Lockheed-California Company, Report No. 10637, October 1956.
- "Propfan Data Package: Weights," Hamilton Standard, United Technologies, SP06A82, May 1982.

BIBLIOGRAPHY

Environmental Protection Agency, "Control of Air Pollution from Aircraft and Aircraft Engines," Federal Register Vol-

ume 38, No. 136, pp 10987-19103, 17 July 1973.

Environmental Protection Agency, "Control of Air Pollution from Aircraft and Aircraft Engines," Proposed Rules (Changes) Federal Register Volume 43, No. 58, pp 12615-12634, 24 March 1978.

Environmental Protection Agency, "Control of Air Pollution from Aircraft and Aircraft Engines," Final Rules, Federal Register Volume 47, No. 251, pp 58462-58474, 30 December 1982.

R. Munt and E. Danielson, Aircraft Technology Assessment, Status of the Gas Turbine Program, U.S. Environmental Protection Agency, Washington, December 1976.

"Advanced Propfan Engine Technology (APET) Definition Study," Technical Proposal, Detroit Diesel Allison, General Motors Corporation, EDR 10790, September 1981.

International Civil Aviation Organization, Committee on Aircraft Engine Emissions, Second Meeting, Montreal, Canada, May 1980.

International Civil Aviation Organization, Committee on Aircraft Engine Emissions, Background Information Paper No. 29, Emissions Data Bank, Montreal, Canada, November 1980.

International Civil Aviation Organization, International Standards and Recommended Practices, Environmental Protection, Annex 16, Volume II, Aircraft Engine Emissions, Montreal, Canada, 1981.

Yarmartino et al, *Impact of Emissions on Air Quality in the Vicinity of Airports*, Volume I: Recent Airport Measurement Programs, Data and Sub-Model Development, Argoune National Laboratory, Federal Aviation Administration Report FAA-EE-80-09A, Washington, DC, July 1980.

Boeing Air Quality Monitor Test at the Seattle-Tacoma International Airport, Boeing Airplane Company, Report D6-51459, Seattle, Washington, 24 June 1982.

Boeing Air Quality Monitor Test at Los Angeles International Airport, Verbal

Report to Aerospace Industries Association, Washington, DC, 1 July 1982.

APPENDIX B

TASK II. ENGINE CONFIGURATION AND CYCLE EVALUATION

TABLE OF CONTENTS

	Page
Introduction	R-1
Cycle and Configuration Selection	B-2
Initial Screening	B-2
Final Screening	B-3
Engine Preliminary Designs	B-9

LIST OF ILLUSTRATIONS

Figure	Title	Page
B-1	Configurations selected for further evaluation	B-3
B-2	Engine configuration evaluation parameters	B-4
B-3	Engine PD436-1B performance relationships (axial compressor)	
B-4	Engine PD436-1B size relationships (axial/axial compressor)	
B-5	Cost trend for engines with axial/centrifugal compressors	
B-6	Cost trend for engines with axial compressors	
B-7	Weight trend for engines with axial/centrifugal compressors	
B-8	Weight trend for engines with axial compressors	
B-9	Diameter trend for engines with axial/centrifugal compressors	
B-10	Diameter trend for engines with axial compressors	
B-11	Length trend for engines with axial/centrifugal compressors	
B-12	Length trend for engines with axial compressors	
B-13	Airplane takeoff gross weight sensitivity to engine overall pressure ratio (axial/centrifugal compressor,	
	1000 nmi)	B-6
B-14	Airplane takeoff gross weight sensitivity to engine cycle pressure and temperature (axial/centrifugal	
	compressors, 1000 nmi)	B-6
B-15	Direct operating cost sensitivity to engine cycle pressure and temperature (axial compressors, 300 nmi)	
B-16	Direct operating cost sensitivity to engine cycle pressure and temperature (axial/centrifugal compressors, 1000	
	nmi)	B-7
B-17	Direct operating cost sensitivity to engine cycle pressure and temperature (axial/centrifugal compressors, 300	
	nmi)	B-7
B-18	Direct operating cost sensitivity to engine cycle pressure and temperature (axial/centrifugal compressors, 1000	
	nmi)	B-7
B-19	Fuel burned sensitivity to engine cycle pressure and temperature (1000 nmi)	B-8
B-20	Fuel burned sensitivity to engine cycle pressure and temperature (300 nmi)	
B-21	Engine performance for scaled EEE component technology	
B-22	PD436-10 engine general arrangement for axial/centrifugal compressor	
B-23	PD436-11 engine general arrangement for axial/axial compressor	
B-24	Low pressure axial compressor common to both Engines PD436-10 and PD436-11	
B-25	Low pressure compressor flow path	B-12
B-26	High pressure centrifugal compressor of Engine PD436-10	B-12
B-27	High pressure centrifugal compressor flow path	B-12
B-28	Rough model stress summary of HP centrifugal compressor	B-13
B-29	High pressure axial compressor of Engine PD436-11	B-13
B-30	APET compressor	B-14
B-31	Fold-back combustor for the axial/centrifugal compressor configuration of Engine PD436-10	
B-32	Axial combustor-reverse diffuser of Engine PD436-11	B-15
B-33	Turbine flow path for the axial/centrifugal compressor configuration (PD436-10)	B-16
B-34	Turbine flow path for the axial/axial compressor configuration (PD436-11)	B-16
B-35	High pressure turbine for Engine PD436-10 (axial/centrifugal compressor)	B-17
B-36	High pressure turbine for Engine PD436-11 (axial/axial compressor)	B-18
B-37	High pressure turbine inlet stator cross section	B-18
B-38	High pressure turbine rotor cross section	B-19
B-39	Low pressure turbine for Engines PD436-10 and PD436-11	B-20
B-40	Low pressure turbine stator vane cross section	
B-41	Low pressure turbine rotor blade cross section	
B-42	Power turbine for Engines PD436-10 and PD436-11	B-21

PRECEDING PAGE BLANK NOT FILMED

LIST OF TABLES

Title	Page
Candidate engine configurations	B-2
Final screening results	B-8
Design specifications of APET turboprop engines	B-9
Combustor design parameters for axial/centrifugal compressor flow path	B-14
Combustor design parameters for axial compressor flow path	B-15
Turbine cooling summary	B-17
High pressure turbine aerodynamic design point conditions for Engine PD436-10	B-17
Estimated design point HP turbine aerodynamics for Engine PD436-10 (axial/centrifugal compressor)	B-17
High pressure turbine aero design point conditions at 0.72 M _N , 32,000 ft	B-18
Estimated design point HP turbine aerodynamics for Engine PD436-11 (axial/axial compressor)	B-18
Low pressure turbine aerodynamic design point conditions for Engines PD436-10 and PD436-11 at 0.72 M _N ,	
32,000 ft	B-19
Estimated design point LP turbine aerodynamics for Engines PD436-10 and PD436-11	B-19
Power turbine aerodynamic design point conditions for Engine PD436-10	B-21
Estimated design point LP turbine aerodynamics for Engines PD436-10 and PD436-11	B-21
	Candidate engine configurations Final screening results Design specifications of APET turboprop engines Combustor design parameters for axial/centrifugal compressor flow path Combustor design parameters for axial compressor flow path Turbine cooling summary High pressure turbine aerodynamic design point conditions for Engine PD436-10 Estimated design point HP turbine aerodynamics for Engine PD436-10 (axial/centrifugal compressor) High pressure turbine aero design point conditions at 0.72 M _N , 32,000 ft Estimated design point HP turbine aerodynamics for Engine PD436-11 (axial/axial compressor) Low pressure turbine aerodynamic design point conditions for Engines PD436-10 and PD436-11 at 0.72 M _N , 32,000 ft Estimated design point LP turbine aerodynamics for Engines PD436-10 and PD436-11 Power turbine aerodynamic design point conditions for Engine PD436-10

INTRODUCTION

The engine configuration and cycle evaluation work performed in the APET study is described in this section along with preliminary designs of the two engines selected for use in the mission analysis work. The procedures and assumptions identified in Task I were used to arrive at the engine configurations and the cycle conditions selected. The selection criteria were designed to place priority on the fuel burned and direct operating cost of the reference turboprop-powered airplane. Therefore, engine specific fuel consumption is a key parameter as are reliability and ease of maintenance. Study guidelines dictate that the component technology levels assumed be advanced for the production date of the early

1990s. Specifically, it is anticipated that new engines in commercial service in the 1990s will have demonstrated component performance representing improvements over the EEE engines. This improved component performance will be in two areas: (1) the ability to scale EEE technology to the smaller size APET turboprop engines in the 9000 to 15,000 shp power class and (2) new design and manufacturing methods directed toward solving the problems associated with smaller size, higher pressure ratio engines. The results of the engine preliminary design activity are available in the form of a computer card deck with an instruction manual and a performance data package.

CYCLE AND CONFIGURATION SELECTION

The candidate engine cycles and configurations for a turboprop-powered commercial airliner were evaluated to arrive at the most favorable match of fuel efficiency and direct operating cost. Two engine configurations were taken through preliminary design and performance analysis to provide engine definition for the reference airplane modeling.

The cycle selection procedure was initiated with the development of engine sensitivity data to evaluate the engine cycle and configuration parameters. Sensitivity data were generated by scaling the reference turboprop engine (PD436-1B) developed in Task I to fit the engine size requirement of the reference airplane and flying the mission to determine fuel burned and direct operating cost. The procedure was then repeated with engines similar to the reference turboprop engine except that the pressure ratio and rotor inlet temperature were changed. The dependent variables of engine size, performance, and cost were adjusted using specific horsepower, specific fuel consumption, and cost relationships. Axial and centrifugal high-pressure compressors were also evaluated to round out the parametric fuel burned and direct operating cost data. These results were weighed against the increased complexity required in each design and the impact on reliability and maintenance.

INITIAL SCREENING

Based on previous Allison engine cycle optimization studies and preliminary engine designs, the seven configurations shown in Table B-I were selected for the initial screening process. These configurations are compatible with pressure ratios in excess of those possible with only single-spool compressors, which are limited to approximately 25:1. The configurations were also chosen to provide an option relative to the type of compressor—axial or centrifugal—and the possibility of driving a booster compressor with the power turbine. The seven candidate engine configurations are identified as follows:

- Configuration 1 is a dual-spool engine with an axial flow compressor and a free power turbine.
- Configuration 2 is a dual-spool engine with an axial/ centrifugal compressor and a free power turbine.
- Configuration 3 is a three-spool engine with axial/ axial dual-spool compressors and a free power turbine
- Configuration 4 is a three-spool engine with axial/ centrifugal dual-spool compressors and a free power turbine.
- Configuration 5 is a dual-spool engine with a centrifugal/centrifugal single-spool compressor and a free power turbine.

Table B-I.
Candidate engine configurations.

Engine configuration	Compressor type Single-spool axial	Total number of spools Dual-spool engine
2. <u>FR</u> 50	Single-spool axial/centrifugal	Dual-spool engine
3	Dual-spool axial	Three-spool engine
4. 2. 40	Dual-spool axial/centrifugal	Three-spool engine
5. <u>44 F</u> P	Single-spool centrifugal	Dual-spool engine
6. <u>4 4 49</u> 7	Dual-spool centrifugal	Three-spool engine
7. 7	Dual-spool axial	Dual-spool engine

- Configuration 6 is a three-spool engine with centrifugal/centrifugal dual-spool compressors and a free power turbine.
- Configuration 7 is a dual-spool engine with an axial flow high pressure compressor and an axial flow low pressure compressor on the power turbine shaft.

The seven candidate engine configurations were subjected to a qualitative examination to arrive at a ranking of their potential. The results of this examination indicate that Configurations 5, 6, and 7, the dual-centrifugal and booster compressor configurations, are the weakest candidates. These three configurations were screened out for the reasons discussed in the following paragraphs.

Configuration 5 was not selected for further evaluation because the two-stage centrifugal compressor on a single spool has several major disadvantages. First, the overall compressor efficiency tends to be less than compressor designs using the low pressure axial flow compressor. Second, having the two centrifugal stages on a single shaft introduces part power surge margin difficulties because of the

speed restrictions of the centrifugal stages. In previous inhouse studies, the dual-centrifugal compressors were found to have weight and size penalties in addition to having poor acceleration and deceleration due to rotor inertia.

Configuration 6, the three-spool engine with dual-centrifugal compressors, was not selected for further evaluation; even with this compressor arrangement solving the part power operational difficulties noted for Configuration 5, the reduced efficiency levels of dual-centrifugal compressors are a significant disadvantage compared with axial/centrifugal and axial/axial stage designs.

Configuration 7, with the LP compressor driven by the power turbine, was not selected for further evaluation primarily because it represents a compromise for off design operation and tends to be more limited in growth potential than free turbine designs. It is recognized that by introducing the additional complexity in controls and safety features the booster design would be satisfactory for the APET mission. However, for purposes of this study, Allison favors the free turbine designs, Configurations 1 through 4, for this application.

FINAL SCREENING

The four configurations selected for further evaluation (see Figure B-1) include dual- and three-spool engines. These have compressor efficiency advantages over dual-centrifugal compressors and offer increased growth potential over boosted compressor designs. In this study the single-spool compressors are limited to a maximum pressure ratio of 25:1. The dual-spool compressors are considered for overall pressure ratios above 25:1. Dual-spool compressor designs have the potential to optimize the work split of the two gas generator turbine stages. This advantage is somewhat offset by the requirement for major component assemblies and balancing, additional mainshaft seals, and additional bearings. This complicates implementation of the modular construction concept.

The four final engine configurations were used to define a matrix spanning a range of curise turbine inlet temperatures from 2000°F to 2400°F; overall pressure ratios from 20:1 to 40:1; and axial, axial/axial, and axial/centrifugal compressors. This array of engine configurations is shown in Figure B-2. Engine 7 of the array is PD436-1B, the 15,000 shp reference turboprop engine described in Appendix A. As indicated in Figure B-2, the reference turboprop engine has a single-spool axial flow compressor with an overall pressure ratio of 25:1. The rotor inlet temperature is 2200°F at the cruise condition. The other 29 engines of the array were defined relative to Engine 7 with respect to specific fuel consumption, weight, cost, size, and airflow size. This was accomplished by applying relationships of engine characteristics as functions of cycle pressure ratio, turbine temperature, and compressor type using PD436-1B as the baseline engine. For example, the performance parameter shaft specific fuel consumption varies with overall pressure ratio and turbine temperature for

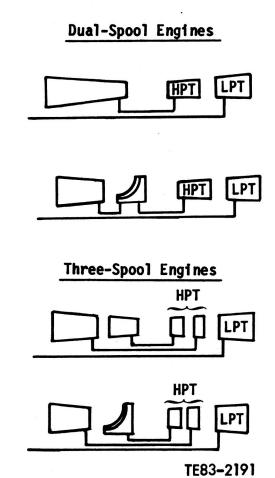
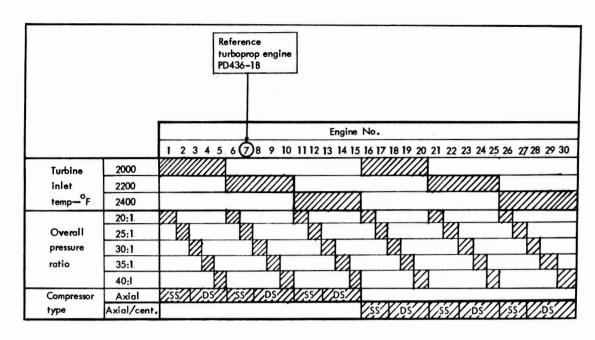


Figure B-1. Configurations selected for further evaluation.

engine PD436-1B, as shown in Figure B-3. This relationship includes the effects of component efficiency and cooling air requirements to maintain a constant metal temperature at the various combinations of gas and compressor discharge temperature. These curves do not exhibit the usual inflection point because the advanced technology level assumed results in the minimum specific fuel consumption at higher pressure ratios than for the less advanced technology level.

The effects of engine size variation with cycle pressure and temperature were determined by the specific horse-power relationships shown in Figure B-4. The trend is toward lower specific horse-power at higher pressure ratios. This effect results in the requirement for larger engines at higher cycle pressures for a given turbine temperature. Increasing turbine temperature reduces engine size for a given power level. Similar relationships were developed for length, diameter, weight, and cost; these are shown in Figures B-5 through B-12. With the engine characteristics defined, the airplane model developed in Task I was flown for each case (30 engines) over the design mission of 1000 nmi and over the alternate 300 nmi mission. Appropriate installation factors, as shown in Appendix A, were applied. The results of these calculations show the effect of engine cycle and configuration



Takeoff power class: 15,000 shp SS—single spool compressor DS—dual spool compressor

Example: Engine No. 7 has 2200°F turbine inlet temperature, 25:1 overall pressure ratio, and axial single-spool compressor

TE83-2192

Figure B-2. Engine configuration evaluation parameters.

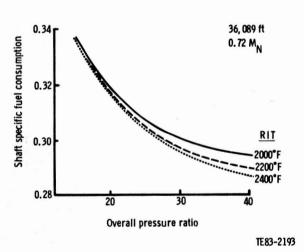


Figure B-3. Engine PD436-1B performance relationships (axial compressor).

parameters on airplane physical size, operating cost, and fuel consumption. These are discussed in the following paragraphs.

Takeoff gross weight (TOGW) was calculated for the 30 cases by making changes to the baseline airplane model (powered by PD436-1B turboprop engines) due to the engine fuel consumption, size, weight, and cost changing with compressor type and cycle conditions. The results of these calcu-

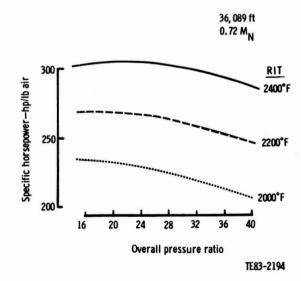


Figure B-4. Engine PD436-1B size relationships (axial/axial compressor).

lations are shown in Figure B-13 for the axial flow compressors and Figure B-14 for axial/centrifugal compressors. Engines using axial compressors result in a lighter weight airplane, as can be seen by comparing Figures 13 and 14. Increasing the overall pressure ratio and cruise temperature causes the airplane to be lighter in all cases. A reduction in

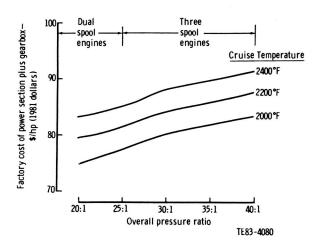


Figure B-5. Cost trend for engines with axial/centrifugal compressors.

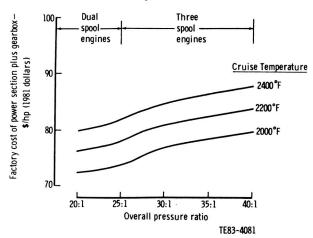


Figure B-6. Cost trend for engines with axial compressors.

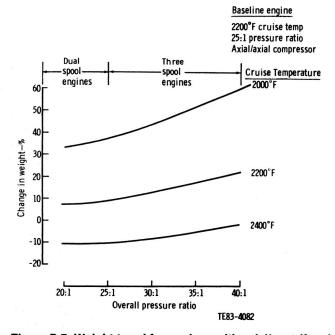


Figure B-7. Weight trend for engines with axial/centrifugal compressors.

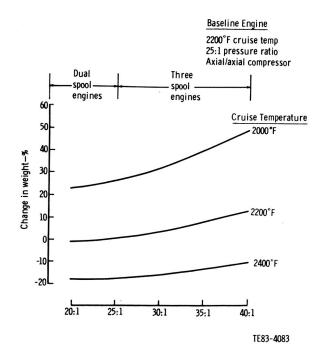


Figure B-8. Weight trend for engines with axial compressors.

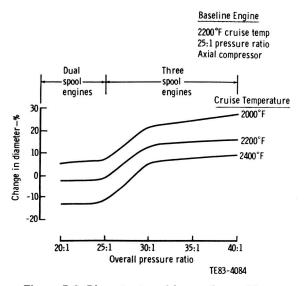


Figure B-9. Diameter trend for engines with axial/centrifugal compressors.

takeoff gross weight of 1.4% is possible by increasing the overall pressure ratio from 25:1 to 38:1 on the axial engine. Substituting an axial/centrifugal compressor results in only a 1.0% TOGW reduction at an overall pressure ratio of 38.1. In addition to the weight savings, direct operating cost (DOC) is 0.8% less than the baseline.

DOC results for 300 nmi and 1000 nmi missions are shown in Figures B-15 and B-16 for the axial compressors and in Figures B-17 and B-18 for the axial/centrifugal com-

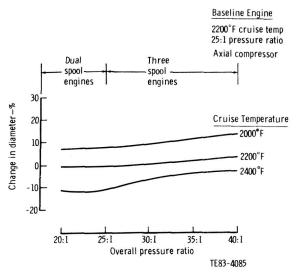


Figure B-10. Diameter trend for engines with axial compressors.

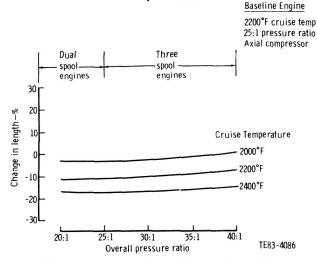


Figure B-11. Length trend for engines with axial/centrifugal compressors.

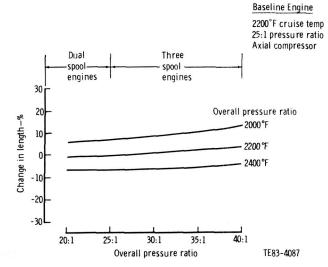


Figure B-12. Length trend for engines with axial compressors.

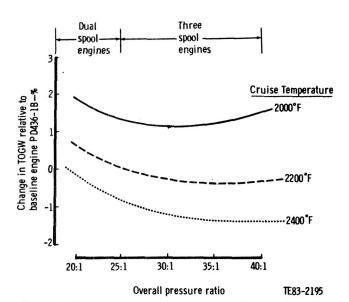


Figure B-13. Airplane takeoff gross weight sensitivity to engine overall pressure ratio (axial/centrifugal compressor, 1000 nmi).

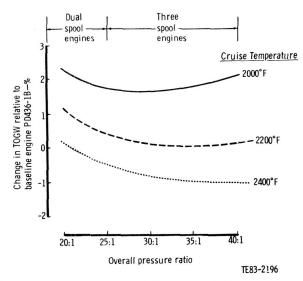


Figure B-14. Airplane takeoff gross weight sensitivity to engine cycle pressure and temperature (axial/centrifugal compressors, 1000 nmi).

pressor designs. As expected, the improved specific fuel consumption of the engine becomes more important for the longer, 1000 nmi case. However, the DOC reduction of 0.5% noted for the shorter mission indicates that significant improvement can be achieved by high pressure ratio engine designs. The case is not as strong for the axial/centrifugal compressors. In fact, the lower pressure ratio axial compressor engines are more cost effective than the higher pressure ratio axial/centrifugal compressor engines.

In the case of fuel burned, as indicated in Figure B-19 for the 1000 nmi mission and in Figure 20 for the 300 nmi mission, the improved engine specific fuel consumption of higher

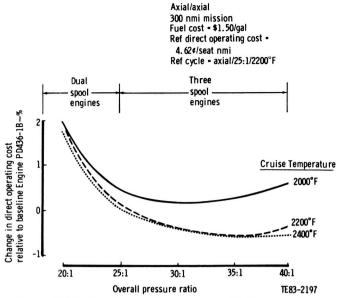


Figure B-15. Direct operating cost sensitivity to engine cycle pressure and temperature (axial compressors, 300 nmi).

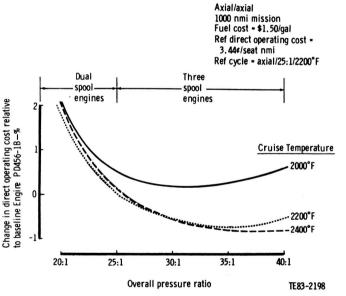


Figure B-16. Direct operating cost sensitivity to engine cycle pressure and temperature (axial/centrifugal compressors, 1000 nmi).

pressure and higher temperature cycles results in increased fuel savings. The benefit of 38:1 compared with the 25:1 baseline is a fuel savings of 6.8% for the axial compressor at 1000 nmi and 6.6% at 300 nmi.

The sensitivity data were applied to the four candidate engine configurations selected in the initial screening process. Based on the trend of fuel burned decreasing with increasing pressure ratio and temperature, the inclination is to design to maximize these values. However, because of other factors involved in high pressure ratio engines such as complexity

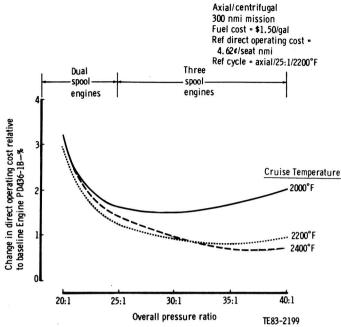


Figure B-17. Direct operating cost sensitivity to engine cycle pressure and temperature (axial/centrifugal compressors, 300 nmi).

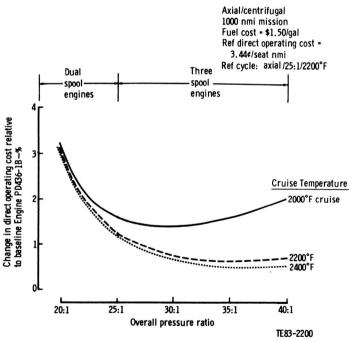


Figure B-18. Direct operating cost sensitivity to engine cycle pressure and temperature (axial/centrifugal compressors, 1000 nmi).

and cost, the direct operating cost advantage is limited at 35:1 to 40:1. For this reason, the design point pressure ratio of the dual-spool compressor designs was set at 38:1 for both compressor types. The turbine temperature of 2400°F

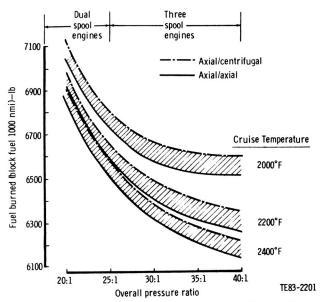


Figure B-19. Fuel burned sensitivity to engine cycle pressure and temperature (1000 nmi).

provides a good match of performance and life requirements for the commercial application.

Increasing the temperature of the initial design would have the effect of making the engine smaller since the specific horsepower increases with temperature, but the impact on improving specific fuel consumption would be marginal. Therefore, the 2400°F cruise temperature is a good choice for the 38:1 overall pressure ratio considering the requirements for long life of the hot section and future growth potential.

The selected pressure ratio and temperature values for the single-spool compressor designs is quite different.

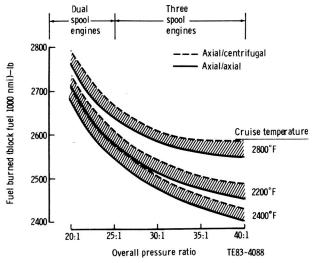


Figure B-20. Fuel burned sensitivity to engine cycle pressure and temperature (300 nmi).

Because of part power surge margin difficulties due to the compressor stages being on a single shaft, the two single-spool compressor designs were limited to an overall pressure ratio of 25:1. The turbine temperature of 2200°F is a good match with the lower pressure ratio. While the single-spool compressor design is limited in pressure level due to off design operational considerations, there are advantages associated with lower pressure ratio engines. These advantages are favorable design, cost, and reliability features associated with the reduced shafting and bearings. As a result, the direct operating cost of the axial flow, single-spool compressor configuration is only 0.7% higher than for the best three-spool engine.

In summary, the DOC and fuel burned data, shown in Table B-II, are the basis for selecting the three-spool engines

Table B-II.
Final screening results.

		Cruise co 32,000 ft		Thrust sfc at	sfc at		Direct operating cost	
Engine No. (Ref Fig B-2)	Engine arrangement	Pressure ratio	Turbine temp	midpoint cruise	300 nmi	1000 nmi	300 nmi	1000 nmi
7 (PD436-1B)	Single-spool axial compressor	25.0	2200	0.476	2580 (+7.1%)	6580 (+7.0%)	4.62 (+0.7%)	3.44 (+0.9%)
22	Single-spool axial/centrifugal compressor	25.0	2200	0.480	2610 (+8.3%)	6660 (+8.3%)	4.68 (+2.0%)	3.49 (+2.3%)
14/15	Dual-spool axia!/axial compressor	38.0	2400	0.451	2410 (Base)	6150 (Base)	4.59 (Base)	3.41 (Base)
29/30	Dual-spool axial/centrifugal compressor	38.0	2400	0.455	2440 (+1.2%)	6220 (+1.1%)	4.62 (+0.7%)	3.46 (+1.5%)

with axial/axial and axial/centrifugal compressors for the preliminary design activity.

ENGINE PRELIMINARY DESIGNS

Two engines, designated PD436-10 and PD436-11. were evaluated in the preliminary design phase. The mechanical design features associated with the HP axial (PD436-11) and centrifugal (PD436-10) compressors were evaluated early in the preliminary design of the two 10,000 shp class turboprop engines. It was determined that the scaling required from the 15,000 shp class PD436-1B turboprop to the 10,000 shp APET size resulted in a reduction in compressor polytropic efficiency from 91 % to 90%. The specific fuel consumption trend with overall pressure ratio for this case is shown in Figure B-21. The minimum specific fuel consumption for this case occurs at 32.5:1 overall pressure ratio. Since fuel burned was the primary criterion for configuration selection, it was decided that the design point of the turboprop engines should be at 32.5:1, the minimum specific fuel consumption point. The turbine temperature was selected at 2200°F because there was not any advantage to higher turbine temperatures, as shown in Figures B-15 through B-18.

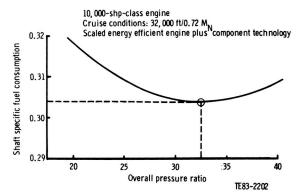


Figure B-21. Engine performance for scaled EEE component technology.

The two APET turboprop engines are defined as indicated in Table B-III. The engine general arrangement for the axial/centrifugal compressor is shown in Figure B-22, and the arrangement for the axial/axial compressor is shown in Figure B-23. These engines are both three-spool configurations with an HP turbine driving the HP compressor, an LP turbine driving an LP turbine, and a power turbine driving the propfan through an 8.9:1 reduction gearbox.

Low Pressure Axial Compressor

The LP axial compressors of these two engines are identical. This compressor features an integral rotor drum and a cast Ti 6Al-4V case to reduce weight. Aluminum graphite abradable tip seals and low leakage sealed rotor dovetails are used to increase the power retention characteristics in service. Materials of the early 1990s would be targeted for

Table B-III.

Design specifications of APET turboprop engines.

	Engine PD436-10	Engine PD436-11
Size—shp	10,000	10,000
Overall pressure ratio	32.5:1	32.5:1
Turbine temperature—°F	2200 cruise	2200 cruise
	2500 takeoff	2500 takeoff
Compressor	Axial/centrifugal	Axial/axial
Turbine	HP/LP/power	HP/LP/power
Number of stages		
LP compressor	6	6
HP compressor	1	7
LP turbine	1	1
HP turbine	1	1
Power turbine	3	3 .

reduced manufacturing cost, weight, and improved strength and stability at high temperature. The use of castings such as cast titanium blades and cast integral ring stator vanes are examples. These features are highlighted in the LP compressor general arrangement drawing shown in Figure B-24. The design goals of the LP compressor are as follows:

- corrected flow = 54.4 lb/sec
- pressure ratio = 8.55:1
- adiabatic efficiency = 86.7 %
- polytropic efficiency = 90 %

The aerodynamic design is targeted toward relatively high stage loadings and low aspect ratios. The 90% polytropic efficiency is consistent with EEE performance goals. Performance will be achieved in six stages by an inlet hub/tip ratio of 0.52, an inlet tip speed of 1590 ft/sec, and an average aspect ratio of 1.44. The overall length is 18.13 in. The minimum blade height is 1.21 in. Minimum rotor and stator chord dimensions are 0.93 in. and 0.86 in., respectively. The flow path of the LP compressor is shown to scale in Figure B-25.

High Pressure Centrifugal Compressor

The HP centrifugal compressor of Engine PD436-10 is shown in Figure B-26. Near-term materials of the HP centrifugal compressor include high temperature Rene 95 for the impeller and cast Inco 718 for dimensional stability and reduced machining of the case. In the 1990s, diffusion bonded titanium aluminide/Ti 829 would have superior strength properties. The design goals of the high pressure centrifugal compressor are as follows:

- corrected flow = 8.8 lb/sec
- pressure ratio = 3.8:1
- adiabatic efficiency = 85.1 %
- polytropic efficiency = 87.6%

Design features of the advanced technology single-stage HP centrifugal compressor, selected to be consistent with technology verification in the late 1980s, are an inlet hub/tip

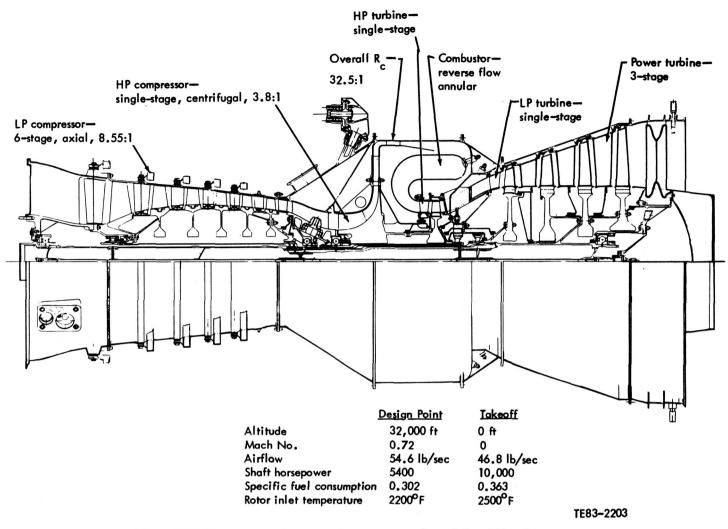


Figure B-22. PD436-10 engine general arrangement for axial/centrifugal compressor.

ratio of 0.66, inlet tip speed of 856 ft/sec, and specific speed of 0.64. The flow path, shown to scale in Figure B-27, consists of an 18-blade impeller with 40 deg of backsweep which discharges into a 2.0 area ratio 24-vane diffuser followed by a 90 deg turn annular dump, deswirl section. This flow path arrangement results in combustion section annulus velocities of 100 ft/sec maximum. The centrifugal compressor is off optimum in terms of basic design parameter selection. It has low specific speed and high hub/tip ratio to achieve the compromise of acceptable stress levels and good performance. Further design studies are needed to pursue optimal centrifugal compressor specific speed.

The centrifugal compressor was subjected to a first order structural analysis to determine the stress levels and degree of difficulty of matching structural and aerodynamic performance requirements. For purposes of the structural analysis, the operating condition of hot-day takeoff was used. At the hot-day takeoff condition, the centrifugal compressor stage has 48.24 lb/sec corrected flow, 27.5 pressure ratio,

and 25,433 rpm mechanical speed. The impeller disk was analyzed using uniform temperature finite element analysis techniques. Material properties were assessed at 800°F. The evaluation criteria used are as follows:

- low cycle fatigue—12,000 zero-max cycles, -3 sigma properties
- no yield—115% mechanical speed, 95% of -3 sigma, 0.2% yield strength
- burst—122% mechanical speed, 95% of -3 sigma, ultimate tensile strength

The results of this limited analysis for two materials, Inco 718 and Rene 95, are shown in Figure B-28. The allowable to calculated stress ratios are satisfactory for Rene 95 (>1). However, for Inco 718 the allowable to calculated stress ratio is less than one, which indicates that Inco 718 would not be a good selection.

The results of this preliminary analysis show that the bore stress and average tangential stress are high but appear to be acceptable for high strength alloys such as Rene 95.

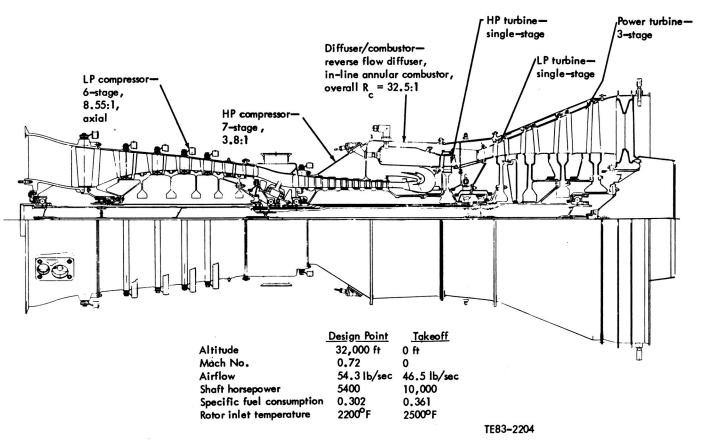


Figure B-23. PD436-11 engine general arrangement for axial/axial compressor.

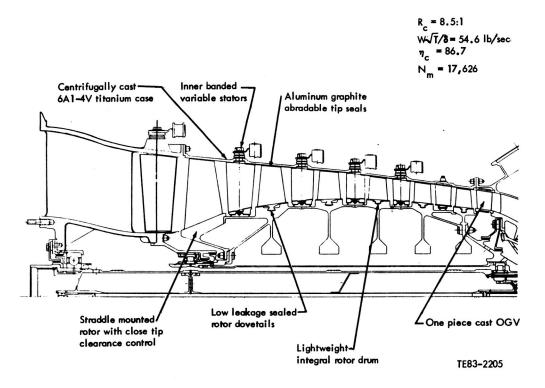


Figure B-24. Low pressure axial compressor common to both engines.

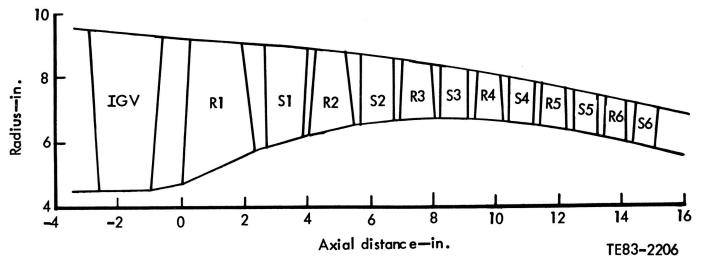


Figure B-25. Low pressure compressor flow path.

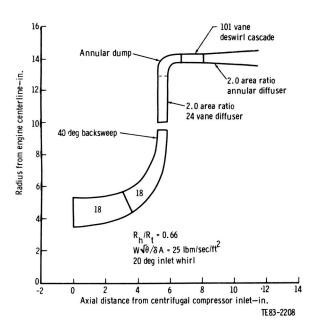


Figure B-26. High pressure centrifugal compressor of Engine PD436-10.

Other materials selected are Inco 718 for the case and aluminum graphite abradable seals.

High Pressure Axial Compressor

The HP axial compressor is shown in Figure B-29. This compressor has a variable inlet guide vane of cast Inco 718, cast Inco 718 case, roll-formed Inco 718 vanes, aluminum graphite abradable seals, and a tie-bolted drum rotor. Ti 829 material is used for first- through fourth-stage blades and cast Inco 718 in the fifth through seventh stages. Increased structural stability could be achieved by the use of a cast titanium aluminide case. Cast integral vanes would further reduce

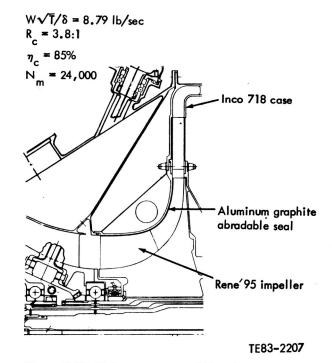
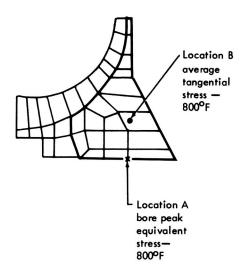


Figure B-27. High pressure centrifugal compressor flow path.

cost. The design goals are as follows:

- corrected flow = 8.8 lb/sec
- pressure ratio = 3.8:1
- adiabatic efficiency = 85.7 %
- polytropic efficiency = 88.1 %

The seven-stage axial HP compressor has been pushed to low flow coefficients and high loading to minimize stage count and maximize blade height. Design features are a hub/ tip ratio of 0.74, inlet tip speed of 991 ft/sec, and average area ratio of 1.37. The key feature is the tie-bolted curvic cou-



René 95 HIP-Processed and Forged

	LCF	<u>Yield</u>	Burst
Location	A	В	В
Allowable stress—ksi	219.5 ksi	113.6	139.1
Calculated stress—ksi	192.4	104.1	104.1
Allowable-to-calculated stress ratio	1.14	1.09	1.34
<u>In∞ 718</u>			
	LCF	<u>Yield</u>	Burst
Location	Α	В	В
Allowable stress—ksi	161.5	86.5	90.6
Calculated stress—ksi	192.4	104.1	104.1
Allowable-to-calculated stress ratio	0.84	0.83	0.87

TE83-2209

Figure B-28. Rough model stress summary of HP centrifugal compressor.

pled rotor drum. The HP axial compressor flow path is shown to scale in Figure B-30. It has an overall length of 10.78 in. The minimum blade height is 0.69 in. Minimum rotor and stator chord dimensions are 0.70 and 0.56, respectively.

Fold-Back Combustor (Axial/Centrifugal Compressor)

The combustor used with engine PD436-10, which has an axial/centrifugal compressor, has an annular fold-back flow path as shown in Figure B-31. With this geometry, the engine is shortened by placing the HP turbine under the combustor. Airflow into the combustor is metered by a combination of orifices and the porosity of the Lamilloy porous material skin.

The combustor geometry is designed to fit a plenum sized radially by the diffuser system of the centrifugal compressor. The discharge of diffuser directly into the combustion chamber plenum is accomplished with a minimum length penalty to the overall engine. Allison has experience with combustors of this type in both the ATDE and MTDE engine designs.

The preliminary design sizing and estimated performance of the fold-back combustor is summarized in Table B-IV.

Axial Combustor—Reverse Diffuser (Axial/Axial Compressor)

The combustor used with Engine PD436-11, which has an axial/axial compressor, has an axial flow path, discharging directly into the high pressure turbine nozzle. The combustor is positioned forward of the last stage of the compressor and the compressor discharge is turned 180 deg and diffused to supply the combustor inlet plenum with low-velocity, high-

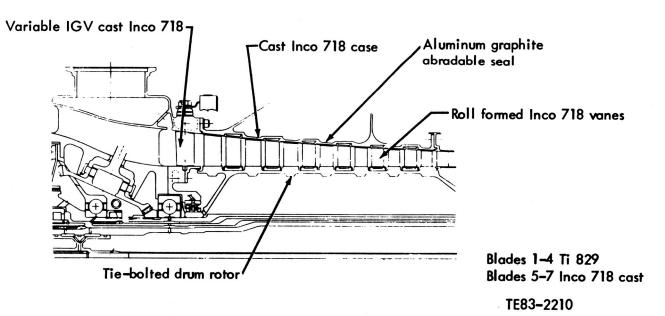


Figure B-29. High pressure axial compressor of Engine PD436-11.

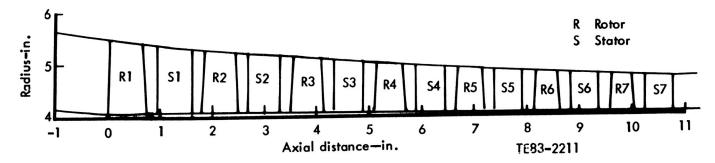


Figure B-30. APET compressor.

$$W = 43.4 \text{ lb/sec}$$

$$T_{\text{inlet}} = 1063^{\circ} \text{F}$$

$$T_{\text{BOT}} = 2558^{\circ} \text{F (RIT} = 2500^{\circ} \text{F)}$$

$$\Delta T = 1495^{\circ} \text{F}$$

$$F/A = 0.024$$

$$\Delta P = 5.0\%$$

$$\eta = 99.9\%$$
Pattern factor
$$\left(\frac{T_{\text{max}} - T_{\text{avg}}}{T_{\text{avg}} - T_{\text{inlet}}}\right) = 0.2$$
Heat release = 2.9 x 10⁶ Btu/ft³-atmos-hr

Figure B-31. Fold-back combustor for the axial/centrifugal compressor configuration of Engine PD436-10.

Table B-IV.

Combustor design parameters for axial/centrifugal compressor flow path.

	Takeoff SLS	Altitude cruise, 32.000 ft, 0.72 M _N
Lines and annual valuation	F0.7	47.0
Liner reference velocity— ft/sec	50.7	47.0
Annulus velocity—ft/sec	106 max	98 max
Pressure drop, ΔP/P—%	5.0	5.0
Length to height ratio, L/h	3.14	3.14
Heat release rate—	2.9×10^6	2.74 x 10 ⁶
Btu/ft3-atmos-hr		
Estimated combustion	99.9	99.9
efficiency—%		
Estimated pattern factor,	0.2	0.2
(T _{max} - T _{avg})/(T _{avg} - T _{inlet})		
Airflow—lb/sec	43.432	20.811
Inlet pressure—psia	404.15	182.79
Inlet temperature—°F	1063	874
Outlet temperature—°F	2500	2200
Temperature rise—°F	1437	1326
Fuel/air ratio, F/A	0.0242	0.0216

static-pressure air, as shown in Figure B-32. This flow path differs from the fold-back configuration of the axial/centrifugal compressor in that in this case the hot gas of the combustor is not subjected to a severe turn ahead of the high pressure turbine. This combustor is also fabricated from Lamilloy porous material for airflow regulation and heat transfer purposes. Preliminary design sizing and estimated performance of the axial combustor is summarized in Table B-V.

The advantage of this flow path is a shorter engine with a conventional flow path from the combustor through the turbine. Test verification of the compressor/combustor flow path is needed.

Turbines

The two turbine flow paths generated are shown in Figures B-33 and B-34. Two distinct HP turbines were necessary because the two compressor configurations (axial/axial and axial/centrifugal) are characterized by different HP rotational speeds. The HP turbine for the axial/centrifugal compressor configuration is designated PD436-10, and the HP turbine

$$W_{a} = 43.1 \text{ lb/sec}$$

$$T_{inlet} = 1060^{\circ} \text{F (RIT} = 2500^{\circ} \text{F)}$$

$$T_{BOT} = 2558^{\circ} \text{F}$$

$$\Delta T = 1495^{\circ} \text{F}$$

$$F/A = 0.024$$

$$\Delta P = 5.0\%$$
Heat release = 5.7 x 10⁶

$$Btu/ft^{3} - atmos - hr$$

$$\eta = 99.9\%$$
Pattern factor
$$\left(\frac{T_{max} - T_{avg}}{T_{avg} - T_{inlet}}\right) = 0.2$$

$$TE83-2213$$

Figure B-32. Axial combustor—reverse diffuser for Engine PD436-11.

Table B-V.

Combustor design parameters for axial compressor flow path.

	Takeoff SLS	Altitude cruise, 32,000 ft, <u>0.72 M_N</u>
Liner reference velocity— ft/sec	75.3	69.9
Annulus velocity—ft/sec	120 max	111 max
Pressure drop, ΔP/P—%	5.0	5.0
Length to height ratio, L/h	3.0	3.0
Heat release rate— Btu/ft³-atmos-hr	5.7 x 10 ⁶	5.3 x 10 ⁶
Estimated combustion efficiency— %	99.9	99.9
Estimated pattern factor, (T _{max} - T _{avg})/(T _{avg} - T _{inlet})	0.2	0.2
Airflow—lb/sec	43.162	20.686
Inlet pressure—psia	404.05	182.79
Inlet temperature—°F	1060	871
Outlet temperature—°F	2500	2200
Temperature rise—°F	1440	1329
Fuel/air ratio, F/A	0.0243	0.0208

corresponding to the axial/axial compressor is designated PD436-11. The LP and power turbines are common to both designs.

Both the HP and LP turbines are air cooled. The power turbine is uncooled. A summary of the cooling air supply conditions and flow rates required to maintain the indicated metal temperatures is presented in Table B-VI. Details of the cooling schemes and estimated turbine performance of each turbine assembly are described in the following paragraphs.

High Pressure Turbine (Axial/Centrifugal Compressor)

The HP turbine design point for the axial/centrifugal compressor configuration, Engine PD436-10, is cruise, 0.72 Mach number, 32,000 ft altitude. The turbine inlet conditions for this design point are defined in Table B-VII.

The HP turbine design criteria used are as follows:

- impeller speed = 24,000 rpm
- single stage air-cooled
- hub/tip ratio = 0.83
- reaction = 0.5
- tangential lift coefficient = 0.65
- stage loading coefficient = 1.24

The design procedure involved estimating free vortex velocity triangles and preliminary throat definition using Allison computer code DE 8. Estimates of losses and overall turbine performance were made with computer code Q 69 at the cruise design point and sea level takeoff condition. The design point aerodynamic characteristics at the cruise design point are shown in Table B-VIII. These parameters are also representative of sea level takeoff. The HP turbine is shown in Figure B-35.

High Pressure Turbine (Axial/Axial Compressor)

The HP turbine design point for the axial/axial compressor configuration, Engine PD436-11, is cruise at 0.72 Mach number, 32,000 ft altitude. Turbine inlet conditions at the design point are shown in Table B-IX.

The design criteria used are as follows:

- axial compressor speed = 27,000 rpm
- single stage

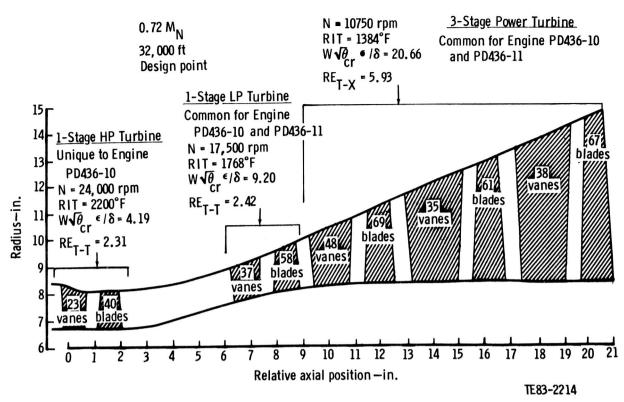


Figure B-33. Turbine flow path for the axial/centrifugal compressor configuration (PD436-10).

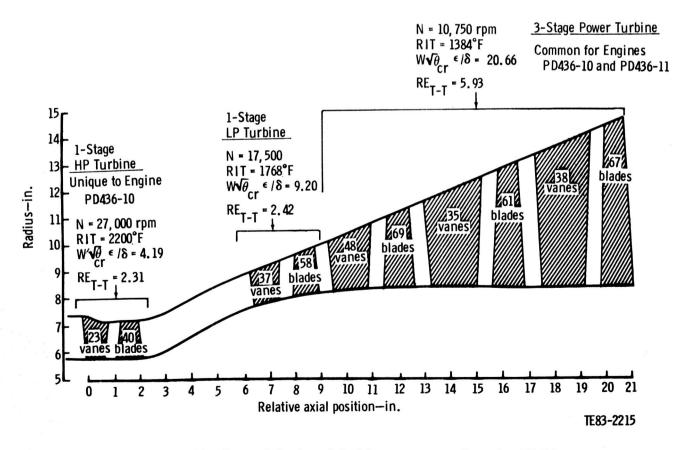


Figure B-34. Turbine flow path for the axial/axial compressor configuration (PD436-11).

Table B-VI. Turbine cooling summary.

	Sea level takeoff conditions			Sea level takeoff conditions				С	Cruise, 32,000 ft, 0.72 Mach No.		
	T _G —	T _M —	T _C —	Wc/Wg-	T _G —	T _M —	T _c —	Wc/Wg-			
Airfoil row	<u>°F</u>	<u>°F</u>	<u>°F</u>		<u>°F</u>	<u>°F</u>	<u>°F</u>	%			
HP NGV	2840	1815	1086	3.80	2530	1815	907	2.05			
HP blade	2330	1725	1186	3.09	2067	1725	1009	1.20			
LP NGV	2314	1778	1086	1.42	2043	1778	909	0.54			
LP blade	1861	1673	695	0.35	1625	1625	550	0.00			

T_G—gas stream relative total temperature (w/burner profile)

T_M—chordwise average metal temperature corresponding to T_G

T_C—cooling air temperature into airfoil

Wc/Wg-cooling flow requirement expressed as percent of compressor inlet flow

Table B-VII. High pressure turbine aerodynamic design point conditions for Engine PD436-10.

Table B-VIII. Estimated design point HP turbine aerodynamics for Engine PD436-10 (axial/centrifugal compressor).

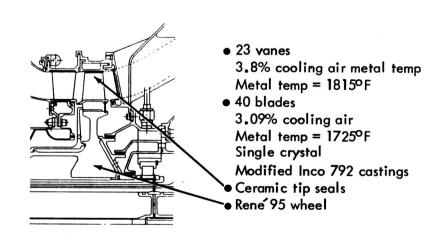
0.72 M _N , 32,000 ft		Stator exit absolute Mach No.	0.77
		Stator exit absolute gas angle—deg	12.2
Turbine inlet temperature—°F	2200	Rotor exit relative Mach No.	0.81
Turbine inlet total pressure—psia	173.7	Rotor exit relative gas angle—deg	-18.4
Turbine inlet equivalent flow—lbm/sec	4.19	Rotor meanline reaction	0.52
Equivalent work—Btu/lbm	24.4	State loading coefficient	1.24
Rotational speed—rpm	24,000	Turbine exit swirl—deg	-16.0
Expansion ratio*	2.31	~	
Goal efficiency*	0.870		

^{*}Total/total basis

$$AN^2 = 3.6 \cdot 10^{10} \text{ in.}^2 - \text{rpm}^2$$

N = 24,000 rpm

Aero Design Point Equivalent work = 24.4 Btu/lbm $\eta_{T-T} = 2.31$ $\eta_{T-T} = 87\%$ $RIT_{cruise} = 2200^{\circ} F$ $Max T_{gas} = 2840^{\circ} F$



TE83-2216

Figure B-35. Axial pressure turbine for Engine PD436-10 (axial/centrifugal compressor).

- area x (speed)² = 4.5 x 10¹⁰ in.²-rpm² maximum permitted at sea level takeoff
- reaction = 0.5
- tangential lift coefficient = 0.65
- stage loading coefficient = 1.30

The design procedure of Engine PD436-10 estimates free vortex velocity triangles and preliminary throat definition were made for the HP turbine. Losses and turbine performance were calculated at the cruise design point shown in Table B-X.

$\frac{\mbox{High pressure turbine aerodynamic design point}}{\mbox{conditions at 0.72 M}_{\mbox{N}}, 32,000 \mbox{ ft.}}$

Turbine inlet temperature—°F	2200
Turbine inlet total pressure—psia	173.7
Turbine inlet equivalent flow—lbm/sec	4.19
Equivalent work—Btu/lbm	24.4
Rotational speed—rpm	27,000
Expansion ratio*	2.31
Goal efficiency*	0.870

^{*}Total/total basis

Table B-X. <u>Estimated design point HP turbine aerodynamics</u> for Engine PD436-11 (axial/axial compressor).

Stator exit absolute Mach No.	0.80
Stator exit absolute gas angle—deg	13.9
Rotor exit relative Mach No.	0.83
Rotor exit relative gas angle—deg	-21.2
Rotor meanline reaction	0.51
State loading coefficient	1.30
Turbine exit swirl—deg	-15.5

The HP turbine design shown in Figure B-36 is cooled with 3.8% of compressor flow. A cross section of the inlet stator vane is shown in Figure B-37. Cooling is accomplished by compartmenting the vane interior cavity so that leading edge, center body, and trailing edge compartments are cooled by different methods with metered cooling air quantities. The leading edge is both impingement and film cooled.

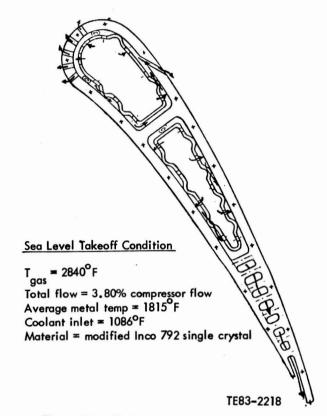


Figure B-37. High pressure turbine inlet stator cross section.

$$AN^2 = 4.0 \times 10^{10} \text{ in.}^2 - \text{rpm}^2$$

N = 27,000 rpm

Aero Design Point

Equivalent work = 24.4 Btu/lbm $R_{C_{T-T}} = 2.31$ $\eta_{T-T} = 87\%$

RIT = 2200° F Max T = 2840° F

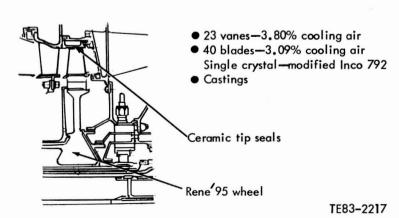


Figure B-36. High pressure turbine for Engine PD436-11 (axial/axial compressor).

Impingement cooling is used in the center body and pin-fin convection cooling in the trailing edge region. The rotor blade cross section shown in Figure B-38 also has three compartments. However, film convection is used in the leading edge compartments and convection cooling with extended surface in the center body and trailing edge. Cooling airflow of 3.09% is required.

Low Pressure Turbine (Common for Axial/ Centrifugal and Axial/Axial Compressors)

The LP turbine is common to Engines PD436-10 and PD436-11. Design point inlet conditions are listed in Table B-XI. The design criteria used for the LP turbine are as follows:

- single stage
- tangential lift coefficient = 0.75

As was the case for the HP turbine previously discussed, preliminary performance and sizing calculations of the LP turbine were the basis for the design. The design point aerodynamic characteristics are shown in Table B-XII. These data are also typical for sea level takeoff conditions. The LP turbine design is shown in Figure B-39.

Both the stator and rotor airfoils are air cooled. The stator airfoil cross section, shown in Figure B-40, contains an impingement tube to cool the leading edge region and confine convective flow in the center body region. The impingement flow passes over pin fins in the trailing edge region and exhausts through trailing edge slots. Cooling airflow is 1.42% of compressor flow supplied from the HP compressor. A cross section of the rotor blade is shown in Figure B-41. The rotor blade is convection cooled, with 0.35% compressor

flow taken from the LP compressor, and therefore is at the lower temperature of 695°F at the blade entrance.

Table B-XI.

Low pressure turbine aerodynamic design point
conditions for Engines

PD436-10 and PD436-11 at 0.72 M_N, 32,000 ft.

Turbine inlet temperature—°F	1768
Turbine inlet total pressure—psia	75.0
Turbine inlet equivalent flow—lbm/sec	9.20
Equivalent work—Btu/lbm	25.7
Rotational speed—rpm	17,500
Expansion ratio*	2.42
Goal efficiency*	0.882

^{*}Total/total basis

Table B-XII.

Estimated design point LP turbine aerodynamics for Engines PD436-10 and PD436-11.

Stator exit absolute Mach No.	0.87
Stator exit absolute gas angle—deg	19.3
Rotor exit relative Mach No.	0.90
Rotor exit relative gas angle—deg	-23.4
Rotor meanline reaction	0.51
State loading coefficient	1.48
Turbine exit swirl—deg	-22.5

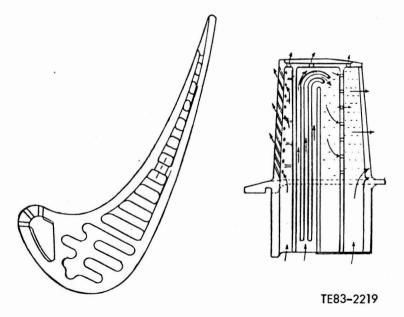


Figure B-38. High pressure turbine rotor cross section.

Sea Level Takeoff Condition

T gas = 2330°F

Total flow = 3.09% compressor flow

Average metal temp = 1725°F

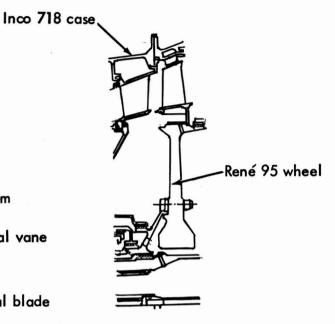
Coolant inlet = 1186°F

Material = modified Inco 792 single crystal

 $N_m = 17,626 \text{ rpm}$ $\eta_T = 88\%$ $Max T_{gas} = 2314^{\circ}F$ $T_{RIT} = 1768^{\circ}F$ Equivalent work = 25.7 Btu/lbm

Modified Inco 792 single crystal vane 1.42% cooling air Metal temp = 1778°F avg

Modified Inco 792 single crystal blade 0.35% cooling air
Metal temp = 1673°F avg



TE83-2220

Figure B-39. Low pressure turbine for Engines PD436-10 and PD436-11.

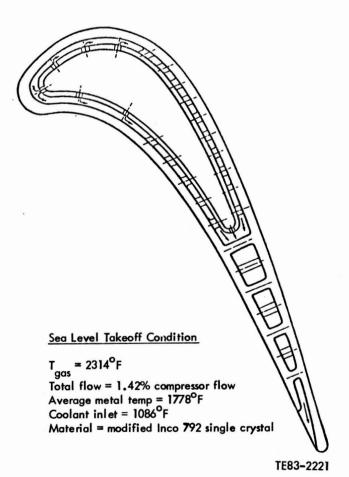
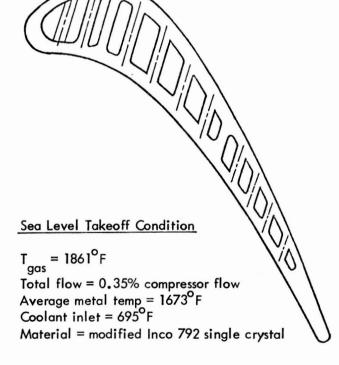


Figure B-40. Low pressure turbine stator vane cross section.



TE83-2222

Figure B-41. Low pressure turbine rotor blade cross section.



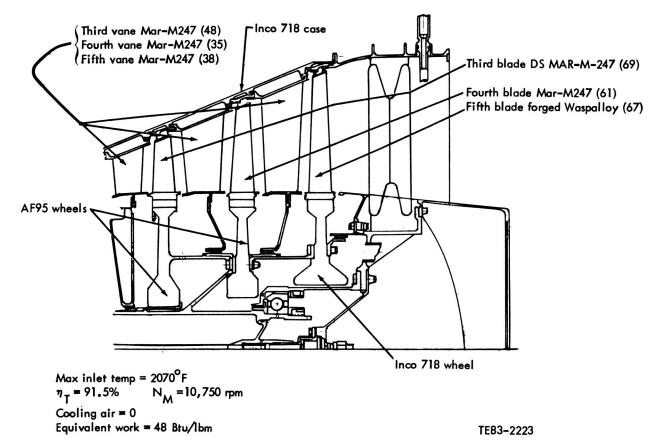


Figure B-42. Power turbine for Engines PD436-10 and PD436-11.

Table B-XIII.

Power turbine aerodynamic design point conditions
for Engine PD436-10.

Turbine inlet temperature—°F	1384
Turbine inlet total pressure—psia	31.0
Turbine inlet equivalent flow—lbm/sec	20.66
Equivalent work—Btu/lbm	48.0
Rotational speed—rpm	10,750
Expansion ratio*	5.93
Goal efficiency*	0.915

^{*}Total/total basis

Power Turbine (Common for Axial/Centrifugal and Axial/Axial Compressors)

The power turbine shown in Figure B-42 is also common to Engines PD436-10 and PD436-11. It has the design point inlet conditions listed in Table B-XIII and the design point aerodynamics summarized in Table B-XIV. Three stages

Table B-XIV.

Estimated design point LP turbine aerodynamics for Engines PD436-10 and PD436-11.

Design point	PT	PT	PT
turbine aero parameter	1	2	<u>3</u> 0.73
Stator exit absolute Mach No.	0.70	0.70	0.73
Stator exit absolute gas angle—deg	28.1	24.1	25.5
Rotor exit relative Mach No.	0.72	0.74	0.87
Rotor exit relative gas angle—deg	-26.6	-25.0	-27.4
Rotor meanline reaction	0.52	0.54	0.62
State loading coefficient	1.62	1.38	1.24
Turbine exit swirl—deg	_		-16.8

were selected with approximately equal work split to achieve the objective of optimum efficiency. No restraints were placed on power turbine speed since the gearbox was designed to provide the reduction required to optimize propfan and power turbine speeds.

APPENDIX C

TASK III. PROPULSION SYSTEM INTEGRATION

TABLE OF CONTENTS

Title .	Page
ntroduction	C-1
Propulsion System Integration	C-2
Propfan Gearbox	C-2
Engine Assemblies	C-3
Propfan Control System	C-3
Torquemeter	C-3
Propfan Brake	
Engine and Aircraft Accessories	
Engine Control System	C-12
Propulsion System Assemblies	
Engine Data Package	
References	

LIST OF ILLUSTRATIONS

Figure	Title	Page
C-1	Candidate gear arrangements selected for further evaluation	
C-2	Scheme to reverse direction of rotation of offset gear configuration	
C-3	Conceptual design drawing of the offset gearbox	
C-4	Conceptual design drawing of the in-line gearbox	
C-5	Losses projected for future-production gearboxes	
C-6	Engine PD436-10 outline drawing	
C-7	Engine PD436-11 outline drawing	
C-8	Engine PD436-12 outline drawing	
C-9	Engine PD436-13 outline drawing	C-9
C-10	Propfan pitch change system	
C-11	Dual idler load sharing torquemeter	C-11
C-12	Phase detector torquemeter	C-11
C-13	Accessorized propeller brake	
C-14	Power extraction penalty to cycle	C-12
C-15	Control system block diagram	C-13
C-16	Installation drawing for Engine PD436-10	C-14
C-17	Installation drawing for Engine PD436-11	
C-18	Installation drawing for Engine PD436-12	C-15
C-19	Installation drawing for Engine PD436-13	C-15
C-20	Propfan installation criteria	C-16
C-21	Engine support structure	

PRECEDING PAGE BLANK NOT FILMED

LIST OF TABLES

Table	Title	Page
C-I	Evaluation results of candidate gear arrangements	. C-3
C-II	Comparison with current production model gearbox	. C-5
C-III	Engine identification	. C-10
C-IV	Accessory drive summary	. C-13
C-V	Engine data summary	. C-17
	Cost and physical characteristics	
C-VII	PD436-10 performance data	. C-19
C-VIII	PD436-11 performance data	. C-25
	Physical characteristics of PD436-12 and PD436-13	

INTRODUCTION

The work described in Appendix C involves the integration of the two engine configurations developed in Task II with the rest of the propfan propulsion system. This includes the propfan gearbox, accessory gearbox, engine inlet, oil cooler, engine torque measuring system, engine controls, propfan, propfan pitch control, engine mount system, conceptual nacelle, engine accessories, aircraft accessories,

inlet anti-ice system, and inlet acoustic treatment requirements. The purpose of this integration effort is to define turboprop propulsion systems for evaluation in the mission analysis portion of the study and to provide preliminary design drawings, propulsion system data packages, and a computer deck for calculating steady-state engine performance.

PROPULSION SYSTEM INTEGRATION

The propulsion system integration utilizes the two power sections developed in Task II. Both power sections are three-spool configurations designed to operate at 32.5:1 overall pressure ratio. The primary difference in the two engines is the type of high pressure compressor—axial or centrifugal. These two selected configurations are combined with the other propulsion system components and accessories in various nacelle arrangements to arrive at recommended propulsion systems for further study. The results of the integration work, beginning with the propfan gearbox and including each major component, are discussed in the following subsections.

PROPFAN GEARBOX

A range of gear arrangements were investigated. These were narrowed to two final configurations which were used with the two power sections of Task II. The resulting engines provided the basis for defining the additional elements of the propulsion system.

After initial screening of the candidate gear arrangements, the four designs shown in Figure C-1 were selected for quantitative evaluation. The four favored gear trains are as follows:

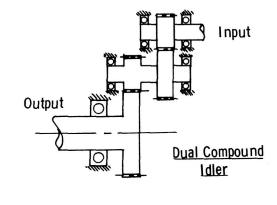
- 1. dual compound idler
- 2. split path planetary
- 3. spur and planetary
- 4. star planetary

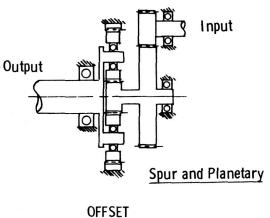
Two of these designs, the dual compound idler and the spur and planetary, result in offset input/output shafting.

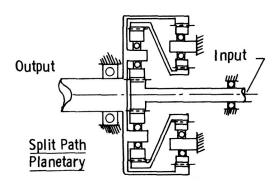
The other two, the split path planetary and the star, have in-line shafting. Evaluation criteria for these configurations were chosen at 10,000 shp power class, 9:1 speed reduction ratio, and 30,000 hours design life (mean time between removals) with the following gear stress levels:

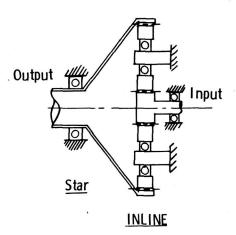
gear crushing stress
 gear bending stress (Lewis)
 unidirectional

gear bending stress (Lewis) reverse 28,000 lb/in.²









TE83-2237

Figure C-1. Candidate gear arrangements selected for further evaluation.

The crushing stress and unidirectional bending stress were selected to be the same as those for the current-production Allison T56 engine. Pitch line velocity was set at 25,000 ft/min, 25% higher than for the current-production T56. Nearterm materials selected were AX92 magnesium housing, vacuum melt 9310 gears, and VIM/VAR M50 bearings. Results of the evaluation relative to seven rating parameters are shown in Table C-I.

The four gear arrangements were narrowed to two—the offset dual idler and the in-line star planetary—based primarily on minimizing the number of power train gears and bearings. Initial cost is favorable for these choices. To reverse the direction of rotation of the in-line configuration, the power turbine direction of rotation would be reversed. Reversing direction of rotation of the offset configuration could be accomplished either by adding idlers as shown in Figure C-2 or reversing the power turbine direction of rotation.

The offset gearbox has an advantage relative to accommodating aircraft accessories. It can provide for limited mounting of aircraft accessories on the rear face and it provides good offset to drive an aircraft-mounted accessory drive system (AMADS) gearbox. An angle drive to the AMADS would be required because of the possible interference of the drive shaft with the engine inlet duct.

The conceptual design drawings of the offset and in-line gearboxes are shown in Figures C-3 and C-4, respectively. These conceptual gearboxes were compared with the Allison production T56/501 gearbox design parameters and are listed in Table C-II. The reduced number of gears and bearings is an important feature relative to improving reliability and reducing maintenance requirements of future-production gearboxes. It is projected that losses for the future-production gearboxes would be similar to the Allison T56/501 gearbox data shown in Figure C-5.

ENGINE ASSEMBLIES

The two power sections developed in Task II were combined with the gearbox configurations previously described to

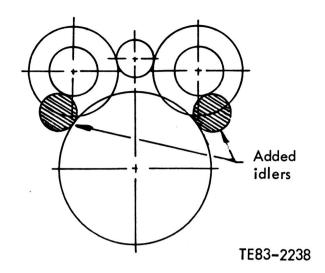


Figure C-2. Scheme to reverse direction of rotation of offset gear configuration.

make four engines identified as PD436-10, -11, -12, and -13 in Table C-III. Drawings of these four engines are shown in Figures C-6 through C-9.

PROPFAN CONTROL SYSTEM

The pitch change actuation system is shown in Figure C-10. Location of the prop control on the offset box provides access to the rear of the prop shaft, allowing location of the pitch change regulator and slip ring assembly on the propfan axis. In the case of the in-line gearbox, this access is not available. The regulator and slip ring assembly would then be placed at the front of the propfan pitch change mechanism. A fixed quillshaft is used to drive the slip ring assembly and transfer electrical signals.

TORQUEMETER

The offset gearbox has a built-in torque measuring system associated with the hydraulic load sharing device of the

Table C-I.
Evaluation results of candidate gear arrangements.

	Power- train gears	Power- train bearing	Weight	Cost	Prop control access	Accy mounting	Opposite rotation mod
Offset*							
dual idler	6	10	107	68	good	good	fair
Offset							
spur/planetary	9	17	100	100	good	good	poor
In line							
split path planetary	17	16	82	143	poor	poor	poor
In line*							
star planetary	5	9	110	54	fair	poor	poor

^{*}Selected for aircraft integration study

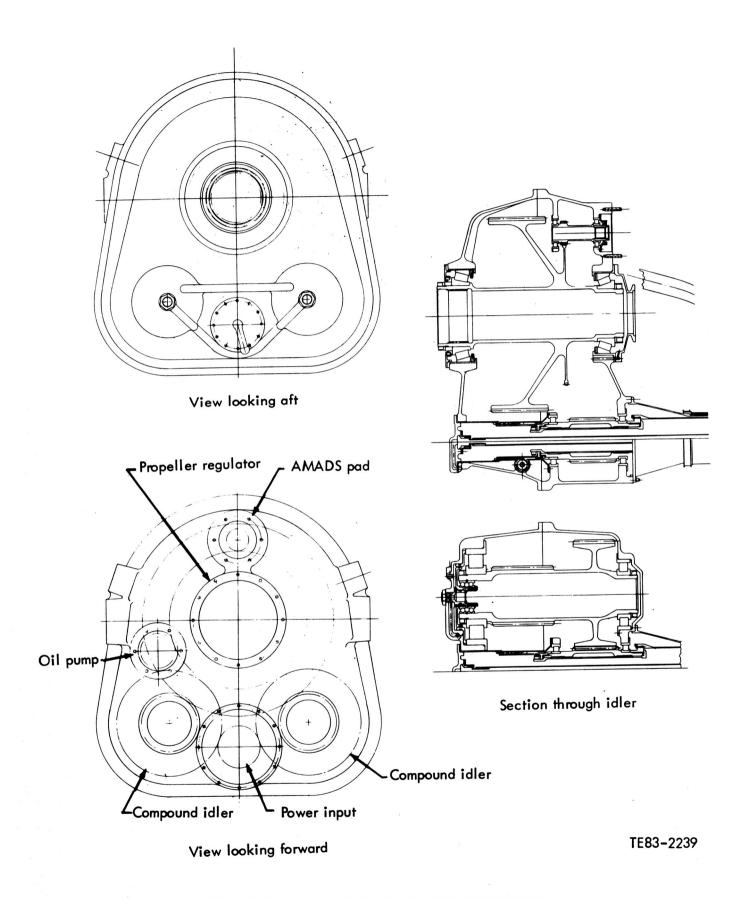


Figure C-3. Conceptual design drawing of the offset gearbox.

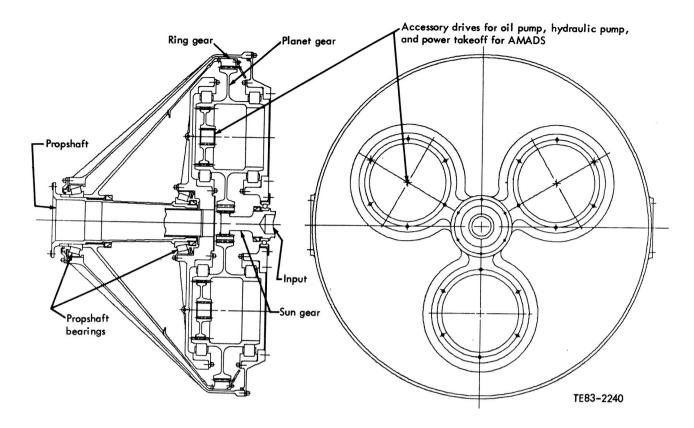


Figure C-4. Conceptual design drawing of the in-line gearbox.

Table C-II.

Comparison with current production model gearbox.

	to the law	production hp class Offset	Current production 5,000 hp class T56/501
Power-train gears	5	6	8
Power-train bearings	9	10	16
Maximum crushing stresslb/in.2	160,000	159,500	161,000
Maximum bending stresslb/in.2	27,500	31,500	41,200
Maximum pitchline velocity—ft.min	13,100	15,950	20,500
Relative cost	0.79	1	
Weight—lb	655	635	562 (T56-A14)
Efficiency at takeoff	99.0	99.0	98.9
Efficiency at cruise	98.8	98.8	98.6

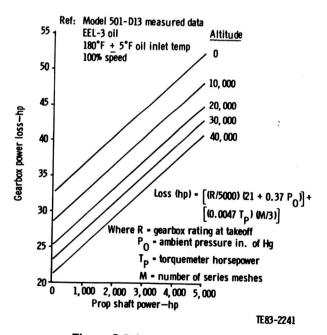
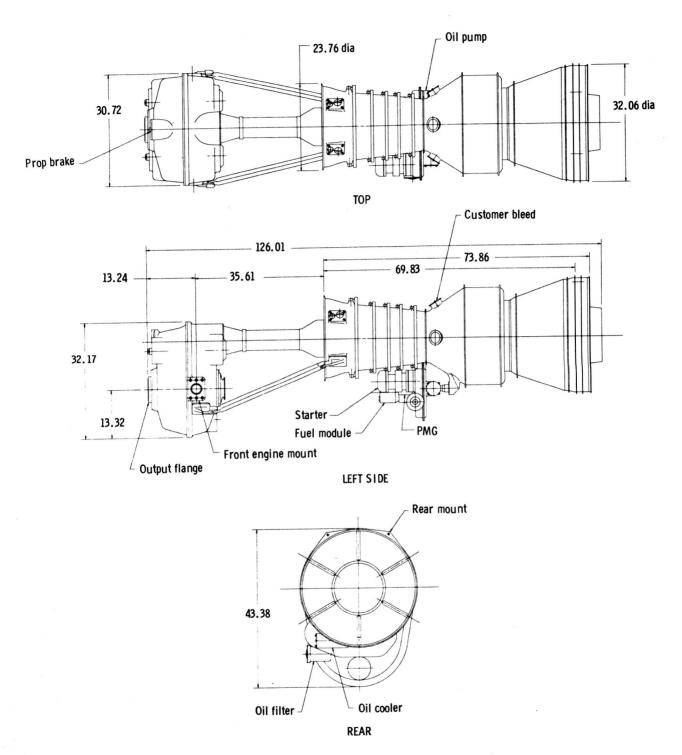


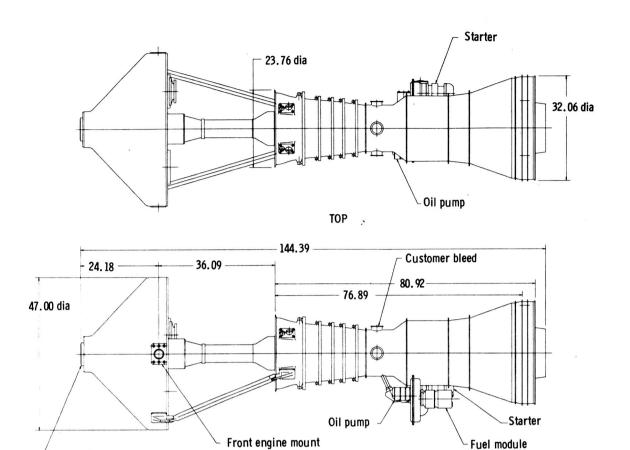
Figure C-5. Losses projected for future-production gearboxes.



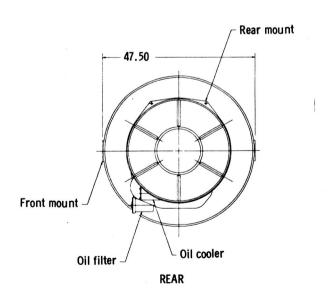
Note: All dimensions are in inches

TE83-2242

Figure C-6. Engine PD436-10 outline drawing.



LEFT SIDE



Note: All dimensions are in inches

∠ Output flange

TE83-2243

Figure C-7. Engine PD436-11 outline drawing.

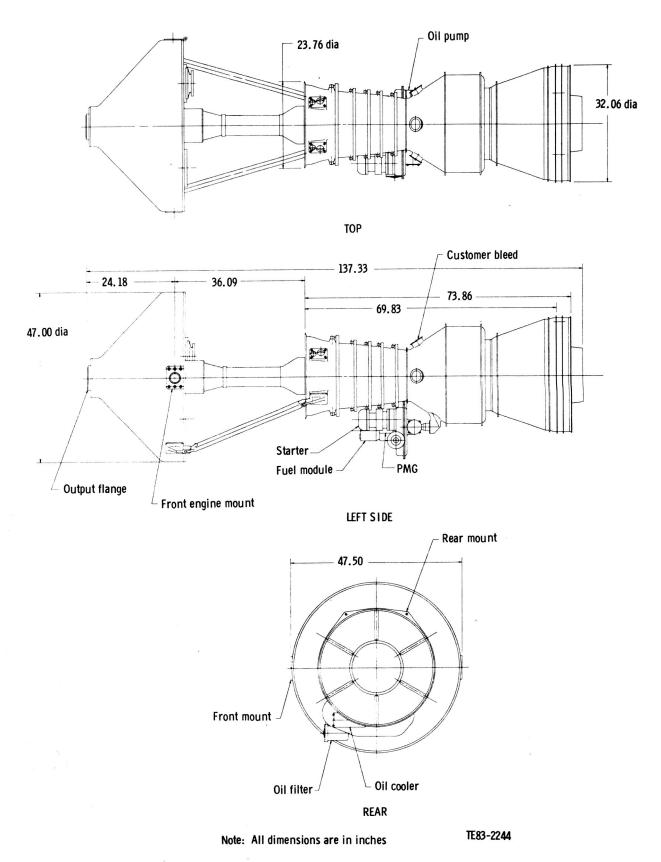
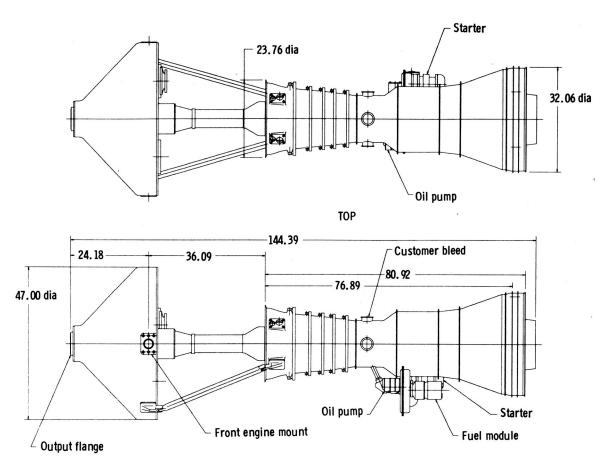
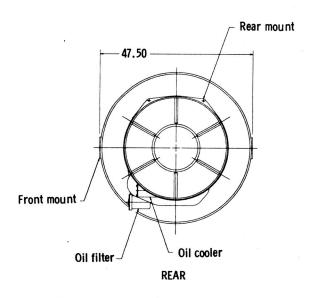


Figure C-8. Engine PD436-12 outline drawing.



LEFT SIDE



Note: All dimensions are in inches

TE83-2245

Figure C-9. Engine PD436-13 outline drawing.

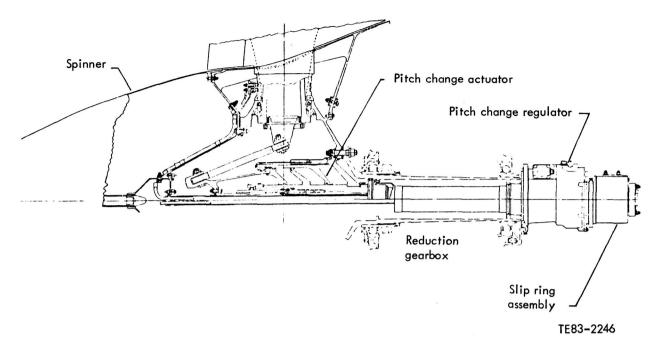


Figure C-10. Propfan pitch change system.

Table C-III. Engine identification.

Engine identification	Compressor type	Gearbox type
PD436-10	Axial/centrifugal	Offset
PD436-11	Axial/axial	Offset
PD436-12	Axial/centrifugal	In-line
PD436-13	Axial/axial	In-line

two idler gears. Since the pressure in the cavity at the end of the idler is a function of load, this pressure is also directly proportional to torque. In a helical gear system the thrust reaction is proportional to the torque reaction. The unbalanced force when the load is not equally shared positions a piston relative to a metering orifice in the hydraulic system, counteracting the unbalanced thrust and establishing the desired load sharing. This system, called a dual idler load sharing torquemeter, is shown in Figure C-11.

The in-line gearbox utilizes a phase detector type torquemeter, as shown in Figure C-12. Allison has experience with both the hydraulic and phase detector torquemeters. The hydraulic type is used on the T63 and Model 250 engines. Its accuracy is rated at +1.5%. There is no weight or cost penalty. The phase detector type is used on the T56 and Model 501 engines. It also is rated at +1.5% accuracy. There is a 20-lb weight penalty and added cost. The load sharing system utilizes the hydraulic torquemeter to take advantage of the potential cost and weight savings.

PROPFAN BRAKE

The advanced turboprop engine incorporates a propeller brake integrated into the reduction gearbox accessory drive train. Previous studies projected a requirement for a propeller brake by some airline operators. The brake will prevent windmilling propeller blades on parked airplanes when windmilling torque from ground winds exceeds engine and accessory drag torque. The brake also decreases the time required to stop the propeller after engine shutdown, thus expediting passenger deplaning. However, it adds some complexity and associated maintenance costs.

The cross section of an accessorized propfan brake is shown in Figure C-13. Both the propfan brake and the oil pumps are external to the gearbox to improve maintainability. In the event of excessive slippage or failure to disengage, the brake could be quickly replaced on the flight line. The features of the brake are the same as for Allison's current Model 501-D13 design except that since it is no longer co-axial with the starter, additional control system tieins to effect release, such as for starting, would be required.

The method of operation of the brake is tied to prop speed. As the speed is decreased, oil pressure in the cavity decreases, allowing a spring to engage the brake surfaces.

ENGINE AND AIRCRAFT ACCESSORIES

Provisions are made on the engine for aircraft and engine accessories. The accessories driven by the power section gearbox are those essential to the operation of the power section: the fuel module, oil pump, starter, permanent

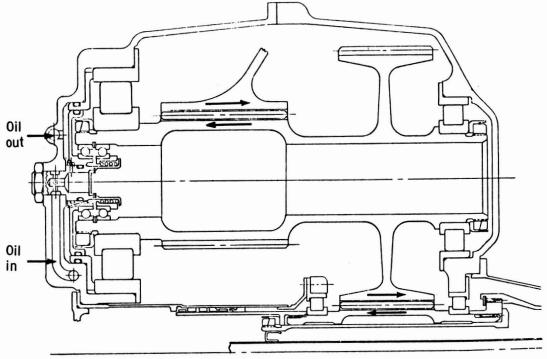


Figure C-11. Dual idler load sharing/torquemeter.

TE83-2247

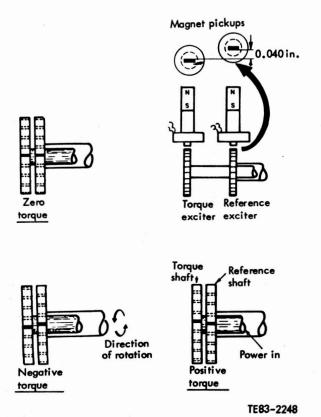


Figure C-12. Phase detector torquemeter.

magnet generator, and air/oil separator. Engine accessories driven off the propfan gearbox are an oil pump, prop brake, prop regulator, and AMADS drive. Also driven by the propfan gearbox are the aircraft alternator and two aircraft hydraulic pumps.

The accessories may be powered by the HP turbine, LP turbine, or power turbine; a trade study was performed to determine the sensitivity of specific fuel consumption to the turbine selected as the power source. These data take the form of increased specific fuel consumption for increasing power extraction from each spool. Results are summarized in Figure C-14 for the takeoff and cruise conditions. There is no independent effect of power extraction source over the range of 0 to 150 hp at the cruise condition. Therefore, unless the selection is made for other reasons, the power turbine source is preferred and the location would be at the propfan gearbox for the convenience of installing accessories and of obtaining the desired gear reduction. A summary of the accessory's drive system is shown in Table C-IV.

ENGINE CONTROL SYSTEM

The propfan propulsion system utilizes a full authority digital electronic control. It integrates the engine and prop control functions and has the following features:

- dual-channel digital controllers
- fly-by-wire inputs
- integrated fuel system

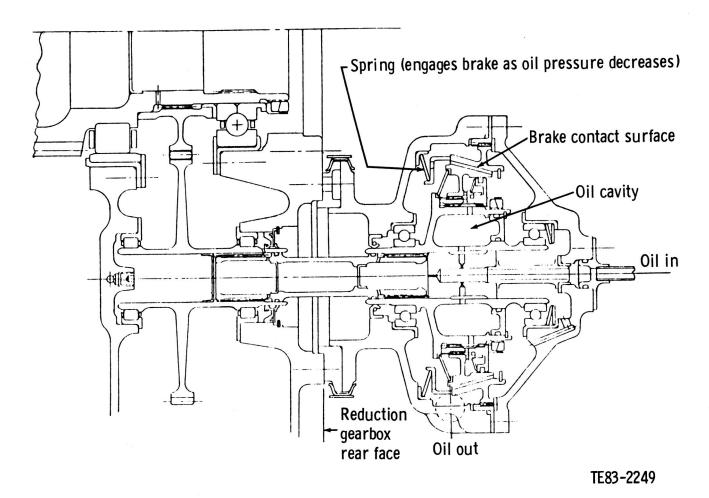


Figure C-13. Accessorized propeller brake.

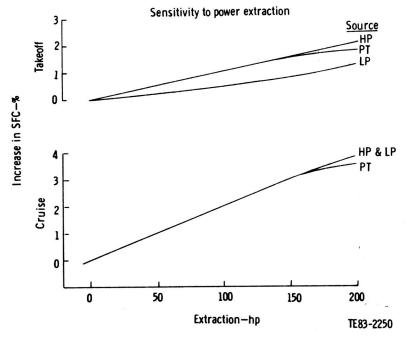


Figure C-14. Power extraction penalty to cycle.

- fuel-powered control guide vanes
- integrated diagnostic-condition monitoring system
- self-contained electrical power
- propeller synchrophasing

Accessories

Table C-IV. Accessory drive summary.

Power source

Location

Power section	HP spool	Top or bottom to be constant with maintenance concept
Reduction gearbox	Power turbine	Mounted on gearbox
Aircraft	Either spool, power turbine recommended Less speed droop on power turbine Easier mechanically on power turbine Separate AMADS box possible for maintenance reasons	AMADS

Key elements of the control system are the engine baymounted, full-authority digital prop-engine control; propfan pitch lock; Beta regulator; permanent magnet generator; accessory gearbox; fuel pump; fuel filter; fuel metering module; radiation pyrometer; and gas stream thermocouples.

It is anticipated that the advanced control system would provide for the following requirements:

- 1. automatic start sequencing
- acceleration/deceleration control of fuel flow, bleed, and compressor geometry for smooth, rapid operation without surge or flameout
- power lever control of thrust through gas generator speed control
- control of propeller/power turbine speed over required range of flight and ground operation
- power turbine inlet temperature limiting for turbine protection
- gas generator turbine blade temperature limiting for extended life
- limit maximum power turbine overspeed by redundant system
- 8. provision for torque limiting for gearbox protection
- provisions for mode selection for optimum thrust control (takeoff, climb, cruise for minimum specific fuel consumption)
- 10. safety features of autofeather and pitch lock
- 11. propeller synchrophasing
- 12. automatic control/prop system self-test

- 13. condition monitoring signals provided
- 14. provisions for interfacing with flight control system
- 15. cockpit display signals of engine parameters
- 16. automatic anti-ice control

The block diagram for the control system is shown in Figure C-15.

PROPULSION SYSTEM ASSEMBLIES

The two engine configurations were combined with the inlet, propfan, and nacelle in the assembly drawings shown in Figures C-16 through C-19 for engines PD436-10, -11, -12, and -13. These arrangements are over-the-wing installations. The axial/centrifugal compressor power section and offset gearbox allow for nacelle contouring to achieve the preferred aerodynamic shape for the over-the-wing mounted propulsion system. A top-mounted, single-scoop inlet is ducted to the compressor face transitioning from the scoop to the full annular shape required for uniform air distribution. This arrangement has a bottom-mounted AMADS gearbox, engine accessory gearbox, and air/oil cooler. Engine mounts are located on the gearbox housing and power turbine case. The axial/ axial compressor power section with the offset gearbox is installed the same way. The only differences are locations of the rear mount and the design of the engine accessory gearbox. Installation of the in-line gearbox dictates a different arrangement. With the in-line gearbox, the engine inlet is forced to be further from the engine centerline. The radial flow path becomes longer, and a bifurcated inlet is preferred. The air/oil cooler location is moved to the top location and the pitch change and AMADS components are relocated. Engine mounts remain in approximately the same locations. This arrangement applies to both engine configurations with the in-line gearbox.

Design considerations of the interfaces between the inlet power section and gearbox are based on previous turboprop engine installation experience. However, propfans and advanced nacelles present new geometric relationships and

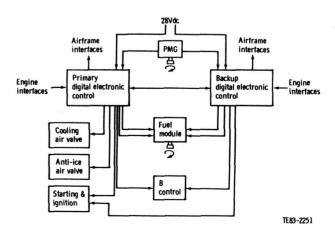


Figure C-15. Control system block diagram.

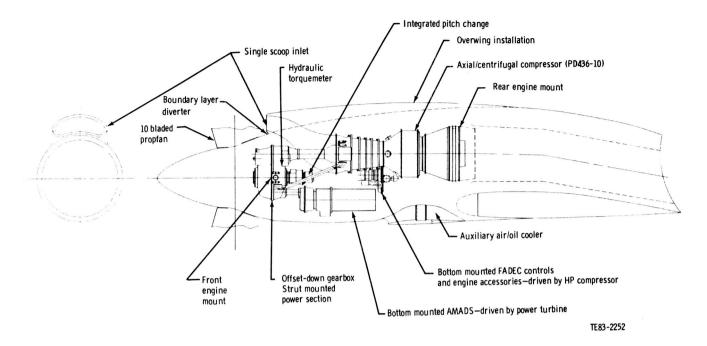


Figure C-16. Installation drawing for Engine PD436-10.

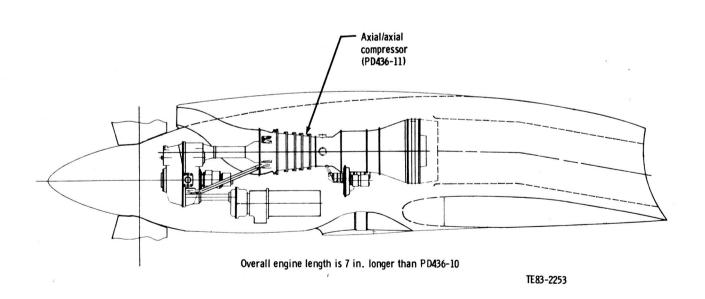


Figure C-17. Installation drawing for Engine PD436-11.

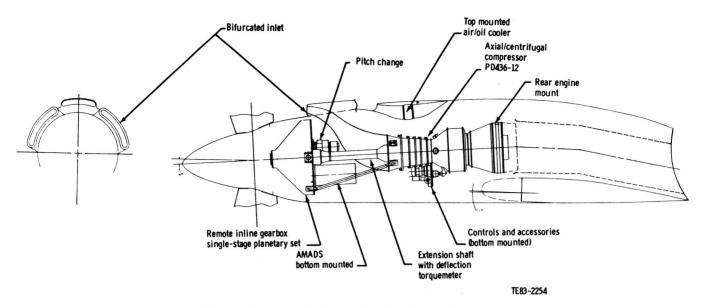


Figure C-18. Installation drawing for Engine PD436-12.

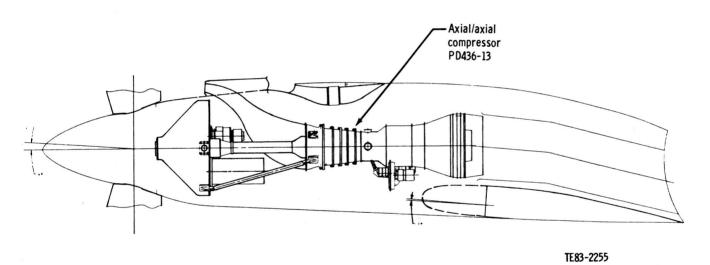


Figure C-19. Installation drawing for Engine PD436-13.

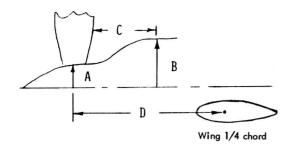
different aerodynamics and dynamics because of the propfan characteristics and the high-speed flight conditions. For example, the 10-blade propfan has a spinner diameter which is 24% of the prop diameter. In this case, the prop diameter is 12.78 ft and the spinner diameter is 3.07 ft. At one blade chord downstream, the hub diameter is 30% to 35% of the prop diameter. The rotor to wing position is a minimum of one prop diameter. These installation criteria and prop clearance requirements are shown in Figure C-20 for a 10-blade, single-rotation propfan loaded to 32 shp/D² at cruise.

The engine mounts and supporting structure are shown in Figure C-21. This possible truss arrangement transfers propulsion system forces to the wing structure. It is recognized that the details of the structure are the airplane company's responsibility and the configuration shown here for study pur-

poses is conceptual only, showing that there is room in the nacelle for supports and identifying engine mount locations.

A data summary of the four engine configurations is given in Table C-V. Although the in-line gearbox has a more favorable acquisition price and is estimated to be cheaper to maintain, other considerations make the offset gearbox more desirable for further study. The offset gearbox is favored for the following reasons:

- 1. Inlets are accommodated with less offset of the S-duct.
- There is more space for accessory drives; therefore, there is less interference with gearbox-mounted accessories, less interference with power section to gearbox structure, and direct drive to the AMADS is permitted rather than bevel drive.
- 3. Opposite rotation is accommodated more easily.



Installation Criteria

- A Spinner dia = 24% of prop diameter
- B Highlight dia = 30% to 35% of prop diameter
- C Highlight = 1 blade chord
- D Rotor to wing 1/4 chord = 100% of prop diameter minimum
- E Fuselage spacing to prop tip = 80% of prop diameter
- F Ground clearance = 2 ft to 3 ft

TE83-2256

Figure C-20. Propfan installation criteria.

- 4. Integration of a hydraulic pitch change mechanism is simplified.
- 5. A hydraulic torquemeter can be used.

Based on the comparison, Engines PD436-10 and PD436-11 with offset gearboxes were selected for further evaluation in the engine-aircraft studies of Task IV. These engines are also available in the form of a performance model and data package. The performance model is a customer card deck furnished on tape with a user's manual, Allison EDR 11321 (Ref 1)*. It contains the steady-state engine parameters normally required for airplane company use. The following features are included:

- Two engines, PD436-10 and PD436-11, both with offset gearboxes, are contained in the same performance model.
- Two additional engines, PD436-12 and PD436-13, both with in-line gearboxes, are also contained in the same performance model.
- Performance model conforms to specification AS68C.
- Performance model may be used as a subroutine to user's computer code or separately.
- Automatic power incrementing is obtained with a single input.
- Customer bleed of up to 5% may be selected at low pressure compressor discharge.
- Customer power extraction of up to 300 shp may be selected from the propfan gearbox.
- Inlet recovery may be specified by user.
- Propfan efficiency may be specified by user.
- Propfan ram may be simulated by specifying inlet temperature and pressure rises.
- Power settings from flight idle to maximum power may be specified at all flight conditions within the operating envelope.

An engine data package was prepared to be used for less extensive analyses. This package, defined in Allison EDR 11375A (Ref 2), includes an engine description with an overall drawing, dimensions, and weight estimates. It also contains acquisition price, maintenance cost data, and performance data over a wide range of altitudes, speeds, and power settings. Scaling procedures are defined for the range of 6,000 shp to 18,000 shp. These data are also summarized in the following subsection.

^{*}The references in Appendix C are listed at the end of this appendix.

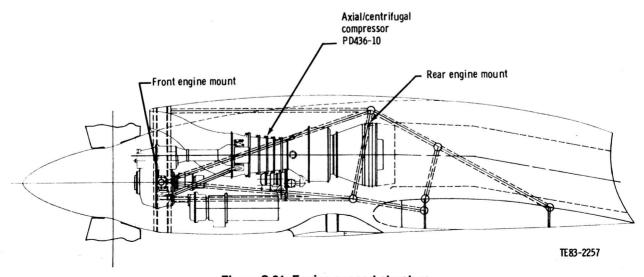


Figure C-21. Engine support structure.

Table C-V.
Engine data summary.

Designation	PD436-10	PD436-11	PD436-12	PD436-13
LP/HP compressor type	Axial/cent	Axial/axial	Axial/cent	Axial/axial
Reduction gearbox type	Offset	Offset	In-line	In-line
Performance				
Max power SLSS, std day-shp	10,000	10,000	10,000	10,000
32,000 ft/0.72 M _N /max cont, sfc—lb/hr/shp	0.305	0.304	0.305	0.304
Weight—lb				
Reduction gearbox	635	635	655	655
Supporting structure	28	28	8	8
Torquemeter		_	40	40
Power section	1499	1473	1499	1473
Total	2162	2136	2202	2176
Dimensions—in.				
Overall length	126.0	133.1	137.3	144.4
Maximum height	43.4	43.4	47.0	47.0
Maximum width	32.1	32.1	47.5	47.5
Acquisition price—1981 \$	1,992,500	1,908,700	1,932,700	1,848,900
Typical maintenance cost—\$/EFH*	132.82	129.05	130.13	126.36

^{*1} flt hr/flight, \$13.75/hr labor rate, 220% burden, 1981 dollars

ENGINE DATA PACKAGE

This subsection presents estimates of performance, weight, dimensional, and cost data for the PD436-10 and -11 turboprop engines. (The performance data are detailed separately in Allison EDR 11375A [Ref 2].) The technology included in these 10,000 shp class propulsion systems is verifiable in the late 1980s and is appropriate for production in the mid 1990s. The two engines have identical overall pressure ratios and turbine temperature levels at the design point. The engine general arrangements are similar except for the HP compressor; PD436-10 employs a centrifugal compressor while PD436-11 utilizes an axial compressor on the HP shaft. The gearbox design for both engines is designed for the propfan speed and employs gearbox/propfan integration features for improved maintainability. The engines have been matched for optimum cruise performance at 32,000 ft altitude and 0.72 Mach number.

Engine Physical Characteristics

A summary of the physical characteristics for both engines is shown in Table C-VI for the unity size of 10,000 shp. The weight data in Table C-VI are dry weights including the engine accessories. They do not include the remote AMADS and interconnecting shafting or the remote oil tank, filter, and cooler. The torquemeter is an integral feature of the

Table C-VI.

Cost and physical characteristics.

	DD 400 40	
5.4	PD436-10	PD436-11
Performance		
SLS, std day, max power		
Power—shp	9999	9999
Specific fuel consumption	0.360	0.359
32,000 ft/0.72 M _N , max continuous		
Power—shp	5337	5331
Specific fuel consumption	0.305	0.304
Dimensions—in.		
Overall length	126.0	133.1
Maximum engine diameter	32.1	32.1
Maximum height	43.4	43.4
Maximum width	32.1	32.1
Weight—lb		
Reduction gearbox	635	635
Supporting structure	28	28
Power section	1499	1473
Total	2162	2136
· otal	2102	2136
Acquisition price—1981 dollars	1,992,500	1,908,700
Typical maintenance costs—\$/EFH*		
Labor	13.49	13.49
Burden	29.67	29.67
Material	89.66	85.89
Total	132.82	129.05

^{*}Assumes 1 flt hr/flight, \$13.75/hr labor rate, 220% burden

reduction gearbox, and its weight is included with the reduction gearbox. The cost data are estimated for 1981 economics. A typical set of maintenance costs is shown in Table C-VI.

Scaling

The following techniques are recommended for scaling performance, weights, dimensions, and cost data over a range of engine sizes from 6,000 shp to 18,000 shp.

The performance data presented herein and the data that can be generated using the customer performance model apply for the unity size 10,000 shp engine. Engines larger or smaller than unity need to be scaled for size effects. The weight and dimensions for the power section and reduction gearbox are scaled separately. In addition, the reduction gearbox weight and dimensions can be modified for overall gear ratios different from the nominal 8.99:1. The acquisition price scaling data use 1981 economics.

1. Performance

Shaft horsepower, shp SF = (shp/9999) $shp = base shp \times 0.9644 e^A$ where $A = 0.01736 SF - 0.001193 SF^2 + 0.02152/SF^2$ SF = scale factorshp = SLS, std day, max power

Specific fuel consumption, shp SFC SFC = base SFC \times 0.9594 e^B where B = (0.005599) (SF²) + (0.03326/SF) + (0.003316/SF²)

2. Dimensions

Engine

Axial dimension = (base dim.) $(shp/9999)^{0.4}$ Diameter = (base dia) $(shp/9999)^{0.5}$

Reduction gearbox

Dimension = (base dim.) $(shp/9999)^{0.5} (GR/8.99)^{0.33}$ where

GR = reduction gearbox overall gear ratio

NOTE: Interconnecting shaft length remains unchanged.

3. Weights

Engine weight = K (shp/9999)^{1.01} where K = 1499 for PD436-10 K = 1473 for PD436-11 Reduction gearbox and interconnecting structure weight = $(635 + 28) (shp/9999)^{1.5} (GR/8.99)^{0.4}$

Interconnecting structure is 4.2% of reduction gearbox weight.

4. Cost

Acquisition price = $X (shp/10^4)^{0.8}$ where $X = 1.9927 \times 10^6$ for PD436-10 $X = 1.9089 \times 10^6$ for PD436-11

Maintenance cost

Labor (manhours/flight/engine)

$$mh = 0.53 \left[\left(0.65 + \frac{0.030 \text{ shp}}{1000} \right) t_f + 0.3 + \frac{0.030 \text{ shp}}{1000} \right]$$

Material (\$/flight/eng/\$ acquisition price) \$ material = $(2.5 t_f + 2.0)/10^5$ where $t_f = flight time per flight$

Uninstalled Steady-State Performance

A performance model is available upon request to predict performance for both PD436-10 and -11 engines over the flight envelope with user-specified installation factors. A user's manual, EDR 11321 (Ref 1), is also available to describe model utilization.

Tables C-VII and C-VIII display steady-state performance data for PD436-10 and -11 over a wide range of altitudes, Mach numbers, and power settings. Both engines are flat rated at maximum power to 86°F ambient day at sea level static. The uninstalled performance data are based on the following assumptions.

- ICAO standard atmosphere unless otherwise specified
- 100% inlet recovery
- 18,400 Btu/lb fuel lower heating value
- zero accessory horsepower extraction
- zero customer bleed extraction
- 100% output shaft speed
- constant jet nozzle effective throat area (PD436-10: 342.7 in.²)

(PD436-11: 340.6 in.2)

The following nomenclature is utilized in the performance tables:

Alt Geopotential pressure altitude—ft M_N Flight Mach number

Power setting

MAX Maximum power (5 min rating)
INT Intermediate power (30 min rating)
MC Maximum continuous power

shp	Shaft horsepower delivered at reduction
	gearbox output flange
W_f	Engine fuel flow—lb/hr
W_{noz}	Nozzle inlet total flow—lb/sec
P_{noz}	Nozzle inlet total pressure—psia
T_{noz}	Nozzle inlet total temperature—°F
FN	Residual jet thrust—lb
$W_{c_{in}}$	Engine inlet corrected airflow—lb/sec

Note that the shaft horsepower and specific fuel consumption are to be adjusted for scaling effects when the engine shp size is different from unity.

Gearbox Trade Data

PD436-12 is identical to PD436-10 except that an in-line reduction gearbox is included. Similarly, PD436-13 is identical to PD436-11 except for the in-line gearbox. The physical characteristics for these engines are summarized in Table C-IX. The performance of PD436-10 and PD436-12 is identical as is the performance of PD436-11 and PD436-13.

Table C-VII.
PD436-10 performance data.

Data	A 14		Power	Power—	w	w	-	D	FN	W
point	Alt	MN	setting	shp	W _f	W _{noz}	T _{noz}	P _{noz}		W _{cin}
				s	TANDARD D	AY				
1	0	0.0	MAX	9,999	3602	48.58	972	16.34	1066	47.58
2	0	0.0	INT	9,225	3371	46.85	954	16.21	982	45.92
3	0	0.10	MAX	10,000	3597	48.62	970	16.35	902	47.34
4	0	0.10	INT	9,264	3378	46.98	953	16.22	827	45.77
5	0	0.20	MAX	10,000	3583	48.75	965	16.35	737	46.63
6	0	0.20	INT	9,381	3399	47.37	951	16.24	679	45.33
7	0	0.30	MAX	10,001	3559	48.96	957	16.35	572	45.47
8	0	0.30	INT	9,573	3433	48.00	947	16.28	535	44.59
				86°F AMBII	ENT TEMPER	RATURE DAY				
9	0	0.0	MAX	9,999	3642	46.95	1038	16.31	1045	47.06
10	0	0.0	INT	7,769	2973	41.95	986	15.93	809	42.12
11	0	0.10	MAX	9,999	3637	46.99	1037	16.31	880	46.82
12	0	0.10	INT	7,800	2978	42.05	985	15.94	666	41.98
13	0	0.20	MAX	9,999	3622	47.11	1031	16.31	718	46.11
14	0	0.20	INT	7,894	2994	42.37	983	15.96	528	41.54
15	0	0.30	MAX	9,999	3598	47.31	1023	16.32	555	44.97
16	0	0.30	INT	8,050	3020	42.89	980	15.99	393	40.83
17	0	0.20	!NT	9,381	3399	47.37	951	16.24	679	45.33
18	0	0.20	MC	7,941	2974	43.99	919	15.99	547	42.14
19	0	0.20		6,474	2547	40.26	889	15.76	423	38.62
20	0	0.20		5,007	2121	36.17	860	15.53	305	34.74
21	0	0.20		3,404	1652	31.11	831	15.30	189	29.93
22	0	0.20		1,761	1143	25.03	792	15.08	83	24.13
23	0	0.20		0	409	14.99	618	14.81	-24	14.52
24	0	0.30	INT	9,573	3433	48.00	947	16.28	535	44.59
25	0	0.30	MC	8,098	3000	44.53	916	16.02	411	41.42
26	0	0.30		6,600	2567	40.73	886	15.78	295	37.93
27	0	0.30		5,097	2134	36.54	857	15.55	189	34.07
28	0	0.30		3,475	1661	31.44	828	15.31	87	29.36
29	0	0.30		1,818	1152	25.35	788	15.09	-0	23.73
30	0	0.30		0	399	15.08	607	14.81	-76	14.19
31	0	0.40	INT	9,837	3479	48.88	943	16.33	393	43.59
32	0	0.40	MC	8,314	3036	45.28	911	16.06	275	40.43
33	0	0.40		6,772	2593	41.36	881	15.81	167	36.97
34	0	0.40		5,220	2150	37.03	854	15.57	71	33.15
35	0	0.40		3,577	1675	31.90	823	15.33	-16	28.60
36	0	0.40		1,900	1164	25.82	783	15.10	-85	23.20
37	0	0.40		0	386	15.23	592	14.81	-130	13.76
38	0	0.50	INT	9,999	3486	49.58	933	16.37	237	41.99
39	0	0.50	MC	8,584	3079	46.22	906	16.12	137	39.18

Table C-VII. (cont)

Data			Power	Power-						
point	Alt	M _N	setting	shp	Wf	W _{noz}	T _{noz}	P _{noz}	FN	Wcin
40	0	0.50		6,987	2625	42.16	876	15.85	37	35.78
41	Ō	0.50		5,374	2170	37.64	849	15.60	-50	31.99
42	0	0.50		3,711	1692	32.50	818	15.35	-122	27.67
43	0	0.50		2,008	1179	26.43	776	15.12	-173	22.55
44	0	0.50		0	371	15.45	573	14.81	-185	13.25
45	0	0.60	INT	10,000	3438	49.95	920	16.37	66	39.76
46	0	0.60	MC	8,906	3128	47.33	899	16.18	-4	37.71
47	0	0.60		7,233	2658	43.05	870	15.90	-97	34.35
48	0	0.60		5,555	2191	38.36	844	15.63	-172	30.64
49	0	0.60		3,880	1714	33.26	811	15.38	-231	26.61
50	0	0.60		2,147	1199	27.20	768	15.14	-265	21.80
51	0	0.60		0	351	15.71	551	14.82	-244	12.67
52	5,000	0.20	INT	8,753	3088	42.58	930	13.71	669	48.11
53	5,000	0.20	MC	7,484	2713	39.68	896	13.48	547	44.89
54	5,000	0.20		6,195	2338	36.52	863	13.26	429	41.37
55	5,000	0.20		4,886	1960	33.02	832	13.05	320	37.45 32.50
56	5,000	0.20		3,426	1538	28.61	800	12.83	206 95	26.09
57	5,000	0.20		1,828	1062	22.92 12.91	762 583	12.60 12.33	-19	14.78
58	5,000	0.20	INIT	0	341		926	13.74	545	47.36
59	5,000	0.30	INT	8,934	3121 2740	43.17 40.21	893	13.74	428	44.16
60	5,000	0.30	MC	7,637	2358	36.96	860	13.28	317	40.65
61	5,000 5,000	0.30 0.30		6,316 4,980	1974	33.39	829	13.20	216	36.77
62 63	5,000	0.30		3,491	1547	28.90	797	12.84	113	31.87
64	5,000	0.30		1,877	1069	23.19	759	12.61	21	25.63
65	5,000	0.30		0	334	13.00	574	12.33	-63	14.45
66	5,000	0.40	INT	9,186	3167	44.00	921	13.80	422	46.33
67	5,000	0.40	MC	7,849	2776	40.94	888	13.55	310	43.16
68	5,000	0.40		6,484	2384	37.57	856	13.31	205	39.66
69	5,000	0.40		5,110	1993	33.90	825	13.09	112	35.83
70	5,000	0.40		3,574	1557	29.26	793	12.85	20	30.98
71	5,000	0.40		1,947	1078	23.57	755	12.62	-55	25.01
72	5,000	0.40		0	324	13.14	560	12.33	-109	14.02
73	5,000	0.50	INT	9,504	3223	45.04	916	13.87	300	45.03
74	5,000	0.50	MC	8,113	2821	41.84	882	13.61	192	41.88
75	5,000	0.50		6,694	2417	38.34	850	13.35	92	38.42
76	5,000	0.50		5,262	2014	34.49	820	13.12	5	34.61
77	5,000	0.50		3,683	1570	29.74	789	12.87	-74	29.89
78	5,000	0.50		2,042	1091	24.08	749	12.64	-134	24.26
79	5,000	0.50		0	312	13.32	542	12.33	-156	13.50
80	5,000	0.60	INT	9,884	3289	46.29	909	13.95	178	43.49
81	5,000	0.60	MC	8,426	2871	42.91	876	13.67	71	40.36
82	5,000	0.60		6,944	2454	39.24	844	13.40	-24	36.95
83	5,000	0.60		5,441	2037	35.19	815	13.15	-104	33.18
84	5,000	0.60		3,829	1588	30.38	783	12.90	-171	28.69
85	5,000	0.60		2,165	1107	24.73	741	12.66	-217	23.41
86	5,000	0.60	INIT	0	296	13.54	522	12.33	-205	12.90
87	10,000	0.20	INT	8,075	2785	37.99	910	11.51	653	50.99
88	10,000	0.20	MC	6,977	2458	35.55	874	11.30 11.10	539	47.78
89	10,000	0.20 0.20		5,847 4,695	2128 1796	32.87 29.90	839 805	10.91	431 327	44.22 40.28
90	10,000 10,000	0.20		3,385	1423	26.12	770	10.70	219	35.25
91 92	10,000	0.20		1,874	984	20.12	732	10.78	105	28.32
93	10,000	0.20		0	285	11.09	551	10.19	-14	15.09
94	10,000	0.30	1NT	8,248	2818	38.56	906	11.55	547	50.24
95	10,000	0.30	MC	7,122	2484	36.05	871	11.33	437	47.03
96	10,000	0.30		5,966	2149	33.30	836	11.13	333	43.49
97	10,000	0.30		4,786	1811	30.25	802	10.92	236	39.56
98	10,000	0.30		3,447	1431	26.39	767	10.71	137	34.57
99	10,000	0.30		1,917	989	21.17	729	10.48	38	27.79
	-,									

Table C-VII. (cont)

Data point	Alt	M _N	Power setting	Power— shp	W _f	W _{noz}	T _{noz}	P _{noz}	FN	W _{cin}
100	10,000	0.30		0	280	11.17	542	10.19	-52	14.75
101	10,000	0.40	INT	8,487	2863	39.34	902	11.61	443	49.20
102	10,000	0.40	MC	7,323	2520	36.73	866	11.38	336	46.00
103	10,000	0.40	WIG	6,131	2177	33.89	832	11.16	237	42.49
104	10,000	0.40		4,911	1830	30.73	798	10.95	144	38.58
105	10,000	0.40		3,534	1443	26.76	764	10.73	55	33.65
106	10,000	0.40		1,978	997	21.49	725	10.49	-29	27.07
107	10,000	0.40		0	272	11.28	530	10.19	-90	14.31
108	10,000	0.50	INT	8,786	2918	40.32	896	11.68	340	47.88
109	10,000	0.50	MC	7,577	2564	37.60	861	11.43	235	44.70
110	10,000	0.50		6,336	2210	34.62	826	11.20	139	41.21
111	10,000	0.50		5,071	1854	31.34	793	10.98	53	37.36
112	10,000	0.50		3,644	1457	27.23	759	10.75	-29	32.51
113	10,000	0.50		2,060	1008	21.91	720	10.51	-98	26.21
114	10,000	0.50		0	262	11.43	513	10.20	-130	13.77
115	10,000	0.60	INT	9,145	2982	41.49	890	11.76	237	46.30
116	10,000	0.60	MC	7,879	2616	38.63	854	11.50	134	43.16
117	10,000	0.60		6,578	2248	35.49	820	11.25	39	39.70
118	10,000	0.60		5,256	1880	32.04	787	11.01	-42	35.89
119	10,000	0.60		3,764	1471	27.74	754	10.77	-116	31.12
120	10,000	0.60		2,164	1021	22.43	713	10.52	-170	25.22
121	10,000	0.60	INIT	0	249	11.62	492	10.20	-171	13.16
122 123	10,000 10,000	0.70 0.70	INT MC	9,558	3055 2672	42.84	883	11.86	131	44.49
123	10,000	0.70	MC	8,223 6,854	2289	39.79 36.46	848 814	11.58	28 -64	41.38
125	10,000	0.70		5,459	1906	32.81	781	11.31 11.05	-04 -141	37.97 34.21
126	10,000	0.70		3,912	1488	28.36	748	10.79	-206	29.61
127	10,000	0.70		2,296	1038	23.10	705	10.75	-245	24.17
128	10,000	0.70		0	232	11.85	469	10.20	-214	12.49
129	15,000	0.30	INT	7,524	2522	34.15	888	9.66	539	53.20
130	15,000	0.30	MC	6,563	2235	32.07	850	9.46	439	50.02
131	15,000	0.30		5,563	1943	29.75	814	9.27	342	46.46
132	15,000	0.30		4,534	1648	27.19	777	9.08	251	42.52
133	15,000	0.30		3,345	1313	23.89	739	8.88	152	37.42
134	15,000	0.30		1,937	914	19.28	698	8.66	57	30.26
135	15,000	0.30		0	234	9.55	512	8.37	-42	15.09
136	15,000	0.40	INT	7,748	2566	34.88	884	9.71	453	52.16
137	15,000	0.40	MC	6,753	2271	32.71	846	9.51	354	48.98
138	15,000	0.40		5,720	1970	30.31	809	9.30	260	45.43
139 140	15,000	0.40		4,656	1668	27.66	773	9.11	173	41.51
141	15,000 15,000	0.40 0.40		3,435	1326	24.26	735	8.90	81	36.48
142	15,000	0.40		1,991 0	921 227	19.54 9.65	695 500	8.67 8.37	-3 -74	29.44
143	15,000	0.50	INT	8,031	2621	35.81	878	9.79	368	14.63 50.84
144	15,000	0.50	MC	6,992	2314	33.52	841	9.56	270	47.66
145	15,000	0.50		5,917	2004	31.01	804	9.34	177	44.14
146	15,000	0.50		4,810	1692	28.24	768	9.14	93	40.25
147	15,000	0.50		3,546	1342	24.73	731	8.92	8	35.30
148	15,000	0.50		2,061	929	19.89	690	8.69	-63	28.45
149	15,000	0.50		0	219	9.77	484	8.37	-107	14.08
150	15,000	0.60	INT	8,369	2685	36.91	872	9.87	284	49.25
151	15,000	0.60	MC	7,278	2365	34.49	834	9.63	184	46.08
152	15,000	0.60		6,155	2044	31.85	797	9.40	93	42.60
153	15,000	0.60		4,992	1720	28.92	762	9.18	10	38.74
154	15,000	0.60		3,674	1359	25.25	725	8.94	-66	33.87
155	15,000	0.60		2,151	940	20.33	684	8.70	-126	27.33
156	15,000	0.60	14.1-	0	208	9.94	464	8.37	-142	13.45
157	15,000	0.70	INT	8,755	2756	38.18	865	9.98	198	47.41
158 159	15,000 15,000	0.70 0.70	MC	7,606	2421	35.60	828	9.71	97	44.27
109	13,000	0.70		6,421	2086	32.79	791	9.46	7	40.82

Table C-VII. (cont)

Data			Power	Power—						
point	Alt	M _N	setting	shp	Wt	W _{noz}	T _{noz}	P _{noz}	FN	Wcin
160	15,000	0.70		5,199	1750	29.70	756	9.22	-74	37.02
161	15,000	0.70		3,814	1376	25.82	719	8.97	-144	32.24
162	15,000	0.70		2,263	954	20.87	677	8.72	-193	26.11
163	15,000	0.70		0	195	10.13	442	8.37	-178	12.77
164	15,000	0.75	INT	8,966	2794	38.87	862	10.04	154	46.41
165	15,000	0.75	MC	7,783	2451	36.20	824	9.76	52	43.27
166	15,000	0.75		6,565	2108	33.30	788	9.49	-38	39.86
167	15,000	0.75		5,310	1765	30.11	753	9.24	-118	36.09
168	15,000	0.75		3,888	1383	26.12	717	8.99	-184	31.35
169	15,000	0.75		2,328	961	21.18	673	8.73	-227	25.47
170	15,000	0.75		0	188	10.24	429	8.37	-197	12.41
171	15,000	0.80	INT	9,188	2833	39.60	859	10.10	109	45.36
172	15,000	0.80	MC	7,975	2483	36.85	821	9.80	6 -84	42.26 38.85
173	15,000	0.80		6,714	2131	33.83	784 749	9.53 9.27	-04 -163	35.12
174	15,000	0.80		5,425	1780 1391	30.54 26.43	749	9.00	-225	30.44
175	15,000	0.80		3,964 2,401	970	21.53	669	8.74	-262	24.84
176	15,000	0.80 0.80		2,401	180	10.36	416	8.38	-217	12.05
177 178	15,000 20,000	0.40	INT	6,981	2279	30.64	867	8.09	453	55.17
179	20,000	0.40	MC	6,148	2028	28.88	827	7.90	363	52.06
180	20,000	0.40	MO	5,268	1769	26.89	788	7.71	276	48.53
181	20,000	0.40		4,348	1507	24.66	750	7.53	190	44.57
182	20,000	0.40		3,281	1208	21.79	709	7.34	106	39.45
183	20,000	0.40		1,992	850	17.77	663	7.13	22	32.23
184	20,000	0.40		0	190	8.22	470	6.82	-60	15.01
185	20,000	0.50	INT	7,249	2333	31.52	862	8.16	385	53.88
186	20,000	0.50	MC	6,374	2070	29.64	822	7.96	294	50.74
187	20,000	0.50		5,454	1803	27.55	783	7.76	207	47.21
188	20,000	0.50		4,498	1532	25.22	744	7.57	123	43.29
189	20,000	0.50		3,390	1224	22.23	704	7.36	44	38.22
190	20,000	0.50		3,051	857	18.05	659	7.14	-32	31.08
191	20,000	0.50		0	183	8.32	456	6.82	-88	14.44
192	20,000	0.60	INT	7,565	2396	32.56	856	8.25	318	52.31
193	20,000	0.60	MC	6,643	2121	30.56	816	8.03	225	49.15
194	20,000	0.60		5,676	1841	28.33	777	7.81	136	45.63
195	20,000	0.60		4,676	1560	25.89	739	7.61 7.39	54 -20	41.75 36.76
196	20,000	0.60		3,519	1243	22.76	698 655	7.15	-20 -88	29.76
197	20,000	0.60		2,124 0	864 175	18.39 8.46	438	6.82	-116	13.79
198 199	20,000 20,000	0.60 0.70	INT	7,926	2466	33.75	850	8.36	251	50.46
200	20,000	0.70	MC	6,950	2176	31.60	810	8.11	154	47.30
201	20,000	0.70	WIC	5,931	1885	29.24	771	7.87	64	43.82
202	20,000	0.70		4,877	1591	26.63	732	7.65	-16	39.97
203	20,000	0.70		3,665	1262	23.34	692	7.42	-86	35.09
204	20,000	0.70		2,219	875	18.83	649	7.17	-145	28.37
205	20,000	0.70		0	164	8.61	416	6.82	-147	13.08
206	20,000	0.75	INT	8,123	2504	34.40	847	8.42	217	49.45
207	20,000	0.75	MC	7,117	2206	32.17	806	8.16	118	46.30
208	20,000	0.75		6,070	1908	29.73	767	7.91	27	42.84
209	20,000	0.75		4,986	1608	27.04	729	7.68	-52	39.01
210	20,000	0.75		3,742	1272	23.65	689	7.43	-120	34.19
211	20,000	0.75		2,273	881	19.09	645	7.18	-175	27.64
212	20,000	0.75		0	158	8.71	405	6.83	-162	12.71
213	20,000	0.80	INT	8,328	2543	35.08	844	8.48	181	48.38
214	20,000	0.80	MC	7,293	2237	32.76	803	8.20	81	45.24
215	20,000	0.80		6,215	1931	30.24	. 764	7.95	-12	41.81
216	20,000	0.80		5,098	1624	27.45	726	7.70	-89	38.00
217	20,000	0.80		3,822	1282	23.97	686	7.45	-156	33.24
218	20,000	0.80		2,334	888	19.36	641	7.19	-205	26.91
219	20,000	0.80		0	152	8.81	392	6.83	-178	12.34

Table C-VII. (cont)

Data			Power	Power—		•••	_	_		
point	Alt	M _N	setting	shp	W _f	W _{noz}	T _{noz}	P _{noz}	FN_	W _{cin}
220	25,000	0.40	INT	6,188	1999	26.59	853	6.69	441	58.08
221	25,000	0.40	MC	5,518	1792	25.23	811	6.52	363	55.19
222	25,000	0.40		4,785	1574	23.63	769	6.36	282	51.76
223	25,000	0.40		4,001	1348	21.79	728	6.20	205	47.78
224	25,000	0.40 0.40		3,085 1,960	1090 779	19.40 16.04	683 633	6.02 5.82	126 43	42.62 35.31
225 226	25,000 25,000	0.40		0 0	158	6.97	443	5.62	-49	15.45
227	25,000	0.50	INT	6,441	2053	27.42	848	6.76	389	56.88
228	25,000	0.50	MC	5,730	1834	25.96	805	6.58	308	53.91
229	25,000	0.50		4,958	1607	24.25	764	6.40	225	50.42
230	25,000	0.50		4,145	1373	22.32	723	6.23	150	46.47
231	25,000	0.50		3,190	1107	19.82	678	6.04	73	41.34
232	25,000	0.50		2,019	787	16.31	629	5.83	-4	34.10
233	25,000	0.50	INIT	0	153	7.05	429	5.51	-72	14.85
234	25,000	0.60 0.60	INT MC	6,741	2116 1883	28.41 26.81	842 800	6.85 6.65	339 253	55.39 52.33
235 236	25,000 25,000	0.60	MC	5,981 5,166	1645	24.99	758 .	6.46	169	48.83
237	25,000	0.60		4,314	1402	22.94	717	6.27	94	44.90
238	25,000	0.60		3,314	1126	20.32	673	6.07	19	39.82
239	25,000	0.60		3,089	795	16.63	624	5.85	-53	32.67
240	25,000	0.60		0	146	7.16	412	5.51	-95	14.17
241	25,000	0.70	INT	7,078	2185	29.54	836	6.96	289	53.60
242	25,000	0.70	MC	6,267	1939	27.79	794	6.74	197	50.48
243	25,000	0.70		5,405	1688	25.83	752	6.52	111	46.98
244	25,000	0.70		4,508	1434	23.66	710	6.32	36	43.10
245	25,000	0.70		3,457	1147	20.88	667	6.10	-37	38.09
246	25,000	0.70		2,166 0	803 138	16.98 7.29	619 392	5.86	-103 -120	31.04
247 248	25,000 25,000	0.70 0.75	INT	7,259	2222	30.15	834	5.51 7.02	263	13.44 52.60
249	25,000	0.75	MC	6,423	1968	28.33	791	6.79	169	49.47
250	25,000	0.75	1410	5,536	1710	26.30	749	6.56	81	45.98
251	25,000	0.75		4,614	1451	24.06	707	6.34	7	42.12
252	25,000	0.75		3,534	1157	21.19	663	6.12	-66	37.15
253	25,000	0.75		2,208	807	17.17	616	5.87	-128	30.18
254	25,000	0.75		0	133	7.37	381	5.51	-133	13.06
255	25,000	0.80	INT	7,447	2260	30.79	831	7.09	237	51.54
256	25,000	0.80	MC	6,586	1999	28.89	788	6.84	140	48.40
257 258	25,000 25,000	0.80 0.80		5,673 4,723	1734 1468	26.78 24.46	745 704	6.60	51	44.92
259	25,000	0.80		3,614	1168	21.50	660	6.37 6.13	-24 -95	41.09 36.18
260	25,000	0.80		2,259	813	17.40	613	5.88	-155	29.34
261	25,000	0.80		0	128	7.45	370	5.52	-147	12.67
262	30,000	0.50	INT	5,613	1779	23.51	836	5.56	379	59.67
263	30,000	0.50	MC	5,064	1605	22.45	791	5.41	309	57.03
264	30,000	0.50		4,441	1417	21.12	747	5.25	237	53.73
265	30,000	0.50		3,760	1218	19.54	703	5.10	169	49.79
266	30,000	0.50		2,952	991	17.49	655	4.92	95	44.63
267 268	30,000	0.50		1,941	714	14.58	600	4.73	19	37.28
269	30,000 30,000	0.50 0.60	INT	0 5,900	128 1843	5.95 24.48	404 831	4.42 5.66	-58 346	15.33 58.39
270	30,000	0.60	MC	5,301	1654	23.26	786	5.48	269	55.55
271	30,000	0.60		4,635	1454	21.81	741	5.31	193	52.15
272	30,000	0.60		3,920	1247	20.13	697	5.14	124	48.21
273	30,000	0.60		3,072	1010	17.97	649	4.95	51	43.08
274	30,000	0.60		2,014	724	14.91	595	4.75	-21	35.82
275	30,000	0.60		0	122	6.04	388	4.42	-77	14.62
276	30,000	0.70	INT	6,213	1912	25.56	826	5.77	311	56.74
277	30,000	0.70	MC	5,568	1709	24.19	780	5.57	228	53.76
278	30,000	0.70		4,858	1497	22.60	735	5.38	149	50.31
279	30,000	0.70		4,105	1279	20.82	691	5.19	78	46.39

Table C-VII. (cont)

Data			Power	Power-						
point	Alt	M _N	setting	shp	Wf	W _{noz}	T _{noz}	P _{noz}	FN	Wcin
280	30,000	0.70		3,209	1032	18.50	643	4.99	5	41.30
281	30,000	0.70		2,094	734	15.26	589	4.76	-64	34.13
282	30,000	0.70		0	116	6.15	370	4.42	-98	13.86
283	30,000	0.75	INT	6,383	1950	26.14	824	5.83	294	55.80
284	30,000	0.75	MC	5,710	1737	24.69	777	5.62	207	52.76
285	30,000	0.75		4,979	1519	23.04	732	5.41	127	49.29
286	30,000	0.75		4,203	1296	21.18	688	5.21	54	45.38
287	30,000	0.75		3,282	1043	18.79	640	5.00	-19	40.33
288	30,000	0.75		2,136	739	15.44	587	4.77	-86	33.21
289	30,000	0.75	.	0	112	6.21	359	4.42	-108	13.47
290	30,000	0.80	INT	6,557 5,857	1988	26.74	821	5.90	276	54.77
291	30,000	0.80	MC	5,857	1766 1542	25.22 23.49	775 729	5.68	187	51.70
292 293	30,000 30,000	0.80 0.80		4,307	1314	23.49	684	5.45 5.24	104 30	48.22
293 294	30,000	0.80		3,360	1054	19.10	636	5.02	-43	44.33 39.32
295	30,000	0.80		2,179	743	15.63	584	4.78	-109	32.26
296	30,000	0.80		0	108	6.28	348	4.42	-119	13.07
297	35,000	0.50	INT	4,350	1371	19.04	776	4.40	296	59.73
298	35,000	0.50	MC	4,350	1371	19.04	776	4.40	296	59.73
299	35,000	0.50		3,906	1233	18.15	732	4.28	241	57.01
300	35,000	0.50		3,357	1069	16.92	685	4.14	180	53.22
301	35,000	0.50		2,686	877	15.27	633	3.99	112	48.10
302	35,000	0.50		1,826	641	12.88	573	3.81	39	40.65
303	35,000	0.50		0	107	5.00	380	3.50	-46	15.90
304	35,000	0.60	INT	4,803	1495	20.27	795	4.55	300	59.73
305	35,000	0.60	MC	4,606	1431	19.89	774	4.49	274	58.66
306	35,000	0.60		4,090	1270	18.81	727	4.34	209	55.53
307	35,000	0.60		3,505	1097	17.47	679	4.18	145	51.65
308	35,000	0.60		2,798	896	15.71	628	4.02	76	46.52
309	35,000	0.60		1,897	651	13.19	568	3.83	5	39.14
310	35,000	0.60 0.70	INT	0	103	5.07 21.75	366	3.50	-62	15.16
311 312	35,000 35,000	0.70	MC	5,343 4,854	1646 1486	20.77	818 770	4.74 4.58	316 247	59.63 57.02
313	35,000	0.70	IVIC	4,034	1312	19.56	721	4.41	177	53.75
314	35,000	0.70		3,675	1128	18.10	673	4.23	109	49.82
315	35,000	0.70		2,928	918	16.22	622	4.05	39	44.71
316	35,000	0.70		1,979	663	13.55	562	3.85	-31	37.42
317	35,000	0.70		0	98	5.16	349	3.50	-79	14.36
318	35,000	0.75	INT	5,508	1685	22.32	816	4.81	307	58.84
319	35,000	0.75	MC	4,986	1515	21.25	767	4.63	233	56.08
320	35,000	0.75		4,407	1334	19.96	718	4.44	161	52.74
321	35,000	0.75		3,768	1145	18.45	670	4.26	92	48.81
322	35,000	0.75		2,998	929	16.49	618	4.07	20	43.71
323	35,000	0.75		2,023	668	13.74	559	3.86	-49	36.48
324	35,000	0.75		0	95	5.21	339	3.50	-87	13.95
325	35,000	0.80	INT	5,672	1722	22.91	813	4.88	298	57.94
326	35,000	0.80	MC	5,123	1545	21.74	765	4.68	220	55.07
327	35,000	0.80		4,520	1356	20.38	716	4.49	144	51.66
328 329	35,000 35,000	0.80 0.80		3,865 3,072	1163 941	18.81 16.79	667 615	4.29 4.09	73 1	47.75
330	35,000	0.80		2,068	674	13.93	557	3.87	-68	42.68 35.50
331	35,000	0.80		0	92	5.27	329	3.50	-96	13.53
332	40,000	0.50	INT	3,395	1071	15.04	763	3.46	232	59.73
333	40,000	0.50	MC	3,394	1071	15.04	763	3.46	232	59.73
334	40,000	0.50	***************************************	3,131	989	14.52	729	3.39	200	57.71
335	40,000	0.50		2,700	859	13.57	681	3.28	150	53.98
336	40,000	0.50		2,168	707	12.27	629	3.15	95	48.88
337	40,000	0.50		1,482	518	10.37	568	3.01	35	41.42
338	40,000	0.50		0	90	4.07	386	2.76	-36	16.38
339	40,000	0.60	INT	3,749	1168	16.01	782	3.57	235	59.73

Table C-VII. (cont)

Data			Power	Power—						
point	Alt	M _N	setting	shp	Wf	W _{noz}	T _{noz}	P _{noz}	FN	Wcin
340	40,000	0.60	MC	3,682	1146	15.89	772	3.55	226	59.28
341	40,000	0.60		3,282	1020	15.06	724	3.44	175	56.25
342	40,000	0.60		2,821	882	14.01	676	3.31	123	52.42
343	40,000	0.60		2,260	723	12.63	623	3.18	67	47.30
344	40,000	0.60		1,541	527	10.63	563	3.02	8	39.90
345	40,000	0.60		0	87	4.12	372	2.76	-49	15.61
346	40,000	0.70	INT	4,191	1294	17.21	807	3.73	249	59.73
347	40,000	0.70	MC	3,885	1192	16.61	768	3.63	206	57.70
348	40,000	0.70		3,450	1054	15.67	718	3.49	150	54.49
349	40,000	0.70		2,959	908	14.53	670	3.35	96	50.58
350	40,000	0.70		2,365	740	13.04	617	3.20	38	45.47
351	40,000	0.70		1,608	536	10.92	557	3.04	-20	38.16
352	40,000	0.70		0	83	4.20	356	2.76	-63	14.79
353	40,000	0.75	INT	4,399	1348	17.83	814	3.82	254	59.45
354	40,000	0.75	MC	3,994	1216	17.00	766	3.67	196	56.79
355	40,000	0.75		3,538	1072	16.00	716	3.53	138	53.49
356	40,000	0.75		3,035	922	14.81	667	3.38	81	49.58
357	40,000	0.75		2,423	750	13.26	614	3.22	23	44.48
358	40,000	0.75		1,644	541	11.08	554	3.05	-35	37.22
359	40,000	0.75		0	81	4.24	347	2.76	-70	14.36
360	40,000	0.80	INT	4,535	1380	18.31	812	3.88	249	58.59
361	40,000	0.80	MC	4,106	1240	17.41	763	3.72	186	55.80
362	40,000	0.80		3,632	1090	16.34	713	3.56	125	52.42
363	40,000	0.80		3,114	937	15.10	664	3.40	67	48.52
364	40,000	0.80		2,483	760	13.50	611	3.24	8	43.44
365	40,000	0.80		1,681	546	11.24	551	3.06	-50	36.23
366	40,000	0.80		0	78	4.28	338	2.76	-77	13.93

Table C-VIII.
PD436-11 performance data.

Data			Power	Power—			_			10.09
point	Alt	MN	setting	shp	W _f	W _{noz}	T _{noz}	P _{noz}	FN	Wcin
				S	TANDARD D	AY				
1	0	0.0	MAX	9,999	3586	48.28	971	16.34	1059	47.28
2	0	0.0	INT	9,237	3359	46.59	953	16.21	977	45.66
3	0	0.10	MAX	9,999	3581	48.32	969	16.34	896	47.04
4	0	0.10	INT	9,276	3366	46.71	952	16.22	822	45.51
5	0	0.20	MAX	10,000	3567	48.45	964	16.35	732	46.34
6	0	0.20	INT	9,392	3387	47.10	950	16.24	675	45.07
7	0	0.30	MAX	10,000	3543	48.66	956	16.35	568	45.19
8	0	0.30	INT	9,584	3421	47.73	947	16.28	532	44.34
				86°F AMBIE	ENT TEMPER	RATURE DAY				
9	0	0.0	MAX	9,999	3626	46.66	1037	16.31	1037	46.77
10	0	0.0	INT	7,783	2963	41.71	985	15.94	804	41.89
11	0	0.10	MAX	10,000	3621	46.70	1036	16.31	875	46.53
12	0	0.10	INT	7,814	2968	41.82	985	15.94	662	41.74
13	0	0.20	MAX	9,999	3606	46.83	1030	16.31	713	45.83
14	0	0.20	INT	7,908	2984	42.13	983	15.96	525	41.31
15	0	0.30	MAX	9,999	3582	47.02	1022	16.31	550	44.69
16	0	0.30	INT	8,064	3010	42.65	979	15.99	391	40.60
17	0	0.20	INT	9,392	3387	47.10	950	16.24	675	45.07
18	0	0.20	MC	7,955	2964	43.74	918	16.00	544	41.90
19	0	0.20		6,490	2539	40.04	888	15.76	421	38.41

Table C-VIII. (cont)

Data			Power	Power-						
point	Alt	M _N	setting	shp	Wt	W _{noz}	T _{noz}	P _{noz}	FN	W _{cin}
20	0	0.20		5,026	2115	35.98	859	15.53	304	34.56
21	0	0.20		3,423	1647	30.95	830	15.30	189	29.78
22	0	0.20		1,779	1140	24.91	791	15.08	83	24.01
23	0	0.20		0	403	14.84	615	14.81	-24	14.38
24	0	0.30	INT	9,584	3421	47.73	947	16.28	532	44.34
25	0	0.30	MC	8,111	2990	44.28	915	16.02	408	41.19
26	0	0.30		6,617	2559	40.51	885	15.78	294	37.72
27	0	0.30 0.30		5,114 3,494	2127 1656	36.34 31.27	856 827	15.55 15.32	188 87	33.88 29.21
28 29	0 0	0.30		1,836	1149	25.23	787	15.09	-0	23.62
30	0	0.30		0	393	14.93	604	14.81	-76	14.05
31	0	0.40	INT	9,849	3467	48.60	942	16.33	391	43.34
32	0	0.40	MC	8,327	3025	45.03	910	16.07	273	40.20
33	0	0.40		6,788	2585	41.14	881	15.81	166	36.77
34	0	0.40		5,239	2143	36.84	852	15.57	70	32.97
35	0	0.40		3,596	1670	31.74	823	15.33	-16	28.45
36	0	0.40		1,918	1161	25.69	782	15.10	-85	23.08
37	0	0.40		0	381	15.09	589	14.81	-130	13.63
38	0	0.50	INT	9,999	3470	49.28	932	16.37	235	41.73
39	0	0.50	MC	8,597	3068	45.96	905	16.12	136	38.96
40	0	0.50		7,003	2616 2163	41.92 37.46	875 848	15.85 15.60	37 -49	35.58 31.84
41 42	0 0	0.50 0.50		5,396 3,730	1687	32.34	817	15.35	-121	27.53
43	0	0.50		2,026	1176	26.30	775	15.12	-172	22.43
44	0	0.50		0	365	15.30	571	14.81	-184	13.13
45	Ō	0.60	INT	10,000	3423	49.65	919	16.37	65	39.52
46	0	0.60	MC	8,919	3117	47.06	899	16.18	-4	37.49
47	0	0.60		7,247	2649	42.81	870	15.90	-96	34.15
48	0	0.60		5,573	2184	38.15	843	15.63	-172	30.47
49	0	0.60		3,898	1709	33.09	811	15.38	-229	26.47
50	0	0.60		2,166	1195	27.07	767	15.14	-265	21.70
51	0	0.60	INIT	0	346	15.56	549	14.81	-242	12.55
52	5,000 5,000	0.20 0.20	INT MC	8,760 7,494	3077 2704	42.33 39.46	929 895	13.71 13.48	665 544	47.83 44.64
53 54	5,000	0.20	MC	6,207	2330	36.32	863	13.46	427	41.13
55	5,000	0.20		4,900	1954	32.84	831	13.05	318	37.25
56	5,000	0.20		3,442	1534	28.46	799	12.83	205	32.33
57	5,000	0.20		1,843	1059	22.81	762	12.61	95	25.97
58	5,000	0.20		0	337	12.79	581	12.33	-19	14.64
59	5,000	0.30	INT	8,942	3110	42.93	925	13.74	542	47.09
60	5,000	0.30	MC	7,647	2730	39.99	892	13.51	426	43.91
61	5,000	0.30		6,329	2350	36.76	859	13.28	315	40.42
62	5,000	0.30		4,995	1968	33.21	828	13.07	215	36.57
63	5,000	0.30		3,507	1542	28.75	796	12.84	113	31.70
64	5,000	0.30		1,892 0	1066 330	23.08 12.89	758 571	12.61 12.33	21 -63	25.50 14.32
65 66	5,000 5,000	0.30 0.40	INT	9,193	3155	43.75	921	13.80	-03 420	46.06
67	5,000	0.40	MC	7,858	2767	40.71	887	13.55	309	42.91
68	5,000	0.40	IVIO	6,496	2376	37.37	855	13.31	204	39.44
69	5,000	0.40		5,120	1986	33.70	824	13.09	110	35.61
70	5,000	0.40		3,589	1552	29.11	793	12.85	20	30.81
71	5,000	0.40		1,962	1075	23.46	754	12.62	-55	24.88
72	5,000	0.40		0	320	13.01	557	12.33	-108	13.89
73	5,000	0.50	INT	9,510	3211	44.78	915	13.87	298	44.77
74	5,000	0.50	MC	8,123	2811	41.61	882	13.61	191	41.65
75	5,000	0.50		6,707	2409	38.13	850	13.36	91	38.21
76	5,000	0.50		5,276	2007	34.30	819	13.12	5	34.42
77	5,000	0.50		3,697 2,057	1565	29.58	788	12.87	-74 122	29.73
78 79	5,000 5,000	0.50 0.50		2,057	1088 307	23.96 13.19	748 540	12.64 12.33	-133 -155	24.13 13.37
19	3,000	0.50		U	307	13.18	340	12.33	-100	13.37

Table C-VIII. (cont)

Data			Power	Power—						
point	Alt	MN	setting	shp	W_{t}	W_{noz}	T _{noz}	P _{noz}	FN	Wcin
80	5,000	0.60	INT	9,891	3277	46.03	908	13.95	176	43.24
81	5,000	0.60	MC	8,434	2861	42.67	875	13.67	70	40.13
82	5,000	0.60		6,955	2445	39.01	844	13.40	-24	36.74
83	5,000	0.60		5,456	2030	35.00	814	13.15	-103	33.00
84	5,000	0.60		3,844	1583	30.22	782	12.90	-170	28.54
85	5,000	0.60		2,180	1104	24.61	740	12.66	-216	23.29
86	5,000	0.60		0	292	13.41	520	12.33	-203	12.78
87	10,000	0.20	INT	8,081	2774	37.77	909	11.51	648	50.70
88	10,000	0.20	MC	6,984	2449	35.35	874	11.30	536	47.50
89	10,000	0.20		5,855	2121	32.68	839	11.10	428	43.97 40.06
90	10,000	0.20		4,706	1790	29.73	805	10.91	325 218	35.06
91 92	10,000 10,000	0.20 0.20		3,397 1,886	1418 981	25.98 20.84	769 731	10.70 10.48	105	28.18
93	10,000	0.20		0 0	282	10.99	549	10.48	-15	14.95
94	10,000	0.30	INT	8,252	2807	38.33	906	11.55	543	49.95
95	10,000	0.30	MC	7,128	2476	35.84	870	11.33	434	46.76
96	10,000	0.30	0	5,975	2141	33.11	835	11.13	331	43.24
97	10,000	0.30		4,797	1805	30.08	801	10.92	234	39.35
98	10,000	0.30		3,460	1427	26.25	767	10.71	137	34.39
99	10,000	0.30		1,930	987	21.06	728	10.48	38	27.65
100	10,000	0.30		0	276	11.06	540	10.19	-52	14.61
101	10,000	0.40	INT	8,489	2852	39.11	901	11.61	440	48.91
102	10,000	0.40	MC	7,329	2511	36.52	866	11.38	334	45.73
103	10,000	0.40		6,140	2169	33.70	831	11.16	235	42.25
104	10,000	0.40		4,924	1824	30.57	797	10.95	144	38.38
105	10,000	0.40		3,546	1439	26.62	763	10.73	55	33.47
106	10,000	0.40		1,991 0	994 268	21.38 11.17	724 527	10.49 10.19	-29 -90	26.94 14.17
107	10,000 10,000	0.40 0.50	INT	8,788	2907	40.08	895	11.68	338	47.60
109	10,000	0.50	MC	7,582	2555	37.38	860	11.43	234	44.44
110	10,000	0.50	IVIC	6,344	2202	34.43	825	11.20	138	40.98
111	10,000	0.50		5,082	1848	31.17	792	10.98	52	37.15
112	10,000	0.50		3,656	1453	27.08	758	10.75	-29	32.33
113	10,000	0.50		2,073	1005	21.80	719	10.51	-98	26.08
114	10.000	0.50		0	258	11.32	511	10.19	-129	13.64
115	10,000	0.60	INT	9,146	2971	41.25	889	11.76	235	46.03
116	10,000	0.60	MC	7,885	2607	38.40	854	11.50	132	42.91
117	10,000	0.60		6,586	2240	35.28	819	11.25	39	39.47
118	10,000	0.60		5,268	1874	31.87	786	11.01	-42	35.70
119	10,000	0.60		3,776	1467	27.59	753 712	10.77 10.52	-115 -169	30.95 25.09
120 121	10,000 10,000	0.60 0.60		2,177 0	1018 245	22.32 11.52	490	10.52	-170	13.04
122	10,000	0.70	INT	9,559	3044	42.59	882	11.86	130	44.23
123	10,000	0.70	MC	8,228	2663	39.57	847	11.58	27	41.14
124	10,000	0.70		6,861	2281	36.26	813	11.31	-63	37.75
125	10,000	0.70		5,468	1900	32.63	780	11.05	-140	34.02
126	10,000	0.70		3,924	1483	28.20	748	10.79	-205	29.45
127	10,000	0.70		2,309	1035	22.98	704	10.55	-243	24.04
128	10,000	0.70		0	229	11.74	466	10.20	-213	12.38
129	15,000	0.30	INT	7,525	2513	33.95	888	9.66	536	52.89
130	15,000	0.30	MC	6,567	2227	31.89	850	9.46	437	49.73
131	15,000	0.30		5,569	1936	29.58	813	9.27	340	46.20
132	15,000	0.30		4,542	1642	27.04	776	9.08	249	42.28
133	15,000	0.30		3,355 1,948	1309	23.76	739 697	8.88 8.66	151 57	37.22 30.11
134 135	15,000 15,000	0.30 0.30		1,948	912 231	19.18 9.46	510	8.37	-42	14.95
136	15,000	0.30	INT	7,749	2557	34.68	883	9.71	450	51.86
137	15,000	0.40	MC	6,757	2262	32.53	845	9.51	352	48.70
138	15,000	0.40	IVIO	5,726	1963	30.14	808	9.30	258	45.18
139	15,000	0.40		4,664	1662	27.50	772	9.11	172	41.28

Table C-VIII. (cont)

Data			Power	Power-						
point	Alt	M _N	setting	shp	W _f	W _{noz}	T _{noz}	P _{noz}	FN	W _{cin}
140	15,000	0.40		3,444	1322	24.13	735	8.90	80	36.28
141	15,000	0.40		2,001	918	19.44	694	8.67	-3	29.29
142	15,000	0.40		0	224	9.56	497	8.37	-74	14.50
143	15,000	0.50	INT	8,032	2611	35.60	877	9.79	366	50.54
144	15,000	0.50	MC	6,995	2306	33.33	840	9.56	268	47.38
145	15,000	0.50		5,923	1997	30.83	803	9.34	176	43.89
146	15,000	0.50		4,817	1687	28.08	767	9.14	92	40.02
147	15,000	0.50		3,556	1338	24.59	730	8.92	8	35.10
148	15,000	0.50		2,072	927	19.79	689	8.69	-64	28.30
149	15,000	0.50		0	216	9.68	482	8.37	-107	13.95 48.96
150	15,000	0.60	INT	8,368	2675	36.70 34.29	872 834	9.87 9.63	283 183	45.81
151	15,000	0.60	MC	7,280	2356 2036	31.67	797	9.40	93	42.35
152	15,000	0.60		6,159 4,999	1714	28.76	761	9.18	10	38.52
153	15,000	0.60 0.60		3,683	1354	25.11	724	8.94	-66	33.69
154 155	15,000 15,000	0.60		2,162	938	20.22	683	8.70	-126	27.19
156	15,000	0.60		0	206	9.84	462	8.37	-141	13.33
157	15,000	0.70	INT	8,753	2746	37.96	865	9.98	197	47.13
158	15,000	0.70	MC	7,608	2413	35.40	827	9.71	96	44.01
159	15,000	0.70		6,426	2079	32.61	790	9.46	6	40.59
160	15,000	0.70		5,205	1744	29.53	755	9.22	-74	36.81
161	15,000	0.70		3,824	1371	25.68	719	8.97	-143	32.06
162	15,000	0.70		2,273	951	20.76	676	8.72	-191	25.97
163	15,000	0.70		0	193	10.03	440	8.37	-177	12.65
164	15,000	0.75	INT	8,964	2784	38.64	862	10.04	153	46.14
165	15,000	0.75	MC	7,787	2443	36.00	823	9.76	52	43.04
166	15,000	0.75		6,569	2101	33.11	787	9.49	-38	39.63 35.89
167	15,000	0.75		5,316	1759	29.94 25.98	752 716	9.24 8.99	-118 -183	31.18
168	15,000	0.75 0.75		3,897 2,338	1379 958	21.07	672	8.73	-225	25.34
169 170	15,000 15,000	0.75		2,336	185	10.14	427	8.37	-196	12.30
171	15,000	0.80	INT	9,184	2823	39.37	858	10.10	108	45.09
172	15,000	0.80	MC	7,975	2474	36.64	820	9.80	6	42.01
173	15,000	0.80		6,718	2123	33.64	784	9.53	-84	38.62
174	15,000	0.80		5,432	1774	30.37	749	9.27	-162	34.92
175	15,000	0.80		3,974	1387	26.29	713	9.00	-223	30.27
176	15,000	0.80		2,411	967	21.41	668	8.74	-260	24.71
177	15,000	0.80		0	178	10.26	415	8.37	-215	11.94
178	20,000	0.40	INT	6,979	2271	30.46	867	8.09	450	54.84
179	20,000	0.40	MC	6,149	2020	28.71	827	7.90	361	51.76
180	20,000	0.40		5,271	1763	26.73	787	7.71	274	48.25
181	20,000	0.40		4,353	1501	24.52	749	7.53	189	44.32
182	20,000	0.40		3,288	1204	21.67	708	7.34 7.13	105 22	39.23 32.06
183	20,000	0.40		2,000	847 188	17.67 8.14	663 469	6.82	-60	14.88
184 185	20,000 20,000	0.40 0.50	INT	0 7,247	2324	31.33	861	8.16	383	53.57
186	20,000	0.50	MC	6,375	2063	29.47	821	7.96	292	50.44
187	20,000	0.50	0	5,457	1796	27.39	782	7.76	205	46.94
188	20,000	0.50		4,503	1526	25.08	744	7.57	122	43.04
189	20,000	0.50		3,397	1220	22.11	703	7.36	43	38.01
190	20,000	0.50		2,060	854	17.95	659	7.14	-32	30.92
191	20,000	0.50		0	181	8.24	454	6.82	-87	14.31
192	20,000	0.60	INT	7,562	2387	32.37	856	8.25	316	52.00
193	20,000	0.60	MC	6,643	2113	30.38	815	8.03	224	48.86
194	20,000	0.60		5,677	1835	28.17	776	7.81	135	45.37
195	20,000	0.60		4,681	1555	25.74	738	7.61	54	41.51
196	20,000	0.60		3,526	1238	22.63	697	7.39	-20	36.55
197	20,000	0.60		2,132	862	18.29	654	7.15	-87	29.61
198	20,000	0.60	INIT	7.022	172	8.38	436	6.82	-116 240	13.66
199	20,000	0.70	INT	7,922	2457	33.55	850	8.36	249	50.16

Table C-VIII. (cont)

Data			Power	Power—						
point	Alt	M _N	setting	shp	Wf	W _{noz}	T _{noz}	P _{noz}	FN	Wcin
200	20,000	0.70	MC	6,949	2168	31.42	809	8.11	153	47.03
201	20,000	0.70		5,934	1878	29.07	770	7.87	63	43.57
202	20,000	0.70		4,881	1586	26.48	731	7.65	-16	39.74
203	20,000	0.70		3,671	1258	23.21	691	7.42	-86	34.90
204	20,000	0.70		2,227	873	18.73	648	7.17	-144	28.22
205 206	20,000 20,000	0.70 0.75	INT	0 8,118	162 2494	8.54 34.19	414 847	6.82 8.42	-146 215	12.96 49.16
207	20,000	0.75	MC	7,116	2198	31.98	806	8.16	117	46.03
208	20,000	0.75	IVIO	6,071	1901	29.56	766	7.91	26	42.59
209	20,000	0.75		4,990	1602	26.88	728	7.68	-52	38.79
210	20,000	0.75		3,749	1268	23.52	688	7.44	-120	33.99
211	20,000	0.75		2,282	879	18.98	644	7.18	-174	27.49
212	20,000	0.75		0	156	8.63	403	6.82	-161	12.60
213	20,000	0.80	INT	8,322	2533	34.87	843	8.48	180	48.09
214	20,000	0.80	MC	7,291	2229	32.57	802	8.21	81	44.98
215 216	20,000 20,000	0.80 0.80		6,217 5,102	1924 1618	30.07 27.30	763 725	7.95 7.70	-12 -89	41.57 37.79
217	20,000	0.80		3,828	1278	23.84	685	7.45	-155	33.05
218	20,000	0.80		2,342	886	19.26	641	7.19	-204	26.77
219	20,000	0.80		0	150	8.72	391	6.82	-177	12.22
220	25,000	0.40	INT	6,185	1991	26.43	853	6.69	438	57.74
221	25,000	0.40	MC	5,518	1786	25.09	810	6.52	361	54.87
222	25,000	0.40		4,786	1568	23.50	769	6.36	280	51.46
223	25,000	0.40		4,004	1343	21.66	727	6.20	203	47.50
224	25,000	0.40		3,090	1087	19.30	683	6.02	125	42.38
225	25,000	0.40		1,966	777	15.95	632	5.82	42	35.12
226	25,000	0.40	INIT	0	156	6.90	441 848	5.51 6.76	-48 386	15.31 56.53
227 228	25,000 25,000	0.50 0.50	INT MC	6,436 5,729	2046 1828	27.25 25.80	805	6.58	306	53.59
229 ·	25,000	0.50	IVIO	4,959	1601	24.11	763	6.40	224	50.13
230	25,000	0.50		4,148	1368	22.19	722	6.23	149	46.20
231	25,000	0.50		3,195	1103	19.71	677	6.04	73	41.11
232	25,000	0.50		2,026	784	16.23	628	5.83	-4	33.92
233	25,000	0.50		0	151	6.99	427	5.51	-71	14.71
234	25,000	0.60	INT	6,736	2108	28.25	842	6.85	337	55.06
235	25,000	0.60	MC	5,979	1876	26.65	799	6.65	251	52.02
236	25,000	0.60		5,167	1639	24.84	758 716	6.46	168 93	48.54 44.64
237 238	25,000 25,000	0.60 0.60		4,316 3,319	1397 1122	22.81 20.20	716 672	6.27 6.07	19	39.59
239	25,000	0.60		2,095	792	16.54	623	5.85	-53	32.49
240	25,000	0.60		0	144	7.09	410	5.51	-95	14.04
241	25,000	0.70	INT	7,072	2177	29.37	836	6.96	287	53.28
242	25,000	0.70	MC	6,264	1932	27.62	793	6.74	196	50.18
243	25,000	0.70		5,405	1681	25.68	751	6.52	110	46.71
244	25,000	0.70		4,511	1429	23.53	710	6.32	36	42.85
245	25,000	0.70		3,462	1143	20.76	666	6.10	-37	37.87
246	25,000	0.70		2,173	801	16.89	618	5.86	-102	30.88
247	25,000	0.70 0.75	INT	0 7,252	136 2213	7.23 29.97	390 833	5.51 7.02	-119 261	13.32 52.29
248 249	25,000 25,000	0.75	MC	6,420	1961	28.16	790	6.79	168	49.18
250	25,000	0.75	MC	5,536	1704	26.14	748	6.56	81	45.71
251	25,000	0.75		4,616	1446	23.92	706	6.34	7	41.88
252	25,000	0.75		3,538	1153	21.06	663	6.12	-66	36.94
253	25,000	0.75		2,215	805	17.08	615	5.87	-128	30.02
254	25,000	0.75		0	131	7.30	379	5.51	-132	12.94
255	25,000	0.80	INT	7,437	2250	30.61	831	7.09	236	51.23
256	25,000	0.80	MC	6,582	1991	28.72	787	6.84	139	48.12
257	25,000	0.80		5,671	1728	26.62	745	6.60	51	44.66
258	25,000	0.80		4,725	1463	24.32	703	6.37	-24	40.85
259	25,000	0.80		3,619	1164	21.38	659	6.13	-95	35.97

Table C-VIII. (cont)

Data point	Alt	M _N	Power setting	Power— shp	W _f	W _{noz}	T _{noz}	P _{noz}	FN	W _{cin}
										
260	25,000	0.80		2,265	810	17.30	612	5.88	-154	29.18
261	25,000	0.80	INIT	0 5 600	126 1772	7.39 23.37	368 836	5.51	-146 277	12.56 59.32
262 263	30,000 30,000	0.50 0.50	INT MC	5,609 5,062	1599	23.37	791	5.56 5.41	377 307	56.69
263 264	30,000	0.50	MIC	4,441	1412	21.00	746	5.25	236	53.43
265	30,000	0.50		3,761	1214	19.43	702	5.10	168	49.50
266	30,000	0.50		2,955	987	17.39	654	4.92	95	44.38
267	30,000	0.50		1,946	712	14.50	599	4.73	19	37.08
268	30,000	0.50		. 0	126	5.90	402	4.41	-57	15.19
269	30,000	0.60	INT	5,894	1836	24.34	830	5.66	344	58.05
270	30,000	0.60	MC	5,297	1648	23.12	785	5.48	267	55.22
271	30,000	0.60		4,634	1449	21.68	741	5.31	192	51.85
272	30,000	0.60		3,921	1243	20.02	696	5.14	123	47.93
273	30,000	0.60		3,075	1007	17.86	648	4.95	51	42.84
274	30,000	0.60		2,019	722	14.82	594	4.75	-21	35.63
275	30,000	0.60		0	121	5.98	386	4.42	-77	14.49
276	30,000	0.70	INT	6,205	1904	25.41	826	5.77	310	56.40
277	30,000	0.70	MC	5,563	1702	24.04	780	5.57	227	53.44
278	30,000	0.70		4,856	1491	22.47	735	5.38	148	50.01
279	30,000	0.70		4,105	1275	20.70	690	5.19	78	46.12
280	30,000	0.70		3,212	1028	18.40 15.18	642	4.99	5	41.07
281 282	30,000 30,000	0.70 0.70		2,099 0	732 115	6.09	589 368	4.76 4.42	-64 -97	33.95 13.74
283	30,000	0.75	INT	6,374	1943	25.98	824	5.83	292	55.46
284	30,000	0.75	MC	5,704	1731	24.54	777	5.62	206	52.44
285	30,000	0.75		4,977	1514	22.90	732	5.41	126	49.01
286	30,000	0.75		4,204	1291	21.06	687	5.21	54	45.12
287	30,000	0.75		3,285	1039	18.69	639	5.00	-19	40.10
288	30,000	0.75		2,141	736	15.36	586	4.77	-86	33.04
289	30,000	0.75		0	111	6.15	358	4.42	-107	13.35
290	30,000	0.80	INT	6,548	1980	26.58	821	5.90	275	54.45
291	30,000	0.80	MC	5,851	1760	25.07	774	5.68	186	51.39
292	30,000	0.80		5,104	1537	23.35	729	5.45	103	47.94
293	30,000	0.80		4,308	1309	21.44	684	5.24	30	44.07
294	30,000	0.80		3,363	1050	18.99	636	5.02	-43	39.09
295	30,000	0.80		2,184	741	15.55	583	4.78	-108	32.08
296	30,000	0.80	INIT	0	107	6.22	347	4.42	-118	12.95
297 298	35,000 35,000	0.50 0.50	INT MC	4,346 4,346	1366 1366	18.92 18.92	776 776	4.40	294 294	59.37
298 299	35,000	0.50	MC	3,904	1228	18.92	776	4.40 4.28	239	59.37 56.68
300	35,000	0.50		3,357	1065	16.82	684	4.14	179	52.91
301	35,000	0.50		2,687	874	15.18	632	3.99	111	47.83
302	35,000	0.50		1,829	639	12.81	573	3.81	39	40.43
303	35,000	0.50		0	105	4.95	378	3.50	-46	15.76
304	35,000	0.60	INT	4,797	1489	20.15	795	4.55	298	59.37
305	35,000	0.60	MC	4,601	1425	19.78	774	4.49	272	58.31
306	35,000	0.60		4,087	1266	18.70	726	4.34	208	55.20
307	35,000	0.60		3,505	1093	17.37	679	4.18	144	51.35
308	35,000	0.60		2,800	893	15.62	627	4.02	76	46.25
309	35,000	0.60		1,901	649	13.12	567	3.83	5	38.93
310	35,000	0.60		0	101	5.02	364	3.50	-61	15.03
311	35,000	0.70	INT	5,338	1641	21.62	818	4.74	314	59.28
312	35,000	0.70	MC	4,847	1481	20.65	770	4.58	245	56.68
313	35,000	0.70		4,292	1307	19.44	721	4.41	176	53.42
314	35,000	0.70		3,675	1124	18.00	673	4.23	109	49.53
315	35,000	0.70		2,929	915	16.13	621	4.05	39	44.44
316	35,000	0.70		1,982	661	13.47	562	3.85	-31	37.21
317	35,000	0.70	INIT	0	97	5.11	348	3.50	-78	14.24
318 319	35,000 35,000	0.75	INT	5,500	1679	22.19	816	4.81	305	58.49
319	35,000	0.75	MC	4,980	1509	21.12	767	4.63	232	55.75

Table C-VIII. (cont)

Data			Power	Power-						
point	Alt	MN	setting	shp	Wf	W _{noz}	T _{noz}	P _{noz}	FN	Wcin
320	35,000	0.75		4,404	1329	19.84	718	4.44	160	52.43
321	35,000	0.75		3,767	1141	18.34	670	4.26	91	48.53
322	35,000	0.75		2,999	926	16.40	618	4.07	20	43.46
323	35,000	0.75		2,026	666	13.66	559	3.86	-49	36.28
324	35,000	0.75		0	94	5.16	338	3.50	-87	13.83
325	35,000	0.80	INT	5,664	1715	22.77	813	4.88	296	57.59
326	35,000	0.80	MC	5,117	1539	21.62	765	4.69	219	54.74
327	35,000	0.80		4,516	1351	20.26	715	4.49	143	51.36
328	35,000	0.80		3,864	1159	18.70	667	4.29	73	47.48
329	35,000	0.80		3,073	938	16.69	614	4.09	1	42.44
330	35,000	0.80		2,071	672	13.86	556	3.87	-68	35.31
331	35,000	0.80		0	91	5.22	328	3.50	-96	13.41
332	40,000	0.50	INT	3,392	1067	14.95	763	3.46	231	59.37
333.	40,000	0.50	MC	3,391	1067	14.95	763	3.46	231	59.37
334	40,000	0.50		3,131	985	14.44	729	3.39	198	57.38
335	40,000	0.50		2,700	856	13.49	681	3.28	149	53.66
336	40,000	0.50		2,170	. 704	12.20	628	3.15	95	48.61
337	40,000	0.50		1,485	516	10.31	567	3.01	35	41.18
338	40,000	0.50		0	89	4.03	384	2.76	-36	16.23
339	40,000	0.60	INT	3,743	1163	15.92	781	3.57	234	59.37
340	40,000	0.60	MC	3,678	1141	15.80	772	3.55	225	58.92
341	40,000	0.60		3,279	1016	14.97	723	3.44	174	55.91
342	40,000	0.60		2,821	879	13.93	675	3.31	122	52.11
343	40,000	0.60		2,261	720	12.55	622	3.18	66	47.02
344	40,000	0.60		1,543	525	10.57	562	3.02	8	39.67
345	40,000	0.60		0	86	4.09	371	2.76	-49	15.47
346	40,000	0.70	INT	4,185	1288	17.11	807	3.73	248	59.37
347	40,000	0.70	MC	3,880	1187	16.51	768	3.63	205	57.36
348	40,000	0.70		3,447	1050	15.58	718	3.49	149	54.17
349	40,000	0.70		2,959	905	14.44	669	3.35	95	50.29
350	40,000	0.70		2,366	738	12.96	616	3.20	37	45.21
351	40,000	0.70		1,610	534	10.86	556	3.04	-20	37.94
352	40,000	0.70		0	82	4.16	355	2.76	-62	14.66
353	40,000	0.75	INT	4,392	1343	17.72	814	3.82	253	59.10
354	40,000	0.75	MC	3,989	1211	16.90	766	3.67	195	56.45
355	40,000	0.75		3,535	1068	15.91	715	3.53	137	53.17
356	40,000	0.75		3,034	919	14.72	667	3.38	81	49.29
357	40,000	0.75		2,424	747	13.19	613	3.22	23	44.22
358	40,000	0.75		1,647	539	11.01	553	3.05	-35	37.01
359	40,000	0.75		0	80	4.20	346	2.76	-69	14.23
360	40,000	0.80	INT	4,529	1374	18.20	812	3.88	247	58.24
361	40,000	0.80	MC	4,100	1235	17.31	763	3.72	185	55.47
362	40,000	0.80		3,629	1087	16.24	713	3.56	124	52.11
363	40,000	0.80		3,112	933	15.02	663	3.40	67	48.23
364	40,000	0.80		2,484	757	13.42	610	3.24	7	43.18
365	40,000	0.80		1,684	544	11.17	550	3.06	-49	36.03
366	40,000	0.80		0	77	4.25	336	2.76	-76	13.81

Table C-IX.
Physical characteristics of PD436-12 and PD436-13.

	PD436-12	PD436-13
Dimensions—in. Overall length Maximum engine diameter Maximum diameter	137.3 32.1 47.0	144.4 32.1 47.0
Weight—Ib Reduction gearbox Supporting structure Torquemeter Power section Total	655 8 40 1499 2202	655 8 40 1473 2176
Acquisition price—1981 dollars	1,932,700	1,848,900
Typical maintenance costs—\$/EFH* Labor Burden Material Total	13.49 29.67 <u>36.97</u> 130.13	13.49 29.67 <u>83.20</u> 126.36

^{*}Assumes 1 flt hr/flight, \$13.75/hr labor rate, 220% burden

REFERENCES

- R. E. Herrold, "Instructions for Use of a Program in the Form of an Object Deck of Digital Computer Cards to Calculate Steady-State Performance of the Detroit Diesel Allison Model PD436-10 and PD436-11 Turboprop Engines," Detroit Diesel Allison, EDR 11321, 15 February 1983.
- "Advanced Propfan Engine Technology (APET) Definition Study, Data Package for PD436-10 and -11 Turboprop Engines," Detroit Diesel Allison, EDR 11375A, 25 March 1983.

APPENDIX D

TASK IV. ENGINE/AIRCRAFT EVALUATION

TABLE OF CONTENTS

	Title	Page
nt	troduction	D-1
	ngine/Aircraft Evaluations	
	Aircraft/Engine Results	
	Fuel Burn	
	Direct Operating Costs	
	Noise Results	
	Sensitivity Results	
		CONTRACTOR OF THE PARTY OF THE

LIST OF ILLUSTRATIONS

igure	Title	Page
D-1	Cruise altitude selection (300 nmi revenue mission)	. D-3
D-2	Block fuel comparison	. D-4
D-3	Installed climb TSFC and thrust comparison with typical climb path altitude/velocity combinations	. D-5
D-4	Installed cruise TSFC comparison	. D-5
D-5	Direct operating cost comparison	. D-7
D-6	DOC breakdown for 300 nmi mission	. D-7
D-7	Engine price comparison	. D-8
D-8	Engine maintenance cost comparisons	. D-8
D-9	FAR part 36 levels for APET turbofan and propfan powered transports	. D-9
D-10	Block fuel sensitivity results	. D-9
D-11	DOC sensitivity results	. D-10
D-12	Estimated effect of study assumption errors	. D-10
D-13	DOC sensitivity to fuel cost	. D-10

PRECEDING PAGE BLANK NOT FILMED

LIST OF TABLES

Table	Title	Page
D-I	Turbofan and propfan study engines	. D-2
D-II	Scaled aircraft/engine results	. D-2
D-III	Propulsion system weight breakdown	. D-3
D-IV	Aircraft weight breakdown	. D-3
D-V	Aircraft aerodynamic comparison for 300 nmi revenue mission	. D-4
D-VI	Block fuel breakdown	. D-4
D-VII	Climb time, distance, and block fuel comparison for 300 nmi revenue emission	. D-6
D-VIII	Climb time and distance comparison	. D-6
D-IX	List price breakdown	. D-8
D-X	Maintenance cost breakdown	. D-8
D-XI	Engine price comparison	. D-9
D-XII	Noise source levels in PNdB at part 36 measurement locations for Engines PD436-10 and PD436-11	. D-9

INTRODUCTION

Appendix D covers the mission performance and economic analysis of the previously discussed reference turbofan and candidate propfan engines. These analyses were conducted during the APET Task IV effort and utilized the evaluation procedures and assumptions presented in Appendix A of this report. These mission analysis procedures consist of two major steps: (1) sizing the airframe to meet specific design mission requirements and (2) evaluating the airframe in a typical revenue environment. The design mis-

sion requirements were selected by Allison with Douglas Aircraft Company (DAC) consultation to define a system appropriate for the next generation short-haul, commercial transport. The DAC inputs were on a no-cost basis.

Revenue mission range was selected from CAB Form 41 data obtained since deregulation. The design mission profile is consistent with ATC procedures, aircraft capability, and reserves definition sufficient for the short-haul transportation concept.

ENGINE/AIRCRAFT EVALUATIONS

Information on the reference turbofan engine and the two propfan engines, including their gearbox arrangement, general inlet and nacelle configuration, and engine parameters at the design cruise condition, is listed in Table D-I. These engines were installed in the reference aircraft, and each of the three aircraft/engine systems were scaled to meet previously specified design mission requirements. Each of the sealed aircraft/engine combinations was then flown in the revenue mission to determine fuel burn (block fuel) and direct operating cost (DOC) results.

AIRCRAFT/ENGINE RESULTS

Characteristics for each of the scaled aircraft/engine combinations are summarized in Table D-II. This table includes the resultant sized aircraft design TOGW, engine thrust or horsepower size, and a summary of the capabilities of each engine in the selected engine sizing requirements. These data show that the propfan-powered aircraft is approximately 2% heavier than the turbofan aircraft. The critical engine sizing condition for the turbofan was the takeoff requirement while both propfans were sized for the 300 ft/min rate of climb requirement at the initial cruise condition—a trend consistent with their respective thrust lapse characteristics. Note that the standard all engine operative takeoff and the balanced field lengths for the propfan engines are approximately 20% less than for the turbofan-powered aircraft.

A weight breakdown of the propulsion system for each of the three study engines is shown in Table D-III. A thrust-to-weight (T/W) ratio comparison for each engine type, excluding nacelle weight, would show the propfan to be approxi-

Table D-II.
Scaled aircraft/engine results.

	Reference	Propfan	engines
	turbofan engine	PD436-10	PD436-11
Design TOGW—Ib	89,580	91,180	91,100
(ΔTOGW-%)	(base)	(+1.8%)	(+1.7%)
Thrust/engine, SLS, std day, takeoff rating—lb	11,500	_	_
Power/engine, SLS, std day, takeoff rating—shp	-	8,005	8,015
Propeller diameter —ft	-	11.4	11.4
Takeoff distance to 35 ft—ft	5,500*	4,270	4,260
Rate of climb at initial cruise —ft/min	380	300*	300•
OEI rate of climb at 15,000 ft—ft/min	100	125	125
Balanced field length—ft	7,400	5,990	5,980

^{*}Denotes critical engine sizing requirement

mately 50% lower than the turbofan. When the nacelle weight is included in a "propulsion system" T/W ratio, the comparison indicates no advantage to either turbofan or propfan system. Note that the turbofan nacelle weight includes the strut or pylon weight plus a penalty for the fan thrust reverser system weight. However, due to the higher

Table D-I.
Turbofan and propfan study engines.

	Reference	APET prop	APET propfan engines		
	engine	PD436-10—	PD436-11-		
	2-spool	3-spool	3-spool		
	mixed flow	axial LP and	axial LP and		
Propulsion system description	turbofan	centrifugal HP	axial HP		
Gearbox	NA	Offset down	Offset down		
Inlet	Conventional	Single scoop	Single scoop		
		—top mtg	—top mtg		
Nacelle	Strut mtg	Overwing	Overwing		
	under wing	-	-		
Design condition	Cruise	Cruise	Cruise		
Design BPR	7.4	NA	NA		
Design R _{coa}	36:1	32.5:1	32.5:1		
Design RIT—F	2200	2200	2200		
Maximum RIT—F	2500	2500	2500		

Table D-III.

Propulsion system weight breakdown for scaled aircraft.

(note: per engine basis)

	Reference	Propfan engines	
	turbofan engine	PD436-10	PD436-11
Engine/power section	1,500	1,220	1,220
Gearbox	_	455	455
Propeller		1,170	1,170
Total engine	1,500	2,845	2,825
Nacelle (incl thrust rev wt)	1,385	850	_850
Total propulsion system	2,885	3,695	3,675
Thrust at SL, 0.15 M _N , 86°F—Ib	9,645	12,235	12,240
Thrust/W _{prop sys}	3.34	3.31	3.33

aircraft thrust loading, the propulsion system weight is heavier for the propfan aircraft. This fact is indicated in the aircraft weight breakdown for each of the scaled aircraft/engine combinations shown in Table D-IV. The operating empty weight fraction for the turbofan aircraft is approximately 0.56, whereas the propfan is at a 0.59 fraction. The higher fraction for the propfan is attributed to the higher propulsion system weight and the fuselage acoustic treatment weight penalty. The fuel fraction for the turbofan is approximately 0.13 and for the propfan is 0.11—an approximate 15% advantage for the propfan aircraft. The rationale for this significant decrease in fuel requirement will be presented in the fuel burn section of this appendix.

Table D-IV.
Aircraft weight breakdown.

	Weight—Ib				
	Reference	Propfan	engines		
	turbofan	PD436-10	PD436-11		
Structure group	24,200	24,500	24,480		
Propulsion system	5,770 (0.06)*	7,390 (0.08)	7,350 (0.08)		
Fixed equipment & system weights	16,760	16,710	16,710		
Fuselage acoustic treatment	_	1,710 (0.02)	1,710 (0.02)		
Operational items	3,250	3,200	3,200		
Operating empty weight	49,980 (0.56)	53,510 (0.59)	53,450 (0.59)		
Payload (including cargo weight)	28,000	28,000	28,000		
Design fuel load	11,600 (0.13)	9,670 (0.11)	9,650 (0.11)		
Design TOGW	89,580	91,180	91,100		

^{*}Weight fractions in parentheses = weight/TOGW.

As explained in Appendix A, the cruise altitude for the 300 nmi revenue mission is selected to obtain the minimum value of DOC. A plot of the DOC variation with cruise altitude for both the turbofan and propfan powered aircraft is shown in Figure D-1. These data show that both turbofan and propfan aircraft DOC are minimized at 30,000 ft cruise altitude. Therefore, DOC results are based on the revenue mission cruise at 30,000 ft.

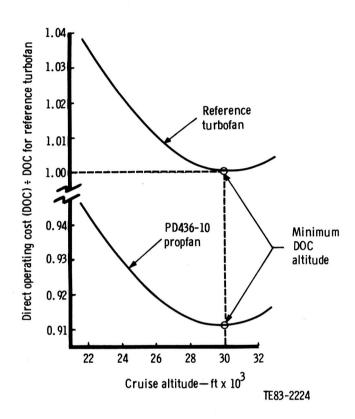


Figure D-1. Cruise altitude selection (300 nmi revenue mission).

A comparison of the 300 nmi revenue mission cruise aerodynamic characteristics of the turbofan and propfan aircraft at the 30,000 ft cruise altitude is shown in Table D-V. These data indicate that at the typical revenue mission cruise midpoint condition, the lift-to-drag ratios (L/D) are essentially the same for both vehicles. The favorable L/D values result from the supercritical wing and high wing aspect ratio selected for the reference aircraft. The major reason for the essentially equivalent L/D values lies in the propfan drag assumptions utilized in this study, which were no penalty for propeller-induced swirl or scrubbing drag and no wing/ nacelle interference drag penalty. This was assumed reasonable since no credit was taken for swirl recovery. Table D-V also lists takeoff and landing wing configuration characteristics representative of the advanced technology assumed for the APET study aircraft. These characteristics provide takeoff and approach/landing velocities within an acceptable range of safety.

Table D-V.

<u>Aircraft aerodynamic comparison</u>
for the 300 nmi revenue mission.

	Reference turbofan	Propfan (PD436)
Cruise altitude/velocity—ft/M _N Typical midpoint weight—lb	30,000/0.72 87,000	30,000/0.72 89.000
Cruise lift coefficient	0.5230	0.5260
C _D (aircraft less nacelle)	0.0279	0.0279
C _D (nacelle & pylon)	0.0025	0.0026
C _D total	0.0304	0.0305
Cruise L/D	17.22	17.25
$C_{L_{max}}$ takeoff configuration ($\delta_F = 20 \text{ deg}$)	2.75	2.75
V _{stall} /V _{LO} —kn	118/142	118/142
$C_{L_{max}}$ landing configuration $(\delta_F = 50 \text{ deg})$	3.20	3.20
V _{stall} /V _{approach} —kn	104/135	104/135

 C_D = drag coefficient C_L = lift coefficient δ_F = flap deflection angle

V = velocity

LO = lift off

FUEL BURN

As evidenced by the previously discussed propfan aircraft fuel fraction advantage, the mission fuel use of the

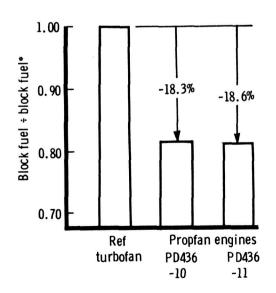
propfan engine is shown to be significantly lower (16.5% to 18.5%) than that of the turbofan-powered aircraft. This result is illustrated by the block fuel comparison of the three study engines shown in Figure D-2. The block fuel comparison is shown for both the revenue and design mission. Note that the axial/axial (PD436-11) propfan engine has a slightly lower fuel burn than the axial/centrifugal (PD436-10) propfan configuration in both the revenue and design missions.

Table D-VI shows a fuel breakdown by mission segment or engine power condition for both revenue and design missions. These data indicate that approximately 85% of the block fuel is consumed during the climb and cruise segments of both missions. However, the most significant fact indicated in this comparison is the shift in the major fuel consuming engine power condition from cruise power in the design mis-

Table D-VI.
Block fuel breakdown.

	block 300	t of total (fuel) nmi o mission	1000 nmi design mission		
	Ref TF	Propfan	Ref TF	Propfan	
Takeoff power	4	4	2	2	
Climb power	56	56	25	25	
Cruise power	26	24	68	67	
Idle power	14	16	5	6	
Total	100	100	100	100	

300 nmi 1000 nmi design mission (Block fuel* = 3280 lb) (Block fuel* = 8170 lb)



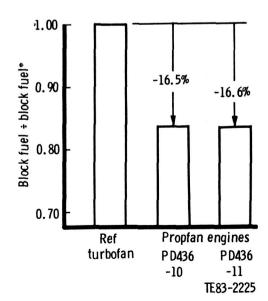


Figure D-2. Block fuel comparison.

sion to climb power in the revenue mission. With this fact, it becomes necessary to examine typical operating conditions for both climb and the cruise phases.

Typical Climb Condition

Figure D-3 shows a comparison turbofan and propfan climb power thrust specific fuel consumption (TSFC) and thrust along a typical climb altitude/ M_N path. The propfan TSFC advantage during climb power operation is shown to vary from 29% to 18% as climb altitude is increased. The difference in thrust lapse between the turbofan and propfan engines is also illustrated in that the propfan falls below the fan as the climb path passes through 20,000 ft altitude. Note that all data in Figure D-3 are for the engines as sized to meet the aircraft/ mission requirements.

Typical Cruise Condition

Figure D-4 shows a comparison of the turbofan and propfan TSFC at $32,000 \text{ ft/0.72 M}_N$. The midpoint operating thrust level, expressed as a percentage of the maximum cruise power thrust, is essentially the same in both revenue and design mission, i.e., approximately 84% maximum cruise power for the turbofan and 87% for the propfan engines. At this thrust condition, Figure D-4 indicates nearly

18% TSFC advantage for the propfan engine with respect to the turbofan. It is now evident why the revenue mission indicates a larger fuel savings for the propfan—the revenue mission has a much larger climb fuel content than does the design mission and this is where the propfan has the greatest TSFC advantage, i.e., 18% to 29% at climb as opposed to 18% at cruise.

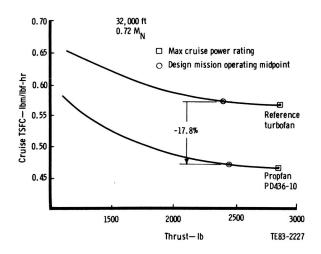
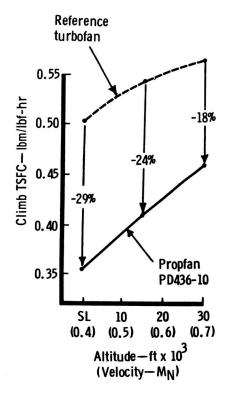


Figure D-4. Installed cruise TSFC comparison.



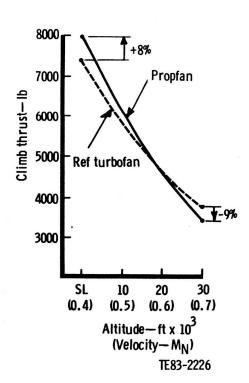


Figure D-3. Installed climb TSFC and thrust comparison.

Table D-VII.

Time, distance, and block fuel comparison for 300 nmi revenue mission.

	Reference turbofan			PD436-10 propfan (axial/centrifugal)			PD436-11 propfan (axial/axial)		
	Time— minutes	Distance— nmi	Fuel—	Time— minutes	Distance— nmi	Fuel— lb*	Time— minutes	Distance— _nmi	Fuel— lb*
Start, warmup, & taxi allowances	15.0	0	239	15.0	0	227	15.0	0	224
Takeoff allowance	1.0	0	129	1.0	0	102	1.0	0	101
First climb—acceleration	4.4	19.8	531	4.0	17.8	368	4.0	17.8	367
Second climb	14.6	91.0	1306	17.1	107.7	1144	17.0	107.3	1141
Cruise at 0.72 M _N **	16.8	118.6	870	14.7	103.9	642	14.8	104.3	643
Descent—deceleration	10.6	70.6	206	10.5	70.6	195	10.5	70.6	_194
Totals	62.4	300.0	3281	62.3	300.0	2678	62.3	300.0	2670

^{*}Mission fuels reflect 5% conservatism

Table D-VII presents a tabulation of the time, distance, and fuel consumption per mission phase or segment for the 300 nmi revenue mission and for each of the three propulsion systems. In Table D-VIII, the difference in the turbofan and propfan engine climb thrust characteristics is evidenced by comparing the climb times and climb distance of the first climb and second climb values. In the first climb, the higher thrust of the propfan provides lower climb time and shorter climb distance. The opposite is shown for the second climb, during which the turbofan has the higher thrust capabilities.

Table D-VIII.
Climb time and distance comparison.

	1	Turbofan		Propfan		
	Time— minutes	Distance— nmi	Time— minutes	Distance—		
First climb (SL to 10,000)	4.4	19.8	4.0	17.8		
Second climb (10,000 to 30,000)	14.6	91.0	17.1	107.7		

DIRECT OPERATING COSTS

Direct operating costs, in terms of cents per seat nautical mile (*/seat nmi), are compared for the turbofan and propfan-powered aircraft in Figure D-5. This figure indicates an 8.5% to 9.5% DOC advantage for the propfan with the largest savings occurring in the revenue mission. This result, generally speaking, reflects the previously discussed fuel savings of the propfan engine. However, additional engine oriented economic factors must be examined before a complete understanding of this DOC result can be obtained.

Elements of total DOC for the turbofan- and propfan-powered aircraft are compared in Figure D-6. Each element is shown as a percent of the total turbofan DOC, and the elements from left to right are in order of their contribution to total DOC. It is noted that only fuel and engine maintenance costs differ significantly from the turbofan value. The rationale for the fuel cost difference between the turbofan and propfan has been discussed in the previous subsection on fuel burn.

Engine maintenance cost consists of spares cost, which is driven by the engine selling price, and labor cost. The turbofan and both propfan engine prices are compared in Figure D-7. (The propfan price includes propeller; the turbofan price does not include thrust reverser.) This figure shows a 5% to 8% advantage for the propfan relative to the turbofan engine with the axial/axial (PD436-11) propfan being the least expensive. If the turbofan reverser had been included, this difference would be larger. Figure D-7 also shows a comparison of the power section, gearbox, and propeller prices for both of the propfan engines. This figure indicates identical gearbox and propeller prices for the propfans with the price advantage of the axial/axial configuration attributed to its lower cost power section.

Engine maintenance costs are compared relative to the turbofan costs in Figure D-8. Propfan engines are indicated to have maintenance costs 14% to 16% lower than the turbofan engine. The maintenance labor costs are shown to constitute approximately one-third of the total engine maintenance cost and are shown to be essentially equal for all three study engines. Therefore, maintenance material cost, which is a function of engine price, provides the difference in the total engine maintenance cost results. How a 5% to 8% propfan engine price advantage could produce 14% to 16% lower engine maintenance costs is explained by detailed examination of the propfan maintenance breakdown. Propfan engine price and maintenance cost breakdowns are presented in Table D-IX and D-X. These data show that the propeller price is a significant portion of the propfan engine price, whereas the propeller maintenance is essentially insignificant compared with the power section plus gearbox (PS + GB) main-

 ^{*}Cruise altitude (optimized for minimum DOC): turbofan at 30,000 ft; propfan at 30,000 ft

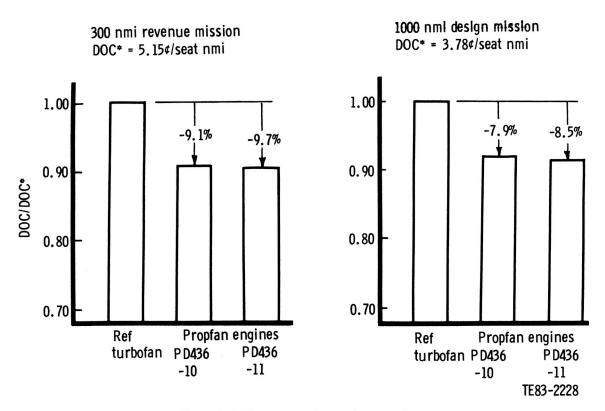


Figure D-5. Direct operating cost comparison.

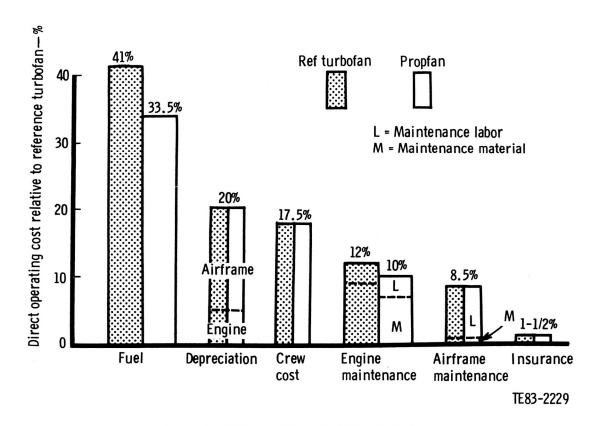


Figure D-6. DOC breakdown for 300 nmi mission.

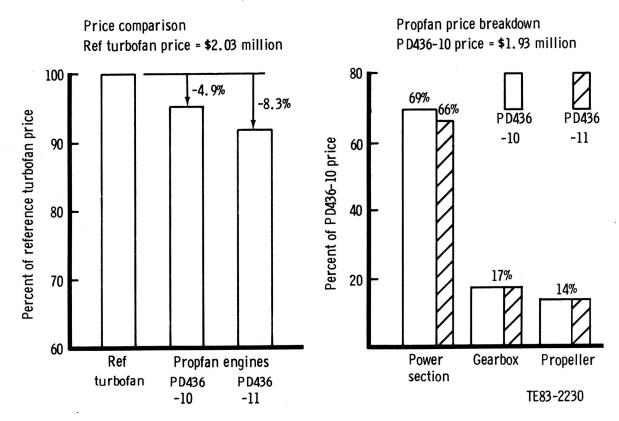


Figure D-7. Engine price comparisons.

Table D-IX. List price breakdown.

(Per engine basis)

PD430	3-10	PD436-11	
\$-millions	% •	\$-millions	% *
1.34	69.4	1.27	65.8
0.33	17.1	0.33	17.1
1.67	86.5	1.60	82.9
0.26	13.5	0.26	13.5
1.93	100.0	1.86	96.4
	\$-millions 1.34 0.33 1.67 0.26	1.34 69.4 0.33 17.1 1.67 86.5 0.26 13.5	\$-millions % • \$-millions 1.34 69.4 1.27 0.33 17.1 0.33 1.67 86.5 1.60 0.26 13.5 0.26

^{*}Percentages based on PD436-10 list price

Table D-X. Maintenance cost breakdown.

(Per engine basis)

	PD43	6-10	PD436-11		
	\$/block hr	%*	\$/block hr	_%*_	
Power section (PS) Gearbox (GB) PS + GB	90.02 0.63 90.65	97.3 0.7 98.0	87.52 <u>0.63</u> 88.15	94.6 0.7 95.3	
Propeller Total	$\frac{1.80}{92.45}$	$\frac{2.0}{100.0}$	1.80 89.95	$\frac{2.0}{97.3}$	

Figure D-8. Engine maintenance cost comparisons.

Propfan engines

Ref turbofan maintenance cost = \$106.25/block hr

-16.2%

M

PD436

-11

Maintenance

Maintenance

TE83-2231

material

labor

-13.8%

M

100

80

60

40

20

Ref

turbofan PD436

-10

Percent of reference turbofan maintenance

^{*}Percentages based on PD436-10 maintenance cost

tenance. With the removal of the propeller price, the propfan PS + GB price becomes 18% lower than the turbofan engine price, as shown in Table D-XI. Therefore, fuel burn or TSFC and engine (PS + GB) price advantage coupled with low propeller maintenance cost constitute the major portion of the propfan engine DOC reduction.

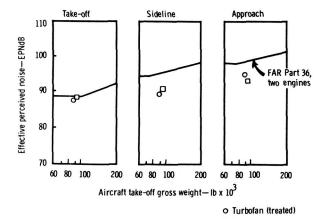
Table D-XI.
Engine price comparison.

	Turbofan price— millions of \$	Propfan price— millions of \$	Difference in price %
First	2.03	1.93	-4.9
comparison		(PS + GB + Prop)	
Second	2.03	1.67	-17.7
comparison		(PS + GB)	

NOISE RESULTS

Noise levels for the APET turboprop- and propfan-powered transports were estimated using Hamilton Standard Division and Allison production methods to determine their compliance with FAR Part 36, Stage 3. Both aircraft met the Part 36 requirements, as shown in Figure D-9. The turbofans require inlet treatment to achieve the levels shown while the turboprop does not.

The main propulsor, fan or propfan, was the dominant noise source at all locations. Table D-XII provides a noise source breakdown and shows that turboprop engine noise is not significant except on approach, at which time the compressor, core combustion, and turbine contribute to the total propulsion noise. The engine contribution to the Part 36 effective perceived noise levels was less than 1 EPNdB for takeoff and about 4 EPNdB for approach. Note that Table D-XII provides source levels in units of PNdB and Part 36 estimated and limit levels in units of EPNdB.



Propfan (untreated)
TE83-2232
Figure D-9. FAR Part 36 levels for APET turbofan- and

propfan-powered transports.

Table D-XII.

Noise source levels in PNdB at Part 36 measurement locations for Engines PD436-10 and -11.

Source	Takeoff	Sideline	Approach
Compressor	68	65	90
Turbine	50	48	79
Jet	63	61	48
Core combustion	69	68	80
Propfan	91	91	94
Effective perceived noise level—EPNdB	88	90	92
Part 36 limit—EPNdB	89	94.5	98.5

SENSITIVITY RESULTS

The following trade studies were completed to determine the effect of a selected set of independent variables on fuel burned and DOC for the 300 nmi revenue mission. The baseline engine used was the PD436-10 propfan engine. Figure D-10 shows the effect of seven propfan aircraft system variables on block fuel. In each case, the block fuel difference resulted from a 10% change in the variable. This figure identifies propfan efficiency, engine specific fuel consumption, and aircraft drag as major fuel burn drivers. These affect fuel consumed on nearly a one-to-one basis. The effect of nacelle drag, propulsion system weight, and acoustic panel weight on fuel burn is one-tenth or less.

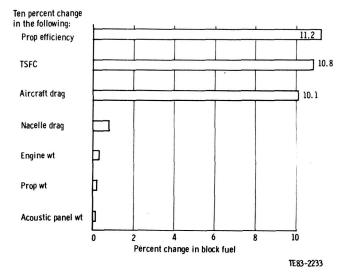


Figure D-10. Block fuel sensitivity results.

The sensitivity of the propfan aircraft DOC to a 10% change in each of 12 variables is shown in Figure D-11. More variables enter the picture when examining DOC sensitivity because "dollar only" items become important. The same three variables that drove fuel burn are again seen to be prominent. However, the additional variables of aircraft cost, power section plus gearbox cost, and power section plus gearbox maintenance cost also have an effect greater than

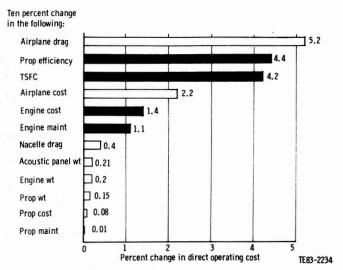


Figure D-11. DOC sensitivity results.

1 % DOC. The effect of the remaining variables is likely below the resolution level of the sensitivity study. The effects of important propulsion system variables are shown with shaded bars. These variables are propfan efficiency, thrust specific fuel consumption, power section plus gearbox cost, and power section plus gearbox maintenance cost. Note that propeller cost, acoustic panel weight, and other weight items have an insignificant effect on the operating cost of the APET aircraft.

Putting the sensitivity or trade study approach into a different context, it is noted that the ranges of estimated variables were selected on the basis of the certainty with which they could be defined; sensitivities to DOC were then calculated to indicate the effect of estimating error on the DOC advantage shown for the propfan propulsion system. The results of this study are shown in Figure D-12. Typical errors in propeller variables and power section plus gearbox costs still show an 8% + DOC advantage for the propfan. Note that doubling the acoustic panel weight reduces the propfan advantage by less than two percentage points; however, a 5% error in aircraft drag could reduce the estimated propfan DOC advantage by one-third. In the unlikely event that all the errors were realized, the combined effect would still show more than a 4% DOC advantage for the propfan propulsion system. Using the following approximation, the combined effect was obtained by subtracting from the baseline DOC advantage a statistically combined effect of the individual deviations from the propfan advantage:

Combine effect propfan advantage = Baseline propfan advantage =
$$\sqrt{\sum_{i=1}^{\Delta} 2^{2}}$$

where

 $\Delta_i = 9.1 \%$ - Propfan advantage for each assumed error (%) in Figure D-12

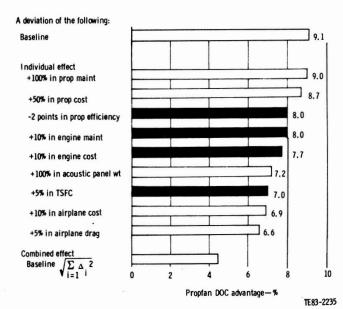


Figure D-12. Estimated effect of study assumption errors.

The sensitivity of DOC to fuel cost is an important consideration; high fuel cost increases emphasis on fuel burn economy. Figure D-13 shows the DOC determined for the reference turbofan and both propfan systems over a range of fuel costs from \$1 to \$2 per U.S. gallon. The propfan DOC advantage over the turbofan varies over this range from 8% to 10%. The implication is that, if fuel costs continue to rise, the importance of propfan technology will increase in direct proportion.

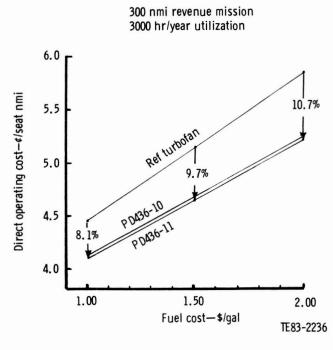


Figure D-13. DOC sensitivity to fuel cost.

APPENDIX E

TASK V. ADVANCED PROPFAN ENGINE TECHNOLOGY PLAN

TABLE OF CONTENTS

Title Control of the	Page
Introduction	E-1
Engine Inlet Technology Plan	E-2
Gearbox Technology Plan	E-4
Compressor Technology Plan	E-7
Turbine Technology Plan	E-11
Control System Technology Plan	

LIST OF ILLUSTRATIONS

Title	Page
Engine inlet design concerns	E-2
Engine inlet program schedule	E-4
Flow diagram of gearbox technology program	E-5
Gearbox program schedule	
Compressor efficiency correlation	E-7
APET low pressure compressor common to both HP compressor systems	E-8
Low pressure compressor program schedule	E-9
High pressure compressor configurations	E-9
High pressure compressor program schedule	E-10
APET turbine technology levels compared to the state of the art	E-11
Schematic of four basic bleed/blow secondary flow control concepts	E-11
Turbine program schedule	E-12
Typical linear cascade assembly for aerothermodynamic cascade facility	E-12
GMA500 power turbine rig hardware	E-13
Control system program schedule	E-14
	Engine inlet design concerns Engine inlet program schedule Flow diagram of gearbox technology program Gearbox program schedule Compressor efficiency correlation APET low pressure compressor common to both HP compressor systems Low pressure compressor program schedule High pressure compressor configurations High pressure compressor program schedule APET turbine technology levels compared to the state of the art Schematic of four basic bleed/blow secondary flow control concepts Turbine program schedule Typical linear cascade assembly for aerothermodynamic cascade facility GMA500 power turbine rig hardware

PRECEDING PAGE BLANK NOT FILMED

INTRODUCTION

The technology definition plan is described in this appendix. Key components of the engine are discussed, and the plans leading to component technology verification are presented. These plans are based on the requirement for technology verification in the late 1980s and for first production in the early 1990s. The six key technology components recommended for technology improvement are as follows:

- engine inlet
- propfan gearbox
- low pressure compressor
- high pressure compressor
- turbines
- engine controls

ENGINE INLET TECHNOLOGY PLAN

High speed propfan inlets operate in flow field environments that demand careful design integration for good performance and stability. Figure E-1 illustrates the many problems facing the design and integration of the propfan inlet. Although flight Mach numbers are subsonic, the inlet system faces many of the same design problems as the inlet design of a supersonic propulsion system. Typical problem areas are the impact on compressor stability, spillage drag, and overall nacelle drag. These concerns are compounded by the skewed and unsteady aerodynamics imposed on the inlet by the propfan blades.

PROPOSED PLAN

A joint NASA/Allison/airframer inlet program is recommended. This program would be interactive with the APET advanced gearbox preliminary design studies. It would extend the existing subscale propfan/inlet data base through evaluation of baseline and alternate inlet designs addressing the following issues:

- offset and in-line gearbox installations
- single and dual scoop S-bend inlets
- wraparound or penetrating shaft

The engine inlet program plan would interface with gearbox configuration studies to optimize installed propulsion system performance. The concept definition phase of the inlet program would assess various configurations and evaluate the compatibility of these configurations with gearbox and drive systems. This would be accomplished by performing a configuration study, designing selected configurations, installing these in propfan propulsion system preliminary designs, and estimating the system performance. Promising inlet configurations would be recommended for test with the propfan and spinner installed and at simulated flight conditions to determine the effects of the propfan flow field on inlet performance and drag. The details of the test configurations and selection of the test facility would be determined concurrent with the configuration study. The program schedule for these tasks is shown in Figure E-2.

PROGRAM BENEFITS

The program benefits of these propfan inlet studies relate directly to future airline engine installations. Technology advancements would be addressed in the following four areas:

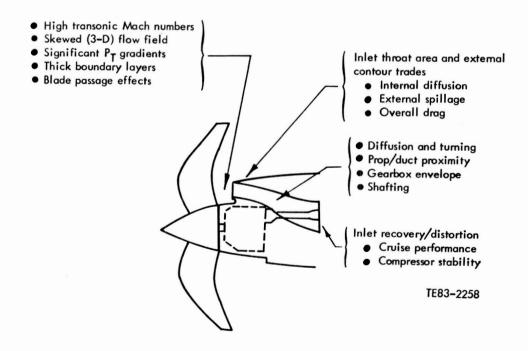


Figure E-1. Engine inlet design concerns.

- high performance inlet duct designs that result in acceptable engine stability over a broad range of installed operating conditions, such as power setting, angle of attack, and cross winds
- duct designs that achieve high installed thrust-minusdrag from high inlet pressure recovery and reduced inlet chargeable drags
- inlet performance variable sensitivity to the gearbox and shafting to achieve minimum weight, frontal area, cost, and reliability
- steady-state and dynamic pressure mapping of the inlet duct exit plane and duct wall pressure distributions for analytical modeling

Particular emphasis should be directed to the definition of inlet flow field and stability limits and the impact of design variables on installed engine/nacelle performance. An additional result of this effort is the trade of case cooling and resulting tip clearance control on engine performance versus possible spillage drag or frontal area drag.

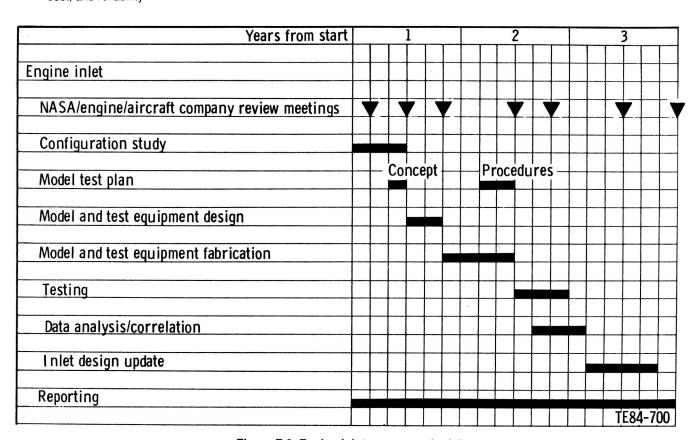


Figure E-2. Engine inlet program schedule.

GEARBOX TECHNOLOGY PLAN

A need exists to develop a modern gearbox in the APET power class of 10,000 shp. Since the gearbox configuration has a major impact on inlet/nacelle integration, it could affect installed engine performance and compromise other propulsion system components. Advanced technology efforts of industry in the field of compact, lightweight, high horsepower speed reducing gearboxes have been almost nonexistent in the past 15 to 20 years. This lack of technology improvement applies not only to mechanical design and manufacturing disciplines but also to basic gearbox design.

PROPOSED PLAN

The proposed program plan for advancing gearbox technology was initiated with a preliminary design study of the gearbox configuration and related propfan pitch change mechanism. These studies will be closely integrated with the propfan inlet development because of the impact these two components have on each other. Included are the investigation of various reduction schemes and gear arrangements, serviceability, cost, weight, reliability, heat rejection, and/or power absorption. An identification of technology needs to advance gearbox technology to the levels of other current gas turbine components will evolve out of these preliminary design studies. These needs are in the area of design analyses, lubrication, materials, manufacturing techniques, bearings, gearing, and housing structures. The key elements of the recommended program are as follows:

1. conduct preliminary design studies of the gearbox to define the configuration in conjunction with the engine

- inlet and propfan pitch change system. This design will consider the requirements for system diagnostics.
- 2. identify design methodology needs and update codes
- 3. identify requirements for advancements in design analyses, lubrication, materials, manufacturing techniques, bearings, gearing, and housing structures
- conduct a detailed design of an advanced technology gearbox
- 5. fabricate gearbox hardware
- 6. perform full-scale gearbox and component tests

The preliminary design studies will result in the selection of a gearbox configuration for detailed design and a definition of the component technology needs, including gearing, bearings, lubrication system, materials, and structural parts. The program would be conducted as shown in the flow diagram of Figure E-3. A schedule is shown in Figure E-4.

PROGRAM BENEFITS

The gearbox technology program will result in a data base for U.S. industry to initiate development of medium to large propfan drive systems in the 1990s. Design approaches based on verified advanced technology gearing, bearings, lubrication, structures, and materials will then be available for application to production-quality gearboxes. Without a concentrated technology effort of the type described herein, the next generation of gearboxes will inherit some of the reliability, maintainability, and performance deficiencies of current gearboxes.

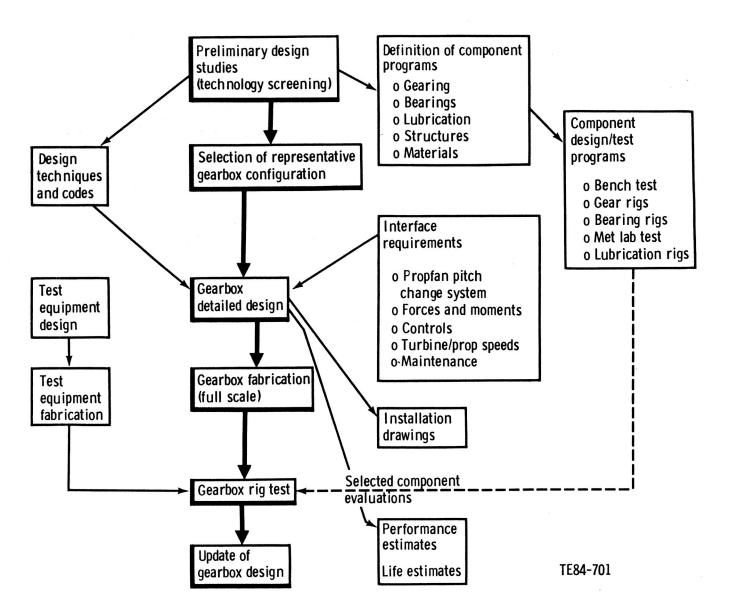


Figure E-3. Flow diagram of gearbox technology program.

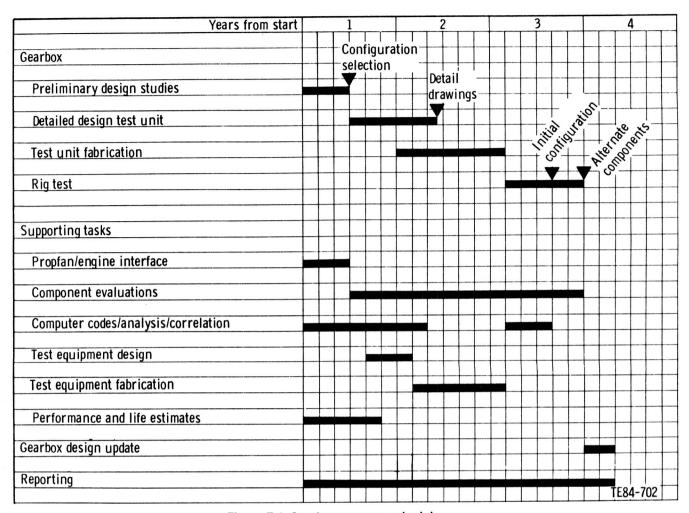


Figure E-4. Gearbox program schedule.

COMPRESSOR TECHNOLOGY PLAN

The key technology components of advanced technology engines described herein are the compressors. Favorable fuel and cost savings projected in the APET study are based on assumed compressor performance not yet demonstrated in 10,000 shp class engines. Verification of these assumptions must be accomplished if the turboprop engine advantages reported herein are to be fully realized.

Figure E-5 illustrates a correlation of compressor polytropic efficiency with compressor exit corrected flow. A current technology band is shown as well as the EEE and APET goals. These data illustrate that the APET goals represent about the same extension of efficiency as the EEE program. The demonstrated performance of the EEE programs is also shown illustrating good advancement toward goals. Test data are shown for the industrial axial/centrifugal compressor supporting the validity of the goals.

LOW PRESSURE COMPRESSOR PROPOSED PLAN

A schematic of the APET low pressure (LP) compressor flow path is illustrated in Figure E-6 in conjunction with the design aerodynamic characteristics. The 90% polytropic efficiency is in agreement with EEE performance goals. Features of this aero design include relatively high stage loadings and low aspect ratios.

The LP compressor program objectives are to demonstrate high polytropic efficiencies in a moderate flow size

compressor utilizing advanced aerodynamic technologies, including the following:

- advanced three-dimensional computation techniques leading to passage designed blading
- higher stage loadings
- low aspect ratios

The program plan is enhanced by the use of an existing Allison 30 lb/sec flow class compressor rig as the baseline. The rig has a six-stage, low aspect ratio design that has undergone initial baseline testing with conventionally designed blading. The rig would also be used to test passage designed blading to increase both the efficiency and loading of the compressor. A schedule for the low pressure compressor program is shown in Figure E-7.

HIGH PRESSURE COMPRESSOR PROPOSED PLAN

Figure E-8 illustrates a comparison between the centrifugal and axial compressors proposed for the high pressure (HP) spool and lists comparative data for the prime design features of both compressors. The major problem to be solved for the centrifugal compressor is the low specific speed (64) brought on by high bore stress. In the axial compressor, the small latter stage blade heights become limiting.

The primary objective of the proposed HP compressor program is the evaluation of the centrifugal compressor compared with the axial compressor in terms of design point and

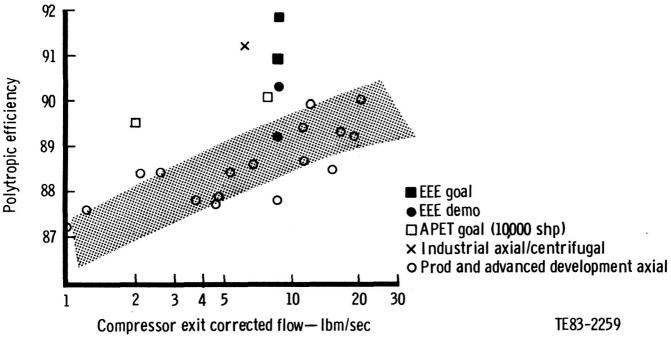


Figure E-5. Compressor efficiency correlation.

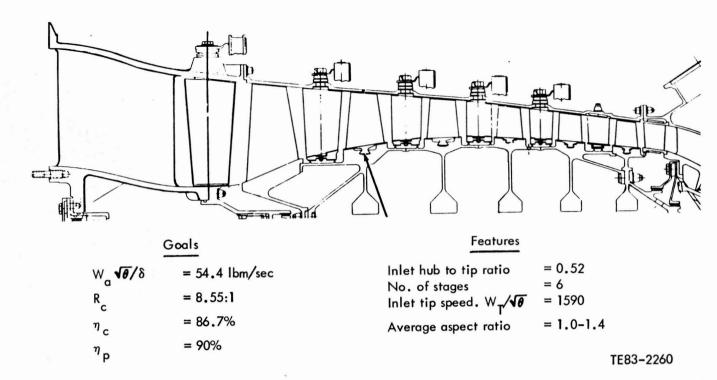


Figure E-6. APET low pressure compressor common to both HP compressor systems.

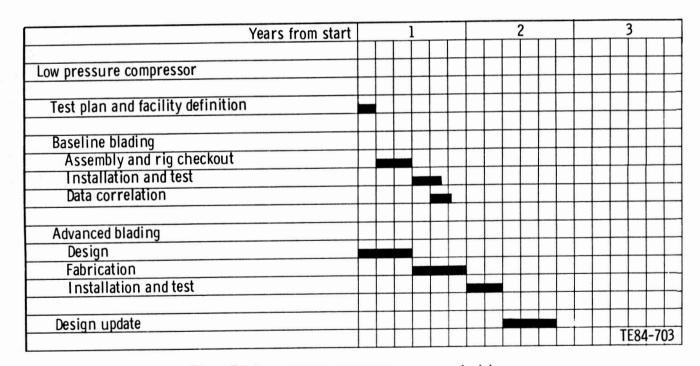
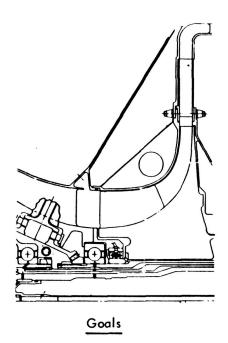
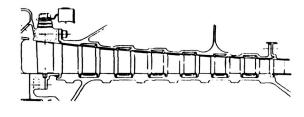


Figure E-7. Low pressure compressor program schedule.





W . √θ/ δ	= 8.8 lbm/sec
R	= 3.8:1
$^{\eta}$ c axial	= 85.7%
η_{p}	= 88.1%
η _{c cent}	= 85.1%
η _p	= 87.6%
۲	

ı eu	10163	
	Axial	Centrifugal
Inlet hub to tip ratio No. of stages Inlet tip speed, U _T /√6	0.74 7 991	0.66 1 856
Average aspect ratio Specific speed	1.37	. 64
		TE83-2261

Faatures

Figure E-8. High pressure compressor configurations.

off-design efficiency, surge margin, and stability. It would initially involve a design-study effort for each compressor type. The centrifugal program would concentrate on ways to ' improve specific speed without excessive bore stress while the axial program would strive to improve blade length while maintaining an acceptable number of stages and turbine stress. Both designs would be fabricated and rig tested. Inlet distortion testing would be included, using new component hardware adapted to existing rigs in Allison's small compressor test facility. Inlet distortion tests for a baseline and one development modification on each compressor would provide a comparative performance evaluation of the axial and centrifugal HP compressor components. A comparison is needed because both components are well off optimum in terms of basic design parameter selection. The centrifugal compressor is designed to operate at low specific speed and high inlet hub/tip ratio to reduce the stress levels. The axial has been pushed to low flow coefficients and high loading to

minimize stage count and maximize blade height. A schedule for the high pressure compressor program is shown in Figure E-9.

PROGRAM BENEFITS

The compressor design and test program will address one of the components most critical to the success of the advanced turboprop engines. With this work accomplished as outlined herein, the state of the art of high pressure compressor design will be advanced to the levels needed for advanced turboprop engines to be competitive. It is anticipated that the level of technology developed in the NASA-sponsored EEE turobfan program will be carried through to the smaller flow size turboprop engines. Although additional tasks are involved, particularly in the centrifugal configuration, many of the advances in compressor design and manufacturing made in EEE are applicable to the APET engines.

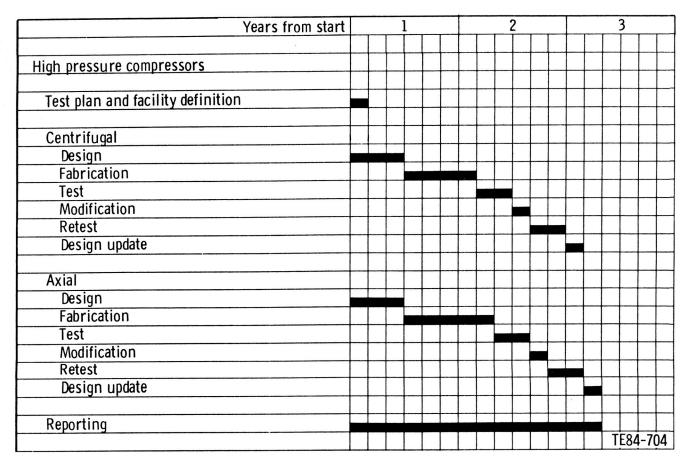


Figure E-9. High pressure compressor program schedule.

TURBINE TECHNOLOGY PLAN

The vane inlet endwall boundary layer and associated velocity profile strongly influence the formation and magnitude of the secondary flows on the vane endwalls. These secondary flows are vortex flows which aggravate the vane endwall heat transfer, produce loss within the vane passage, and have a detrimental effect on the downstream rotor performance.

PROPOSED PLAN

Figure E-10 illustrates the trend of turbine overall polytropic efficiency for an overall expansion ratio of approximately six. The APET HP/LP turbines and power turbine are combined in the figure. These efficiency levels compare to the state of the art. Much effort has been devoted toward improving efficiency of small air-cooled gasifier turbines, but very little work has been directed toward one of the prime sources of loss in any turbine, which is the loss associated with endwall secondary flows. Therefore, the objective of the proposed program is to increase stage aerodynamic performance and/or reduce endwall cooling requirements through the control of secondary flows. This work is applicable to both cooled and uncooled turbines, with the primary emphasis on uncooled stages.

The proposed program consists of three phases. Phase I employs 2-D cascades to quantify and qualify schemes such as those shown in Figure E-11 to control secondary flows.

Phase II would carry the most promising configurations to a full annular cascade to investigate detailed rotor inlet flow conditions. Phase III consists of complete stage testing to fully investigate overall performance characteristics.

The test program is summarized as follows:

- Phase I—2-D Cascade Tests
 Quantify and qualify the effects of bleed and/or blowing concepts on
 - 1. endwall loss reduction
 - 2. improved rotor inlet flow conditions

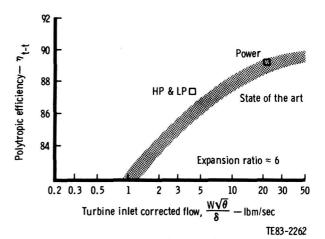


Figure E-10. APET turbine technology levels compared to the state of the art.

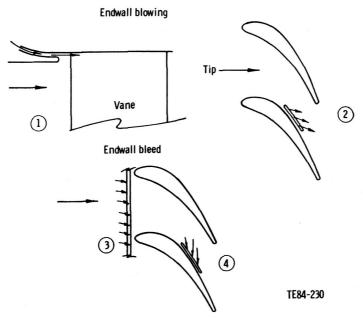


Figure E-11. Schematic of four basic bleed/blow secondary flow control concepts.

ORIGINAL PAGE IS OF POOR QUALITY

- 3. endwall heat transfer (where applicable)
- Tests would incorporate
- 1. flow visualization
- 2. detailed exit flow field mapping
- 3. intrapassage mapping (locally)
- 4. endwall heat transfer characterization
- 5. bleed/blow flow rates
- 6. vane expansion ratio
- 7. bleed/blow locations
- Phase II—Full Annular Cascade Tests
 - select two most promising configurations from Phase I, and fabricate and test two vane cascades
 - investigate the effecs of bleed/blow flow rates and vane expansion ratio incorporating detailed vane exit flow surveys
- Phase III—Full Stage Rotating Rig Tests
 For each of the configurations of Phase II, conduct full stage rotating rig test to obtain
 - 1. overall stage performance
 - 2. detailed insight into changes in rotor performance resulting from reduced endwall secondary flows

The schedule for accomplishing the proposed turbine technology plan is shown in Figure E-12.

FACILITIES

Allison has the facilities necessary to conduct this comprehensive three-phase test program. The linear cascade work will be performed in the Allison aerothermodynamic cascade facility. This Phase I effort will require the design and fabrication of a 2-D cascade test section that is capable of accommodating the various endwall bleed/blow geometries and is suitable for flow visualization. A typical 2-D cascade test section assembly designed for this facility is shown in Figure E-13. The vane annular cascade and rotating rig tests will be conducted in the Allison small turbine test facility. It is recommended that the available Allison GMA500 two-stage

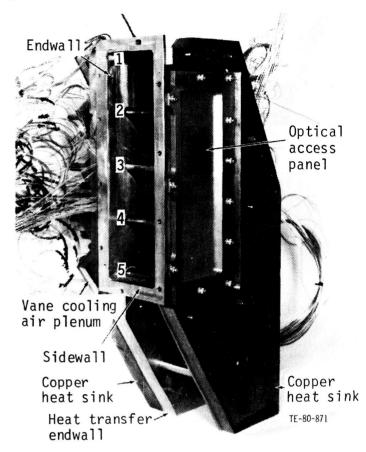


Figure E-13. Typical linear cascade assembly for aerothermodynamic cascade facility.

power turbine test rig hardware (shown in Figure E-14) be modified and employed in the Phase II and Phase III testing. This turbine has demonstrated excellent aerodynamic performance in previous testing.

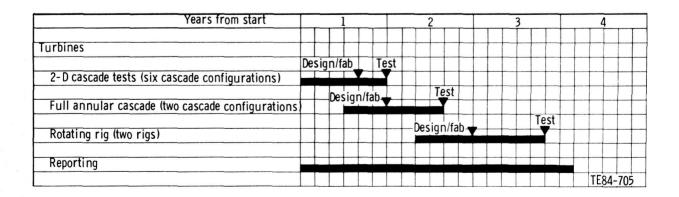
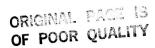


Figure E-12. Turbine program schedule.



PROGRAM BENEFITS

The benefits provided by secondary flow loss reduction extend to all turbines. Combining secondary flow concepts, such as bleeding in forward stages and injecting this air in a downstream stator, is obviously more applicable to an uncooled turbine. A primary example of this concept is a low pressure turbine located aft of a rather long transition duct,

such as is encountered in the APET engine. However, endwall blowing concepts could in certain cases be combined with the vane endwall cooling scheme for HP turbines that require cooling air. It is anticipated that improved performance could also be realized in the aft stages of the low pressure turbine, which must operate far off design (low expansion ratios relative to design).

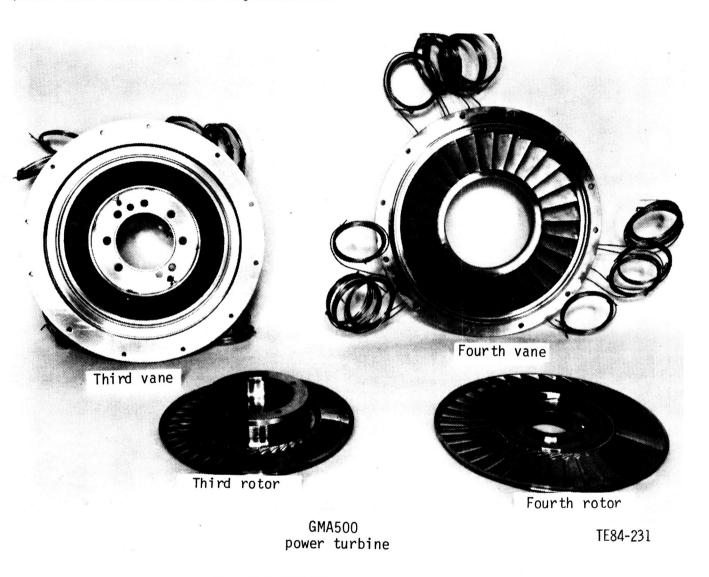


Figure E-14. GMA500 power turbine rig hardware.

CONTROL SYSTEM TECHNOLOGY PLAN

The major problem with many current gas turbine turboprop propulsion systems is the division of control management between the propeller and the engine. These systems are designed independently and, although coordinated, seldom achieve optimum performance, reliability, and cost effectiveness.

PROPOSED PLAN

A joint venture into a combined or integrated control system is a primary element of the program. This work would include computer modeling of the engine and the propfan system from which control modes would be investigated. As a result of these studies an overall system design and component interface can be defined. The recommended program would be performed jointly by the engine and propfan companies working with an airframer to define an integrated system concept. It involves the design and procurement of hardware for demonstration testing using an integrated BREADBOARD system. The schedule for accomplishing the proposed control system technology plan is shown in Figure E-15.

PROGRAM BENEFITS

The major benefit of this program will be control system definition for the propfan and the engine that are compatible and potentially enhance overall performance in terms of response, failure modes, and overall performance. This program requires a joint effort by the engine and propfan companies to define an integrated control system concept to achieve the following objectives:

- 1. optimum propulsion system performance throughout the range of ground and flight operations
- failure mode accommodation to ensure optimum performance and safety in the backup mode of operation
- 3. incorporation of control system self test features for fault isolation for reduced maintenance
- 4. control system interface definition between engine and propfan systems
- 5. overall system concept validation through simulations and hardware test programs

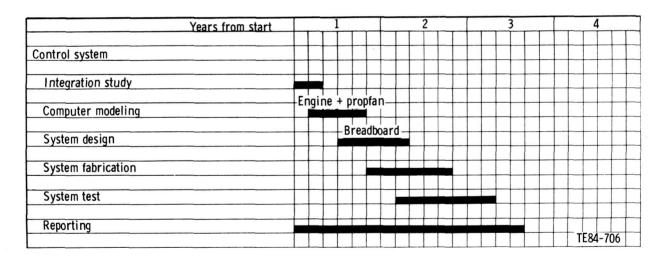


Figure E-15. Control system program schedule.

APPENDIX F

TASK VII. PRELIMINARY DESIGN OF THE SINGLE-ROTATION PROPFAN REDUCTION GEARBOX

TABLE OF CONTENTS

Title	Pa	ge
ntroduction	F	F-1
reliminary Design of the Single-Rotation Propfan Reduction Gearbox		-2
Program Defined Design Constraints	200 11 12 12 13 14 15 16 16 16 16 16 16 16	-2
Trade Study		2
Design Criteria		-4
General Arrangement		F-5
Accessories	3. 112. 4 (4. 1) (1. 1)	F-6
Design Details	47. CH. CH. CH. CH. CH. B. B. CH. CH. CH. CH. CH. B. CH. B. C. CH. CH. CH. CH. CH. CH. CH. CH. CH.	-12
Gears		-13
		-15
Bearings		-17
Heat Generation and Efficiency		
Lubrication System	F-	-18
Housings	F-	-20
Propfan Interfaces	F-	-20
Gearbox Physical Dimensions	F-	-21
Gearbox Weight	. N. S. B. B. B. S. S. B.	-21
Acquisition and Maintenance Cost		-21
Power Scaling	18km (15km (15km) 15km) 전 시간 (15km) 15km	-21
Opposite Rotation	[18] [18] [18] [18] [18] [18] [18] [18]	-22
References		-23
11010101000		

LIST OF ILLUSTRATIONS

igure	Title	Page
F-1	Offset and in-line candidate gearbox arrangements	F-3
F-2	Candidate offset and in-line gearboxes shown installed in a contoured nacelle	
F-3	Gearing/bearing schematic common for current and advanced designs	F-5
F-4	Comparison of input pinion designs	F-6
F-5	Comparison of compound dual idler designs	F-7
F-6	General arrangement of the state-of-the-art gearbox	F-8
F-7	General arrangement of the advanced technology gearbox	F-8
F-8	Modular accessories of the back face of the state-of-the-art gearbox	F-9
F-9	Propfan brake and drive mechanism	F-9
F-10	Oil pump drive system	F-10
F-11	Torquemeter/load sharing system	F-11
F-12	Torquemeter/load sharing system oil transfer line	F-12
F-13	Modifications required for reversing direction of rotation of propfan	F-22

PRECEDING PAGE BLANK NOT FILMED

LIST OF TABLES

Table	Title	Page
F-I	Weighted-decision analysis	F-3
F-II	Criteria for the two technology levels	F-4
F-III	APET mission parameters used to compute cubic mean power	
F-IV	Gear geometry comparison	F-13
F-V	Gear operating condition comparison	F-14
F-VI	Bearing geometry data	
F-VII	Bearing life comparison	F-16
F-VIII	Bearing operating conditions	
F-IX	Gearbox power loss and efficiency	
F-X		
F-XI	Bearing losses	
F-XII	Lubrication system design conditions	
F-XIII	Gearbox physical dimensions	
F-XIV	Scaled gearbox external dimensions	
F-XV	Scaled gearbox weights	

INTRODUCTION

Task VII involved the preliminary design of a single-rotation gearbox for the 10,000 shp advanced propulsion system of Task III. This design is an extension of the work performed in Task III in which in-line and offset gearbox configurations were considered. The basis for the offset gearbox is the "Study of Turboprop Systems Reliability and Maintenance Costs" reported in NASA CR-135192, June 1978.

The in-line configuration is a single-stage reduction system selected specifically for the APET program to take advantage of the large-diameter spinner of the propfan.

Early on in the APET program both the in-line and offset gearboxes were found to be acceptable candidates. However, to be consistent with the engine installation assumptions and particularly the selection of a contoured nacelle, the offset arrangement was favored. These installation assumptions also apply to the Task VII preliminary design configuration selection.

The purpose of this preliminary design is to define the optimum propfan gearbox configuration and identify the advanced technology issues that need additional effort and verification as indicated in Appendix J. Task VIII provides for the same kind of thing for the pitch change system except at the conceptual design level. Pitch change-gearbox interfaces are resolved so that these systems are compatible with each other and the overall propulsion system.

PRELIMINARY DESIGN OF THE SINGLE-ROTATION PROPFAN REDUCTION GEARBOX

A preliminary design study was conducted under Task VII to provide an advanced flight weight gearbox that uses the propfan pitch change control and mechanism described in Appendix G.

The objectives of this preliminary design study are as follows:

- Select and rank two 10,000-shp gearbox configurations compatible with the APET propulsion system defined in Tasks I through VI.
- Select one gearbox configuration and prepare a preliminary design of this configuration at two technology levels, stressing long life, good efficiency, low maintenance cost, low initial cost, and high aircraft dispatch reliability. The two technology levels are state-of-the-art technology (1980s—available now for commercial application) and advanced technology (1990s—available in the early 1990s for commercial application).
- Compare the two designs to identify the advanced technology required for the advanced technology gearbox.
- Prepare a research and technology plan that would result in gearbox technology verification in the late 1980s and allow for first production in the early 1990s.

PROGRAM DEFINED DESIGN CONSTRAINTS

The gearbox designs were required to be compatible with the Allison APET propulsion system. Therefore, the gearbox was designed for a 10,000-shp class, three-spool, advanced technology, free turbine engine. The inlet corrected airflow is 56 lb/sec, and the overall pressure ratio is 32.5:1 at the design point cruise condition of 0.72 Mach number at a 32,000-ft altitude. The propfan power at this initial cruise point is 5,227 hp as dictated by the aircraft and mission described in Appendix A. The compressor is a dual-spool unit with each spool driven by a single high-pressure turbine stage. The maximum turbine inlet temperature is 2500°F. The power turbine consists of three axial-flow stages. These stages provide input to the propfan gearbox at its optimal rotational speed of 10,750 rpm. The APET engine was configured during preliminary design studies and installed in wing-mounted nacelles with all the propulsion system components to establish interface requirements for the drive sys-

The gearbox was designed for a propfan characterized by blades having thin swept profiles to achieve high effi-

ciency at the cruise condition. The propfan has the following characteristics:

- 10 blades
- 800 ft/sec maximum tip speed
- 32 shp/dia² disk loading at the initial cruise condition
- 1,196 rpm rotational speed
- 12.78 ft propfan diameter

Using the characteristics of the APET power section and propfan requires that the reduction gearbox be designed with 8.99 speed reduction ratio.

TRADE STUDY

In early APET tasks, four gearbox configurations were evaluated. Two of the four configurations were selected as the best candidates at the start of the preliminary design. These two configurations are the offset dual compound idler and the in-line star planetary shown schematically in Figure F-1.

These two gearbox configurations were evaluated in a trade study to select one for the preliminary design effort. The trade study consisted of a weighted-decision analysis as well as installation and torquemeter considerations. The weighted-decision analysis results are shown in Table F-I. Both normal gearbox rotation and opposite gearbox rotation were considered in the selection. Evaluation parameters having the greatest influence over the configuration decision were assigned weighting factors according to their relative influence on the configuration selection. Design coefficients for each parameter and each configuration were determined. These coefficients are the relative parametric difference between each configuration and are based on estimates obtained through preliminary drawing and design work. Each design coefficient was then multiplied by the corresponding weighting parameter to obtain a parametric total for each configuration total. As shown, the offset dual compound idler rating of 1.916 was approximately 10% higher than the star planetary rating of 1.798.

Because of the closeness of the weighted-decision analysis results, the selection process was extended to include installation effects and torque sensing schemes. The installation considerations included the following five criteria:

- adaptability of the configuration to over and under the wing mounting
- 2. impact on inlet duct efficiency
- impact on reliability and maintainability of gearbox and airframe accessory drives
- 4. impact on torquemeter design

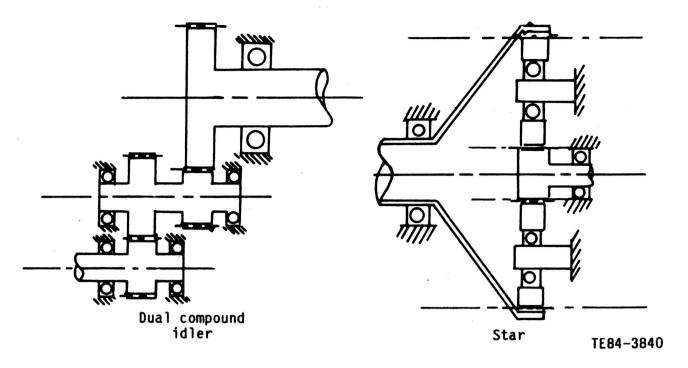


Figure F-1. Offset and in-line candidate gearbox arrangements.

Table F-I.
Weighted-decision analysis.

		In-line star planetary			Offset dual compound idler				
		Standard rotation		Opposite rotation		Standard rotation		Opposite rotation	
	Weighting factor	Design coeff	Total	Design coeff	Total	Design coeff	Total	Design coeff	Total
Reliability	0.18	1	0.18	0.9	0.162	1	0.18	0.83	0.149
Efficiency	0.17	0.99	0.168	0.99	0.168	0.99	0.168	0.986	0.168
Maintenance cost	0.13	0.98	0.127	0.95	0.124	1	0.13	0.87	0.113
Acquisition cost	0.12	1.26	0.152	0.95	0.114	1	0.12	0.87	0.104
Pitch control access	0.12	0.6	0.072	0.5	0.06	1	0.12	1	0.12
Weight	0.11	0.97	0.107	0.9	0.099	1	0.11	0.87	0.096
Technical risk	0.08	1	80.0	1	80.0	1	80.0	1	0.08
Ease of scaling	0.05	8.0	0.04	0.6	0.03	1	0.05	1	0.05
Spatial envelope	0.04	0.38	0.015	0.051	0.020	1	0.04	0.95	0.038
Parametric total	1.00		0.941		0.857		0.998		0.918
Configuration total				1.798				1.916	

5. adaptability to an aerodynamically contoured nacelle

The offset configuration is the most adaptable gearbox to over the wing or under the wing installations. The propfan centerline to power section centerline offset is the main reason for this adaptability.

Inlet ducting is much better for the offset configuration. The duct length is less, and the radial transition from duct inlet to outlet is less severe.

The offset configuration is better suited for the mounting of accessories on the back face of the gearbox. The

accessories for this configuration are also more accessible for maintenance purposes.

The offset configuration is more adaptable to the contoured nacelle defined in Figures C-16 and C-17 and shown in Figure F-2. The need for aerodynamic contouring is influenced by the geometric relationships and aerodynamics of propfans in high-speed flight conditions.

Lastly, the offset dual compound idler configuration is better suited for a hydraulic torquemeter. This type of torquemeter offers a 20-lb weight and cost savings over the phase detector type torquemeter that would be required on the in-line star planetary configuration. The hydraulic torquemeter also can be used to provide a load sharing system.

Based on the weighted-decision results and the installation/torquemeter considerations, the offset dual compound idler configuration was selected for the preliminary design effort.

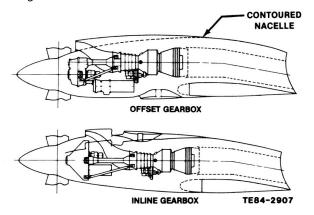


Figure F-2. Candidate offset and in-line gearboxes shown installed in a contoured nacelle.

DESIGN CRITERIA

Criteria for the two gearbox technology levels used in this design study were established as shown in Table F-II. The state-of-the-art technology criteria are based on current Allison gearbox design procedures. The advanced technology criteria are selected to reflect improvements estimated to be available by the 1990s.

The gear tooth bending stresses are based on the Lewis calculation method at the high point of single-tooth contact. Tooth contact stresses are based on the Hertzian calculation method for the pitch diameter meshing condition. Bending and contact stress allowables for the advanced technology case were increased by 25% over current levels based on estimates of improved materials and lubrication life factors. This increase is justified by fatigue testing of new gear materials that have shown life improvements as great as 10 times that of currently used materials, as reported by D. P. Townsend in Ref 1*.

Gear pitch-line velocity limits were held to the same value for both technology levels because increased velocity is not required for the advanced technology design. With the increased gear material allowables, the advanced technology gearbox would tend to have lower pitch-line velocities than the state-of-the-art design due to smaller gears.

Gear surface finish improvements for the advanced technology gearbox are recommended to achieve gear life factor improvements. By improving the surface finish, the ratio of oil film thickness to flank surface finish between meshing teeth is increased and the mesh life is improved, as indicated in Ref 2. Gear finish for the advanced technology case was increased by 40% over current technology levels.

Table F-II.

Criteria for the two technology levels.

	State-of-the-art (1980s)	Advanced technology (1990s)	
Gear teeth			
Lewis bending stress limit—lb/in.2	40,000	50,000	
Hertzian contact stress limit—lb/in.2	160,000	200,000	
Pitch-line velocity—ft/min	25,000	25,000	
Surface finish—microinches			
(arithmetic average)	10	6	
Bearings			
life factor	10	30	
B ₁₀ set life—hr	18,000	18,000	
Finish—microinches			
(arithmetic average)	6	3	
Allowable temperature rise— °F	60	90	
Flash temperature index	370	440	
Gearbox efficiency cruise —%	98 .8	99.3	

^{*}The references in Appendix F are listed at the end of this appendix.

Bearing criteria for spalling fatigue life factor, bearing set life factor, and race/roller surface finish were established.

The bearing life factor was increased by 200% over current levels. This improvement is a very aggressive goal obtainable through improved materials and lubrication life factors. This increased life factor also is influenced by indications that current life factors may be conservative, as indicated by D. G. Lewicki in Ref 3.

Both gearboxes were designed to the same reliability level for comparison purposes. The mean time between unscheduled removal (MTBUR) was established at 30,000 hr. To meet this goal, a bearing set life goal of 18,000 hr is required.

Surface finish improvements of 40% for the advanced technology gearbox over current technology were specified for the bearings. The improved finish is needed to achieve the life improvements reflected by the increased life factor goals. A process development program is needed to evaluate a number of manufacturing process changes which are discussed in Appendix H.

Criteria were established for lubrication-influenced parameters including allowable oil temperature rise, flash temperature index, and gearbox efficiency.

The oil temperature rise for the 1980s gearbox was limited to 60 °F, which is typical for current gearboxes. Oil temperature rise across the gearbox was increased by 50% for the advanced technology design to allow for a reduction in oil flow. Reduced oil flow would tend to decrease energy losses associated with gear and bearing windage and oil pumps.

The flash temperature index for the 1980s gearbox was limited to 370. This value is higher than the 290 recommended by the American Gear Manufacturers Association (AGMA) but is within successful Allison experience. The flash temperature index was increased approximately 20% for the advanced technology gearbox. This index is calculated using the AGMA method. It is an indicator of the probability of gear tooth scuffing. Successfully operating to higher flash temperature indexes would be made possible through use of high hot hardness materials, improved surface finishes, improved oils, and tooth surface treatments.

Lastly, improvements in gearbox efficiency for the advanced technology gearbox were desired. The values selected as goals at the takeoff condition were 98.8% for the 1980s and 99.3% for the 1990s.

GENERAL ARRANGEMENT

General arrangement drawings were prepared for both the state-of-the-art and advanced technology designs. These drawings include the front and rear views and sections showing the gearing and bearing configuration for the main drive and auxiliary drives. Portions of these drawings will be discussed and compared. However, it is necessary to first establish a clear definition of the gearing

arrangement, which, on a schematic basis, is common for both the current and advanced designs. The gearing/bearing schematic is shown in Figure F-3. In both designs, an input pinion drives two compound idler gears. The second-stage gear on each compound idler shaft meshes with the single output gear, thus recombining the power paths to drive the single prop shaft. The function of the dual idlers is to provide a split path load sharing capability, thereby reducing the overall size and weight of the gearbox. Details of the gearing and bearings are discussed with the mechanical arrangements described in the following paragraphs.

The input pinion is a spur gear mounted on two cylindrical roller bearings. The state-of-the-art input gear is a standard spur gear while the advanced design incorporates a high contact ratio gear set. A sketch of the input pinions for both designs is shown in Figure F-4. The high contact ratio gears were selected for the advanced design to provide a gear size reduction at this mesh. The front and rear pinion bearings in both cases are supported by the rear housing in a similar manner. The pinion bearings have flange-mounted outer races to eliminate the need for pressed-in-steel sleeves. Bearing lubrication is supplied through the pinion shaft from a forward-located jet. The input gear is lubricated by a spray bar on the out-of-mesh side of the gear.

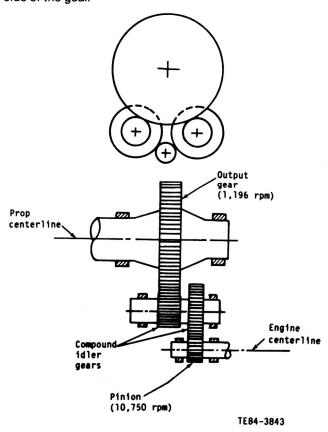


Figure F-3. Gearing/bearing schematic common for current and advanced designs.

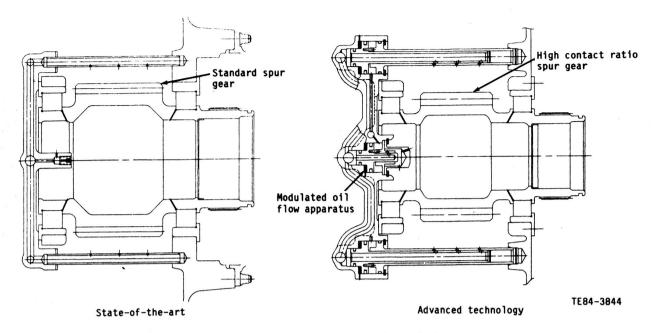


Figure F-4. Comparison of input pinion designs.

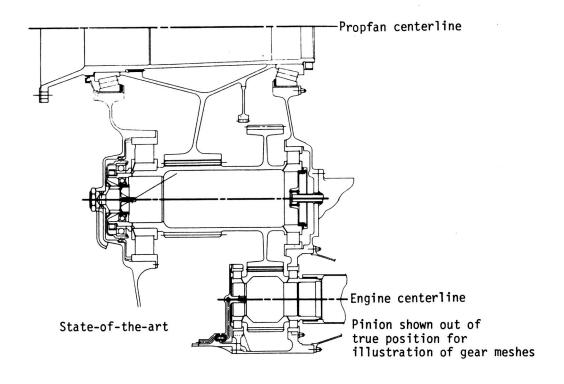
The compound dual idler gearing arrangements are shown in Figure F-5. The compound dual idlers have two gears on each idler. The first-stage idler gear is a spur gear. The second-stage idler gear is a helical gear. Each idler is supported radially by two cylindrical roller bearings. These are flanged outer race type bearings. The helical gear is lubricated on the out-of-mesh side by a spray bar. The helical gear thrust load is reacted by the torquemeter/load sharing assembly ball bearing. The bearings are lubricated through the idler shaft. The shaft inside diameter is supplied by a jet from the torquemeter/load sharing assembly.

The output gear is a helical gear shown in mesh with the second stage of the compound idler in Figure F-5. The output gear is splined and piloted to the prop shaft. The pilots are located next to the prop shaft bearings to prevent prop moment and side load reactions from being transmitted through the output gear and adversely affecting gear mesh alignment. The prop moments and side loads and their resulting deflections take place within the prop shaft. The output gear is supported by two tapered roller bearings. The forward bearing is supported by the front housing. The aft bearing is supported by the rear housing. These bearings are lubricated by jets directed at the small end of the bearing (inner race). Belleville springs preload these bearings.

The general arrangements of the current and advanced technology gearboxes are shown in Figures F-6 and F-7 for comparison of overall size and shape. On an overall comparative basis, the advanced gearbox is smaller and lighter than the current technology design. These results are discussed in detail following a description of the accessory drives and special mechanical features of the designs.

ACCESSORIES

A number of engine and airframe accessories are driven by the main gearbox. In each case modularity is considered to be an important design feature. In the case of the airframe, accessories such as alternators and hydraulic pumps are driven by a modular accessory drive mounted on the rear of the gearbox housing at the upper pad shown in Figure F-8. This modular arrangement is favored to allow removal of the accessory module while the main gearbox remains installed in the nacelle. The airframe accessory drive receives its input from an accessory drive gear in mesh with a gear attached by an electron beam weld to the rear of the output shaft. The accessory drive gear is supported by the cylindrical roller bearings in the rear and front housings. A splined coupling shaft is provided at the airframe accessory drive pad.



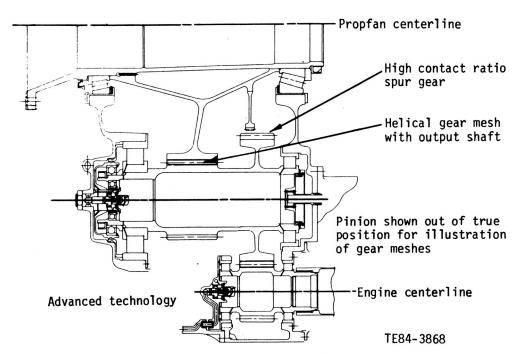


Figure F-5. Comparison of compound dual idler designs.

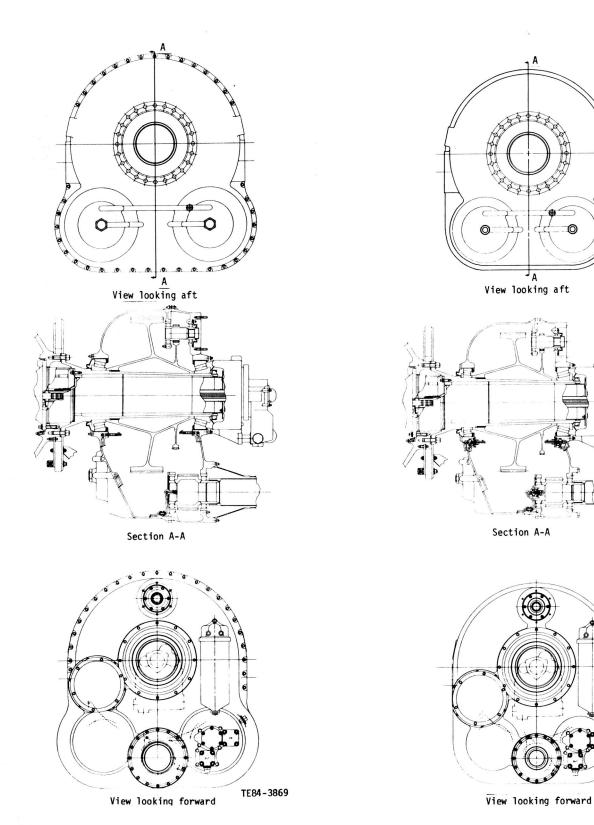


Figure F-6. General arrangement of the state-of-the-art gearbox.

Figure F-7. General arrangement of the advanced technology gearbox.

TE84-3842

Propfan Brake

The gearbox also drives a modular cone type propfan brake mounted on a pad at the back of the rear housing, as shown in Figure F-8. This unit, including its drive gear, can be removed as a module with the gearbox installed in the nacelle. The propfan brake drive gear meshes with a spur

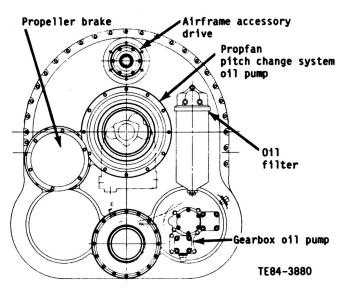


Figure F-8. Modular accessories of the back face of the state-of-the-art gearbox.

gear on the left compound idler as viewed from the rear. Previous studies have indicated a need for a propeller brake by some airline users to prevent propfan rotation after a feather. The propfan brake is designed to reduce rotation time during an engine shutdown and to prevent windmilling of propfan blades on parked airplanes when windmilling torque from ground winds exceeds engine and accessory drag torque. The propfan brake is similar to Allison's current Model 501 propeller brake design. Since the brake is not co-axial with the engine starter control system, activation will be required to release the brake as part of the engine start sequence.

The braking achieved is proportional to propfan rotational speed. As propfan speed decreases, oil pressure in the brake cavity that holds the brake surfaces apart decreases. At the prescribed speed setting, a spring force exceeds the oil pressure force, and the braking surfaces are engaged. A schematic diagram of the propfan brake and the associated drive mechanism is shown in Figure F-9.

Gearbox Oil Pump

The right compound idler gear as viewed from the rear drives the gearbox/propeller oil pump, as indicated in Figure F-10. This pump is driven by a splined coupling shaft. The coupling shaft is driven by a hub splined at the coupling shaft junction and pinned at the compound idler shaft

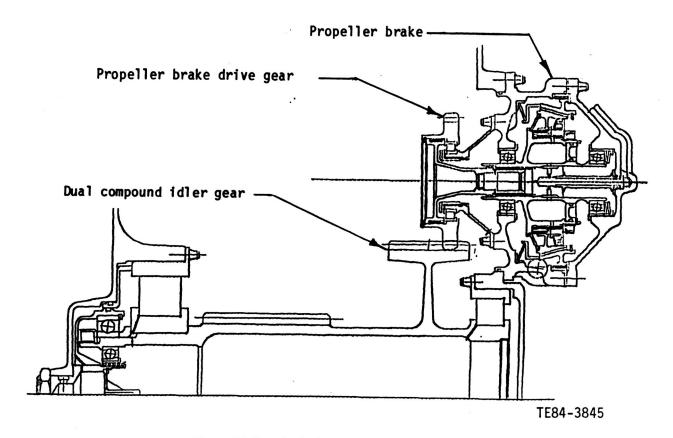


Figure F-9. Propfan brake and drive mechanism.

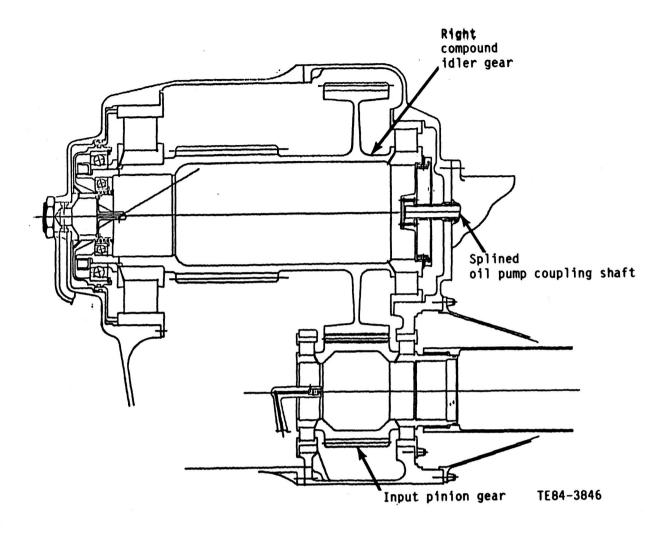


Figure F-10. Oil pump drive system.

junction. The pump is mounted external to the gearbox to achieve the desired modularity assumed in the study.

Torquemeter/Load Sharing System

The gearbox incorporates a torquemeter/hydraulic load sharing system. Load sharing devices are located at the front of each compound idler gear, as shown in Figure F-11. Each device consists of two ball bearings, a spring, an oil distribution assembly, and a slide valve. The oil distribution assembly is threaded and is fastened to the front housing by a nut. Oil enters this assembly through forward radial holes. The radial holes are supplied by oil from a cored passage. Upon entering this assembly, oil flows to the bearing lubrication jets and to the slide valve. The lubrication jets supply the shaft inside diameters of the compound idlers, as discussed previously.

The slide valve is free to axially move on the oil distribution assembly. The orifice area in the slide valve, exposed to the radial supply holes in the distribution assembly, increases as the slide valve moves forward. Therefore, moving the valve forward increases the equivalent orifice size and decreases the oil flow restriction. Upon passing through the radial distribution holes and the slide valve holes, oil enters an oil chamber. This chamber is bounded by the front housing in the front and the outer radial positions, by the slide valve piston in the rear position, and by the oil distribution assembly in the inner radial position. All leak paths but two are sealed by O-rings or ring seals. The slide valve inside diameter to distribution assembly junction clearance provides one controlled leak path. Some leakage is desirable at this location to provide a low coefficient of friction for the moving inside diameter of the valve. The second leak path is provided by an orifice drilled axially through the slide valve wall. This orifice provides oil lubrication to the larger ball bearing and allows flow out of the oil chamber. The oil flow allows chamber oil pressure to vary based on the chamber inlet orifice size.

In summary, the chamber inlet orifice size is variable and is a function of the axial slide valve position, while the

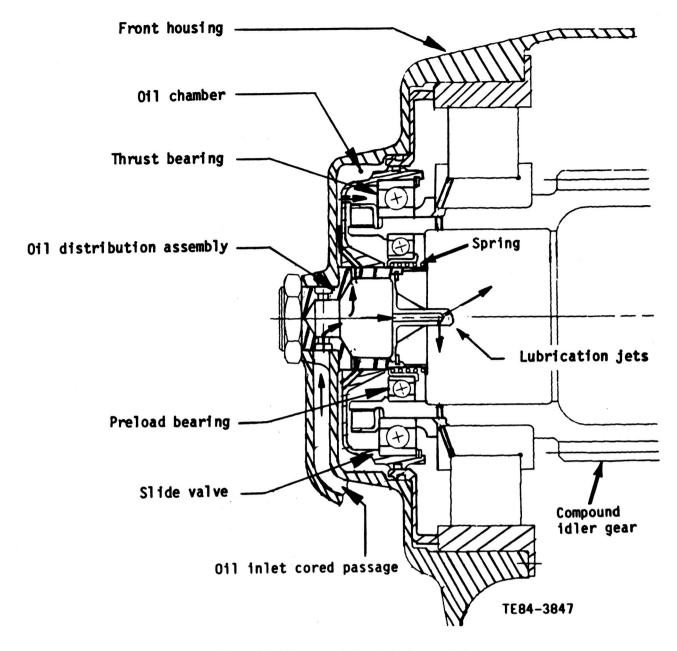


Figure F-11. Torquemeter/load sharing system.

chamber outlet orifice size is fixed. Therefore, the chamber oil pressure increases as the slide valve moves forward due to the increasing inlet orifice size.

As torque increases, the axial load caused by the helical gear set increases. This axial load is transmitted through the large ball bearing into the slide valve piston. The increased axial load causes the forward load on the slide valve piston to be greater than the aft load caused by the chamber oil pressure. The slide valve moves forward, increasing the chamber inlet orifice and increasing the chamber oil pressure. The axial movement will continue until the oil pressure increases enough to counterbalance the increased axail load.

Load sharing is accomplished by coring a common passage between the two compound idler oil chambers, as shown in Figure F-12, to ensure that the oil pressure in both chambers is equal. With equal pressure, the axial gear loads on each chamber are equal and the transmitted torque through each idler gear is also equal.

The load sharing devices also serve as a torquemeter. A torque sensing system is provided by porting the oil chamber oil to a pressure sensing device. As torque increases, the oil pressure in the chamber increases linearly. Torque can be registered on a gage by calibrating oil pressure with torque. The torque signal could be combined with the speed sensor signal to obtain horsepower.

A small ball bearing and spring have also been added to the torquemeter device to preload the system. This preload provides positive oil pressure at zero and negative torque. Thus, the system will always have positive pressure and can be calibrated to read negative torque.

DESIGN DETAILS

The details of the preliminary design, supporting analyses, and resulting gearbox definition are discussed in this

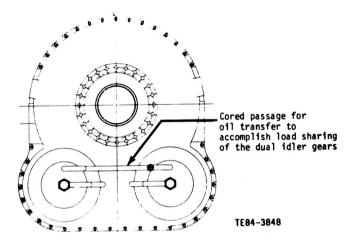


Figure F-12. Torquemeter/load sharing system oil transfer line.

section. Information is provided on materials, bearing and gear sizing, lubrication, structure, propfan interfaces, acquisition and maintenance costs, scaling, and opposite rotation.

Three power levels were used in the design of the gearbox. The 10,000-hp takeoff rating was used to size all gears and determine gearbox maximum heat generation and takeoff condition efficiency. The initial cruise power of 5,227 hp (maximum cruise power) was used to determine gearbox cruise condition heat generation and efficiency. Individual bearing life, bearing set life, and lubrication life factors were determined at the cubic mean power (CMP) condition. This power level of 5,980 hp is based on the 300 nautical mile APET mission defined in earlier tasks and shown in Table F-III. The cubic mean effective power is calculated using the following equation:

$$CMP = \begin{bmatrix} n & t_i \\ \Sigma & shp_i^3 & \frac{t_i}{t} \end{bmatrix}$$

where: n = number of mission segments
t_i = time of mission segment
t = total mission time
shp_i = power setting

Table F-III.

APET mission parameters used to compute cubic mean power.

	APET 300 nautic	al mile missio	n results		Propulsion s power requ	
Mission phase	Time (ti)— min	Alt— ft	Velocity— Mach number	Power setting	Power turbine shp (shp _i)	Propfan* shp
Start and warm- up allowance	15.0	Sea level	0	6% max cruise power	480	351
Takeoff allowance	1.0	Sea level	0	Takeoff power	10,000	9,776
First climb (sea level to 10,000 ft)	4.0	5,000	0.4	Climb power	9,280	9,063
Second climb (10,000 ft to 30,000 ft)	17.1	20,000	0.6	Climb power	7,630	7,430
Cruise	14.7	32,000	0.72	87% initial cruise power	4,700	4,529
Descent (30,000 ft to sea level)	10.5	15,000	0.6	6% initial cruise power	440	312
Total time (t) =	62.3			• 30 00		

^{*}Includes gearbox efficiency losses and accessory losses.

Propfan loads were also included in the life analysis of the prop shaft bearings. The propfan loads used were a 1P moment load of 4,643 ft-lb in the horizontal plane, a 1P side load of 1907 lb acting down in the vertical plane, and a 5000lb thrust load.

Gears

Materials and Manufacturing

The gears for the current technology gearbox are designed to be manufactured from AISI 9310 steel, which is a consumable electrode vacuum melting (AMS 6265) process. Gears for the advanced gearbox use an advanced gear steel that provides improvements in fatigue strength/stress allowables and hot hardness compared with AMS 6265. Both powder metal steels such as MCR 2001 and wrought low-carbon steels such as CBS 600 are candidates to meet the above goals. These steels will be VIM/VAR melted, and the powders will be rapidly solidified to provide a high degree of cleanliness and fine grain structures.

Current technology gears are machined using conventional manufacturing process techniques. These processes include hobbing/shaper cutting, carburizing, shot peening, grinding, and honing. Advanced manufacturing techniques will be developed and applied to the advanced gears. These advanced processes include hot isostatic press/hot forged to near net shape and advanced contour

induction hardening for the powder metal steels. Both powder and wrought steels will be machined to ultrasmooth surface finishes with flank surfaces treated by techniques such as ion implantation or TiN coatings. These processes will contribute to fatigue life/stress allowable improvements, manufacturing cost reductions, and reduced heat generation during tooth meshing.

Geometry

The gear geometries for the current and advanced gearboxes are tabulated in Table F-IV.

Improved stress allowables and high contact ratio spur gears have significant effects on gear geometry. The advanced technology high contact ratio gears have approximately 20% smaller pitch diameter. The advanced high contact ratio gears are 33% smaller than the state-of-the-art gears on a volume basis. The advanced helical gears are approximately 9% smaller on a pitch diameter basis and 27% smaller on a volume basis compared with the state-of-the-art gears.

Operating Conditions

Gear operating conditions for the 1980 and 1990 gear-boxes are shown in Table F-V.

Crushing and bending stress values are derived from the Hertzian and Lewis stress equations, respectively. The crushing stress is calculated at the pitch diameter, and the

Table F-IV.

Gear geometry comparison.

	Current technology (1980s)	Advanced technology (1990s)
Overall gearbox ratio	9.008	8.983
(Pinion to idler)		
Gear type	Spur	Spur
Diametral pitch	6	7
Pressure angle	25	20
Face width—in.	3.25	2.7
Number of pinion teeth	32	30
Pinion pitch diameter—in.	5.3333	4.2857
Number of gear teeth	76	72
Gear pitch diameter—in.	12.6667	10.2857
Profile surface finish—microinches (arithmetic average)	10	6
(Idler to output)		
Gear type	Helical	Helical
Diametral pitch—in.	5	6
Pressure angle	25	25
Helix angle	5	5
Face width—in.	5.0	4.0
Number of pinion teeth	32	35
Pinion pitch diameter—in.	6.4244	5.8556
Number of gear teeth	121	131
Gear pitch diameter—in.	24.2924	21.9167
Profile surface finish—microinches (arithmetic average)	10	6

Note: The 1990s first-stage gears are high contact ratio.

Table F-V.

Gear operating condition comparison.

	Current technology (1980s)	Advanced technology (1990s)
First stage		
Crushing stress, S _C	165,000	198,000
Bending stress, S _B	31,000	50,000
Contact ratio	1.38	2.32
Pitch-line velocity—ft/min	15,010	12,061
Sliding velocity—ft/min	2,371	4,107
Flash temperature index	328	304
Scoring index	30,322	39,041
Load carrying ability—lb/in.	3,732	5,391
Oil film thickness—microinches	13.4	9.2
Lambda ratio	1.1	1.2
Lubrication life factor	0.7	0.8
Second stage		
Crushing stress, S _C	160,000	195,000
Bending stress, S _B	32,000	51,000
Contact ratio	1.42	1.40
Face contact ratio	0.695	0.68
Pitch-line velocity—ft/min	7,589	6,845
Sliding velocity—ft/min	1,374	1,023
Flash temperature index	297	312
Scoring index	24,595	29,845
Load carrying ability—lb/in.	4,801	6,633
Oil film thickness—microinches	10.9	9.8
Lambda ratio	0.9	1.2
Lubrication life factor	0.4	0.8

bending stress is calculated at the high point of single-tooth contact.

The gears were sized by the safe stress method. This method is based on the assumption that AMS 6265 steel has a fatigue endurance limit greater than the stress criteria. Thus, designing the gears to the stress criteria, at the maximum power condition, results in an infinite gear fatigue life. The values in Table F-V were calculated at the maximum horsepower of 10,000 and the maximum gearbox input speed of 10,750 rpm.

The use of high contact ratio gears in the first stage of the advanced gearbox results in significant size and weight savings compared with low contact ratio gears. This compactness is derived from the load sharing characteristics of this type of gearing. The transmitted load is always shared by at least two teeth. However, the load is not shared equally among the meshing teeth, and this must be accounted for in the design. The unequal load distribution is a result of the differences in the compliance of each of the meshing tooth pairs. Individual tooth loads must be determined to compute gear stresses and size the gears required. This can be accomplished through a deflection analysis such as finite element modeling, which is beyond the scope of this preliminary design. Instead, load distribution was based on results of strain measurements as discussed in Ref 4. These measurements showed that the

maximum load on a tooth is 63% of the total transmitted load for the gears evaluated. Based on these results it was decided to conservatively use a maximum single tooth load of 70% of the transmitted load. The resulting loads were then used in the Lewis and Hertzian methods to determine the bending and contact stresses, respectively.

Pitch-line velocity, sliding velocity, flash temperature index, scoring index, and load carrying ability are also computed. These parameters are estimates of scoring/scuffing probability. Scoring is a form of surface damage on the tooth flank that results from breakdown of the lubrication film that separates the meshing gear teeth. The film breakdown allows metal to metal contact resulting in radial scratches due to localized welding. This scoring is a function of gear blank temperature, contact pressure, surface finish, and the relative sliding velocity. High blank temperature, excessive heat generation due to high sliding velocities, and high contact pressure tend to reduce film thickness and metal separation. Excessive surface roughness effectively reduces the metal to metal separation distance.

Pitch-line velocity and sliding velocity are indicators of the severity of the sliding environment. Load carrying ability is an indicator of the contact pressure severity. Scoring index reflects the effects of all the important parameters except surface finish. Flash temperature index accounts for the effects of all the important parameters.

The scoring/scuffing parameters for both gearbox designs fall wthin Allison experience levels with the exception of sliding velocity and scoring index for the high contact ratio gears. These parameters do not directly reflect the effects of the improved surface finishes used in the advanced design. However, surface finish effects are included in the flash temperature index, and this parameter is within Allison experience levels. Ion implantation of the tooth flanks will also be incorporated. This reduces friction during asperity contact, thus improving the wear properties of the surfaces and preventing further breakdown of the oil film due to frictional heat generation. Based on these considerations, scoring should pose no problem for either gearbox design.

Table F-V includes values for oil film thickness, film thickness to composite surface roughness ratio, and the lubrication life factor for each gear mesh. The thickness and ratio parameters affect both scoring and spall fatigue life of the tooth flanks. The life factor parameter reflects only the spall fatigue life effects of the lubrication environment.

Film thicknesses were calculated using the Dowson and Hamrock equations from Ref 5. The Cheng thermal reduction factor developed in Ref 6 was used to correct the film thicknesses for the inlet oil shear heating that occurs in high-speed elastohydrodynamic contacts.

The lambda ratio is the ratio of oil film thickness to the composite surface roughness of the contacting surfaces. The conditions indicated by this ratio have a significant effect on pitting fatigue as shown in Ref 2. This ratio also indicates the likelihood of asperity contact. As shown in Table F-V, the advanced gears should significantly benefit from improved surface finish. Although these gears have lower film thicknesses, the improved surface finish prevents a significant degradation in life in comparison with the current technology gearbox. Also, scoring is unlikely since the improved surface finish results in lambda ratios that are within Allison experience levels.

Bearings

Materials and Manufacturing

Bearings for the current gearbox are manufactured from double vacuum melted (VIM/VAR) M50 steel. Bearings for the advanced gearbox are manufactured from an advanced bearing steel providing improvements in fatigue strength, corrosion resistance, fracture toughness, microdamage tolerance, and wear/skid resistance over VIM/VAR M50. Both powder metal steels such as MRC 2001 and low-carbon wrought steels such as CBS 600 are candidates to meet the above requirements. The major focus in many of these materials has been in the area of improved hot hardness and life improvements. These steels will be VIM/VAR melted, and the powders will be rapidly solidified to provide a high degree of cleanliness and fine grain structures.

The current technology bearings are machined using conventional manufacturing processes. These processes include hot/cold forming, lathe cutting, hardening, grinding, and honing. Advanced manufacturing techniques are needed for the 1990s bearings. These advanced processes include hot isostatic pressing and advanced contour induction hardening for the powder metal steels. Ultrasmooth surface finishing techniques will also be used on both types of steels. These processes provide fatigue life improvements and cost reductions.

Geometry

The bearing geometry data for both gearboxes are summarized in Table F-VI. These bearings for both gearboxes were sized to provide a bearing B_{10} set life of 18,000 hr at the cubic mean effective horsepower of 5,980. As shown, the improved material life factors for the 1990s gearbox result in significant bearing envelope reductions.

Bearing Life

It was determined that the 18,000-hr set life would be required to meet the gearbox MTBUR goal of 30,000 hr. This derivation is based on the following considerations:

Table F-VI.
Bearing geometry data.

	Ве	Bearing size		
Bearing	Current technology	Advanced technology		
Pinion front (R)	80 x 140 x 26 mm	75 x 130 x 25 mm		
rear (R)	80 x 140 x 26 mm	75 x 30 x 25 mm		
Idler front (R)	130 x 280 x 58 mm	110 x 240 x 50 mm		
rear (R)	130 x 230 x 40 mm	110 x 240 x 50 mm		
thrust (B)	120 x 165 x 22 mm	100 x 140 x 20 mm		
Output front (TR)	8.0 x 11.5 x 2.28 in.	8.0 x 10.8 x 1.6875 in.		
rear (TR)	7.0 x 10.9 x 2.50 in.	7.0 x 10.9 x 2.50 in.		
R = cylindrical roller				
B = ball				
TR = tapered roller				

- 30,000-hr MTBUR represents a removal rate of 0.033/1,000 hr.
- 50% of unscheduled high-power gearbox removals are assumed to be due to bearing failures. Thus, the gearbox removal rate due to bearing failures is 0.017/1,000 hr.
- 10% of bearing problems are assumed to be associated with contact fatigue. Nonfatigue bearing failures will be reduced by improved design techniques for separators, lubrication management, etc. Therefore, assuming 33% of the bearing failures will be fatigue oriented results in a bearing failure rate associated with unscheduled gearbox removal of 0.006/1,000 hr.
- 50% of the bearing fatigue failures are assumed to be discovered at disassembly and do not cause

- a gearbox removal. Therefore, the total bearing fatigue failure rate is 0.011/1,000 hr, or, by taking the reciprocal, the B_{50} set life is 90,000 hr.
- A typical Weibull slope of 1.1 results in a bearing B₁₀ set life of 18,000 hr.

The individual bearing life and the bearing set life are shown in Table F-VII.

Weibull slopes for the current and advanced gearboxes are 1.3 and 1.5, respectively. These slopes represent reasonable levels for the materials and technology levels assumed.

Operating Conditions

Table F-VIII contains the important gearbox operating conditions.

Advanced technology

Table F-VII.
Bearing life comparison.

Bearing AFBMA* B₁₀ life (hr)**

Current technology	Advanced technology
95,640	73,195
95,640	73,195
123,795	56,513
55,140	51,753
108,810	85,260
250,440	125,540
1 x 10 ⁶	1 x 10 ⁶
108,810	85,260
304,062	148,500
70,800	137,200
18,460	18,379
	95,640 95,640 123,795 55,140 108,810 250,440 1 x 10 ⁶ 108,810 304,062 70,800

^{*} Antifriction Bearings Manufacturer's Association.

C...... 4 4 - a b - a l - m - l

Table F-VIII.
Bearing operating conditions.

	Current technology			Advanced technology				
Bearin	DN—	Film thickness— microinches	Lambda factor	Lub life factor	DN— mm-rpm	Film thickness— microinches	Lambda factor	Lub life factor
Pinion								
Fron	t 860,000	13.0	1.9	2.1	806,000	11.6	3.2	2.6
Rear	860,000	13.0	1.9	2.1	806,000	11.6	3.2	2.6
Right ic	dler							
Fron		13.2	2.0	2.1	493,000	10.6	2.9	2.5
Rear	588,000	10.8	1.6	1.7	493,000	10.8	3.0	2.5
Thrus	st 543,000	9.7	1.4	1.5	448,000	8.8	2.4	2.3
Left idle	er							
Fron	t 588,000	13.5	2.0	2.1	493,000	10.8	3.0	2.5
Rear	588,000	12.1	1.8	2.1	493,000	11.8	3.3	2.6
Thru	st 543,000	9.8	1.4	1.5	448,000	8.9	2.4	2.3
Output								
Front	t 242,000	5.3	8.0	0.3	243,000	4.7	1.3	1.2
Rear	212,000	4.1	0.6	0.2	213,000	4.7	1.3	1.2

^{**}Based on a cubic mean power of 5,980 hp.

The product of the bearing bore diameter and speed (DN) indicates the severity of the application and suggests the technology level required for the application. Both gearbox designs have DN values well within current Allison experience.

The oil film thicknesses, lambda factors, and lubrication life factors for each bearing are also shown in Table F-VIII. The roller bearing film thicknesses listed are the minimum thicknesses based on a formula developed by Grubin in Ref 7. The ball bearing film thicknesses are the minimum thicknesses based on a formula developed by Archard and Kirk in Ref 8. As expected, the high-speed bearings have the greatest oil film thicknesses. The slower speed prop bearings have the lowest film thicknesses. The prop bearings are in a lubrication regime (lambda factor < 1) in which these low film thicknesses lead to significant life penalties. Therefore, the prop bearings would benefit the most from surface finish improvements.

It is estimated that the prop bearing improvement in fatigue life due to improved surface finishes would be 500%. The other bearings also benefited from improved surface finishes in the advanced gearbox but to a lesser extent of approximately 25% life improvement.

It should be noted that the bearing factors shown in Table F-VIII have not been incorporated in the lives shown in Table F-VII. Therefore, the actual bearing lives should be higher than those shown in Table F-VII with the exception of the 1980s prop bearings.

Heat Generation and Efficiency

Heat generation and power losses were determined for the gears, bearings, and oil pumps in both gearboxes. The results of this analysis are presented in Table F-IX for the cruise and takeoff power conditions.

The results of the power loss analysis show that the efficiencies of both gearboxes are approximately the same. The 1990s gearbox gear losses are higher than those in the 1980s gearbox.

The higher loss is attributed to the use of high contact ratio gears, which have higher sliding losses due to longer

addendums. The high contact ratio gear sliding losses are slightly offset by the reduced gear windage, gear rolling, and bearing losses attributed to the smaller gears and bearings in the 1990s gearbox. The pump losses in the 1990s gearbox are also lower. The reduced pump loss is the result of the lower oil flow rates and oil pressures in the 1990s gearbox. The lower flow rates are a result of using a higher temperature rise across the gearbox. The advanced gearbox did not require as high an oil pressure to provide the required jet penetration into the pinion gear. The lower pinion supply oil pressure also contributed to the lower pump losses.

The advanced gearbox was designed with a modulated oil system. This system allows the gearbox oil flow to be modulated according to gearbox transmitted torque. Thus, oil flows are significantly reduced at lower power conditions such as cruise. Lower oil flows result in lower churning/windage type losses.

Gear sliding losses should also be lower than predicted on the 1990s gearbox. These gears have ionimplanted tooth flanks. Ion implantation has demonstrated the ability to lower frictional forces. Thus, this flank treatment should lower the gear sliding losses.

Gears

The power losses associated with the gears were determined by using formulas developed in Ref 9. These formulas account for gear losses due to windage, mesh sliding, and mesh rolling. These formulas were developed for standard spur gears lubricated by a mineral oil. For this study it was required to modify the Ref 9 formulas to allow their use with high contact ratio gears. These gears have longer than standard addendum and two teeth sharing the transmitted load at all times. The formulas were also modified to allow their use with MIL-L-23699 type oils. Also, helical gears were treated as spur gears in this analysis. Due to the low helix angle used in these helical gears, only a small error would be introduced by this assumption. A summary of the gear power loss analysis is presented in Table F-X.

Table F-IX.

Gearbox power loss and efficiency.

	Current technology		Advanc	ced technology
	Cruise	Takeoff power	Cruise	Takeoff power
Gears-hp	40.80	73.57	40.31	79.22
Bearings—hp	14.68	19.80	14.33	19.12
Oil pumps—hp	8.60	8.60	6.80	6.80
Total loss—hp	64.08	101.97	61.44	105.14
Gearbox efficiency—%	98.77	98.98	98.82	98.95

Table F-X. Gear losses.

	Sliding loss	Rolling loss	Pinion windage loss	Gear windage loss	Total individual gear loss
Current technology					
Cruise					
First stage—left First stage—right Second stage—left Second stage—right Access drive	5.485 5.485 8.659 8.659 1.300	0.678 0.678 0.367 0.367 0.028	0.885 0.885 0.191 0.191 0.008	2.522 2.522 0.890 0.890 0.113	9.570 9.570 10.107 10.107 1.449
Total gear loss					40.803
Takeoff Power					
First stage—left First stage—right Second stage—left Second stage—right Access drive	12.294 12.294 18.277 18.277 1.300	0.649 0.649 0.351 0.351 0.028	0.885 0.885 0.191 0.191 0.008	2.522 2.522 0.890 0.890 0.113	16.350 16.350 19.710 19.710 1.449
Total gear loss					73.567
Advanced technology					
Cruise					
First stage—left First stage—right Second stage—left Second stage—right Access drive	8.265 8.265 8.822 8.822 1.342	0.346 0.346 0.242 0.242 0.022	0.292 0.292 0.113 0.113 0.007	0.799 0.799 0.539 0.539 0.109	9.702 9.702 9.716 9.716 1.480
Total gear loss					40.315
Full Power					
First stage—left First stage—right Second stage—left Second stage—right Access drive	18.110 18.110 18.454 18.454 1.342	0.331 0.331 0.231 0.231 0.022	0.292 0.292 0.113 0.113 0.007	0.799 0.799 0.539 0.539 0.109	19.532 19.532 19.337 19.337 1.480
Total gear loss					79.218

Note: Losses are measured in horsepower.

Bearings

The cylindrical roller and ball bearing power losses were calculated by the method outlined in Ref 10. The tapered roller bearing power losses were calculated by the method shown in Ref 11. These formulas account for losses associated with speed and load effects. The results of the bearing power loss analysis are shown in Table F-XI.

Oil Pumps

Oil pump losses were calculated using the following equation:

$$HP_{loss} = \frac{(Q)(H)}{(33,000)(Eff)}$$

where:

HP_{loss} = oil pump horsepower loss
Q = oil flow rate—lb/min
H = oil pressure head—ft

Eff = pump mechanical efficiency

The oil flow rates and oil pressure head were determined as discussed in the lubrication section. The pump efficiency was assumed to be 25%.

Lubrication System

The primary function of the lubrication system is to remove the heat generated by the gears, bearings, and oil

pumps to maintain the desired component temperatures. The lubrication also provides lubricant to separate mating surfaces with an oil film to reduce friction and the resultant heat generation. The lubricant is also needed to protect the gearbox components from corrosion and foreign particles.

The lubrication system flow requirements are initially based on the predicted gearbox heat generation and the allowable temperature rise across the gearbox components. The design value for lubrication system oil pressure depends on the required gear tooth penetration depths.

Heat generation estimates at cruise and full power for both gearboxes are shown in Table F-XII. The gearbox allowable temperature rises are also listed in this table and were established during the criteria definition phase. To maintain these gearbox temperature rises during the full power condition requires oil flow rates of 144 lb/min and 99 lb/min for the current and advanced gearboxes, respectively. The advanced gearbox oil flow will be regulated to 58 lb/min at the cruise condition to reduce gearbox losses.

The gearbox oil pump also supplies the oil needed for the propfan pitch change system. The oil flow rate, temperature rise, and maximum continuous heat rejection for the propfan are also listed in Table F-XII. The temperature rise across the propfan is lower than the temperature rise across the gearbox. Thus, the combined temperature rise across the common propfan and gearbox lubrication system is also lower than the gearbox temperature rise. The combined temperature rise for the gearbox and propfan is the temperature difference that must be maintained by the oil cooler.

Table F·XI.
Bearing losses.

	Current to	echnology	Advanced	technology
Bearing	Cruise loss	Takeoff power loss	Cruise loss	Full power loss
Pinion front	1.085	1.376	1.052	1.404
Pinion rear	1.085	1.376	1.052	1.404
Idler front—right	2.642	3.750	2.243	3.340
Idler rear—right	1.943	2.797	1.999	2.933
Idler thrust-right	0.375	0.513	0.272	0.404
Idler front—left	2.319	3.209	1.895	2.759
Idler rear—left	1.019	1.252	1.372	1.491
Idler thrust—left	0.375	0.513	0.272	0.404
Prop front	2.163	2.567	2.041	2.423
Prop rear	1.975	2.333	2.058	2.443
Accessory front	0.051	0.082	0.051	0.082
Accessory rear	0.023	0.036	0.023	0.036
Total bearing loss	14.680	19.805	14.331	19.123

Note: Losses are measured in horsepower.

Table F-XII.

Lubrication system design conditions.

	Current technology		Advanced technology	
	Cruise power	Takeoff power	Cruise power	Takeoff power
Flow rate—Ib/min				
Gearbox	144	144	58	99
Propfan	82	82	82	82
Combined	226	226	140	181
Temperature rise— °F				
Gearbox	38	60	90	90
Propfan	9	9	9	9
Combined	27	42	43	53
Maximum continuous heat rejected to oil—Btu/min				
Gearbox	2720	4328	2608	4462
Propfan	367	367	367	367
Combined	3087	4695	2975	4829
Oil pressure required—Ib/in.2				
Pinion gear teeth	110	110	80	80
Other jets	80	80	80	80

Table F-XII lists the lubrication system oil pressures. The current technology gearbox requires a pressure of 110 lb/in.² to provide adequate oil penetration into the pinion gear teeth. Restricting the 110 lb/in.² pressure to the pinion gear mesh is favored to lower the oil pump power requirements. Oil pressure of 80 lb/in.² is adequate for all the other oil jets in this gearbox. The required advanced gearbox oil pressure is 80 lb/in.² at all jet locations.

The advanced technology gearbox incorporates a modulated oil system feature designed to adjust oil flow based on the transmitted torque. Since heat generation is a function of the transmitted torque, oil flow is adjusted proportional to the heat generation rate. Thus, only the oil flow needed to maintain a constant temperature rise is provided. Avoiding excess flow at the lower power points reduces heat generation associated with excess windage/churning. This system is discussed in more detail in the general arrangement and technology sections.

Three micron filtration is incorporated in both gearbox designs. In the past, typical turboprop gearbox installations have used filtration in the 38-80 micron range. Testing discussed in Ref 12, with 3-micron filtration, has shown improvements in bearing fatigue life and significant improvements in bearing surface appearance and wear levels. In Ref 13, use of 3-micron filtration in Army UH-1/AH-1 transmissions resulted in much cleaner components and less seal wear. Therefore, to meet the gearbox 30,000-hr MTBR a 3-micron filter is recommended.

A full flow debris monitoring system is included in both designs. The system selected for both gearboxes is a TEDECO Quantitative Debris Monitoring type. This system captures, counts, and discriminates by size the ferrous particles generated by the gearbox. A trending capability allows differentiation between progressive and noncritical debris generation conditions.

Higher oil bulk temperatures, self-cleaning filters, and improved oils are featured in the 1990s gearbox and discussed in the gearbox technology plan section.

An oil system common to both the engine and gearbox is incorporated for both designs. This type of lubrication system leads to reduced lubrication system complexity in comparison with separate gearbox and engine systems. Only one oil tank and a common scavenge oil filter and oil cooler are required in this system.

The potential for smaller air/oil coolers is greater with a common system since optimizing the size of a hybrid air/oil and fuel/oil system is more feasible. Development of new oils with higher load carrying capacity than those currently available would make it more desirable to separate the gearbox and power section lubrication systems. However, if these oils were developed with high temperature capabilities it would be advantageous to use a common system.

Housings

The housing material used in the current design is magnesium (AZ92-T6). These housings would be coated with AMS 2475 (HAE) to protect them from corrosion.

The advanced gearbox housings would be manufactured from composite materials to reduce weight and increase stiffness. Greater stiffness in the advanced design would reduce deflections, which result in misalignment of gear and bearing contacts. The operating stresses would be reduced, further justifying higher design allowable stresses and increased material life factors. Either metal matrix or resin matrix composites will be selected for the advanced design. This decision would be based on the results of the technology program. Further details on the composite housing materials are discussed in the technology section.

Propfan Interfaces

A number of mechanical and hydraulic interfaces between the gearbox and propfan were required. As discussed previously, the gearbox and propfan oil systems are common. The gearbox oil pump supplies 80 lb/in.² oil to the high-pressure propfan hydraulic pumps, which boost the pressure to 4,750 lb/in.². The high-pressure oil is used for the pitch change mechanism and returned to the propfan hydraulic power module for scavenging by the gearbox scavenge pumps. The propfan oil system flow, pressure, and heat dissipation requirements are as follows:

- required oil flow rate = 45 qt/min
- required hydraulic pump inlet oil pressure = 75 lb/in.² gauge
- maximum continuous heat rejection = 22,000 Btu/hr

The gearbox also provides a high-speed drive for the propfan module. This drive is powered by an internal gear mounted to the aft end of the prop shaft. The drive speed is increased to 20,000 rpm through two gear stages. The drive supplies power to the propfan rotating generator and hydraulic pumps. The high-speed drive power requirements are as follows:

- maximum continuous drive power
 - no de-icing = 8.7 hp
 - de-icing = 15.0 hp
- maximum transient
 - no de-icing = 35.5 hp
 - de-icing = 42.0 hp

Lastly, the gearbox provides mounting provisions for the propfan rotating module, hydraulic power module, and capacitive coupling. The propfan rotating module is mounted to and driven by the prop shaft curvic coupling, which has flange requirements as follows:

outside diameter = 13.25 in.

- inside diameter = 10.75 in.
- bolt circle diameter = 12 in.
- number of bolts = 24
- bolt size diameter = 9/16 in.

The hydraulic power module is mounted on a pad on the rear of the gearbox housing. The capacitive coupling stationary member is mounted on a pad on the front of the gearbox housing. This pad is concentric with the prop shaft.

Gearbox Physical Dimensions

Important overall dimensions of both gearbox designs are listed in Table F-XIII.

The size reductions obtained in the advanced design are primarily a result of the higher material allowables and use of high contact ratio spur gears for the pinion-to-idler mesh.

Gearbox Weight

The gearbox weight for the current technology gearbox is 800 lb and for the advanced gearbox, 640 lb. The weight savings is primarily a result of using higher material allowables and high contact ratio spur gears for the pinion-to-idler mesh. The major weight contributors are the gears (40% of total) and bearings (20% of total). The shafting and housing contribute approximately 10% each with the balance being pumps and miscellaneous hardware.

Acquisition and Maintenance Cost

The estimated acquisition cost of the current technology gearbox is \$220,000 and for the advanced gearbox, \$165,000. These costs were determined using an Allison material index factor procedure. The primary reason for re-

duced cost of the advanced technology gearbox is the use of powder metal gears and bearings, near net shape manufacturing processing, and smaller size and weight. Acquisition cost is based on a cumulative average of 500 units at 20/month and quoted in 1984 dollars.

The maintenance cost for the current technology gear-box is \$1.31/engine flight hour and for the advanced technology gearbox, \$1.08/flight hour.

The MTBR for both gearboxes was equal, and the manhours required for maintenance actions on each gearbox were the same. The primary reason for the reduced maintenance cost of the advanced technology gearbox is the reduced cost of parts needed for maintenance actions. The maintenance costs were projected using T56 engine experience as a base and assuming on-condition maintenance practice.

Power Scaling

Dimensions and weights for both gearboxes were scaled from 8,000 to 20,000 hp. The scaled gearbox external lengths, heights, and widths are shown in Table F-XIV.

The scaled gearbox weights are shown in Table F-XV. Weights and dimensions were scaled using the following equations:

(Weight) scaled = (weight) base
$$\left(\frac{hp}{hp}\right)$$
 scaled $\left(\frac{hp}{hp}\right)$ 1.5

(Dimension)_{scaled} = (dimension)_{base}
$$\left(\frac{hp_{scaled}}{hp_{base}}\right)^{0.5}$$

These equations are based on the assumption that turbine and propeller tip speeds and disk loading remain constant over the scaled power range for a given technol-

Table F-XIII.

Gearbox physical dimensions.

Dimension	Current technology	Advanced technology
Frontal area—in. ²	900.0	745.1
Height—in.	34.31	31.62
Length—in.	24.38	23.22
Width		
Between mounts—in.	28.44	26.75
Maximum—in.	32.06	26.75
Centerline offset (engine-propeller)—in.	15.375	14.375

Table F-XIV.
Scaled gearbox external dimensions.

	Current technology			Adv	anced techno	nnology
Horsepower	Length	Height	Width	Length	Height	Width
8,000	21.8	30.7	28.7	20.8	28.3	23.9
10,000	24.4	34.3	32.1	23.2	31.6	26.8
20,000	34.5	48.5	45.4	32.8	44.7	37.9

Note: Dimensions are in inches.

Table F-XV. Scaled gearbox weights.

Horsepower	Current technology	Advanced technology
8,000	570	460
10,000	800	640
20,000	2263	1810

Note: Weights are in pounds.

ogy level. Compressive stress levels are assumed to remain constant over the horsepower range. Also, it is assumed that the output torque has the greatest influence over gear-box weight and size. This is reasonable since the output stage is the largest weight contributor due to the high torque transmitted through this stage.

Opposite Rotation

Reversing propfan rotation is a possible requirement by the airframe designer to achieve aerodynamic performance and reduction of noise level. Opposite rotation for both gearbox designs can be achieved in two ways. Either the engine power turbine rotation could be reversed or idler gears could be added to the gearbox.

Adding opposite rotation idlers to the dual compound idler gearbox requires a modification to the design as shown in Figure F-13. First, two additional helical idler gears and four supporting bearings would be required. These gears would be located between the second-stage idler gear and the output gear. The main drive gear would require an opposite helix hand. A slightly larger second-stage compound idler gear would be needed to maintain acceptable gear stresses. Finally, larger housings would be required to accommodate the gear center distance changes.

To minimize manufacturing costs, the larger housings and larger compound idler gears would be used for both rotational designs. Thus, the only changes from one design to the other during manufacturing would be machining of

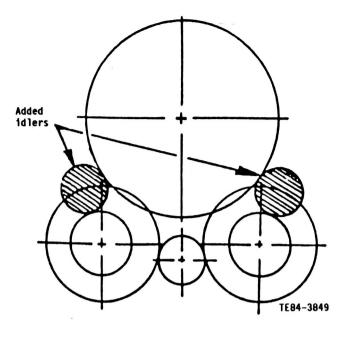


Figure F-13. Modifications required for reversing direction of rotation of propfan.

the housing bearing bores and output gear teeth and the addition or deletion of idler gears and bearings.

Opposite rotation is not without penalties if it is achieved through gearbox changes. Additional gears and bearings are required at the expense of increased costs, lower overall efficiency, and possibly reduced reliability. The additional hardware would result in increased oil flow requirements and a larger oil cooler and housing. These issues would need to be compared with the complexity of reversing the turbine direction of rotation.

Deciding which way to proceed would also depend on the requirements of the airline since right- and left-hand gearboxes and power sections affect engine maintenance and replacement operations.

REFERENCES

- D. P. Townsend, R. J. Parker, and E. V. Zaretsky, "Evaluation of CBS 600 Carburized Steel as a Gear Material," NASA TP 1390, 1979.
- E. N. Bamberger, T. A. Harris, W. M. Kacmarsky, C. A. Moyer, R. J. Parker, J. J. Sherlock, and E. V. Zaretsky, "Life Adjustment Factors for Ball and Roller Bearings—An Engineering Design Guide," ASME, 1971.
- D. G. Lewicki, J. D. Black, M. Savage, and J. J. Coy, "Fatigue Life Analysis of a Turboprop Reduction Gearbox," AIAA-84-1384, presented at the AIAA 20th Joint Propulsion Conference, Cincinnati, 11-13 June 1984.
- R. Drago, "Heavy Lift Helicopter Brings Up Drive Ideas," Power Transmission Design, March 1974, pp 49-63.
- B. J. Hamrock and D. Dowson, "Isothermal Elastohydrodynamic Lubrication of Point Contacts III—Fully Flooded Results," *Journal of Lubrication Technology*, Vol 99, No. 2, April 1977, pp 264-276.
- H. S. Cheng, "Prediction of Film Thickness and Traction in Elastohydrodynamic Contacts," ASME
 Design Engineering Technology Conference, ASME,
 New York City, 1974, pp 285-293.
- A. Grubin and I. Vinogradova, "Investigation of the Contact of Machine Components," TsNIITMASH,

- Book No. 30, 1947 (D.S.I.R., London, Translation No. 337).
- 8. G. Archard and M. Kirk, "Lubrication at Point Contacts," Proceedings of the Royal Society, A. 261, 1961, pp 532-550.
- N. E. Anderson and S. H. Loewenthal, "Spur-Gear-System Efficiency at Part and Full Load," NASA TP 1622, 1980.
- 10. T. A. Harris, "Roller Bearing Analysis," John Wiley and Sons, Inc., 1966.
- D. C. Witte, "Operating Torque of Tapered Roller Bearings," Preprint No. 72 LC-2C-1, presented at the ASME/ASLE International Lubrication Conference, New York City, 9-12 October 1972.
- S. H. Loewenthal and D. W. Moyer, "Filtration Effects on Ball Bearing Life and Condition in a Contaminated Lubricant," *Journal of Lubrication Technology*, Vol 101, April 1979, pp 171-176.
- Dr. T. Tauber, W. A. Hudgins, and R. S. Lee, "Full-Flow Debris Monitoring and Fine Filtration for Helicopter Propulsion Systems," Preprint No. RWP-24, presented at the Rotary Wing Propulsion System Specialist Meeting, Williamsburg, VA, 16-18 November 1982.

APPENDIX G

TASK VIII. CONCEPTUAL DESIGN OF THE SINGLE-ROTATION PITCH CONTROL AND MECHANISM

TABLE OF CONTENTS

Title	Page
Introduction	G-1
Conceptual Design of the Single-Rotation Pitch Control and Mechanism	G-2
Current Technology Overview	G-2
Trade Studies	G-3
Conceptual Design of Selected Concept	G-8
Description of Pitch Control Concepts	
Pitch Control Parameters	G-16
Reliability	G-17
Maintenance Cost	
Acquisition Cost	G-18

LIST OF TABLES

Table	Title	Page
G-I	Power system concept ranking	. G-5
G-II	Blade angle feedback sensor ranking	. G-8
	Signal transfer ranking	
G-IV	Control system ranking	. G-8
G-V	Pitch control concept evaluation	· G-16
G-VI	Slew rates	. G-16
G-VII	Blade angle settings	· G-17
G-VIII	Unscheduled removals (all causes)	· G-17

INTRODUCTION

Task VIII focused on the conceptual design of a singlerotation pitch control and mechanism for the 10,000-shp
advanced propulsion system of Task III. This design is an
extension of work performed in Task III, which assumed a
state-of-the-art linear hydraulic piston type actuator, a beta
control valve, blade drive links, a mechanical in-place pitch
lock, an input shaft, and an oil transfer housing. The advanced system defined in Task VIII provides for improved
reliability and maintenance required for commercial airliners and expected of propfan propulsion verification. The
mission is a 120-passenger advanced design airliner capable of cruising at 0.72 Mach Number at a 32,000-ft altitude.
It is assumed that the 10-blade, 12.78-ft-diameter propfan of

Task III is used with the advanced technology gearbox of Task VII.

This pitch change system conceptual design was fully integrated with the advanced gearbox of Task VII so that maintenance of the pitch change control, pitch change mechanism, propfan, and gearbox can be accomplished in an economical and efficient manner. Sufficient details were defined to establish estimates of acquisiton and maintenance costs and the anticipated reliability.

To fully realize the benefits projected for the advanced pitch change system requires implementation of the research and technology plan described in Appendix H.

CONCEPTUAL DESIGN OF THE SINGLE-ROTATION PITCH CONTROL AND MECHANISM

A conceptual design study was conducted under Task VIII to provide an advanced flight weight pitch change control and mechanism design compatible with the offset gearbox designed in Task VII. The conceptual design study used data from a Hamilton Standard-funded conceptual trade study conducted before the conceptual design in determining the concept for further design effort under the APET contract. The favored concept incorporates a linear hydraulic actuator with hydraulic and electrical power generated within the propfan assembly. A digital electronic control and a rotary capacitor signal transfer assembly are also incorporated in the propfan assembly.

A modular design of all pitch control components was used to enhance serviceability and thereby reduce maintenance cost. Drawings of three conceptual arrangements were generated for the linear hydraulic pitch control system. The final selection achieved improved maintainability by locating the hydraulic power module at the rear of the gearbox on the propfan axis of rotation. This arrangement is possible with the offset gearbox, which has access to the rear of the output shaft.

The concept-level drawings, descriptions of the propfan pitch control operation and estimates of acquisition cost, MTBUR, and maintenance cost are presented in this section.

Also, blade angles, twisting moments, and slew rates are provided for selected operating conditions of the APET mission.

CURRENT TECHNOLOGY OVERVIEW

Blade pitch controls on new commuter turboprops generally incorporate a linear hydromechanical actuator with a metering valve and a mechanical pitch lock mounted in the rotating hardware. Mechanical, hydraulic, and electrical inputs must be transmitted from the fixed, nacelle-mounted components (i.e., the gearbox). Rotary mechanical inputs position the metering valve and pitch lock and use either differential gearing or a bearing-mounted ball screw to transmit rotary motion across the rotating interface. High-pressure oil is transmitted to the metering valve and actuator through a low-clearance oil transfer bearing and transfer tubes. Electrical power for ice protection is transmitted to the propeller through contact brushes running on a rotating slip ring assembly.

The propeller assembly shown in Figure G-1 defines a current pitch control concept adapted to an offset gearbox installation. The offset gearbox permits pitch control components to be easily mounted in accessible modules on the axis of rotation. This minimizes the impact on the gear-

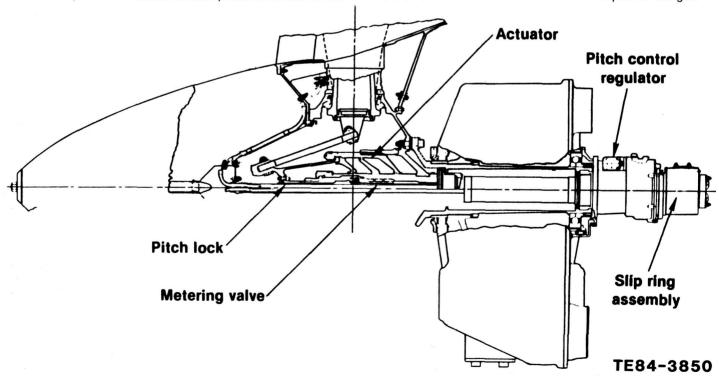


Figure G-1. Current pitch control concept adapted to an offset gearbox configuration.



box design and greatly improves maintainability. Other features include the relatively small-diameter oil transfer bearing and compact differential gearing in the regulator module and the small drum-type slip ring module, which contribute to a more reliable system for less weight. Propellers installed on today's large commuter aircraft incorporate most of these features.

Current technology for transmitting rotary mechanical and hydraulic pitch control inputs to a turboprop installed on an in-line planetary gearbox are shown in the sectional drawing of Figure G-2. In this configuration, access to the axis of rotation from the rear of the gearbox is restricted by the drive shaft from the engine. Therefore, the mechanical signal must be transmitted from the rear face of the gearbox housing to the turboprop through differential gearing around the sun gear shaft, lay shafts through the planet cage, and additional gears to reach the axis of rotation. Similarly, high-pressure pitch change oil must be transmitted through a large-diameter (high leakage) transfer bearing around the sun gear shaft and oil transfer tubes through the planet cage to the turboprop shaft.

Unlike the offset gearbox configuration, the integration of nonmodular pitch control inputs within the in-line gearbox introduces several complexities. In addition to the complex gearing and large-diameter transfer bearing, there is a significant impact on the gearbox design. The overall effect is a reduction in reliability and an increase in maintenance costs. This configuration emphasizes the need to develop advanced pitch control systems that are more reliable and easily maintained.

TRADE STUDIES

Before the APET pitch control study, Hamilton Standard conducted company-funded pitch control trade studies to identify advanced technology concepts. The primary criterion was that the pitch control system be adaptable to both in-line and offset gearbox configurations with minimal impact on the gearbox design. The pitch change system was considered as two parts: a power system and a control system. A comprehensive matrix of the most viable concepts was prepared for each system to be evaluated separately.

The power system matrix in Figure G-3 shows several concepts of pitch change mechanisms, prime movers, and power supplies. Several methods of power transfer across the rotating interface were considered. All components were comparatively evaluated using the following parameters listed in order of decreasing criticality: safety, reliability, maintainability, weight, performance (accuracy of blade an-

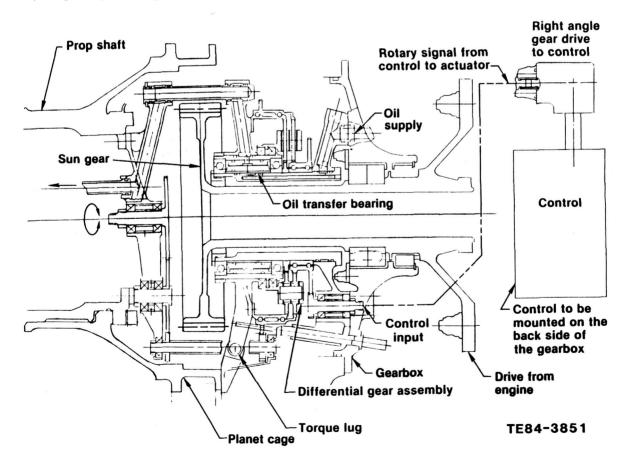


Figure G-2. Current pitch control concept adapted to an in-line gearbox configuration.

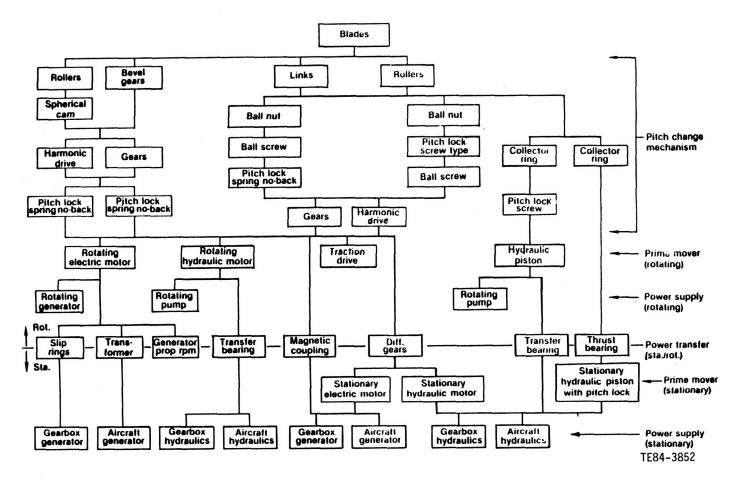


Figure G-3. Propfan power system matrix.

gle control for Synchrophasing® *), acquisition cost, impact on gearbox, technical risk, envelope, and heat generation (efficiency). (Synchrophasing is a fine-tuning control of blade pitch through very small angles that do not require high slew rates.) These evaluation parameters were assigned weighting factors and were used in conjunction with a forced decision rating technique.

A first round of rating concepts of the same function, one to another, eliminated several concepts. This resulted in a reduced matrix of seven power systems represented by the shaded boxes in Figure G-4. Pitch change mechanisms at the far left of the matrix were eliminated primarily because of weight penalties associated with the large bevel gears and cams required to actuate the propfan blades mounted in the large-diameter hub. The ball screw and ball nut coupled with a spring no-back pitch lock in the left center of the matrix were eliminated because of unsatisfactory blade angle control. The backlash required to release and engage the pitch lock caused excessive hysteresis in the pitch control loop. Most of the power transfer components on the rotating interface were eliminated

because of their low reliability when compared with systems incorporating dedicated propfan-mounted power supplies. In addition, slip rings incur high maintenance costs; tranformers and generators driven at propfan speed are heavy; oil transfer bearings have low reliability and maintainability for the large diameters required by in-line gear-box installations; and the thrust bearing that transmits pitch change and pitch lock loads across the rotating interface rates low on reliability, maintainability, and weight.

One of the final seven power system candidates incorporates a linear hydraulic piston that acts directly on a collector ring, links, and blade trunnions (crank arms) to change pitch. The remaining six systems incorporate a ball screw that, when rotated, translates a ball nut and links to change blade pitch. The ball screw can be driven by either a traction drive or motors (electric or hydraulic; rotating or stationary) powered by generators or pumps (rotating or stationary). Hydraulic pumps and motors are considered to be gear types operating at a system pressure of 6000 lb/in.². Electric generators and motors are considered to be the samarium-cobalt permanent magnet brushless type with

^{*}Synchrophasing is a registered trademark of Hamilton Standard.

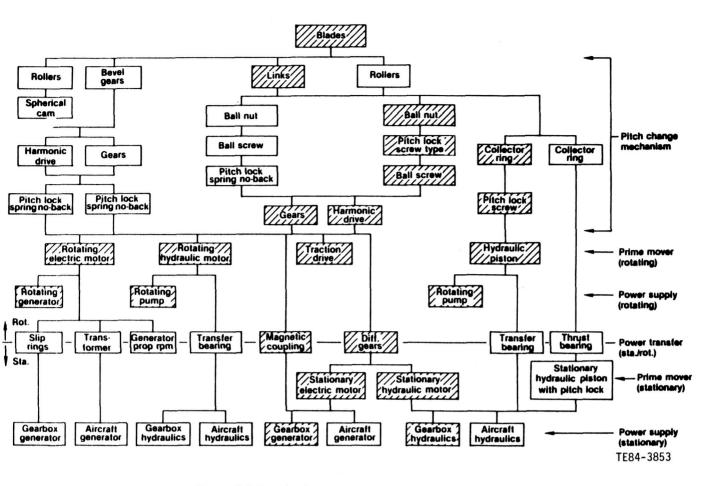


Figure G-4. Propfan intermediate power system matrix.

appropriate electronic controls. The required motor size for maximum pitch rate is approximately 25 hp.

The magnetic coupling is an electric motor mounted on the rotating interface with the stator fixed to the gearbox and the rotor driving the ball screw through appropriate gearing. During fixed pitch operation, the rotor reacts blade torque and rotates at a reference speed dependent on propfan speed. Rotor speed is increased or decreased from the reference speed to change pitch toward high or low pitch. The traction drive is a toroidal variable ratio type with associated planetary gearing. This type of traction drive was selected rather than a constant-ratio, multistage roller traction drive because it offered a mechanical method of providing bidirectional, variable-speed pitch control.

The seven power system concepts were comparatively evaluated, and they are listed in Table G-I in order of ranking. The simplicity of the hydraulic piston concept resulted in high ratings for reliability, performance, and cost, resulting in the highest total rating. Of the remaining ball screw concepts, electric motor drives rated second to hydraulic motor drives based on reliability and weight. Differential gear concepts rated lower on reliability based on higher parts count. The toroidal traction drive was rated low on reliability, performance, and technical risk. The hydrau-

Table G-I.
Power system concept ranking.

Ranking	Power system concept
1	Hydraulic piston actuator
2	Ball screw, hydraulic motor
3	Ball screw, electric motor
4	Ball screw, differential gears, hydraulic motor
5	Ball screw, magnetic coupling
6	Ball screw, differential gears, electric motor
7	Ball screw, traction drive

lic piston actuator (linear hydraulic) and the hydraulic motor-driven ball screw (rotary hydraulic) were considered the two final candidates for selection since they rated significantly higher than the other five concepts.

The linear hydraulic concept rated high in comparison with the rotary hydraulic concept for all evaluation parameters except weight and adaptability to counter-rotating propellers. The latter was a consideration secondary to the evaluation parameters listed at the beginning of this section. Both concepts have a minimum impact on the gearbox. Based on the higher evaluation rating, the linear hydraulic power system was selected for the APET pitch control conceptual design study. This system is highlighted by the

shaded boxes in the power matrix of Figure G-5. Gearbox interface requirements of this self-contained hydraulic power system are minimal, consisting only of a high-speed pump drive shaft from the sun gear and a nominal amount of cooling oil flow.

The control portion of the advanced pitch control trade studies will now be described. Figure G-6 is a diagram representing a digital electronic aircraft propulsion control system in which a full authority digital electronic engine control (EEC) coordinates and commands engine fuel flow, compressor vane positions, and propfan blade angle to control power and speed. The control is provided diagnostic feedback data from the engine and propfan. This system was reported in a NASA-sponsored study completed in 1978 (Report No. 135192) and is still considered a desirable system for advanced propfans. The control system matrix shown in Figure G-7 identifies different methods of transmitting a blade pitch command signal to the propfan power matrix from the EEC. Several methods of transmitting the digital signal across the rotating interface to a propfan-mounted electronic controller are shown with several types of blade angle (β) feedback sensors. A stationary nacelle-mounted electronic controller mounted on the gearbox side of the rotating interface was also considered in this analysis.

All control system components were comparatively evaluated using parameters and weighting factors similar to those employed in the power system study. These parameters are listed in order of decreasing criticality as follows: safety, reliability, maintainability, acquisition cost, accuracy (Synchrophasing control), weight, technical risk, adaptability (to single and counter-rotating propellers; in-line and offset gearbox configurations), and envelope. Five blade angle feedback displacement sensors were considered: (1) linear variable differential transducer (LVDT), (2) rotary variable differential transducer (RVDT), (3) linear variable-phase transducer (LVPT), (4) resolver, and (5) optical encoders. The LVDT and LVPT measure linear displacement, the RVDT and resolver measure rotary displacement, and optical encoders can measure either linear or rotary displacements.

The ranking of the sensors determined by comparative evaluation are shown in Table G-II.

All sensors were found to provide sufficient accuracy, but each differed significantly in reliability, maintainability, and cost. The first three rated sufficiently higher than the last two to qualify as candidates for selection. The LVDT and RVDT measure displacement as a function of output voltage amplitude and are widely used today. In contrast, the LVPT represents a relatively new technology. It mea-

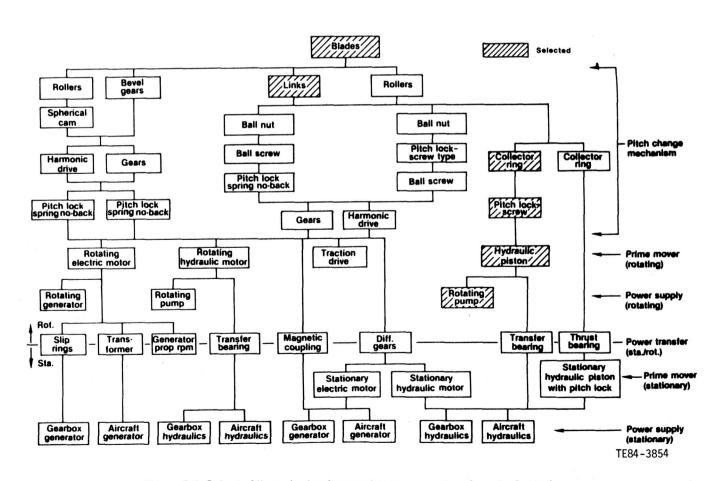


Figure G-5. Selected linear hydraulic propfan power system from trade study.

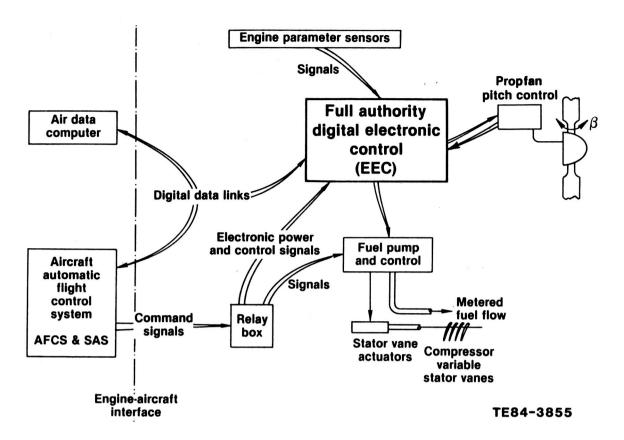


Figure G-6. Propfan propulsion system control diagram.

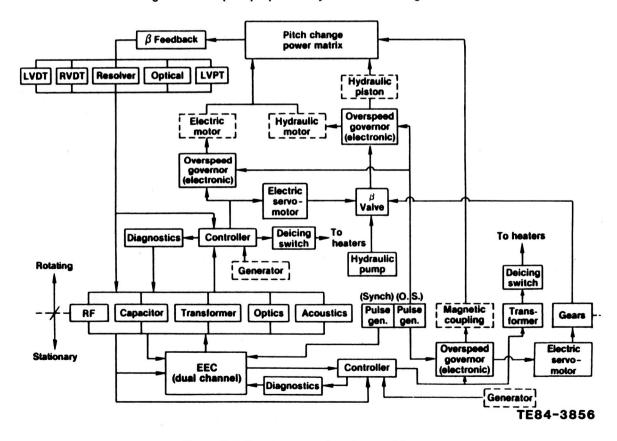


Figure G-7. Propfan control system matrix.

Table G-II.
Blade angle feedback sensor ranking.

Ranking	Sensor
1	LVPT
2	LVDT
3	RVDT
4	Resolver
5	Optical

sures displacement as a function of phase difference of two output voltages, and unlike the LVDT, it doesn't require an analog/digital converter. Because of this latter feature, the LVPT rates slightly higher than the LVDT and was selected for use with the linear hydraulic power system in the APET study.

Five methods of transmitting digital control signals across the rotating interface were evaluated. These are: (1) radio (radio frequency [RF]), (2) capacitor, (3) optics, (4) transformer, and (5) acoustics. Table G-III shows them listed in order of relative ranking following the evaluation.

Table G-III.
Signal transfer ranking.

Ranking	Signal transfer method	
1	Capacitor	
2	Transformer	
3	Optics	
4	Radio	
5	Acoustics	

Rating variations were based primarily on reliability, with particular emphasis on susceptibility to external interference. Optics rated lower than the capacitor and the transformer concept because it was considered more difficult to protect optical components from contamination than to shield the capacitor and transformer from electromagnetic interference (EMI). Radio and acoustics were considered very difficult to protect from RF and acoustic interference. The capacitor concept was selected based on high reliability and simplicity.

Three of the five control system concepts shown in Figure G-7 use a fractional horsepower, direct current (dc) electric servomotor to position a metering valve to provide high-pressure oil to either a linear piston or a gear motor prime mover. The servomotor and its electronic controller are mounted in the rotating propfan in two of these concepts and on the stationary gearbox in the third concept. The remaining two concepts incorporate an electronic controller to directly control a large, dc electric motor (approximately 25 hp) prime mover. One of these concepts has the

controller and motor mounted in the rotating propfan; the other concept has the controller mounted on the gearbox to control the motor (magnetic coupling).

Comparative evaluation of the control systems resulted in the ranking list shown in Table G-IV.

Table G-IV.
Control system ranking.

Ranking	Control system concept
1	Electric servomotor, metering valve, hydraulic piston
2	Electric servomotor, metering valve, hydraulic motor
3	Electric servomotor, gears, metering valve
4	Electric motor (magnetic coupling)
5	Electric motor

The first two servomotor control systems are identical and share the same rating. They differ only in the prime movers being driven, and their rating is significantly higher than ratings of the remaining three concepts. The third servomotor system was penalized on reliability and accuracy for transmitting the control input to the metering valve through differential gearing. Low ratings were assigned to the two large electric motor control concepts because the solid-state components currently available for large motor and generator controls are less reliable and are heavy. Considerable research and development effort is being expended to improve this technology for use in aerospace applications (i.e., the all-electric aircraft). When electrical prime movers become competitive with hydraulic prime movers, they can easily be adapted to the rotary pitch change mechanism.

The pitch control system components selected for the linear hydraulic power system are highlighted by the shaded control matrix boxes in Figure G-8. Interface with the gearbox is minimal and consists of a support bracket for the stationary half of the capacitor signal transfer coupling and a high-speed generator drive shaft from the sun gear. This is the same shaft that drives the pumps in the power system.

In summary, the trade studies showed that: (a) the linear hydraulic actuator rates best overall but is heavier and less adaptable to counter-rotating propfans, (b) hydraulic systems are more reliable and have a higher power density capability than electrical systems, (c) a power supply located on the rotating side of the interface is more reliable than transmitting power across the rotating interface from the stationary side, and (d) the capacitor control signal transfer across the rotating interface is simple and reliable.

CONCEPTUAL DESIGN OF SELECTED CONCEPT

The two primary design objectives for the APET pitch control conceptual design were: (1) to minimize impact on

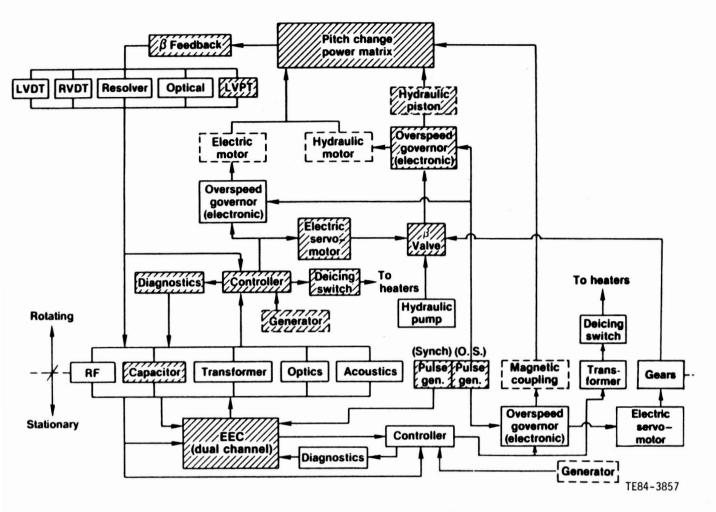


Figure G-8. Selected control system linear hydraulic concept.

the gearbox and (2) to maximize accessibility and maintainability. These objectives were attained by applying modularity to the pitch control design. The modular approach increases reliability by simplifying the interface with the gearbox and reduces maintenance cost by providing accessible, easily maintained modules.

The linear hydraulic pitch control system components were incorporated in three conceptual arrangements. Concept 1 is compatible with either offset or in-line gearbox within the propfan assembly. Concepts 2 and 3 are compatible only with an offset gearbox installation since some components are mounted at the rear face of the gearbox housing on the propfan axis of rotation.

Description of Pitch Control Concepts

The propfan is flange-mounted to the gearbox output shaft through curvic face splines at the rear face of the hub. Each blade is retained in the hub with a single-row angular contact ball bearing. Additional support for static blade pitch operation is provided by an external blade clamp. Blade retention bearings are lubricated by a fixed amount of oil in the

hub. A lip seal at the blade root prevents external leakage. A sectional assembly drawing of the propfan with pitch control Concept 1 is shown in Figure G-9. Blade trunnion arms splined to the inboard end of the blades are used to rotate the blades about the pitch axes. Links with spherical rod-end bearings connect the trunnion arms to a collector drive ring that translates to change blade pitch. The drive ring is strad-dle-mounted on hub-mounted support rings. Link forces impose a torque on the drive ring, which is reacted by a sliding splined sleeve fixed to the rear of the hub.

The link drive ring is translated by a hydraulic power module that consists of a linear piston-type actuator, a four-way metering valve (beta control), a mechanical in-place pitch lock, pumps, oil sumps, pressure regulating and relief valves, and a generator. Two bolted flanges are used to mount the hydraulic power module in the propfan. A flange on the actuator piston extension is bolted to the rear of the hub, and a flange on the actuator cylinder is bolted to the blade link drive ring. Blade pitch is changed toward high or low pitch by the cylinder, which translates in response to pressurized oil applied to the high or low side of the grounded piston. The actuator cylinder also incorporates a pitch lock

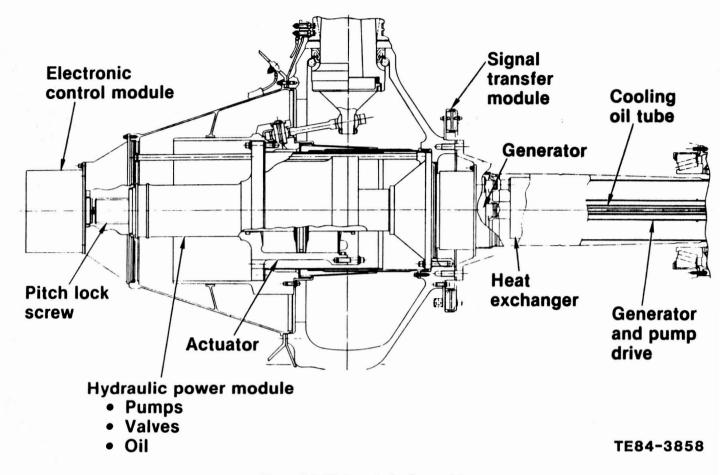


Figure G-9. Pitch control—Concept 1.

nut and screw on the axis of rotation. A small axial gap is maintained between the end of the translating screw and the grounded piston in operation. This prevents the blade pitch from decreasing toward low pitch more than one degree if hydraulic power is inadvertently lost anywhere in the blade operating range.

The pitch lock screw is driven by a small bidirectional do servomotor to control pitch upon command from the electronic control module. Each axial position of the screw and each equivalent rotary position of the motor shaft represents a discrete blade angle setting in the operating range. This position is measured by an RVDT geared to the motor shaft and fed back to both the electronic control module and the nacelle-mounted EEC.

Hydraulic System

Figure G-10 is a diagram showing the functional relationship between the actuator, pitch lock, and hydraulic components. All hydraulic components except the heat exchanger are located within the piston centerbody. The hydraulic system is designed to conserve power and reduce heat generation. Over 95% of propfan pitch control operating time is spent at power levels less than 20% of peak power. This is because commercial aircraft require peak

pitch rate power only for large blade angle excursions, i.e., reversing and feathering.

A small displacement main gear pump supplies highpressure oil to the actuator via the beta metering valve for all low-power pitch control requirements. Although the pump can provide the peak system pressure set by the high pressure relief valve, the pump supply (discharge) pressure is regulated to a few hundred pounds per square inch above actuator operating pressure requirements. This is accomplished by the main and standby regulating valve, which regulates main pump supply pressure to the metering valve at a level slightly above the higher of high and low pitch pressures as indicated by the shuttle selector valve. The pressure regulation coupled with the small pump size reduces pitch control power generation to the low levels required for most of the flight spectrum. A standby gear pump with approximately four times the capacity of the main pump circulates oil back to the pressurized sump at low pressure (low power) most of the time. When the beta metering valve is positioned for high flow (pitch rate), the regulating valve and standby check valve combine both the standby pump flow and the main pump flow, at high pressure, to provide the required high power. This is a transient condition, and heat generation is minimal.

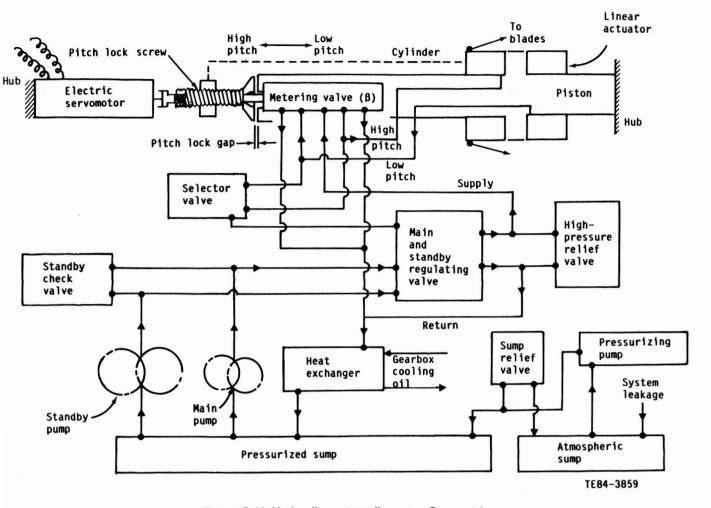


Figure G-10. Hydraulic system diagram—Concept 1.

A pitch control system pressure versus weight trade study showed that 6,000 lb/in.2 is the optimum pressure for minimum weight. However, 4,750 lb/in.2 was selected because it results in higher reliability and lower cost for a weight penalty less than 2% of pitch control weight. The pressurized sump is charged to 75 lb/in.2 minimum by a small scavenge pump on the atmospheric sump where system leakage collects. This pressure ensures that the main and standby high-speed pumps are adequately supplied with oil to prevent cavitation. A small oil-to-oil heat exchanger is mounted in the gearbox output shaft to provide cooling for oil returning to the pressurized sump. Cooling oil from the gearbox lube system is circulated through the gearbox side of the heat exchanger. An optional cooling configuration eliminates the heat exchanger and uses gearbox cooling oil to mix directly with pitch control oil and return filtered oil to the gearbox cooler.

The power module pumps and generator are driven by a high-speed shaft from the gearbox on the axis of rotation. The generator is a lightweight, samarium-cobalt, permanent magnet, externally commutated alternating current (ac) type; ac output is rectified to dc by the electronic control module.

Dual generator windings provide separate voltage supplies for pitch control and blade de-icing. An overrunning clutch is provided at the generator drive shaft to permit the generator to be powered as a motor for static ground operation of the pitch control. Auxiliary ground cart power supplied to the generator with the engine inoperative drives the pumps to develop pressurized oil for pitch change.

Electronic Control System

The electronic control module incorporates the printed circuit boards and solid-state components required to (a) provide control of the dc servomotor under pitch control command from the nacelle-mounted full authority digital EEC and from separate overspeed pitch control circuitry in the module, (b) transmit blade angle feedback and other diagnostic signals to the EEC, and (c) provide power switching for blade de-icing.

A rotary capacitor signal transfer module, located at the rear of the hub, transmits serial digital pitch control signals bidirectionally between the EEC and the rotating electronic control module. The transfer module contains two electrical paths. Each path consists of two parallel annular metal disks,

one on each side of the rotating interface, separated by an air gap.

Under normal operating conditions, the electronic control module provides only blade pitch control as commanded by the EEC. All intelligence for governing speed, Synchrophasing, feathering, reversing, and ground handling is located in the dual-channel EEC. This permits the more complex electronic control circuitry to be located in the stationary nacelle where it is more accessible for maintenance and for modification of control parameters. In the event of either an erroneous signal or loss of signal from the EEC, the electronic control module has a solid-state speed governor with separate power supply, circuitry, and speed sensor that will govern speed at a set percentage of normal speed. The flight may then continue with only the loss of Synchrophasing and reversing capability. Provision is made to conduct a preflight check of this backup control circuit.

Blade pitch angle change originates with a requirement and a command signal from the EEC to change pitch a discrete amount toward either high or low pitch. The signal is transmitted across the capacitor signal transfer module to the electronic control module, which powers the dc servomotor to rotate the pitch lock screw and translate the metering valve spool. Pressurized oil is metered to the actuator causing the cylinder screw and valve spool to translate in the opposite direction, thereby nulling the valve. The actuator cylinder will continue to move as long as the motor is rotating and the in-place pitch lock gap between the screw and ground toward low pitch is continuously maintained within 1 deg of blade angle (i.e., full metering valve authority is sustained within the pitch lock gap). Blade angle position is continuously measured by the RVDT and fed back to the control to terminate the signal when the commanded angle is reached.

Maintainability Features

The modular component design of pitch control Concept 1 satisfies the primary design objectives of minimum impact on the gearbox and maximum accessibility and maintainability for any gearbox configuration. After removal of the propfan spinner, the electronic control module can be easily removed by removing bolts from the mounting flange and then pulling the module forward on guide pins to release the plug-in wiring connectors. Removal of the dc servomotor mounting bolts permits the motor, RVDT, and associated reduction gearing to be removed as a unit. The hydraulic power module can be removed following removal of the conical control support housing, which is flange-mounted. The hydraulic power module is removed on guide dowels after removing the forward and rear mounting flange bolts. A lightweight hoist and lifting fixture is required for removal of the module. Flange bolts are trapped in the rear flange to facilitate reinstallation. Check valves are incorporated in the oil transfer tubes to seal against oil loss when disengaged from the heat exchanger. The heat exchanger, cooling oil tubes, and generator and pump drive shaft are accessible for removal and replacement from inside the hub.

Access is gained to the blade links and drive ring for inspection or maintenance action by removing the conical support housing from the hub at the bolted flange. The electronic control, dc motor, RVDT, and reduction gearing are mounted on this housing and do not need to be removed separately. Blades can also be removed and replaced, if required, due to foreign object damage, as follows: (a) disconnect the blade link at the trunnion arm, (b) disengage the de-icing brush assembly from the blade slip rings, (c) remove the external split clamp and lip seal from the hub, (d) move the blade into the hub a small distance and remove the retention bearing balls, self-contained in a flexible plastic retainer, and (e) remove the blade from the hub. The capacitor signal transfer module is fabricated in segments that are easily removed for replacement or repair.

It is possible to remove and replace all propfan components without removing the hub or gearbox from the aircraft. The extent to which this disassembly is performed on the aircraft must be decided by the user, but the capability exists.

Alternate Concepts

Pitch control Concepts 2 and 3 were considered as optional configurations compatible only with offset gearbox installations. A sectional drawing and a hydraulic system diagram for Concept 2 are presented in Figures G-11 and G-12, respectively. The system functions basically the same as Concept 1 with the links, drive ring, actuator, pitch lock, metering valve, selector valve, and generator located within the propfan hub. The primary difference is in the location of the hydraulic power module and electronic control module, which are mounted in the nacelle on the rear face of the gearbox on the axis of rotation. These modules are readily accessible, impose minor impact on the gearbox, and significantly reduce the number of components mounted in the rotating hub.

Three inputs are required from the rear of the gearbox to the propfan across the rotating interface: (a) high-pressure oil supply to the metering valve, (b) rotary mechanical input to the pitch lock screw, and (c) a high-speed generator drive shaft. The high-pressure oil supply is delivered from the pumps to the metering valve through a small-diameter transfer bearing and a transfer tube rotating at propfan speed. A separate concentric tube transmits selector valve reference pressure through the transfer bearing from the actuator to the regulating valve in the power module. The electronic control module transmits a pitch control command to the pitch lock screw by sending an electrical signal to an electrohydraulic valve (EHV), which meters pressurized oil to a servo piston that translates a bearing

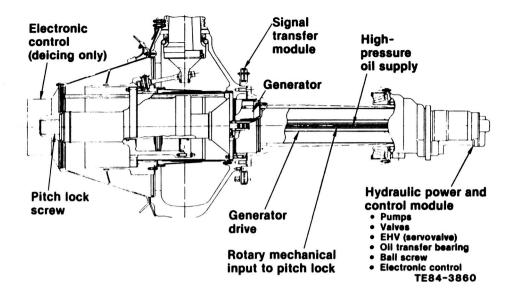


Figure G-11. Pitch control—Concept 2.

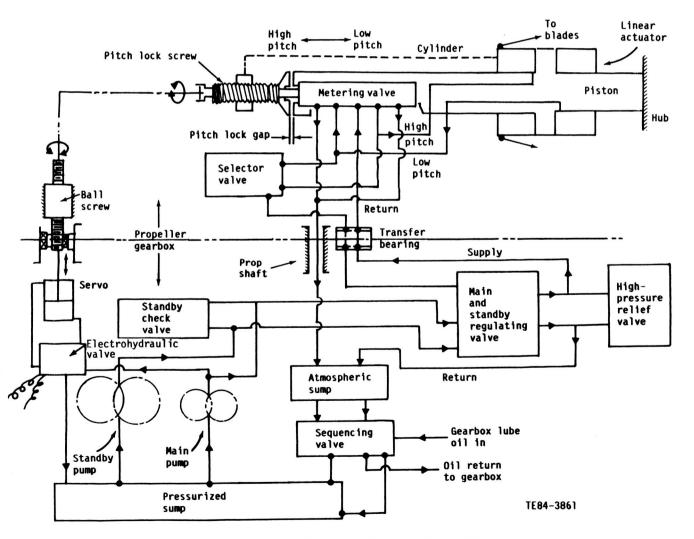


Figure G-12. Hydraulic system diagram—Concept 2.

mounted ball screw, thus providing rotary mechanical input to the pitch lock screw. An LVPT measures blade angle from servo piston position and transmits it to the electronic control and EEC. The generator drive shaft is driven through compound speed increaser gearing from the gearbox output shaft to the propfan. Generator power is used only for blade de-icing and is distributed by solid-state power switching located in the forward-mounted electronic control (de-icing only). The capacitor signal transfer module is used only for transmitting de-icing on/off signals to the on-board de-icing system.

A common oil system is achieved by providing pitch control oil to the power module from the gearbox lube system. Filtration is provided in each system, and a sequence valve in the power module seals off sufficient oil in the module sumps to maintain pitch control in the event of a lube system failure. Oil cooling is unavailable during this failure condition, but pitch control can easily be sustained for as long as the gearbox can operate in this condition.

Concept 3 is configured with similarities to both Concepts 1 and 2, as shown in Figures G-13 and G-14. It is most similar to Concept 1 except that the pressurized oil is supplied to the metering valve from the hydraulic power module (pumps, valves, and oil transfer bearing) located at the rear face of the gearbox. This makes the power module more accessible for maintenance and utilizes the gearbox cooler for heat rejection. Concept 2 not only mounts the hydraulic

power module at the rear of the gearbox, as in Concept 3, but also locates the electromechanical input to the metering valve and the electronic control module there.

A comparative evaluation of the three concepts was made to select the best offset gearbox installation. The same evaluation parameters and rating system used in the earlier trade studies were used for this evaluation. Table G-V shows a relative evaluation of the three concepts, one to another, based on parameters listed in order of decreasing criticality. The concepts were rated equal for safety, reliability, and cost, and therefore these parameters are not included in the table. Concept 2 rated lowest, primarily on weight, performance, and envelope. The large power module, including the rotary mechanical input drive mechanism, mounted on the rear of the gearbox could interfere with the engine air inlet duct and has limited installation space. The remote rotary mechanical input to the pitch lock results in additional weight and hysteresis. Concepts 1 and 3 rated essentially the same, with Concept 3 rating slightly higher based on better maintainability. The hydraulic power module is more accessible and more easily maintained as a separate unit when mounted on the rear of the gearbox. Concept 3 was therefore selected for this offset gearbox installation, and the components are indicated by the shaded boxes in the power matrix of Figure G-15. Earlier trade study results selected Concept 1 as the preferred linear hydraulic system, and that selection is still valid for an in-line gearbox installation.

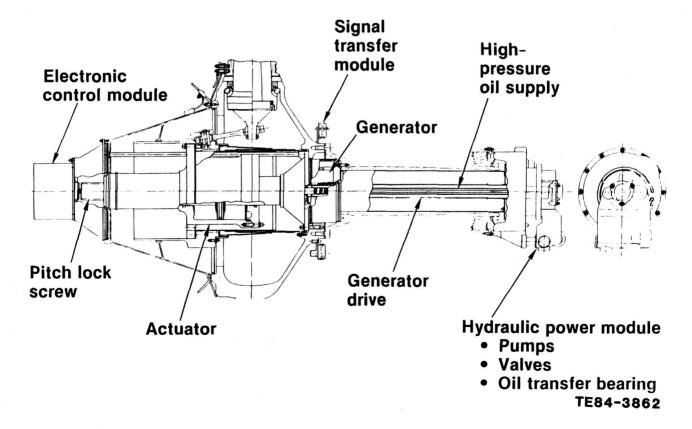


Figure G-13. Pitch control—Concept 3.

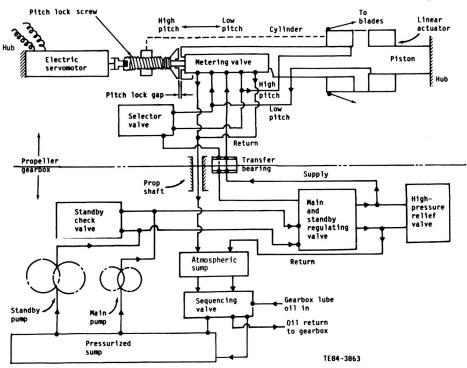


Figure G-14. Hydraulic system diagram—Concept 3.

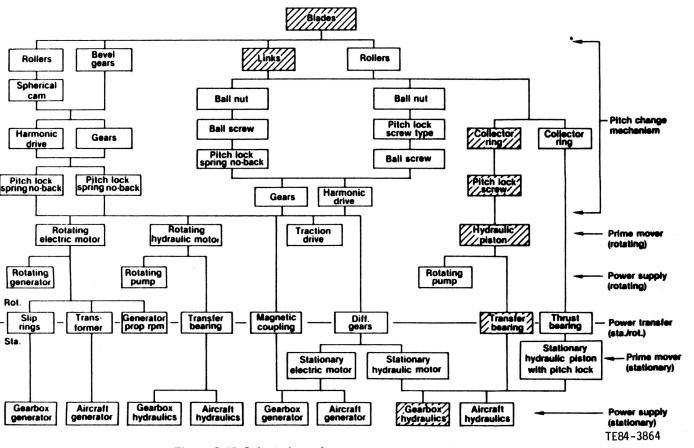


Figure G-15. Selected propfan power system for offset gearbox.

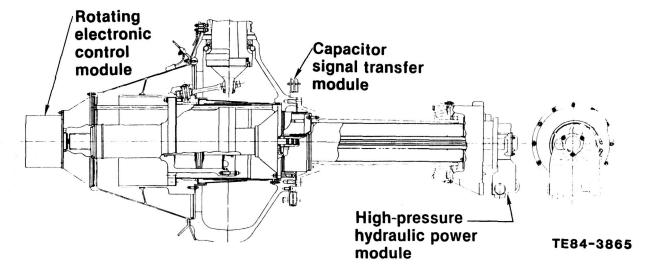


Figure G-16. Advanced technology components requiring additional development.

Table G-V.
Pitch control concept evaluation.

	Concept			
Parameter	1	2	_3_	
Maintainability	-	-	+	
Weight	+	-	+	
Performance	+	-	+	
Impact on gearbox	+	-	-	
Technical risk	-	+	-	
Envelope	+	-	+	
Heat generation	+	-	+	

Technology for the three components shown in Figure G-16 is not completely developed for an advanced propfan application. An efficient shielding system against EMI must be developed for the rotary capacitor signal transfer module. Electronic control components must be mounted and packaged in the module to withstand the G-field environment of the rotating propfan (approximately 40 G's per inch of radius from the axis of rotation). Hydraulic gear pumps must be developed for the high-speed, high-pressure application of the power module. A detailed description of the technology development required for the three components is provided in the technology plan (see Appendix H).

Pitch Control Parameters

The primary propfan design parameters used in the conceptual design of the advanced technology pitch control were blade pitch slew rates, blade angles, and blade twisting moments. These are presented in the following sections.

Slew Rates

Blade pitch slew rate requirements for various propfan operating conditions are shown in Table G-VI. Normal slew

rate requirements for most of the flight spectrum are low. Blade pitch angle is held essentially constant at each flight condition with small excursions of less than ± 0.1 deg during Synchrophasing.

The maximum slew rate is normally set by the aircraft requirements based on the time to reach the full reverse angle on landing. The rates shown are based on the capability to fully reverse from flight idle in three seconds. These rates are judged to be satisfactory for advanced turbuprop propulsion systems. However, different rate requirements can be easily satisfied with minor changes to the pitch control.

Table G-VI. Slew rates.

Condition	Blade pitch rate (deg/sec)
Normal control	0-3
Synchrophasing	0-1
Feathering	15
Reversing	15
Ground operation	
(engine inoperative)	0-3

Blade Pitch Angle Settings

The blade angle settings are given in Table G-VII for various operating conditions. Angles are specified at the blade 3/4 radius. Allison finds that the engine can start with the blades at any angle, including feather. The mimimum propfan torque blade angle is therefore somewhat academic for this propulsion system. Emergency blade angles are set by the mechanical in-place pitch lock, which follows approximately 1 deg below any commanded blade angle.

Table G-VII. Blade angle settings.

Condition	β3/4 (deg)
Takeoff (0 M _N)	+ 30
Maximum climb (0.2 (M _N))	+ 36
Cruise (0.72 M _N)	+ 54
Flight idle (0.3 M _N)	+ 37
Maximum reverse	- 7
Feather	+ 85
Minimum propfan torque	
(static conditions)	0
Emergencies	1 below β setting when condition occurs

Blade Twisting Moment

The pitch control system must be capable of rotating the blades about the pitch axis, counteracting the total blade twisting moment. The total moment consists of the following individual twisting moments: (1) centrifugal, acting toward flat pitch, (2) aerodynamic, acting toward either high or low pitch depending on the flight condition, and (3) friction, acting to impede motion toward either high or low pitch. Centrifugal twisting moment results from centrifugal forces on the blade mass as a function of distance from the pitch axis and makes up most of the total moment. Highly swept propfan blades have significantly higher twisting moments than more conventional blades with less sweep because of the increase in overhang from the pitch axis.

The maximum total blade twisting moment that the pitch control must overcome to move 10 blades toward high pitch is 474,000 in-lb. The maximum total twisting moment required to hold the blades in position is slightly less than this value due to exclusion of the friction moment. It is this reduced moment that the pitch control or the pitch lock must react to hold the blades at a fixed blade angle setting.

Weight

Results of a weight analysis conducted on the pitch control conceptual design were compared with the data base referenced in Table A-XI on page A-8. The net result is a 4% reduction in total propfan weight. This reduction is attributable to the advanced technology pitch control design concept, since the weight of the remainder of the propfan parts is the same as the data base reference.

RELIABILITY

A component failure rate and unscheduled removal rate analysis was performed for all the pitch control modules. These rates were then added to the respective rates of the remaining propfan hardware to arrive at the total propfan system rates.

Failure rate is defined as any event chargeable to the hardware. Removal rates include additional nonchargeable events such as maintenance damage, unsubstantiated removals (no failures), and accident and foreign object damage (where applicable), in addition to the chargeable removal rates. The mean time between unscheduled removals (MTBUR) for all causes is the inverse of the total removal rate.

The MTBUR of 5200 hr for the advanced technology propfan system is derived in Table G-VIII. It is based on propfan assembly removals as well as removals of replaceable components such as the electronic control, hydraulic power module, electric motor module, actuator, and spinner.

Table G-VIII.
Unscheduled removals (all causes).

Component		Removal rate (events/ 1000 flight hours)
Spinner		0.0086
Disk and aft fairing		0.0029
Blades		0.0530
Forward cover and fairing		0.0055
Electronic control module		0.0490
Actuator module		0.0293
Motor module		0.0124
Hydraulic power module		0.0241
Capacitor coupling		0.0002
Nonmodular components		0.0069
	Total	0.1919

MTBUR = (1/0.1919)(1000) = 5200 hr

This MTBUR represents an improvement of 93% over the 2700 hr MTBUR for the baseline propfan system defined in NASA report CR 135192, "Study of Turboprop Systems Reliability and Maintenance Costs," June 1978, Table 4.4-I, page 231. Baseline removal rates were revised for 10 blades instead of 8 to compare with the advanced technology propfan system.

The predicted MTBUR (chargeable events) of 28,700 hr for the advanced technology propfan system is based on those failures that require removal of the entire propfan assembly. This represents a 56% improvement over the 18,400 hr for the baseline propfan system. The increase in MTBUR is a result of the high reliability of the individual components in the advanced pitch control system.

MAINTENANCE COST

Maintenance costs for the advanced technology pitch change system were estimated using an on-condition philos-

ophy established for the propfan. This philosophy, which is in line with present day turboprop field service experience, involves repair or replacement of only the faulty module as determined by built-in health monitoring diagnostics.

The maintenance cost was developed for the 10-bladed, 12.78-ft-diameter propfan by considering all the elements of maintenance, which follow:

- scheduled inspections
- scheduled line repairs
- scheduled removals

Scheduled inspections consist of four basic checks: a routine walk-around check performed a minimum of every 10 flight hr; a line check performed approximately every 35 hr; a base check performed approximately every 1,000 hr (which can be made to coincide with the periodic check of the engine or aircraft); and a major check performed approximately every 18 months (about 4,500 operating hr) to coincide with a major shop aircraft check. Unscheduled maintenance includes blade repairs on the line and unscheduled removals of major components such as the spinner, disc and aft fairing, pitch change modules, blades, and forward cover and fairing. A significant factor in the maintenance cost of the propfan hardware is the design philosophy used at Hamilton Standard. This philosophy includes designing both the propfan blade and hub for infinite life. Consequently, these items will require replacement only in the event of an accident or significant foreign object damage. Blades are repairable for all foreign object damage except spar damage. Therefore, there will be no life limit on major parts, and, accordingly, maintenance costs associated with scrap will be low. Another design characteristic is the absence of major components that will be subjected to replacement due to wearing out. Periodic replacement of the few secondary parts subject to wear is not a significant contributor to maintenance cost.

Maintenance cost estimates for the unscheduled removals of the propfan system were obtained by adding costs for removals of all the advanced technology pitch change modules to maintenance costs of the spinner, blades, disc, and fairing. Costs for unscheduled removals reflect both line manpower and shop costs to repair the faulty component.

The maintenance cost projections for the advanced turboprop propulsion system were generated by multiplying the Hamilton Standard Operations Effectiveness Group's line and shop labor cost estimates (converted to dollars using 1984 fully burdened labor rates) and material charges per maintenance action by the corresponding rate of maintenance action or repair.

Parts cost per event were developed using estimated acquisition costs and historical data relating per repair material costs to acquisition costs on a percentage basis. The propfan acquisition costs were developed by the Cost Engineering Group based on analysis of the hardware as defined on the concept drawings and the developed parts list. The analyses use standard techniques for estimating production hardware costs, including comparisons with costs for similar parts currently in production. The maintenance manhours per 1,000 flight hr include both scheduled inspections and all unscheduled maintenance and are based on fully burdened labor rates. The parts cost assumes 1984 economy and includes all unscheduled maintenance. Based on the maintenance philosophy established by Hamilton Standard for the propfan system, all unscheduled actions have been accounted for. This includes maintenance actions where hardware is removed as well as actions where repair is accomplished on the aircraft.

The total maintenance cost for the advanced technology propfan system represents a 15% decrease from the baseline propfan system maintenance cost referenced in Table A-XII on page A-10. Baseline costs were escalated for the 1984 economy. The lower maintenance cost of the advanced system results primarily from a reduction in the frequency of maintenance actions.

ACQUISITION COST

The acquisition cost for the advanced technology propfan system is approximately 7% less than for the baseline propfan system. Acquisition cost estimates were developed as described in the section on maintenance costs.

APPENDIX H

TASK IX. RESEARCH AND TECHNOLOGY PLAN FOR TASKS VII AND VIII

TABLE OF CONTENTS

Title Title	Page
ntroduction	 H-1
ingle-Rotation Gearbox Technology Plan	 H-2
Gear and Bearing Material	
Gear and Bearing Manufacturing Processes	 H-4
High Contact Ratio Gearing	 H-7
Tapered Roller Bearing-Powder Metal Rib	 H-8
Lubrication System	 H-9
Housing	 H-11
Single-Rotation Gearbox Technology Plan Schedule	H-14
ingle-Rotation Pitch Control and Mechanism Technology Plan	
References	

LIST OF TABLES

Table	Title	Page
H-I	Design allowables for SiC particulate MMCs	. H-13
H-II	Comparison of Model 250-C30 front housing gearbox materials in terms of required	
	wall thickness, weight, and cost	. H-10

INTRODUCTION

Both the single-rotation gearbox and pitch change system designs have incorporated advanced technology features that are not yet demonstrated or verified for the conditions encountered in a propfan propulsion system. Since the first production of these systems is intended to be in the early 1990s, advanced technology issues would need to be verified during the late 1980s before finalizing production designs. The objective of Appendix H is to present the specific advanced technologies applied in the designs.

SINGLE-ROTATION GEARBOX TECHNOLOGY PLAN

This study has attempted to quantify the benefits of incorporating advanced technology in future commercial gearboxes. This has been accomplished by comparing the preliminary design results of a state-of-the-art and an advanced technology gearbox. The gearbox technology areas are discussed on four component levels:

- 1. gears
 - materials
 - manufacturing processes
 - high contact ratio
- 2. bearings
 - materials
 - manufacturing processes
 - tapered roller—powder metal flange
- 3. lubrication system
 - modulated flow
 - higher temperature—rise and level
 - new oils
 - finer filtration
- 4. housings-composite

In this section, the background, benefits, and recommended technology plan regarding each of these technology items are discussed.

GEAR AND BEARING MATERIAL

Background

AMS 6265 (AISI 9310) steel has been used to meet gearing material requirements for the majority of Allison's gearbox designs. New gear materials will be needed if technology is to be advanced in future gearboxes. Materials such as Vasco X2, Pyrowear 53, and CBS 600 have demonstrated some advantages over AMS 6265 in component testing. The major focus with many of these materials has been in the area of improved hot hardness for oil-off capability. Some of these materials have also demonstrated life improvements in limited testing. Greater improvements are needed to meet the goals that have been established in this study for the advanced technology gearbox.

The following requirements offer the greatest potential for gear materials:

- high hot hardness
- increased allowable stresses/improved fatigue life

These requirements must be met without sacrificing the beneficial properties that AMS 6265 has demonstrated, such as good fracture toughness, machinability, hardenability, and scuff/wear resistance. AMS 6265 has been relatively free of corrosion problems in Allison gearing applications, although this material is not classified as cor-

rosion-resistant. Any new material must have this corrosion-resistant property.

Both powder metal steel and wrought low-carbon steels will be evaluated in this program. Powder metal steels have the potential to meet all the advanced gear requirements assumed in the preliminary design.

The powder will be processed by a VIM/VAR process followed by a rapid solidification operation. Steel is double vacuum melted and then dropped in the liquid state onto a rotating chill roll, which rapidly solidifies the steel and slings it into a pulverizer. The pulverizer converts the steel to a fine powder that is segregated with respect to size by passing it through a mesh. The powder is to be reduced to a 200-270 mesh powder in this program. Steels such as Pyrowear 53 and CBS 600 have demonstrated fatigue life and hot hardness improvements over AMS 6265. Clean melted versions of these steels will be included in this program.

Traditional aircraft bearing materials primarily consist of intermediate carbon (0.5%-1.0%) through hardening type steels. VIM/VAR M50 (AMS 6491) steel fits this classification and has been used in a major portion of gearbox bearing applications. M50 has demonstrated properties, such as fatigue strength, that are far superior to other types of steels. However, M50 is also deficient in a number of properties. Corrosion resistance and low fracture toughness have been a problem for this type of steel.

The low fracture toughness properties are primarily due to the through-hardened condition of these steels. The low fracture toughness leads to race fractures, which are catastrophic type failures. The race fracture is initiated by spalling or pitting. Only a relatively small spall or pit is needed to reach a critical crack size for this material. Upon reaching the critical crack size, race fracture progresses rapidly. Intermediate carbon-level steels with better fracture toughness properties obtained through improved manufacturing processing or chemistry changes are needed.

Corrosion has also been a significant problem for these bearing materials. In a number of gearbox bearing locations, corrosion has been the primary problem. Therefore, more corrosion resistance is needed in advanced bearing materials.

Various steels that are corrosion resistant or have good fracture toughness have been examined. While these materials demonstrated excellent results in the corrosion and/or fracture toughness areas, they exhibited deficiencies in areas such as fatigue (spall) strength. Thus, compromises in material properties are required in the selection of current bearing materials. The goal is to develop a bearing material that avoids these compromises for future gear-boxes.

The bearing material properties that will provide the greatest improvements for the advanced technology gear-box are as follows:

- improved fatigue strength
- improved corrosion resistance
- improved fracture toughness
- equivalent hot hardness

As with gear materials, powder metal steels have the potential of meeting all these requirements without compromises. The powder would be processed as outlined for gears:

- VIM/VAR melting
- rapid solidification
- pulverizing to 200-270 mesh powder

Benefits

Most powder metal work has been done with air melt processed steels. In this program, cleaner melt steels, such as VIM/VAR, will be used in the rapid solidification process to further improve fatigue life. The cleaner steels improve fatigue life by greatly reducing nonmetallic inclusions, which serve as fatigue initiation sites.

The rapid solidification technique produces powder metals with much finer grain microstructures than conventionally processed steels. The grain size throughout a powder particle is also very uniform due to rapid solidification. This fine uniform grain microstructure provides fatigue life improvements. The fine grains impede slip band progressions that result in fatigue failures.

The rapid solidification process will be conducted in a protective atmosphere. The atmosphere is needed to protect the powder from oxidation contamination, which reduces fatigue life.

Powder metal materials also provide a more homogeneous and finer carbide microstructure. In wrought steels with the carbon levels proposed (0.5%-1.0%), large carbides limit the steel's performance. These carbides are very brittle and clump together throughout the finished part. If these large carbide stringers form in highly stressed regions, early fatigue can result. The large carbides also make it difficult to obtain the surface finish goals selected for future gears and bearings. These large carbides tend to pull out at machined surfaces, degrading surface finish. Powder metal parts, however, could be machined to much better surface finishes because of the finer carbides. Also, any nonmetallic inclusions are more evenly dispersed in the microstructure of the final part, reducing the likelihood of stringer formations that could lead to fatigue.

By eliminating the large carbides in powder metals, more carbon is available for saturation of the martensite. Thus, the potential for higher hardnesses is present. The higher hardnesses should provide better fatigue strengths and wear resistance.

Powder metal also will provide metal chemistries that are not obtainable in conventionally wrought materials. For example, a higher percentage of vanadium can be used in powder steels than in conventionally wrought steels. Vanadium content is limited in conventional steels due to problems caused by vanadium carbide segregation. Large carbide clusters are very brittle and lead to early fatigue failures. Higher vanadium content can be used in powder metals since the small powder sizes limit carbide size and provide more uniform carbide distribution.

The ability to process new chemistries provides the potential for improved material properties. For the above example, higher vanadium content will provide higher hardnesses and better hot hardness since the vanadium tempers out during the heat treat cycle.

More flexibility in steel chemistry selection provides a better opportunity for developing a steel that provides all the properties desired for future materials. Conventional wrought steels do not have this flexibility, and thus property compromises are required.

Materials Plan

The objective of this program is to develop, test, and select steel chemistries with the following improvements and equivalent properties relative to AISI 9130 for gears and M50 for bearings:

- gears
 - improved fatigue properties
 - high hot hardness
 - equivalent properties
 - scuff/wear resistance
 - fracture toughness
 - corrosion resistance
 - manufacturing processibility
- bearings
 - improved fatigue strength
 - improved corrosion resistance
 - improved fracture toughness
 - improved microdamage tolerance
 - equivalent hot hardness

In the material selection phase, six powder metal chemistries, such as MRC 2001, D6AC, and M50, will be selected. These steel chemistries will be in the 0.5%-1.0% carbon range to allow heat treatment with the Allison advanced induction hardening technique. These chemistries will be melted by a VIM/VAR process. The melted steel will be rapidly solidified and pulverized to powder sizes in the 200-270 mesh size.

The powder will be consolidated into ingots of 100% density using a hot isostatic pressing process. Test specimens will be fabricated from the ingot. These specimens will be conventionally heat treated for use in the following tests:

Jominy (hardenability)

- Izod (fracture toughness)
- hot hardness
- tensile
- corrosion
- metallography investigation

GEAR AND BEARING MANUFACTURING PROCESSES

Background

A number of benefits can be realized through improved gear and bearing manufacturing techniques. The techniques being proposed consist of the following:

- hot isostatic pressing—gears and bearings
- hot forging to near net shape—gears
- advanced contour induction hardening—gears and bearings
- ultrasmooth surface finishing—gears and bearings
- ion implantation—gears

Hot isostatic pressing is used to consolidate powder metals. In this process a powder metal is sealed in a disposable container. The powder container is placed in a sealed chamber, which is pressurized by a gas to consolidate the powder. The container is shaped to provide a consolidated preform requiring fewer post-machining steps than would be required for a wrought part. The density of the consolidated preform is 100%.

The hot forging process is used to convert a powder metal preform or a wrought blank to a near net shape part. Dies shaped to the desired final part configuration are used to meet this objective. A preform or blank is heated to approximately 2000 °F and placed in heated forging dies. The preform or blank is subsequently compressed by the dies to near net shape. Some grinding stock will be provided on the tooth flanks.

Allison is currently involved in the development of an advanced induction hardening technique. This technique has demonstrated the ability to harden gear teeth surfaces, with resulting uniform case depths and fast heat treat cycle times. The same technique can also be used to harden bearing races.

Improved finishing techniques will provide improved surface finishes. Improved gear profile finishes will be provided by better grinding, shot peening, and honing methods. Improved bearing race finishes will be provided by better grinding and lapping methods.

Ion implantation techniques are used to implant ions such as Ta⁺ and Mo⁺ into the surface layers of steels. The implantation method involves the use of a current implanter, which uses a beam to raster the ions onto the steel surface.

Benefits

The hot isostatic press process provides powder metal preforms that are 100% dense and are closer to final part shape than is obtainable with conventional wrought processing. Density of 100% is required to ensure optimum fatigue strength. Providing a near net shape preform thus eliminates a number of machining steps required in conventional wrought processing. These reduced steps provide cost reductions.

Hot forging to near net shape provides both gear cost savings and potential gear performance improvements. The cost savings result from the elimination of processing steps such as hobbing. At the current technology level, the forged parts would require grinding and honing of gear teeth to provide aircraft-quality gears. However, with technology improvements it may be possible to eliminate some or all of these finishing steps. Cost savings are also realized through better use of the raw material. Material isn't wasted through chip scrap.

The gear performance improvements are a result of the ideal forging flow patterns that this process produces. Current forged gears are processed from forged blanks. When the teeth are hobbed, the flow lines are severed, and the resulting flow pattern is not the optimum desired. With hot forging, the teeth are forged to net shape, and the resulting flow lines are parallel to the free surfaces, which is the preferred orientation. This improved flow pattern should result in fatigue life improvements.

The advanced induction hardening process offers a number of gear and bearing improvements. These improvements include the following:

- better fracture toughness for intermediate carbon steels
- cost savings
- better surface durability (spall) life due to better residual compressive stresses
- less part distortion

Traditional aircraft gear materials are composed of low carbon type steels. Intermediate carbon steels (0.5%-1.0%) have been avoided due to their low fracture toughness properties. The low fracture toughness is primarily a result of the through-hardened condition of these steels. The fracture toughness could be greatly improved if the core could be left at a lower hardness level while the case was fully hardened. Lasers and electron beam heat treatment methods have focused on this goal in recent work. Allison has developed a contour induction hardening technique that also meets these goals while avoiding the difficulties that have been encountered in the laser and electron beam methods, such as special atmospheres for lasers, beam directing/raster pattern development complexities, high capital costs, and high reflectivity associated with beam heating.

Bearings will also benefit from the contour induction hardening process by eliminating the race cracking prob-

lems that have occurred in some gearbox applications. As stated previously, the race cracking is caused by low fracture toughness properties. Case hardening these steels with the induction hardening technique will improve fracture toughness and eliminate this problem.

This process also can provide a cost savings compared with carburizing. Aircraft gears are normally selectively carburized. Only areas requiring a fully hardened surface, such as gear teeth, are carburized and hardened. Areas not to be carburized must be protected from the carbon atmosphere with maskings, such as copper plating. This time-consuming process can be eliminated with the contour induction hardening process, resulting in a cost savings. Other savings associated with this process, in addition to labor, include energy, facilities floor space, and cycle time.

Contour-hardened gears have also demonstrated a better residual stress condition when compared with carburized gears. Carburized residual compressive stresses have been shown to peak near the surface and quickly reduce in magnitude with increasing depth beneath the surface. Contour-hardened gears have been shown to maintain equivalent to better compressive stresses near the surface with very little magnitude reduction at points as deep as 0.007 in. below the surface. This property should result in improved surface fatigue life. The improved life is a result of the improved stress condition in the fatigue initiation region. This region is normally located in the maximum shear stress region, which is below the free surface. The same benefits are expected in bearings.

Lastly, the contour-hardening process has demonstrated a much lower part distortion level compared with carburizing. The lower distortion levels reduce grinding cycle times and part scrap.

Improved surface finishes offer potential for life improvements. Better finishes improve the lubrication film thickness to surface asperity height relationship. This relationship is normally expressed as the ratio of the film thickness to the composite surface finish and is known as the lambda ratio. Testing has shown that improvements in the lambda ratio result in an improvement in fatigue life in the lambda ratio regime that applies to the components in this study.

lon implantation techniques offer gear efficiency improvement potential. Implantation of Ta⁺ and Mo⁺ ions into AISI 9310 has demonstrated a 30% reduction in the coefficient of friction in tests run in a no-lubrication environment.

It is anticipated that ion-implanted gear teeth would also demonstrate a lower coefficient of friction for gear meshes in typical lubricated aircraft gearbox environments. Lambda ratios less than two are typical for many aircraft gear sets. In this study the lambda ratio was less than one. For these types of lambda ratio (lambda ratio <2) and in this type of lubrication regime where some metal to

metal contact exists, the performance of the tooth pair is very sensitive to the condition of the tooth surfaces. Therefore, ion-implanted gear teeth should show a reduction in heat generation with a corresponding improvement in gear efficiency.

Surface finish improvements offer fatigue life improvements and efficiency improvements. As it has been shown, predicted fatigue life improvements range anywhere from 15% to 2200% for this study. The slow speed gears and bearings would theoretically benefit the most. This is because the film thickness to composite surface finish ratio is the lowest for these components. Small ratio changes in this regime result in large life changes. Surface finish improvements also should provide gear efficiency improvements. The improved surface finish should lower frictional forces between teeth in the elastohydrodynamic lubrication regime.

Gear and Bearing Manufacturing Process Plan

The following program is recommended to develop processes for application to gear and bearing fabrication. Development of these fabrication methods will be targeted for commercial application into full-scale gearboxes by the early 1990s. The following processes are to be developed:

- hot isostatic pressing—gears and bearings
- hot forging to near net shape—gears
- advanced contour induction hardening—gears and bearings
- ultrasmooth surface finishing—gears and bearings
- ion implantation—gears

Material Selection

The first step in this program will be material selection. AMS 6265 (AISI 9310) and M50 will be used as a baseline for comparison purposes. Five other materials will also be selected and tested. These materials will consist of three intermediate carbon level (0.5%-1.0%) steels and two low carbon level (0.1%-0.2%) steels. Two options are available in the selection of the intermediate carbon level steel. If the proposed powder metal program is undertaken, the steel will be selected from this work. Otherwise three steels such as M50 or D6AC will be selected from a current in-house screening program. The low carbon steel will be selected from the proposed material screening program consisting of materials such as CBS 600 and Pyrowear 53. The contour induction hardening technique cannot be used for the lower carbon steels, and carburizing will be used on these materials.

Hot Isostatic Press

The objective of this phase will be to develop a hot isostatic press process for manufacturing powder metal gear and bearing preforms and test specimens. The preforms and specimens will be hot isostatic pressed to 100% density. No major obstacles are anticipated in this phase since hot isostatic press technology is well beyond the infancy stage. The test specimens will be taken from a hot isostatic pressed ingot. A ceramic container will be developed to provide the desired consolidated preform shape for the hardware items. An inert gas will be used to develop consolidation pressures in the vicinity of 15,000 lb/in.². Dwell times of approximately 4 hr with a peak cycle temperature of approximately 1900 °F-2075 °F will be used. The hot isostatic press equipment needed for this work is available outside of Allison. Use of this equipment will be pursued on a subcontract basis.

Hot Forging to Near Net Shape

The objective of this phase is to develop a hot forging process that provides parts requiring minimal finishing processes. Powder metal preforms and/or wrought blanks would be required for this phase. Dies will be developed for test specimens and for full-scale hardware. No major problems are anticipated for processing test specimens.

Some challenges are anticipated for processing full-scale hardware. Selection of adequate die lubricants and selection of optimum die pressures, temperatures, and dwell times have posed problems in the past. When excessively high temperatures and pressures have been attempted, ejection of the part from the die has posed a problem. When the temperatures and pressures have been too low, 100% die fill has been a problem. Better die lubricants will be needed to ensure ejection. Therefore, this phase will require effort in finding an adequate die lubricant and determining the optimum forging parameters to ensure proper die fill and part ejection.

The forging equipment needed for this program is available from outside sources. Use of this equipment will be pursued on a subcontract basis. Dies will also be fabricated outside Allison.

Advanced Contour Induction Hardening

The objective of this phase is to develop a contour induction hardening technique that provides a uniformly hardened case and low part distortion in intermediate carbon level steels. Allison currently has the induction hardening equipment needed for this program.

Fabricated test gears and test bearing components will be induction hardened. The case hardness gradient in the root and profiles of the gears and races and roller/balls of the bearings will be examined. The process parameters, primarily the heating levels and heating dwell times, will be varied to determine the optimum settings. Full-scale and test gear and bearing hardware will be heat treated and tested following the process cycle development phase.

Ultrasmooth Surface Finishing

The objective of this phase is to develop a cost-effective finishing process that provides parts with surface finishes that are 40%-50% better than finishes produced on current production gears and bearings. Current production gears are produced with finishes of 0.000025 in. peak-to-valley (approximately 10μ in arithmetic average [AA]). The goal would be to produce gears with finishes of 0.000015 in. peak-to-valley (approximately 6μ in AA). Current gear finishing practice is a three-part process. Gears are normally full-form ground by a single grinding wheel. The grinding process is followed by shot peening the roots and profiles twice. Finally, the profiles are honed by a fine grit hone.

Current production bearings are produced with finishes of approximately 6 AA for races and 3 AA for balls and rollers. These finishes are produced by a grinding operation followed by a honing operation. To improve the surface finish beyond the 0.000025 in. peak-to-valley for gears and the 6 AA/3 AA for bearings will require a process development program. A number of manufacturing process changes offer potential improvements. These changes will focus on grinding, honing, coolants, and grit materials for the gears and bearings. Shot peening changes will also be explored for gears.

Improving the after-grind finish should provide a better finish for the honing step. Thus, finer grit hones could be used to provide better surface finishes without increasing hone cycle time. Improving after-shot-peen surface finishes also offers potential for improving the final finish. The after-peen finish could be improved with finer, more uniform shot and/or reduced shot intensity. This again would allow finer grit hones to be used without increasing hone cycle times.

Modifying the hone procedure could provide surface finish benefits. The use of a coarse grit hone followed by a fine grit hone could provide benefits.

Coolants used during the grind process also affect finishes. Various coolants will be used during the grind process and their effects on surface finish evaluated.

Finally, investigating new grinding wheel and hone grit materials may offer improvements. Materials such as Borazon will be used and their effects on surface finish evaluated.

The program will consist of modifying one parameter at a time in the current manufacturing process. Surface finish will be measured after each process step to determine the benefits of each process change. Gears and bearings will be fabricated, tested, and compared with the current baseline to quantify benefits.

Ion Implantation

The objective of this phase will be to ion implant gear teeth and verify efficiency and scoring/scuffing improve-

ments. Erdco test gears will be fabricated and implanted with ions such as Ta⁺ and Mo⁺. The Erdco test head will be insulated, and oil flow and oil temperature rise will be measured to determine the efficiency improvements. The scoring/scuffing test will be conducted according to the standard ASTM D1947 procedure.

Gear Testing

These processes will be evaluated through a testing program. Test gears will be fabricated using the materials and manufacturing processes discussed. These gears will be evaluated in the following tests:

- efficiency test—modified Erdco rig
- scuff test—Erdco rig
- spall life test—Erdco rig
- single-tooth bending test—shaker rig

Specimens will be fabricated to provide 20 data points for all testing except the efficienty test. Three sets of specimens will be provided for the efficiency test. The test results will be compared with an AMS 6265 (AISI 9310) baseline.

The test results will be used to select one material for full-scale hardware development. These tests will also be used to quantify the benefits offered by the proposed manufacturing processes. Those processes demonstrating significant benefits will be developed for fabrication of full-scale gears. The full-scale hardware will be evaluated in back-to-back gearbox testing. This full-scale development work and testing is aimed at identifying problems associated with the increased gear size and operating in an actual gearbox environment.

Bearing Testing

The bearing manufacturing processes will be evaluated through a testing program. Test balls and rolling contact specimens will be fabricated using the materials and manufacturing processes discussed. The test specimens will be evaluated in the spall life test, which involves three ball tester balls and rolling contact tester rolls.

Specimens will be fabricated to provide 20 data points for each type of test.

The test results will be used to select one material for full-scale hardware development and to quantify the benefits offered by the proposed manufacturing processes.

The full-scale hardware will be tested in a bearing rig. Three types of bearings will be tested. Five tests of each bearing type will be conducted. The bearing types that will be tested are cylindrical roller bearings, tapered roller bearings, and ball bearings. The M50 bearings will also be tested for a baseline comparison. Following successful rig testing, full-scale bearings will be tested in a back-to-back gearbox rig.

HIGH CONTACT RATIO GEARING

Background

Aircraft gearing has traditionally been designed for low contact ratio (LCR). The contact ratios (CRs) of most Allison gearing are in the 1.2 to 1.4 range. Gears with a CR in this range spend a portion of time in the mesh cycle with one tooth pair carrying the full load.

High contact ratio (HCR) gears offer the potential for improvements over LCR designs. HCR gears are characterized by CRs greater than two. Stated another way, HCR gears operate with a minimum of two tooth pairs carrying the loads at all times during the meshing cycle.

HCR gears can be created in a number of ways. Finer pitches, lower pressure angles, and longer addendums can all be used to meet this objective.

Benefits

HCR gears offer the potential for smaller and lighter weight or higher reliability and life gear designs in comparison with LCR gears. The potential for lower noise levels is also offered by HCR gears.

The higher capacity inherent in HCR gear designs is due to the load sharing, which is a characteristic of these designs. Since a minimum of two tooth pairs are in contact at all times, the maximum load on each tooth is greatly reduced when compared with LCR gears. The reduced loads also lower the bending and crushing stresses, thus increasing the gear capacity. These capacity gains are counteracted slightly by the lower pressure angles, longer addendums, and finer pitches needed in these designs. However, the net result is a significant gain in gear capacity. Approaches such as buttressing also can be used to increase the capacity gains. The buttress design has a higher pressure angle on the coast side of the gear tooth than on the drive side. This approach improves the bending strength of the tooth.

Lower-noise gear designs are also important in today's environment. Because HCR gears have more teeth in contact at all times, a smoother transition between load sharing regimes (e.g., from two-tooth contact to three-tooth contact) occurs in comparison with LCR gears. The accelerations and decelerations associated with the transition from one regime to another are reduced, lowering the dynamic tooth loads and thus reducing noise.

This characteristic has not been satisfactorily demonstrated to date. However, this can probably be attributed to the need for more development and analysis work in the HCR gear design area. More effort in establishing optimum parametric settings, such as profile modifications, could provide the changes needed for satisfactory demonstration.

High Contact Ratio Gearing Plan

The objective of this program is to design, develop, test, and evaluate HCR spur and helical gear sets.

Design will be done using finite element methods. This approach provides the best method for defining tooth deflections, stresses, and the optimum profile modifications required. Both nonbuttress and buttress designs will be analyzed.

Test gears and full-scale gears will be fabricated. These gears will be fabricated using the beneficial processes developed in the manufacturing process program. If the process program is not funded, conventional forge, hob, shot peen, grind, and hone techniques will be used.

A tooth surface treatment program will be pursued if not undertaken in the manufacturing process program. One of the problems with HCR gears is their increased tendency to scuff and their high heat generation characteristics due to their increased sliding velocities. Developing treatments that provide low-friction, hard tooth surfaces should eliminate this tendency. Ion implantation and some of the new coatings offer the most potential for improvement. Gear pair flank surfaces will be implanted with ions such as Ta and Mo. These coatings have demonstrated the ability to reduce friction in some testing and therefore should reduce heat generation. Reducing heat generation increases oil film thickness and therefore scuffing tendency is also reduced. Gear pair flank surfaces will also be coated with hard coatings such as TiN. The hard coatings should increase scuffing resistance. These coatings should also provide lower friction coefficients and thus less heat generation. The treated gears will be tested in a scuff rig and an efficiency measurement rig. A fastresponse infrared radiometric microscope will also be used to measure temperatures along the tooth profile during operation. The treatment demonstrating the biggest gain will be used in the fatigue test.

Before testing, a profile modification development effort will be undertaken. This effort will consist of testing gears with various profile modifications. The optimum modification will be determined by measuring noise levels and examining tooth contact patterns. Noise levels will be compared with a standard LCR set to quantify benefits.

Spalling fatigue tests of the following designs will be conducted (20 data points per design will be obtained):

- HCR spur buttress
- HCR spur buttress—surface treated
- HCR helical buttress
- HCR helical buttress—surface treated

A single-tooth bending test will also be conducted to quantify the benefits of the buttress design over the conventional approach. The following types will be tested:

- HCR spur
- HCR spur—buttress
- HCR helical
- HCR helical—buttress

All test results will be compared with LCR gear baseline data.

The four HCR designs and one LCR design will also be strain gaged. The strain gages will be located in the roots to measure the bending stress during the meshing cycle. This testing will also determine the amount of load sharing that can be expected. Thus, compressive stress advantages can also be quantified.

Finally, the best spur and helical designs from the test programs will be selected and developed for full-scale hardware tests. Tests will be conducted on a back-to-back gear-box rig. The gears will be strain gaged in the roots to determine bending stresses, load distribution, and compressive stresses when subjected to gearbox operating conditions. Profile modification development will also be undertaken.

TAPERED ROLLER BEARING—POWDER METAL RIB

Background

Tapered roller bearings provide the most compact design for applications such as prop shafts. In these applications both thrust and radial loads must be reacted. The conventional approach has been to use two cylindrical roller bearings with one ball bearing. The cylindrical roller bearings provide most of the needed capacity. They cannot carry the thrust load; therefore, a ball bearing is needed to react the thrust. Tapered roller bearings can carry both radial and thrust loads and also have the high capacity inherent in roller bearings. Therefore, only two bearings are needed in these applications. Reducing envelope requirements and part count results in improvements in size, weight, and reliability/set life.

One of the disadvantages of tapered bearings pertains to the rib/roller contact. This contact is primarily a sliding interface, and scoring or wear problems can occur. In high-speed applications, oil must be applied directly to the interface to ensure problem-free operation. Also, oil interruption and oil-off conditions very quickly lead to failure. Since gearbox oil-off capabilities are becoming very important, improvements in tapered roller bearings are required.

One of the most promising approaches to the tapered roller bearing oil-off problems is the use of impregnated powder metal ribs. Timken is involved in a three-year NASA program in this area. Powder metal ribs with densities ranging from 65%-85% show the most promise.

Another approach is to ion implant the ribs and roller ends. Ions such as Ta⁺ and Mo⁺ have shown significant reductions in friction coefficients under dry running conditions. This should reduce heat generation and improve oil-off operating performance.

Benefits

Improving the oil-off capability of tapered roller bearings will make this type of bearing more viable for use in future gearboxes. Using tapered roller bearings in place of the conventional ball and cylindrical roller bearing arrangement for thrust and radial load environment provides the following benefits:

- reduced size
- reduced weight
- increased bearing reliability/set life

Tapered Roller Bearing—Powder Metal Rib Plan

Tapered roller bearing ribs will be ion implanted with two types of ions. Powder metal ribs using the optimum parameters from the Timken program will also be fabricated.

These bearings will be oil-off tested in a bearing rig under rated loading conditions.

LUBRICATION SYSTEM

Background

Modulated Oil System

The primary function of the oil system is to lubricate and cool bearings and gear meshes. The cooling requirements vary with speed and load. Cooling requirements increase with the increase in speed and/or load. The normal design practice in the past has been to provide optimum oil flow for cooling and lubrication at the maximum speed and load condition. This practice results in excessive flow at reduced speed and power points. The unnecessary flow contributes to windage losses and heat generation due to churning.

A system that could modulate oil flow over the power range would be beneficial. Fuel savings would result due to a reduction in gearbox heat generation at lower power levels such as cruise.

A modulated lubrication system was designed for the 1990s gearbox. This system modulates oil flow proportionally to power transmitted through the gearbox. This system maintains constant velocity oil flow at each of the gear meshes to provide adequate oil penetration. This arrangement consists of two tubes with offset radial circular orifices. As gearbox torque is increased, the oil pressure from a hydraulic torquemeter (load sharing) increases. The increased pressure causes the inner tube to move axially, exposing a larger area of the inner tube radial holes to the outer tube radial holes. Thus, the orifice size is increased, resulting in a corresponding oil flow increase. Also, since the lubrication oil pressure is held constant, jet velocity will remain constant.

Increased Temperature and Temperature Rise

Future gearbox systems will benefit from higher upper oil temperatures and higher temperature differentials. Current gearbox oil-in temperatures range from 180°F-220°F. Gearbox oil-out temperatures range from 240°F-280°F. Thus, the normal temperature differential is approximately 60°F. Oil coolers could be designed to allow gearboxes to operate at higher oil-in and oil-out temperatures as well as higher temperature differentials.

Improved Oils

Oils better than MIL-L-23699 will provide significant benefits. To derive benefits, oils are needed with higher temperature capabilities, higher load carrying abilities throughout the temperature range, and improved efficiency characteristics. These oils must be equivalent to or better than MIL-L-23699 with regard to other properties.

Self-Cleaning, Fine Filtration Filters

Future gearboxes will benefit from self-cleaning, fine filtration oil systems. Current systems use filters in the 38-80 micron mesh range and must be replaced periodically due to clogging. Future self-cleaning systems in the 3-micron range are being proposed.

Benefits

Modulated Oil System

The modulated oil system will provide the following two primary benefits:

- improved cruise efficiency
- smaller air/oil cooler

This system provides reduced oil flow at part power conditions. Thus, losses associated with excess lubrication in a conventional constant-flow type system are reduced.

Also, the potential for reducing cooler size exists. The system that has been proposed for the APET propulsion package is a combination fuel/oil and air/oil type heat exchanger. At high power conditions, the fuel/oil cooler will remove most of the heat due to the high fuel flow rates for this condition. At part power, heat generation is lower, but fuel flow is also lower. The lower fuel flow may require that the air/oil cooler remove a major portion of the heat. Therefore, the air/oil cooler, which has an associated drag penalty, may be sized by part power conditions. If this is true, then reducing oil flow at part power also allows the oil cooler to be downsized. A smaller cooler reduces aircraft drag and weight.

Increased Temperature and Temperature Rise

Increasing gearbox inlet and outlet temperatures will provide the following benefits:

reduced oil flow requirement

- reduced oil pumping losses
- smaller air/oil cooler
- improved efficiency

Higher temperature differentials across the gearbox allow oil flow rates to be reduced. The low-flow, high ΔT system can be designed to remove the same amount of heat as the conventional higher-flow, lower ΔT type system. Reducing oil flow reduces oil pump losses and churning/windage type losses. On the other hand, the higher temperature differential would tend to increase air/oil cooler size since the differential across the cooler is also increased. However, this effect is offset by the reduced flow rate that leads toward smaller air/oil coolers.

Gearboxes operating to higher inlet and outlet temperatures allow smaller air/oil coolers to be used. This occurs since the difference between cooler oil inlet temperature and outside air temperatures is increased. Increasing this temperature difference increases heat transfer rate between the oil and the air, thus leading to smaller air/oil coolers. Gearbox components that are stable at these higher temperatures are needed.

Improved Oils

Advanced oils will provide a number of benefits for future gearboxes and offer the following improvements/ characteristics in comparison with MIL-L-23699:

- elevated temperature capabilities
- higher load carrying capacity throughout the temperature regime
- improved oil film/contact environment
 - higher pitting fatigue life
 - lower heat generation
- compatibility with other MIL-L-23699 requirements

This advanced oil will allow gearboxes to operate to higher bulk temperatures and temperature rises.

Higher load carrying capacity allows gears to operate to higher loads and sliding velocities without scoring/scuffing damage. This capability would be highly beneficial to HCR gear designs, which experience high sliding velocities and have shown a tendency toward these types of failures in testing.

Improving the characteristics of the oil film that separates the contacting surfaces results in improved pitting fatigue life and lower heat generation. Thus, gearbox reliability/life and efficiency are improved.

Self-Cleaning, Fine Filtration Filters

Finer, self-cleaning filters in gearbox oil systems will provide several benefits. Filters in the 3-micron range will improve gear and bearing fatigue life as well as wear life of various components. Life is improved by not allowing particles to circulate through the system causing microdenting

*The reference in Appendix H is given at the end of this appendix.

and accelerating wear of contacting surfaces. The microdenting can lead to early fatigue for materials such as M50. The particles cause wear by acting as abrasives between contacting surfaces.

One of the expected disadvantages of finer filtration is lower filter life. Just the opposite has been demonstrated in an Army helicopter program (Ref 1*). Life of fine micron filters was improved. This improvement was attributed to the reduction in debris being generated by abrasive wear as a result of the high cleanliness level of the oil. The improved oil cleanliness keeps the filters from becoming contaminated as quickly.

Although fine filtration does not require technology advancements, a self-cleaning feature would require development. Developing a filter that cleans away accumulated debris would eliminate the need for frequent filter removal. Thus, downtime and maintenance costs are greatly reduced. Also, the chance of oil system contamination caused during filter removal and debris entering the system during filter bypass operation is almost eliminated.

Lubrication System Plan

Modulated Oil System

The objective of this program is to design, fabricate, and test a modulated oil system to verify and quantify the expected gearbox efficiency benefits.

The program will be started with the design of a modulated orifice for rig testing. Two modulated orifices will be fabricated for rig testing. The rig will be composed primarily of a pressure-regulating pump, the modulated orifice, and a variable oil pressure source to simulate torquemeter pressure.

The effects of varying torquemeter pressure and system oil pressure will be evaluated during rig testing. This testing will be used to evaluate jet velocity, jet length-to-diameter ratio, jet quality, and jet targeting.

Following successful rig testing, hardware will be designed and fabricated for testing in a back-to-back gearbox. The gearbox will be tested with both a conventional lubrication (baseline) system and a modulated system. The gearbox will be run at various power and speed settings. Gearbox heat generation and efficiency will be determined at each of the set points. The conventional and modulated data will be compared to quantify the benefits of the modulated system.

Increased Temperature and Temperature Rise

The objective of this program is to quantify the benefits of increasing gearbox temperatures and increasing the temperature rise across the gearbox.

This program will be initiated by an oil cooler sizing study. Oil coolers will be designed for various temperature

levels, temperature drop levels, and flow rates that would be expected for a typical mission. The cooler system will consist of in-line fuel/oil and air/oil coolers. The study will be directed toward reducing the air/oil cooler size and associated drag and weight penalties. Cooler size, weight, and drag will be determined for each temperature setting.

A back-to-back gearbox rig will be used for high-temperature testing. Gearbox component materials that can withstand the higher temperatures will be used. Gearbox inlet and outlet temperatures will be varied during operation at various speed and power settings. Heat generation and gearbox efficiency will be measured to determine any gearbox benefits.

Improved Oils

Allison will work with an oil company to develop a gearbox oil that provides the following:

- satisfactory performance over a temperature range of -40°F to 600°F
- adequate load carrying ability with respect to scuffing and spalling over this temperature range
- improved friction characteristics in comparison with MIL-L-23699
- properties equivalent to MIL-L-23699 with respect to other requirements

Five oils will be subjected to evaluation tests, which will consist of the following:

- scuff testing—Erdco rig
- heat generation and efficiency measurements modified Erdco rig
- spall testing—Erdco rig and Rockwell C tester
- other tests outlined in MIL-L-23699 specification

These oils will also be tested in a back-to-back gearbox, which will be operated at various gearbox oil-in and oilout temperatures and flow rates. Gearbox heat generation and efficiency will be determined for each one of these test points.

Self-Cleaning, Fine Filtration Filters

The objective of this program is to develop and test a 3-micron filter system that will clean itself.

Two system types will be designed. One filter system will be a continuous-cleaning type. The second system will be a periodic-cleaning type.

The designs will be fabricated and tested on an oil rig, which will be a closed-loop system composed of an oil pump, a self-cleaning filter, valves, a heater/temperature controller, and an oil tank. The tank will be capable of adding contaminants at a controlled rate.

The rig will be operated at various oil temperatures, flow rates, and pressures. Contaminants will be added to the system at each of the test points. The pressure drop across the filter will be measured and used to evaluate the success of each of the self-cleaning designs.

HOUSING

Background

The gearbox housing structure's primary function is to support and maintain alignment of the gears, bearings, and propfan. These structures must react and transmit loads from the gears, propfans, and engine. These load reactions must then be transmitted to the nacelle and airframe structure.

A number of requirements will receive increased emphasis for gearbox housings in the early 1990s. These requirements consist of improvements in the following:

- high-cycle and low-cycle fatigue strength and analysis
- creep resistance
- stiffness-to-weight ratio
- strength-to-weight ratio
- noise damping
- corrosion
- thermal expansion properties for compatibility with other gearbox components

Requirements such as reliability and durability will receive much greater emphasis. Future gearboxes will be designed for much longer intervals between gearbox removals, such as the 30,000 MTBR used in this study. These long intervals will put much more emphasis on high-cycle and low-cycle fatigue of housings. Better materials and improved analysis techniques are needed to ensure adequate housing fatigue strength.

Materials with improved creep resistance are also needed. Magnesium and aluminum housings have historically shown a tendency to creep in a relatively short time in gearbox housings. The creep allows bores to shift and misalign, decreasing gear and bearing life. This problem is compounded when gearboxes must operate for 30,000 hr compared with current lives, which are less than 10,000 (MTBR) hr.

The material creep also allows datum features to shift. Thus, problems are created at overhaul when trying to rework bores or other housing features.

Materials with greater stiffness are also desirable for future housings. Gear and bearing lives could be improved with stiffer housings. Housing deflections cause misalignment of bearings and gear meshes due to bore movement. The misalignment creates high bearing and gear stresses and reduces their life. Housing materials with a higher specific stiffness will reduce these deflections without increasing housing weight.

Also, use of analysis techniques, such as finite element modeling, provides a better method of controlling housing deflections without increasing weight.

Noise reduction will also receive increased emphasis in the 1990s. Materials that provide improved noise damping characteristics can be used to reduce noise generated by gears and bearings.

Weight reduction will continue to be an important requirement for future gearboxes. Materials with high strength-to-weight ratio and improved analysis techniques are needed to provide weight improvements.

Housing corrosion continues to be a slight problem in housings fabricated from magnesium. This problem has been drastically reduced by the use of coatings (e.g., HAE) available today. Problems still occur when the coatings are damaged, however. Corrosion-resistant materials would eliminate the need for coatings and eliminate the potential for any corrosion problems.

Housing materials with thermal properties more compatible with other gearbox components are needed. The thermal expansion characteristics of the cast magnesium and aluminum gearbox materials pose a problem for the design of bearings and gears. Gears, bearings, and bearing liners are fabricated in steel with a thermal expansion coefficient much lower than that of the all-magnesium or aluminum gear housings. Adequate clearances must be provided so that cold-temperature operation (startup at -65°F) is possible, yet the clearances must not be so great that excessive clearance exists at high temperature.

These differential thermal expansions create a number of problems. Bearing liners are normally pressed or bolted into bearing bores. The thermal expansions cause relative movement between the liners and the housings. This movement causes bearing bore fretting and wear problems. The need for extra clearance in bearing bores also allows gears to move out of mesh. This movement, combined with the bore wear, can compromise the gear contact ratio. This movement also makes it difficult to incorporate center distant sensitive gear systems, such as Novikov, which offer some advantages over involute systems. The differential thermal expansion can also aggravate gear and bearing misalignment due to temperature differences at each of the support bearing bores.

Composite materials show great potential for meeting the 1990s gearbox housing requirements. Composite materials offer high specific stiffness and strength, corrosion resistance, creep resistance, and favorable thermal expansion properties and damping characteristics. A period of accelerated progress is now expected in the applicability of composite materials as a result of the increased emphasis on efficient use of strong, stiff, lightweight materials. The combination of factors such as innovative design concepts and development of lower-cost fabrication processes and constituent material shows great promise in making composites cost competitive and in achieving weight reduction and performance goals.

The composites that show the most promise for use in gearbox housings are of the following two general types:

- MMCs
- resin matrix composites

MMC materials in general consist of a high-strength fiber such as silicone carbide (SiC), which is distributed in a

metal matrix such as magnesium or aluminum. Two types of MMCs will be examined in this program. These types are continuous fiber types and whisker fiber types.

The continuous fiber MMCs are processed by wrapping fibers in a die in a desirable orientation. The die is then filled with a metal such as aluminum or magnesium.

The whisker fiber MMCs are processed by mixing a metal such as aluminum or magnesium with very short fibers (whiskers) such as SiC. The whisker-reinforced MMC materials are then cast, forged, or powder metal pressed into the desired component.

The resin matrix composites consist of a highstrength fiber distributed in a resin matrix such as polyimide. The resin matrix fibers that will be used in this program will be composed of both long and short fibers. The short fibers will be used to simplify fabrication. The long fibers will be selectively used in locations requiring higher stiffness and strength than attainable with the short fibers.

The resin matrix materials in this program will be fabricated by a compression molding technique, which consists of developing a composite preform in the general housing shape. The preform is then put in a mold that subjects the preform to pressure and temperature. The mold shapes the preform to the desired housing shape.

Benefits

MMCs

MMCs provide high mechanical properties that are isotropic. These types of material can be processed into complex shapes with such low-cost techniques as powder metal processing, forging, and casting. These materials offer improvements in the following areas, relative to magnesium or aluminum materials:

- specific stiffness
- specific strength
- creep resistance
- noise damping
- thermal expansion compatibility with other gearbox components

A data survey (USAAVRADCOM-TR-81-D-33) was conducted at Allison in 1981 to define the state-of-the-art technology in the field of MMC material systems with respect to turbine engine applications. At the same time, Boeing Vertol Company completed a study (USAAVRADCOM-TR-81-D-34) on the applicability of MMCs to helicopter propulsion drive systems.

In general, an MMC offers the following advantages when compared with other composite systems:

- high off-axis properties
- moderate temperature capabilities
- good environmental stability
- improved joining capabilities

Table H-I shows design allowables for 30% by volume (V/O) SiC particulate/Mg (AZ 61) and 30% by volume (V/O) SiC particulate/A1 (CT 90-T6). Results of the Allison study for the Model 250-C30 helicopter gearbox are given in Table H-II

These studies have shown structural and weight advantages. Application of MMC materials with increased stiffness and strength potentially offers an effective option to provide increased gear and bearing life as a result of reduced wall deflection and thermal expansion.

Fiber/Resin Matrix Composites

Fiber/resin matrix materials compared with cast magnesium and aluminum for gearbox housing applications offer advantages in the following areas:

- specific stiffness
- specific strength
- thermal stability—creep resistance
- noise damping
- corrosion resistance
- thermal expansion compatibility with other gearbox components

In addition, low-cost (compared with MMC) fabrication techniques for these composites and lower constitutent material costs make them attractive for large static components in moderate temperature environments.

With the high-temperature polyimide matrix, the stiffness and strength of the assembly can be maintained to 450°F or even higher.

Weight savings of up to 20% have been projected for the use of graphite/resin composites in gear case structures. However, processing difficulties in controlling thickness and fiber orientation with the hot-melt winding resins have prevented the demonstration of such weight savings.

Table H-I.

Design allowables for SiC particulate MMCs.

Property	SiC/Mg	SiC/AI
Yield strength (10³lb/in.²)	35.0	100.0
Modulus (10 ⁶ lb/in.²)	12.5	21.0
Density (lb/in.³)	0.0755	0.102

Further developments in room-temperature winding resins, such as procedures resulting in better control of thickness, resin content, and fiber orientation, could enhance the applicability of this class of materials to the design of this gear case.

Housing Plan

The objective of this program is to develop a composite housing material that provides the following areas of improvement with respect to aluminum and magnesium:

- stiffness-to-weight ratio
- strength-to-weight ratio
- creep resistance
- noise damping
- corrosion resistance
- thermal expansion more compatible with the steel gearbox components

A number of areas that have inhibited the use of composites will be dealt with in this program.

MMCs are still difficult to fabricate, and constituent material costs are high. As composites come into more widespread use, constituent prices should drop to reasonable levels. However, improved fabrication techniques are needed. Low fracture toughness properties also pose a problem from a fatigue standpoint. Solutions to these MMC problem areas will be addressed in this program.

Resin matrix composites also have disadvantages for which solutions must be sought. First, these composites undergo a strength degradation due to moisture content. Processing difficulties in controlling thicknesses and fiber orientation with the hot-melt winding resins have impeded the demonstration of weight savings. Thermal conductivity of these materials is also low. Thus, more heat would be rejected to the oil, requiring a larger cooler system. The resin matrix materials also have low fracture toughness properties.

The key areas that will be addressed in the composite materials program are the following:

- improving moisture protection—resin matrix
- improving fabrication techniques—MMC and resin matrix

Table H-II.

Comparison of Model 250-C30 front housing gearbox materials in terms of required wall thickness, weight, and cost.

	Baseline	Thick	C:O/Ma-	COAL
	Mg	Mg	SiC/Mg	SiC/AI
Thickness—in.	0.180	0.321	0.254	0.214
Deflection—in.	0.142 (0.025)*	0.025	0.025	0.025
Maximum stress—Ib/in.2	35,000	11,000	17,000	24,600
	(15,000)*	(15,000)*	(35,000)*	(100,000)*
Weight—Ib	28.6	41.2	38.3	41.8
estimated cost—\$	2,135	2,765	6,700	4,600

Allowable values

- improving fracture toughness—MMC and resin matrix
- improving design analysis techniques

The development program will be conducted as follows:

- material selection
- resin matrix moisture protection
- test specimen development and testing
- full-scale housing fabrication
- full-scale housing tests

Both resin matrix composite and MMC materials will be evaluated. A study will be conducted to determine the optimum resin matrix and metal matrix compositions. This study will identify the optimum fiber type, fiber size, and matrix material for each composite type. A finite element analysis will be conducted to determine the housing shape, size, and fiber orientation. A magnesium or aluminum housing will be designed for a baseline comparison. These housings will be designed for a life greater than 30,000 hr.

A moisture protection effort will be undertaken for development of the resin matrix composites. This phase will be directed toward finding a system that will protect the resin matrix composites from material property degradation due to exposure to moisture.

Specimens of both composite types will be fabricated for testing. The specimen tests will be used to determine creep resistance, fatigue properties, and fracture toughness characteristics. These properties will be determined in fiber and transverse fiber directions for the resin matrix materials. Moisture/strength degradation and long-term oil exposure effects will also be determined through specimen testing. The effects of other environmental factors will also be determined.

The specimen testing will be followed by a full-scale housing development phase. This phase will be directed

toward developing less complex fabrication techniques to reduce cost for full-scale housings. This cost reduction effort will focus on development of automated fabrication techniques.

A preform design and development effort will be undertaken for the resin matrix composite. This effort will be directed toward development of a low-cost preform that will provide a finished housing demonstrating the expected weight, stiffness, and strength benefits. The resin matrix housings will be fabricated by the compression molding technique discussed earlier.

An MMC housing fabrication study will also be undertaken. This study will be aimed at identifying the optimum MMC housing fabrication technique. The optimum technique is one in which all the expected benefits are demonstrated. Front and rear housings of each type of composite will be fabricated.

These housings will undergo a number of tests. A static deflection test will be conducted first. This test will be used to verify the expected stiffness benefits. Thermal testing will be conducted to determine thermal expansion. The housings will be submitted to 150 hr of back-to-back gearbox endurance testing to evaluate the effects of an actual gearbox environment. During the endurance test, noise levels and oil heat rejection will be measured and compared with baseline magnesium or aluminum housings. Bore locations will be measured following endurance testing to evaluate creep effects. Test specimens will also be taken from each housing. These specimens will be subjected to strength testing.

SINGLE-ROTATION GEARBOX TECHNOLOGY PLAN SCHEDULE

A schedule for the single-rotation gearbox technology program is shown in Figure H-1.

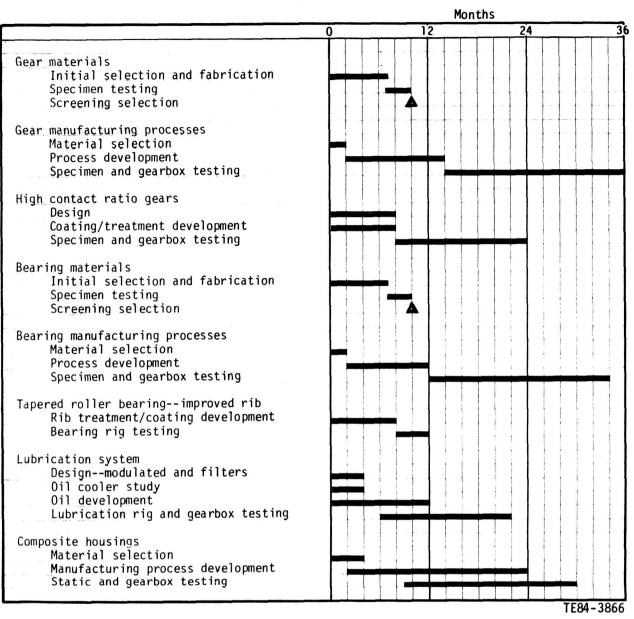


Figure H-1. Single-rotation gearbox technology plan schedule.

SINGLE-ROTATION PITCH CONTROL AND MECHANISM TECHNOLOGY PLAN

The conceptual design of a pitch change system developed under the SRP APET Add–On contract specifies advanced technology features that will require technology programs to establish their acceptability for future production development programs. These technology features are a capacitor signal transfer, a high–pressure hydraulic power module, and a rotating electronic control module.

BACKGROUND

Current turboprops transmit an electrical signal across a rotating interface. This is accomplished through the use of brushes and slip rings, which have inherent problems. The most notable problem is carbon buildup due to brush wear and susceptibility to contamination from oil. These problems result in high maintenance requirements.

Current turboprop systems use low-pressure hydraulics with the hydraulic power components mounted on the stationary side. The oil required for changing pitch is supplied to the rotating components through a transfer bearing. Experience has demonstrated that large-diameter transfer bearings used in many current systems are a high-maintenance item. Also, independent studies by Hamilton Standard indicate that system weight can be reduced through the use of high-pressure hydraulics.

Current turboprop systems use hydromechanical pitch change controls, which are mounted on the stationary side of the system. Mechanical signal transfer is required from the control to the pitch change actuator across the rotating interface. This task is particularly difficult for in-line gearbox configurations and results in pitch change hardware being located within the gearbox. This has a significant impact on gearbox reliability and maintenance cost.

PROPOSED PLAN

The proposed technology plan for the single-rotation pitch change system includes three areas of development:

- capacitor signal transfer
- a high-pressure rotating hydraulic power module
- a rotating electronic control

CAPACITOR SIGNAL TRANSFER

There are two major areas of concern with regard to the capacitor signal transfer concept. The first is susceptibility to electromagnetic interference and vulnerability to lightning strike interference. The second is ensuring that the capacitor does not emit electromagnetic interference. The program includes the design, fabrication, and testing of a shielded capacitor system. This system will be adaptable to an existing turboprop barrel. It includes a breadboard transmitter/receiver, and it will be subjected to an electromagnetic interference survey test for susceptibility and emission. If necessary, additional shielding systems should be concepted, fabricated, and tested.

Lightning transient tests are needed to determine if the capacitor ring can withstand high-voltage transients without damage or signal quality degradation. This program will result in a control signal transfer technique that is adaptable to both current and future turboprop systems and eliminate the need for brushes and slip rings.

HIGH-PRESSURE HYDRAULIC POWER MODULE

A system has been devised for changing pitch on future turboprops with high-pressure hydraulic supply components. For in-line gearbox systems, the components would be mounted on the rotating portion of the system. This eliminates the need for a transfer bearing and permits removal of hydraulic pitch change hardware from the gearbox. For offset gearbox configurations, the option exists to mount the hydraulic supply components on the stationary side of the system. A concept has been developed whereby this can be achieved with a reliable, small-diameter transfer bearing and without impacting the gearbox. The use of high-pressure hydraulics results in reduced size and weight of these components for optimized installation and maintenance. The objective of the pitch change technology program for offset gearbox configurations is to establish an acceptable gear pump that will operate at 4,750 lb/in.2 with an operating life design goal of 30,000 hr.

The recommended approach is to design and build a gear pump sized for the requirements of a potential propfan system. Testing to determine torque characteristics, leakage, endurance, and susceptibility to cavitation will be conducted.

This program will establish the feasibility of a 4,750 lb/in.² gear pump and define hardware suitable for development on advanced pitch change systems.

ROTATING ELECTRONICS

The objective of this technology program is to determine both the operational characteristics and the reliability of the electronic controller when mounted and operating in a rotating field. (The electronic controller includes the interfacing electronics package for signal conditioning, feed-

back signals, and control of the electrohydraulic servomotor.) Electronic circuits operating in a high level "g" field, such as the hub of a propeller, are the technology issue.

It is first necessary to establish the environmental requirements. Concepts for the structural packaging of the electronics for survival in this environment will be developed and a breadboard differential input digital data transmitter/receiver circuit constructed for dynamic test

evaluation. These tests include both whirl and vibration over the total frequency spectrum anticipated for propfanmounted hardware. This program will establish the feasibility of a rotating electronic control and define hardware suitable for development on advanced pitch change systems.

A schedule for the single-rotation pitch control and mechanism technology program is shown in Figure H-2.

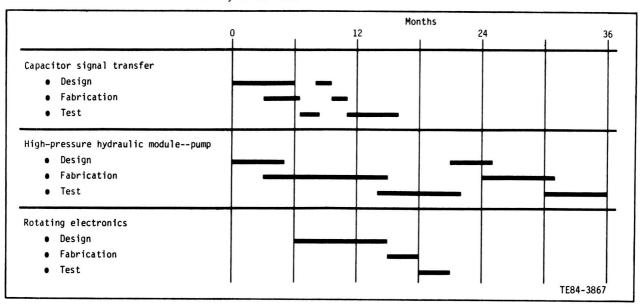


Figure H-2. Single-rotation pitch control and mechanism technology plan schedule.

REFERENCES

 Dr. T. Tauber, W. A. Hudgins, and R. S. Lee, "Full-Flow Debris Monitoring and Fine Filtration for Helicopter Propulsion Systems," Preprint No. RWP-24, presented at the Rotary Wing Propulsion System Specialist Meeting, Williamsburg, VA, 16-18 November 1982.

APPENDIX I

TASK XI. PRELIMINARY DESIGN OF COUNTER-ROTATION PROPFAN REDUCTION GEARBOX

TABLE OF CONTENTS

Title Title	Page
roduction	I-1
eliminary Design of the Counter-Rotation Propfan Reduction Gearbox	I-2
Program Defined Design Constraints	I-2
Counter-Rotation Gearbox Configuration Selection	I-2
Counter-Rotation Gearbox Gear and Bearing Type Selection	I–6
Counter-Rotation Gearbox Design Criteria	I–9
Counter-Rotation Gearbox General Arrangement	
Counter-Rotation Gearbox Design Results	
Counter-Rotation Gearbox Power Loss	
Counter-Rotation Gearbox Lubrication System	I-19
Modifications for Pusher Configuration	
ferences	

LIST OF ILLUSTRATIONS

Figure	Title	Page
I - 1	Differential planetary gear set	1-2
1-2	Gearbox ratio effect on the power split	
1-3	Compound planetary gear set	1–3
1-4	Split path parallel offset gear set	1-4
1-5	Triple command idler gear set	
1-6	Differential epicyclic gear set	
I - 7	Split path planetary gear set	1–5
1-8	Tapered roller bearing and helical gearing	1–7
I - 9	Single row spherical bearing and high contact ratio spur gear	1–8
I-10	Local temperature index of the gear mesh	1–8
I-11	Counter-rotating gearbox cross section	I-10
I-12	Thrust diagram for the helical gearing	
I-13	Planet gear arrangement	
I -14	Outer prop shaft bearing cross section	
I-15	Input shaft bearing cross section	
I-16	Planet gear assembly	
I-17	Front carrier bearing cross section	
I-18	Rear carrier bearing cross section	I-12
I-19	Sun gear cross section	
I-20	Prop brake cross section	I-13
I-21	Oil pump cross section	I-13
I-22	Counter-rotation gearbox side view	I-13
I-23	Propfan/counter-rotation gearbox assembly	
1-24	Propfan/gearbox attachment	I-14
1-25	Counter–rotation gearbox propulsion system	
I-26	Counter–rotation gearbox power loss breakdown	
I-27	Lubrication schematic diagram	I-20
I-28	Oil conditioning unit schematic diagram	I-21
1-29	Ram air oil cooler specifications	
1–30	Nacelle-mounted ram air cooler	I-22
I-31	Blower/air cooler arrangement	

PRECEDING PAGE BLANK NOT FILMED

LIST OF TABLES

Table	Title	Page
1-1	Major part count comparison	. I–5
1-11	Initial forced decision analysis	. I–6
1-111	Weighting categories	. 1–7
I-IV	Weighted decision analysis	. 1–7
I–V	Final forced decision analysis	. I–7
I-VI	Candidate advanced technology gear sets	. I–8
I-VII	Candidate gear set evaluation data	. 1–8
I-VIII	Candidate bearing life comparison	. I–9
I-IX	Planet form selection	. 1–9
I-X	CR gearbox design criteria	. I–10
I-XI	Parameters used to establish overall CR gearbox gear ratio	. I–10
I-XII	CR gearbox mission requirements	. I–15
I-XIII	Planetary gear set geometry	. I–15
I-XIV	Planetary gear set operating parameters	. I–16
I-XV	CR gearbox bearing geometry summary	l-17
I-XVI	CR gearbox bearing life summary	I-17
I-XVII	Planet bearing design parameters	I-17
I-XVIII	Prop shaft bearing design parameters	l-17
I-XIX	Input shaft bearing design parameters	l-17
I-XX	Carrier bearings design parameters	I-17
I-XXI	Propfan-gearbox curvic coupling dimensions	I-18
I-XXII	Inner output shaft drive spline parameters	I-18
I-XXIII	Comparison of single-rotation and counter-rotation gearboxes	I-18
I–XXIV	CR gearbox gearing losses	I-19
I-XXV	CR gearbox bearing losses	I-19
I-XXVI	Oil pump parameters and power loss.	I-19
-XXVII	CR gearbox power loss breakdown	I-19

INTRODUCTION

Task XI involved the preliminary design of a counter–rotation (CR) gearbox for the 10,000–shp advanced propulsion system of Task III. This design incorporates the requirements of a tractor arrangement of a wing–mounted CR propfan propulsion system. It also provides for optimizing the power turbine and propfan speeds thereby permitting the propfan and power turbine to operate at their respective optimum design speeds.

CR gearbox preliminary design is integrated with the propfan pitch change mechanism designed in Task XII relative to both functional and operational characteristics. It is intended that the design features of these systems represent technologies verifiable in the late 1980s, suitable for production in the early 1990s time period. Alternate technology fea-

tures that would further enhance the CR gearbox were considered and are included in the research and technology plan developed in Task XIII.

While the design objectives were specifically for a wing-mounted tractor installation, additional work was performed to determine the qualitative change that would be required if it were to be used in a pusher propfan configured aircraft.

The engine (input) side of the gearbox was well defined by the APET advanced technology engine study. The counter-rotating propfan was selected to determine the output side requirements. The basis for the propfan selection was the APET mission and propfan data furnished by Hamilton Standard.

PRELIMINARY DESIGN OF THE COUNTER-ROTATION PROPFAN REDUCTION GEARBOX

A preliminary design study was conducted in Task XI to provide an advanced flight weight CR gearbox that is integrated with the propfan pitch change control and mechanism designed in Task XII and described in Appendix J.

The objectives of this preliminary design study are as follows:

- Select and rank two 10,000 shp gearbox configurations compatible with the APET propulsion system defined in Tasks I through VI.
- Select one gearbox configuration and prepare a preliminary design of this configuration at an advanced technology level, stressing long life, good efficiency, low maintenance cost, low initial cost, and high aircraft dispatch reliability.
- Compare the counter-rotation design to the singlerotation, advanced technology gearbox described in Appendix F.
- Define modifications required of the CR gearbox for a pusher application.
- Prepare a research and technology plan that would result in gearbox technology verification in the late 1980s and allow for first production in the early 1990s.

PROGRAM DEFINED DESIGN CONSTRAINTS

The gearbox designs were required to be compatible with the Allison APET propulsion system. Therefore, the gearbox was designed for a 10,000 shp three-spool advanced technology, free turbine engine. The inlet corrected airflow of this engine is 56 lb/sec, and the overall pressure ratio is 32.5:1 at the design point cruise condition of 0.72 Mach number at 32,000 ft altitude. The propfan power at this initial cruise point is 5227 hp. The compressor is a dual-spool unit with each spool driven by a single stage high-pressure turbine stage. The maximum turbine inlet temperature is

2500°F. The power turbine consists of three axial flow stages. These stages provide input to the propfan gearbox at its optimal rotational speed of 10,750 rpm. The APET engine was configured during preliminary design studies and installed in wing–mounted nacelles with the propulsion system components to establish interface requirements for the drive system.

The CR gearbox was designed for a propfan characterized by advanced technology blades having thin swept profiles to achieve high efficiency. The propfan had the following characteristics:

- 12 blades at 6 per row
- 750 ft/sec maximum tip speed
- 45 shp/dia² disk loading at the initial cruise condition

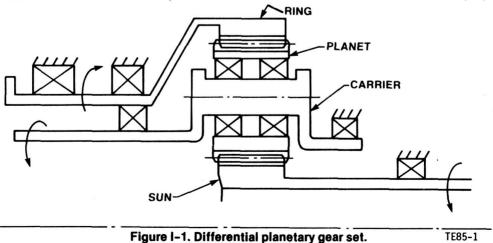
Using the characteristics of the APET power section and propfan described above requires that the reduction gearbox be designed with the following characteristics:

- 10.78 ft propfan diameter
- 1329 rpm propfan speed
- 8.185 speed reduction ratio

COUNTER-ROTATION GEARBOX CONFIGURATION SELECTION

Six candidate configurations were evaluated for the counter-rotating gearbox. The best configuration for preliminary design was determined through a series of competitions between the candidate configurations. The candidate configurations included the differential planetary, the compound planetary, the splitpath parallel offset, the triple compound idler, the differential epicyclic, and the split path planetary concepts.

The differential planetary gear set, schematically shown in Figure I-1, differs from a simple planetary system in



that the ring gear is allowed to rotate. With the sun gear as the input, both the ring gear and the planet carrier can be attached to output shafts and the output shafts will rotate in opposite directions. The fixed torque relationship between the two output shafts is established in a differential system by the following relationship:

$$T_c/T_R = R + 1/R - 1$$

where:

 T_c = output torque at carrier

 T_R = output torque at ring gear

R = gear ratio as defined by equal speed output shafts

 $R = 2N_R + N_S/N_S$

N_R, N_S = Number of teeth on ring gear and sun gear, respectively

Since the torque relationship is fixed, the output speeds are controlled by the power demand at the shafts. For equal but opposite output speeds, the power split is the same as the torque split. Figure I–2 shows the effect gearbox ratio has on the power split (also, the torque split).

The compound planetary gear set, shown schematically in Figure I-3, differs from a differential planetary system in that there is a second gear on each planet meshing with a fixed ring gear. This second gear mesh fixes the output shafts speed relationship. Typically this relationship is equal speeds in opposite directions. By fixing the output speeds, the output torques may vary. If the output torques are equal to the differential torque split, the second ring gear is not loaded. As the torques vary from the nominal split, the second ring gear load is increased.

The split path parallel offset gear set, shown schematically in Figure I-4, is based on two sets of parallel shaft gearing. One input pinion meshes with two idler gears. The first idler gear drives one output shaft through a gear train. The second idler gear drives a second output shaft through a second gear train. One output shaft is driven in the opposite direction from the outer output shaft by putting a second idler gear in one of the gear trains. The output speeds can be designed equal or at any fixed speed relationship.

The triple compound idler gear set, shown schematically in Figure I–5, is a modified lay shaft design. The input pinion drives three lay shafts spaced equally around the pinion. These three lay shafts drive two output gears, one through an external mesh and the second through an internal mesh. The opposite meshes cause an opposite direction of rotation on the two output shafts.

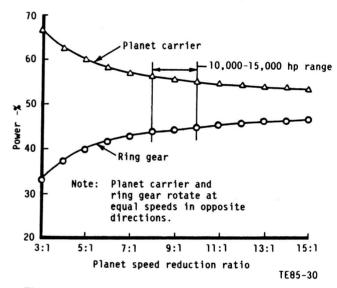


Figure I-2. Gearbox ratio effect on the power split.

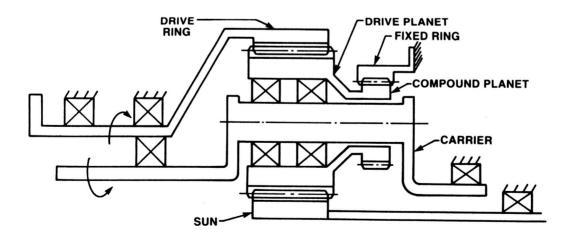


Figure I-3. Compound planetary gear set.

TE85-2

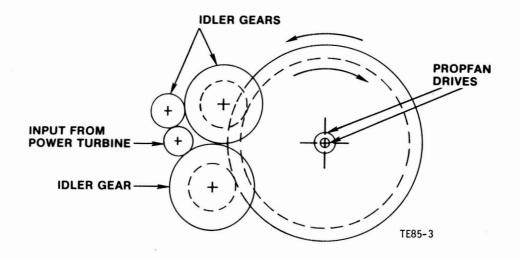


Figure I-4. Split path parallel offset gear set.

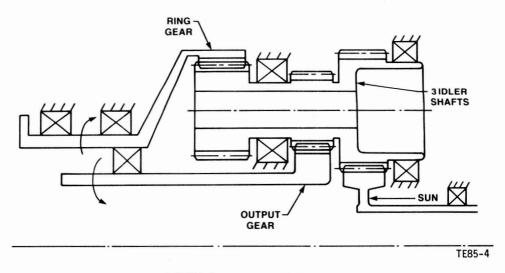


Figure I-5. Triple compound idler gear set.

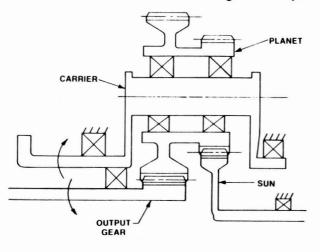


Figure I-6. Differential epicyclic gear set.

The differential epicyclic gear set, shown schematically in Figure I–6, is two planetary systems connected through the planets and with no ring gears. The sun gear to the first planetary system drives the planets. The sun gear to the second planetary system is one output, and the planet carrier is the second output. There are no fixed gears so the torque split between the two output shafts is fixed. This torque relationship is as follows:

$$T_{So}/T_{C} = R + 1/R - 1$$

where:

TE84-5

 T_{SO} = Torque at output sun gear

T_C = Torque at planet carrier

R = Gear ratio as defined by equal speed output shafts

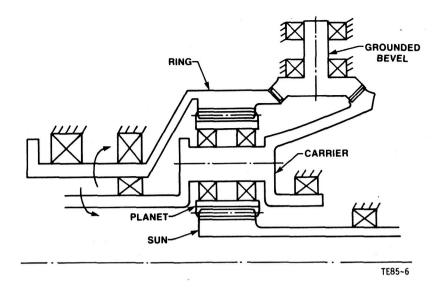


Figure I-7. Split path planetary gear set.

Table I-I.

Major part count comparison.

No. of planet bearings	No. of bearings	No. of gears	No. or bearings and gears	No. of power paths
8.	13	6	19	4
8	13	11	24	4
_	12	8	20	2
	10	12	22	3
6	10	8	18	3
8	19	11	30	4
	planet bearings 8 . 8	planet bearings No. of bearings 8 13 8 13 — 12 — 10 6 10	planet bearings No. of bearings No. of gears 8 13 6 8 13 11 — 12 8 — 10 12 6 10 8	planet bearings No. of bearings No. of gears bearings and gears 8 13 6 19 8 13 11 24 — 12 8 20 — 10 12 22 6 10 8 18

 $R = 2[(N_{PI}N_{SO})/(N_{PO}N_{SI})] - 1$

where:

 N_{SI} , N_{SO} , N_{DI} , N_{PO} = Number of teeth on the sun gears and planet gear at the input planetary and output planetary

Since the torque relationship for the differential epicyclic system is the same as the torque relationship for the differential planetary system, the power relationships are equal (see Figure I-2).

The split path planetary gear set, shown schematically in Figure I–7, is a simple planetary system combined with a bevel gear train. There are large diameter bevel gears attached to both the carrier and the ring gear that mesh with a series of small bevel gears mounted in the housing. These bevel gears fix the output speed relationship betwen the two opposite rotation output shafts. If the two large diameter bevel gears have the same pitch diameter, the output shaft speeds have the same magnitude.

The gearbox candidate configurations were first compared by a count of the major parts. A major part count is defined in this case as the number of gears and bearings required in the main power train. This comparison, listed in Table I–I, shows the number of major parts directly affecting the reliability of each gearbox configuration, with the number of bearings being more important.

Assumptions made so that the comparison would be consistent include equal output shaft speeds and opposite in direction, 8:1 reduction gear ratio, number of power paths limited by geometry or ability to load share, input shaft in-line with the two concentric output shafts, and two bearings maximum per shaft (combined radial and thrust loads would be supported by the same bearing).

The differential planetary, compound planetary, and split path planetary concepts have four planets with load sharing accomplished by a floating sun gear and a flexibile ring gear. Each have two prop shaft bearings, two bearings supporting the planet carrier, two bearings for each planet, and one bearing supporting the input end of the input shaft

Table I-II.
Initial forced decision analysis.

Category (weight factor)	Differential planetary	Compound planetary	Split path parallel offset	Triple com- pound idler	Differential epicyclic
Reliability (25)	75	50	25	0	100
Efficiency (22)	88	66	22	44	0
Maintenance (18)	36	18	72	54	0
Cost (16)	64	48	0	32	16
Weight (12)	48	36	12	24	0
Size (7)	17.5	17.5	28	. 7	0
	328.5	235.5	159	161	116

(the other end floats with the sun gear). The split path planetary has six more bearings supporting three speed fixing bevel gears.

The triple compound idler gear set and the differential epicyclic gear set have three lay shafts of planets that give three power paths with geometrically balanced loads. Each planet shaft and the outer prop shaft are supported on two bearings. The inner prop shaft and the input shaft are supported at one end with a bearing, and the other end is allowed to float with its sun gear.

The split path parallel offset gear set has a total of six shafts, each supported by two bearings. There are two power paths, one for each output shaft.

The split path planetary concept was eliminated at this point because of the large number of bearings it required. It also would require bevel gears of 16 to 20 in. diameter that would need close alignment, a disadvantage relative to maintainability.

The second comparison of the remaining five configurations involved the initial sizing of gears and bearings.

The differential epicyclic gear set was eliminated from further consideration based on the size evaluation. The diameter of the output planet gear is dictated by stress, which is the controlling parameter in establishing the center distance. As a result the input planet pinion becomes large. The diameter of the gearbox then becomes very large, greater than 80 in. The differential epicyclic configuration cannot be effectively packaged beyond a ratio of 4:1 or 5:1.

The differential planetary and compound planetary gear sets are approximately the same size, and their simplicity offers advantages of reliability and size. Smaller size results in cost and weight advantages.

The split path parallel offset gear set is the simplest gearbox. It has a maintainability advantage because of the use of parallel-shaft gearing. It also has a size advantage because a large portion of the gearbox can be placed to one side of the shaft's centerline.

Table I-II displays the results of a forced decision analysis of the five candidate configurations. The differential and compound planetaries were chosen for further analysis because of reliability, efficiency, and cost. Although comparable, the split path parallel offset was chosen over the triple

compound idler for further analysis because of maintainability and size advantage.

The three configurations were subjected to a weighted decision analysis that compared them in each of the 10 categories listed in Table I–III. The results of these comparisons are shown in Table I–IV. Based on this comparison, the differential planetary gear set was selected for the preliminary design study.

The weighted decision method described above yields point values that are a measure of comparison. For example, the differential planetary was 5% lighter than the compound planetary and its point value is 5% higher. This method of comparison yields small differences even with an overwhelming winner. Therefore, these results were verified by a second forced decision. These results are shown in Table I–V.

COUNTER-ROTATION GEARBOX GEAR AND BEARING TYPE SELECTION

The initial phase of the preliminary design was the selection of the gear type and bearing type. Gear type refers to helical gears, spur gears, or high contact ratio spur gears. Bearing type refers to cylindrical or tapered roller bearings. The gear types and bearing types were selected primarily for potential of increased life.

Dynamic loads between gear teeth have a detrimental effect on the life of gears and bearings. By reducing dynamic loads, the surface fatigue life of the gears and bearings increases. These loads occur due to non-conjugate action during the transferring of load from one tooth to the next. Spur gears use profile modifications to improve load transfer. This method only corrects for deflection effects. To reduce the impact of index errors or tooth-to-tooth errors, gears are designed with a higher contact ratio. High contact ratio spur gears have a greater tooth height than standard spur gears. which lengthens the zone of contact and places at least two teeth in contact at all times. Helical gears increase the total contact ratio by adding an axial contact ratio. Helical gears also have a rolling velocity component in the axial direction. These two gear types were compared in the preliminary design and the most promising was chosen.

Table I-III.
Weighting categories.

Reliability

All gearbox configurations defined equal. Part

life will be designed for 30,000 hr MTBR in

	each case.
Efficiency	Differential planetary is slightly more efficient than compound planetary because of the compound ring gear tare losses. The parallel offset has only external meshes so it is the least efficient.
Maintenance	This was determined by major part count with planet bearings being more time consuming to replace than shaft bearings.
Acquisition Cost	Estimations of production cost based on weight.
Pitch control	High and low pressure oil glands and a high speed power shaft.
Weight	Estimates or production weight based on steel gears and bearings and aluminum housings.
Technical risk	Number of technical risk items in each gearbox. Example, tapered plant bearings.
Ease of scaling	Increase in frontal area with a doubling of horsepower.
Spacial envelope	All three configurations have close to the same length; therefore, this rating is based on frontal area.
Propeller shafts	Number of brakes required to stop all shafts.

Table I-IV.
Weighted decision analysis.

Category (weight factor)	Compound planetary	Differential planetary	Offset parallel
Reliability (18)	18	18	18
Efficiency (17)	16.8	17	16.7
Maintenance (13)	8.2	9.6	13
Initial cost (12)	11.5	12	9
Pitch control (12)	12	12	12
Weight (11)	10.5	11	7.3
Technical risk (6)	4.5	4.8	6
Ease of scaling (5)	5	5	4.4
Spacial envelope (4)	4	4	1.5
Propeller brakes (2)	2 .	1	2
4	92.5	94.4	89.9

One method of increasing bearing life is to reduce bearing contact stress. To reduce contact stress, the area of contact between the roller and raceways is increased. Planet bearings are typically cylindrical rollers or two row spherical rollers. Tapered roller bearings typically have a larger length to diameter ratio than comparable cylindrical roller bearings,

Table I-V. Final forced decision analysis.

Category (weight factor)	Compound planetary	Differential planetary	Offset parallel
Reliability (18)	18	18	18
Efficiency (17)	17	34	0
Maintenance (13)	0	13	26
Initial cost (12)	12	24	0
Pitch control (12)	12	12	12
Weight (11)	11	22	0
Technical risk (6)	0	6	12
Ease of scaling (5)	7.5	7.5	0
Spacial envelope (4)	6	6	0
Propeller brakes (2)	3	0	3
	86.5	142.5	71.0

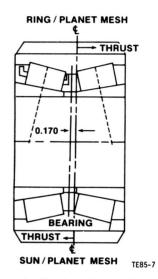


Figure I-8. Tapered roller bearing and helical gearing.

which results in a larger area of contact and longer life. A single row spherical bearing has a larger area of contact than a double row spherical because the center rib area of the double row bearing is replaced by the roller and raceway in the single row bearing. Therefore, the tapered roller bearing and the single row spherical bearing were compared in preliminary design.

In a planetary gearbox the planet bearing size and the gear size directly effect one another. If the bearing is designed at its limit, the gears may be larger than necessary. This is a bearing limited design. Most planetary gearboxes are bearing limited. The emphasis of this comparison was to pick a gear and bearing combination that will give the longest life. The candidate forms to be compared are a tapered roller planet bearing mounted with a helical gear, and a single row spherical roller planet bearing mounted with a high contact ratio spur gear.

The tapered roller bearing mounted with a helical gear for a planet system is shown schematically in Figure I–8. Tapered rollers with the tapers facing outward are required over spherical rollers for helical gears to resist the overturning

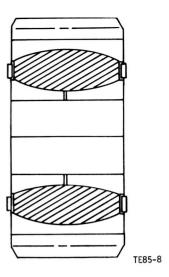


Figure I-9. Single row spherical bearing and high contact ratio spur gear.

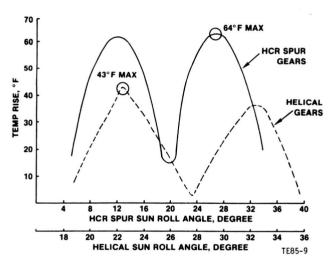


Figure I-10. Local temperature index of the gear mesh.

moment caused by the thrust loads at the meshes. The overturning moment causes a radial load on the two bearing rows that is additive to centrifugal load on one row and subtractive on the other row. To get equivalent resultant radial loads on the two bearing rows, the bearing centerline is offset from the gear mesh centerline. The bearing thrust rib is located at the outer race to provide for continuous cooling.

The single row spherical bearing mounted with a high contact ratio spur gear for a planet system is shown schematically in Figure I–9. The spherical seat allows the spur gears to locate themselves and reduce some misalignment errors. Because oil jetted at the outside of the roller may not get to the center of contact, lubrication is provided at the center of the inner race to ensure oil along the entire length of contact.

Two planetary gear sets were sized, each with one candidate planet form. The gear geometry of these gear sets are

Table I-VI. Candidate advanced technology gear sets.

High contact ratio spur gears	Helical gear
28	27
36	35
100	97
6	6
19	25
8.143:1	8.185:1
1320	1313
745	741
	ratio spur gears 28 36 100 6 19 8.143:1 1320

Table I-VII.
Candidate gear set evaluation data.

	High contact ratio spur gears	Helical gears
Face width — in. Center distance — in. Planet pitch diameter — in.	2.43 5.333 6.000	2.43 5.325 6.012
Sun/Planet Mesh		
Profile overlap face overlap Max sliding velocity — ft/min Contact stress — lb/in.² Sun bending stress — lb/in.² Planet bending stress — lb/in.²	1.34 5375 153,400 30,600 26,500	1.33 1.16 3042 168,300 25,500 22,500
Planet/Ring Mesh		
Profile overlap face overlap	2.95	1.44 1.15
Contact stress — lb/in.2	108,300	126,400

listed in Table I–VI. The results of these gear sets under 10,000 hp load is listed in Table I–VII. Because the planer pitch diameters, gear ratios, and diametral pitches are so similar, the comparisons are realistic. The high contact ratio spur gears have lower contact stresses but higher sliding velocity. This higher sliding velocity tends to produce elevated local temperatures. The local temperature index was calculated to quantify this case. The results of this calculation are shown in Figure I–10. High contact ratio spur gears have a significantly higher temperature rise than the helical gears.

Load parameters and results for each candidate bearing are listed in Table I–VIII. Bearing life is higher for the tapered roller bearing with a much lower stress level. Carrier rotational speed is equal in each case so separator centrifugal loads would be the same.

Table I–IX lists the significant comparisons between the two candidate planet forms. The gear forms are practically equal but the tapered roller bearings show a greater potential for life improvement because of their lower raceway contact stress. Therefore, the preliminary design will be based on a helical gear with tapered roller planet bearings in a differential planetary configuration.

COUNTER-ROTATION GEARBOX DESIGN CRITERIA

The gearbox technology level was established to be consistent with an early 1990s time period for first production. The design criteria assumed is summarized in Table I–X.

The gear tooth bending stresses are based on the Lewis calculation method at the high point of single tooth contact. The tooth contact stresses are based on the Hertzian calculation method for the pitch diameter meshing condition. The bending and contact stress allowables for the advanced technology gearbox were increased by 25% over current levels. This increase would be obtained through improved materials and lubrication life factors. An increase is justified based on the favorable fatigue testing of new gear materials that have shown life improvements as great as ten times that of currently used materials (Ref 1).

Gear pitch-line velocity limits were assumed to be identical for current and advanced technology designs. No need for increased velocity allowables are anticipated for the ad-

Table I-VIII.

Candidate bearing life comparison.

	Single row spherical	Tapered roller
Planet rotational speed — rpm	6,014	5,966
Carrier rotational speed — rpm	1,320	1,313
Relative rotational speed — rpm	7,334	7,279
Radial load from gear force — Ib	7,512	7,560
Gear centrifugal force — Ib	1,500	1,500
Roller centrifugal force — Ib	300	300
Bearing resultant load — rpm	7,725	4,435
Bearing radial rating — Ib	75,800	50,900
Life improvement factor	15	15
Individual bearing life — hr	68,900	117,000
Planet system life — hr	27,300	29,300
Raceway contact stress — lb/in.2	233,000	136,000

vanced technology design. This assumption was made because the increased gear material allowables anticipated for the advanced technology gearbox would tend to reduce pitch-line velocities due to the use of smaller gears.

Gear surface finish improvements for the advanced technology CR gearbox would provide gear life factor improvements. By improving the surface finish, the ratio of oil film thickness to flank surface finish between meshing teeth is increased and the mesh life is improved (Ref 2). The gear finish for the advanced technology CR gearbox was improved by 40% over current technology levels.

Three bearing criteria parameters were selected. These parameters consist of a spalling fatigue life factor, a bearing set life factor, and race/roller surface finish.

For the advanced technology CR gearbox, the bearing life factor was increased by 200% over current levels. This improvement would be obtained through improved materials and lubrication life factors. This increased life factor also is based on indications that current life factors may be conservative (Ref 3).

The mean time between unscheduled removal (MTBUR) was established at 30,000 hr. To meet this goal, a bearing (B_{10}) set life goal of 18,000 hr is required (refer to the Bearings description of the CR Gearbox Design Results section of this Appendix.)

Surface finish improvements of 40% for the advanced technology gearbox over the current technology gearbox were also specified for the bearings. The improved finishes were needed to provide the life improvements specified by the life factor goals.

Criteria was established for lubrication influenced parameters that includes allowable oil temperature rise, flash temperature index, and gearbox efficiency.

The oil temperature rise across the gearbox was increased by 50% for the advanced technology gearbox. This increase would allow a reduction in oil flow. Reduced oil flow decreases energy losses associated with gear and bearing windage and oil pumps.

The flash temperature index for current gearbox designs is limited to 370. This value is higher than the 290 rec-

Table I-IX.

Planet form selection.

	Single row spherical bearings with high contact ratio spur gears	Tapered roller bearings with helical gears
Gear contact stress — lb/in.2*	153,400	168,300
Gear bending stress — lb/in.2*	30,600	25,500
Sliding velocity — ft/min	5,374	3,042
Temperature index rise — °F	43	64
Bearing life — hr	68,900	117,000
Raceway stress — lb/in.2	233,000	136,000

Planet-Sun mesh

Table I-X.
CR gearbox design criteria.

Gear teeth	
Bending stress limit, Lewis — lb/in.2	50,000
Contact stress limit, Hertzian — lb/in.2	200,000
Pitch line velocity — ft/min	25,000
Finish, AA	6
Bearings	
Life factor	30
B ₁₀ set life — hr	18,000
Finish, AA	3
Allowable temperature rise — °F	90
Flash temperature index — °F	440
Gearbox efficiency — %	99.3

ommended by AGMA but is within successful Allison experience. The flash temperature index was increased approximately 20% for the advanced technology CR gearbox. This index, calculated using the AGMA method, is an indicator of the probability of gear tooth scuffing. Successful operation at higher flash temperature indexes is anticipated through use of high hot hardness materials, improved surface finishes, improved oils, and tooth surface treatments.

Improvements in gearbox efficiency for the advanced technology design achieve fuel savings and reduce the oil cooler size. Efficiency goals of 98.8% and 99.3% were selected for the 1980s and the 1990s gearboxes respectively. These efficiencies are at the take-off condition.

Table I-XI.

Parameters used to establish overall

CR gearbox gear ratio.

Engine power at take off — hp	10,000
Prop power at max (initial) cruise — hp	5,227
Disk loading at max cruise — shp/D ²	45.0
Prop diameter — ft	10.78
Prop tip speed — ft/sec	750
Prop rotational speed — rpm	1,329
Power section rotational speed — rpm	10,750
Desired gear set ratio	8.089:1

The gearbox design points are based on engine and propeller requirements. From the early phase of the APET the flight mission and engine power and speed relationships were determined. Using this data, Hamilton Standard defined the CR propfan size and speed. This formed the basis in the gearbox design points. Table I–XI lists the parameters defining the overall gear ratio.

COUNTER-ROTATION GEARBOX GENERAL ARRANGEMENT

A general arrangement of the advanced technology CR propfan gearbox is shown in Figure I–11. The gearbox main power gear train is a differential planetary gear set with four planet gears. The sun gear is driven by the input shaft, the outer output shaft is driven by the ring gear, and the inner out-

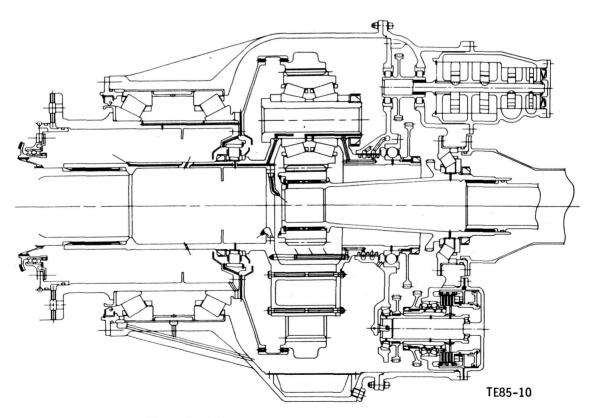


Figure I-11. Counter-rotation gearbox cross section.

but shaft is driven by the planet gear carrier. The single helical gears have the thrust load on the ring gear opposing the propfan thrust. The thrust is diagrammed in Figure I–12.

Cross section of a planet gear arrangement is shown in Figure I–13. The planet bearings are tapered roller bearings mounted in the indirect method that provides maximum stiffness. The thrust rib is on the outer race so that oil will be rapped by centrifugal action to provide continuous lubrication and cooling. The inner races are separated by an accuately ground spacer to set the correct amount of axial preload or endplay. Cooling oil is supplied to the bearings at he "sun" side of the small diameter of the rollers. Centrifugal orce will then carry the oil across the rollers as well as to the 'ring" side of the bearing. The cage is one piece machined steel and outer raceway guided to provide stiffness and strength at 260 g. The ring gear floats radially with two invoute splines providing the flexibility. These splines transmit hrust loads through captured snap rings.

The outer prop shaft bearings, shown in Figure I–14, are steep angled tapered roller bearings mounted in the indirect nethod. The steep angle creates a large, 12.8 in., base for support of the propfan. Loads from both propfan blade rows are supported by these bearings. A thrust rib located on the outer race provides continuous cooling. Fresh oil is supplied o the small end of the rollers. An oil dam on the inside of the outer output shaft separates areas of fresh and used oil. Fresh oil flows in the forward section to the propfan and the prop shaft bearings. Used oil from the propfan and the gear-pox flows in the rear area.

The input shaft bearing, shown in Figure I–15, is a steep angle tapered roller bearing. Only one bearing is located on the shaft since the other end of the shaft floats allowing the sun gear to locate itself among the planets. The steep angle, which provides a high thrust capacity bearing, supports the thrust from the helical sun gear. Lubrication is supplied under the inner race with oil jet holes at both the small end of the rollers and the thrust rib. At the outer race and the large

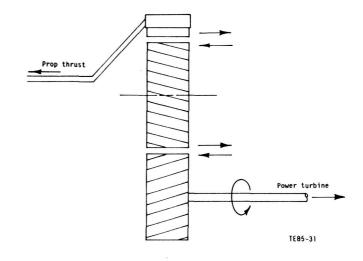


Figure I-12. Thrust diagram for the helical gearing.

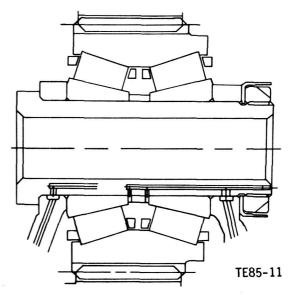


Figure I-13. Planet gear arrangement.

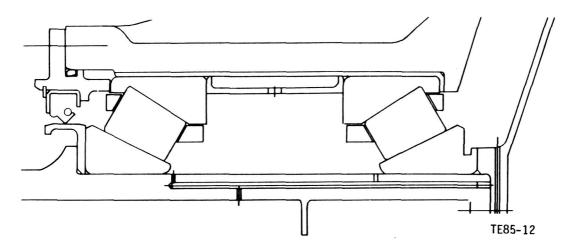


Figure I-14. Outer prop shaft bearing cross section.

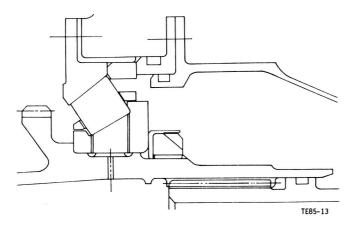


Figure I-15. Input shaft bearing cross section.

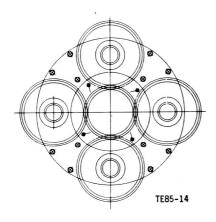


Figure I-16. Planet gear assembly.

roller end, there is a second thrust rib. This rib carries reverse thrust on the bearing and is estimated to be small and short in duration. Because the accessory gear is close to the bearing, its radial load has little effect on the floating sun gear.

The planet carrier is a combined shaft and structure that supports four planets equally spaced around the sun gear. The carrier also has a series of oil channels and jets that direct the fresh oil flow through the gearbox. Figure I-16 shows a cross-section of the carrier with the four planet gears. The large clearance between planet gears helps reduce heat generation. The oil jets on the sun gear are spraying on the out-of-mesh sides of the gear teeth.

The planet carrier is supported by a cylindrical roller bearing and a split inner ball bearing. The front carrier, shown in Figure I–17, is a cylindrical roller bearing with under the race lubrication. Baffles around the bearing direct the used oil from the bearing to the sump. On the inside of the inner output shaft is an oil dam that separates fresh oil in the rear area from used oil returned from the propfan located in the front area.

The rear carrier bearing, shown in Figure I–18, is a split inner ring ball bearing with under the ball lubrication supplying oil directly to the balls. Two oil glands, transferring fresh

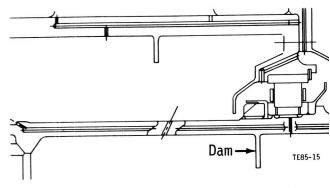


Figure I-17. Front carrier bearing cross section.

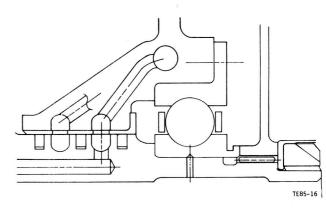


Figure I-18. Rear carrier bearing cross section.

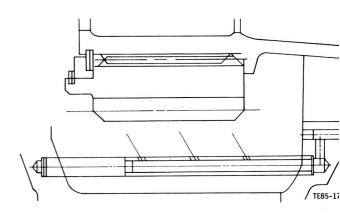


Figure I-19. Sun gear cross section.

oil from the housing to the carrier, are connected to the hig pressure line and the low pressure line, respectively. An accessory gear is attached to the carrier rear of the carried bearing.

The sun gear, shown in Figure I–19, is mounted to the input shaft on a helical spline. This helical spline transmit the thrust from the sun gear to the input shaft and keeps axis contact between the two on the thrust shoulder. Reverse thrust is held by snap rings. The spline is crowned and lubrated to provide flexibility to the sun gear.

In a differential system two of the three rotating part must be stopped to stop the system. The brake shown in Fig ure 1-20 stops both the input shaft and the planet carrier with one mechanism. One accessory gear is connected, through a series of idlers, to the input shaft while the other accessory gear is connected, through a second set of idlers, to the planet carrier. Each gear is also connected to a flat

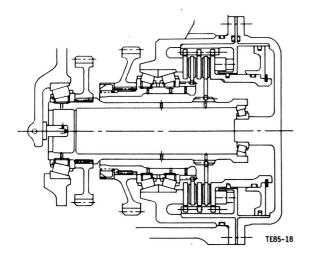


Figure I-20. Prop brake cross section.

friction disk by a shaft. These two friction disks can be clamped with non-rotating reaction disks in a brake mechanism. This brake is spring applied and oil pressure released for a fail safe feature. The brake assembly is modular so it can be replaced quickly.

The oil pump, shown in Figure 1–21, is a modular unit base on Gerotor type pumps. There are four separate pumps in the pump unit: two scavenge pumps, one high pressure lubrication pump and one low pressure lubrication pump. Each pump will be capable of scavenging all the gearbox and propfan oil. Inlets to each pump would be at locations to insure scavenging to all attitudes.

The airframe to gearbox mount points are located in the front section of the gearbox near the prop shaft bearings to reduce the effect of propfan loads on the housing. These mount points are displayed in Figure I–22. Additional mount points toward the input end of the gearbox are provided for gearbox–to–engine brackets.

Figure I-23 shows a cross-section of the gearbox, propfan spinners, and propeller pitch change mechanism.

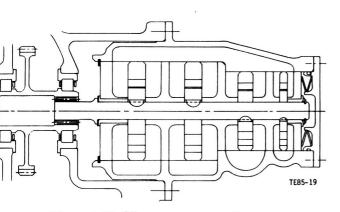


Figure I-21. Oil pump cross section.

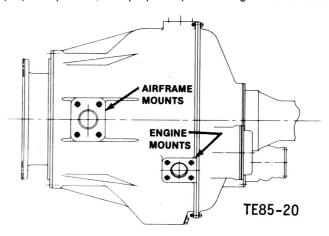


Figure I-22. Counter-rotation gearbox side view.

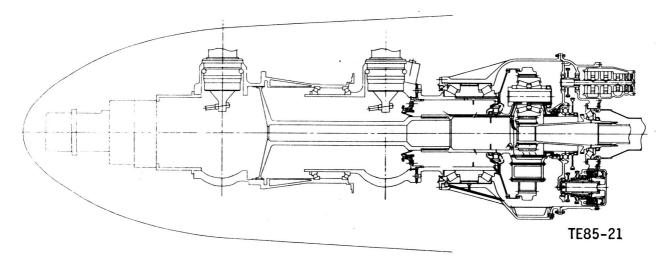


Figure I-23. Propfan/counter-rotation gearbox assembly.

Tapered bearings are used to connect the front spinner with the rear spinner. Lateral, axial and moment prop loads from both rows of blades are carried through the rear spinner, through the curvic face coupling to the outer output shaft and the gearbox prop bearings. Torsional load from the ring gear drives the rear spinner through the curvic while the planet carrier drives the front spinner through the quill shaft. The prop end of the quill shaft works through a large diameter spline that promotes flexibility and reduces thermally induced thrust loads on the rear carrier bearing.

The connection area between the propfan and the gearbox is shown in Figure I–24. The quill shaft in the propfan extends farther than the curvic coupling so this spline can be aligned while still visible. The spline connecting the quill shaft with the carrier is a crowned helical spline. The helix angle of the spline pulls the shaft tight against the thrust seat to axially fix the shaft. The thrust seat is spherical and combines with the crowning of the spline to enhance flexibility.

A scale view of the APET engine, gearbox and counter rotation propfan is shown in Figure I–25.

COUNTER-ROTATION GEARBOX DESIGN RESULTS

Gearbox Loading

The three power levels used in the design of the gearbox were 10,000 hp takeoff, 5,227 hp initial cruise, and 5,980 hp cubic mean power. The 10,000 hp takeoff rating was used to

size all gears. Gearbox heat generation and efficiency were also determined at this power level.

The 5227 hp initial cruise power (maximum cruise power) was used to determine the gearbox heat generation and efficiency.

The individual bearing lives, bearing set lives, and lubrication life factors were determined at 5980 hp cubic mean

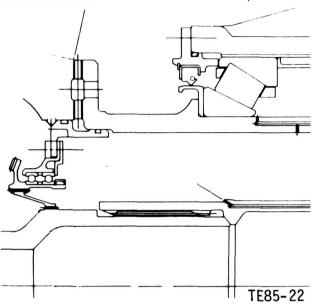


Figure I-24. Propfan/gearbox attachment.

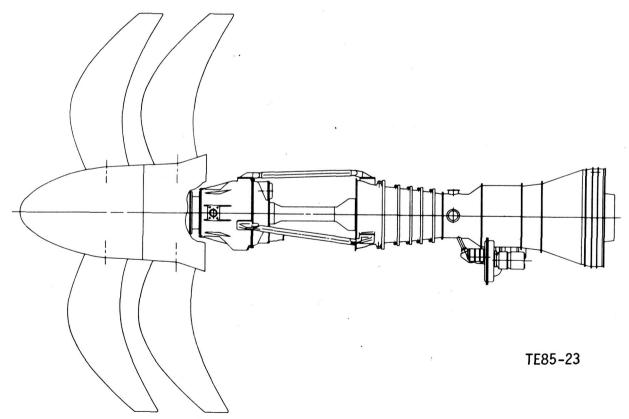


Figure 1-25. Counter-rotation gearbox propulsion system.

Table I-XII. CR gearbox mission requirements.

10,000 shp size engine at SLS rated power — unity engine uninstalled shp (PD436-10) axial/centrifugal

APET 300 nmi revenue mission results

Mission phase	Time — min	Alt —	Velocity — M _N	Power setting	Power turbine shp	Propfan* shp
Start and warm-up allowance	15.0	SL	0	6% max cruise power	480	351
Take off allowance First climb	1.0	SL	0	Take off power	10,000	9,776
(SL to 10,000) Second climb	4.0	5,000	0.4	Climb power	9,280	9,063
(10,000 to 30,000)	17.1	20,000	0.6	Climb power	7,630	7,430
Cruise	14.7	32,000	0.72	87% max cruise power	4,700	4,529
Descent (30,000 to SL)	10.5	15,000	0.6	6% max cruise power	440	312
Total time	62.3					

^{*}Includes gearbox efficiency losses and accessory losses

power. This power level was based on the 300 nautical mile mission defined in earlier tasks and shown in Table I–XII. The cubic mean effective power was calculated as shown in the following equation:

CMP =
$$[(480)^3 (15.0/62.3) + (10,000)^3 (1.0/62.3) +$$

 $9280^3 (4.0/62.3) + (7630)^3 (17.1/62.3) + (4700)^3$
 $(17.1/62.3) + (440)^3 (10.5/62.3) = 5980 \text{ hp}]^{1/3}$

Propfan loads were also included in the life analysis of the propshaft bearings. The propfan loads used were a 1P moment load of 4643 ft-lb in the horizontal plane, a 1P side load of 1907 lb acting down in the vertical plane, and a 5000 lb thrust load.

Gears

The gears will be manufactured from an advanced gear steel. The advanced steel would have improved fatigue strength/stress allowables and hot hardness characteristics in comparison to AMS 6265, which is used for current gears. This advanced gear steel is discussed in Appendix K, Task XIII, Research and Technology Plan for Tasks XI and XII. Powder metal steels such as MCR 2001 and wrought low carbon steels such as CBS 600 are also discussed. These steels would be VIM VAR melted, and the powders would be rapidly solidified to provide high cleanliness and fine grain structures.

Advanced manufacturing techniques would need to be developed and applied to the advanced gears. These processes include hot isostatic press/hot forged to near net shape and advanced contour induction hardened for the

Table I-XIII.
Planetary gear set geometry.

Number of teeth, sun	27
Number of teeth, planets	35
Number of teeth, ring	97
Pitch diameter, sun — in.	4.5818
Pitch diameter, planets — in.	5.8569
Pitch diameter, ring — in.	16.2319
Center distance — in.	5.1875
Face width — in.	2.43
Pressure angle — deg	22.11
Helix angle — deg	14
Diametral pitch	5.976
Profile surface finish — microinches	6

powder metal steels. Both the powder and wrought steels would be machined to ultra smooth surface finishes, and flank surfaces would be treated with techniques such as ion implantation or TiN coatings. Fatigue life/stress allowable improvements, cost reductions, and reduced heat generation during tooth meshing would result from these advanced processes.

The gear geometry for the planetary gear set is shown in Table I-XIII.

The results of gear analysis at the maximum horse-power condition are listed in Table I–XIV.

Contact and bending stress values are derived from the Hertzian and Lewis stress equations, respectively. The contact stress and the bending stress are calculated at the high point of single tooth contact. The gears were not stressed to the maximum levels defined in CR Gearbox Design Criteria because the planet bearing life is the limiting criteria. This forced the planet gears to be larger.

The gears were sized by the safe stress method. This method is based on the assumption that the gear steel has a fatigue endurance limit greater than the stress criteria. Thus, designing the gears to the stress criteria, at the maximum power condition, results in an infinite gear fatigue life. The values in Table I–XIV were calculated at the maximum horsepower of 10,000 and the maximum gearbox input speed of 10,878 rpm.

The helical gears result in a low bending stress. Low bending stress results from the axial load sharing between adjacent gear teeth created by the face overlap of gear teeth. A face overlap greater than one ensures that there are always two teeth or more in contact.

Pitchline velocity, oil film ratio, lubrication life factor, maximum sliding velocity, and scoring index, also listed in Table I–XIV, are used as indications of scoring/scuffing probability. Scoring is damage on the tooth flank that results from a breakdown of the lubrication film between the gear teeth.

The film breakdown allows metal to metal contact resulting in radial scratches due to localized welding. This scoring is a function of gear blank temperature, contact pressure, surface finish, and the relative sliding velocity. High blank temperature, excessive heat generation due to high sliding velocities, and high contact pressure tend to reduce film thickness. Thus, metal to metal separation is also reduced. Excessive surface roughness also allows a reduction in the metal to metal separation distance.

Pitchline velocity and sliding velocity are indicators of the severity of the sliding environment. Oil film ratio and lubrication life factor are indicators of the quality of the lubrication film. Flash temperature index accounts for the effects of temperature, pressure, velocity, film thickness, and surface roughness.

The maximum sliding velocity falls within Allison experience. The pitchline velocity is low for set lubricated gears

Table I-XIV.

Planetary gear set operating parameters.

Input speed — rpm	10,878
Ring/carrier speed — rpm	1,329
Planet speed — rpm	6,037
Pitch line velocity — rpm	11,300
Contact stress, sun to planet — lb/in.2	180,400
Contact stress, planet to ring — lb/in.2	98,500
Bending stress, sun — lb/in.2	32,900
Bending stress, planet — lb/in.2	24,600/27,600
Bending stress, ring — lb/in.2	2,470
Oil film ratio, lambda	1.31
Lubrication life factor	1.0
Maximum sliding velocity — ft/min	3,364
Scoring index — °F	211
Profile overlap, sun to planet	1.459
Profile overlap, planet to ring	1.408
Face overlap	1.15

and the scoring index is in the low probability of scoring region. The oil film ratio, calculated by the Hamrock–Dowsor method (Ref 4 and 5), shows a stable oil film. For these reasons scoring should pose no problem.

Bearings

The bearings for current CR gearbox designs are manufactured from double vacuum melted (VIM VAR) M50 steel. The bearings for the advanced CR gearbox would be manufactured from an advanced bearing steel. This steel would provide improvements in fatigue strength, corrosion resist ance, fracture toughness, micro-damage tolerance, and wear/skid resistance over VIM VAR M50. The advanced stee will be derived from the technology program discussed in Appendix K. The steel would also need to have excellent geal properties since the planet bearings are integral with the gear.

Advanced manufacturing techniques would be developed and employed on the bearings. These processes in clude hot isostatic pressing (HIP) and advanced contou induction hardening for the powder metal steels. Ultramooth surface finishing techniques will also be used o both types of steels. These processes contribute to fatigulife improvements and cost reductions.

There are 13 bearings in the advanced CR gearbox Eleven of these bearings are tapered roller bearings the have good properties for gearboxes because of their high capacity, thrust carrying ability and stability in close mount situations. There is also one cylindrical roller bearing and on split inner ring ball bearing. Table I–XV lists the bearing geometry.

It is estimated that a 18,000 hr set life will satisfy th gearbox MTBUR goal of 30,000 hr. The derivation, based o Allison T56 experience, is as follows:

- 30,000 hr MTBUR represents a removal rate of 0.033/1000 hr.
- Allison's experience indicates that 50% of unscheduled high-power gearbox removals are due to bearing failures. Thus, the gearbox removarate due to bearing failures is 0.017/1000 hr.
- Allison experience indicates that 10% of bearing problems are associated with contact fatigue. This record can be improved for advanced gearbox designs. Non-fatigue bearing failures will be reduced by improved design techniques for separators, lubrication management, etc. Therefore, assuming 33% of the bearing failures will be fatigue oriented results in a bearing failure rate associated with unscheduled gearbox remova of 0.006/1000 hr.

Table I-XV. CR gearbox bearing geometry summary.

or tapered
1.20 K
0.59 K
0.50 K
nm 15 mm x 17 mm
nm ²¹ / ₃₂ "
r

Table I-XVI. CR gearbox bearing life summary.

Location	Quantity	B10 life, hours
Planets	8	83,700
ront prop shaft	1	1,380,000
Rear prop shaft	1	1,870,000
nput shaft	1	300,400
Front carrier	1	45,000,000,000
Rear carrier	1	237,100
system life		20,300

- Approximately 50% of the bearing fatigue failures are discovered at disassembly and do not cause a gearbox removal. This establishes the total bearing fatigue failure rate of 0.011/1000 hr. Taking the reciprocal results in a 50% bearing life failure (B₅₀) set life of 90,000 hr.
- Assuming a typical Weibull slope of 1.1 gives a bearing life failure (B₁₀) set life of 18,000 hr.

The individual bearing lives and the bearing set lives are shown in Table I-XVI. The Weibull slope for the gearbox bear-

The operating conditions of the planet bearings are isted in Table I-XVII. Comparing the lives of the individual pearings shows the planet bearings to be the critical component in the bearing life of the gearbox. The planet bearing ives are largely influenced by the weight of the planet. For his reason the planet design must be optimized for maxinum stiffness with minimum weight.

Tables I-XVIII, I-XIX and I-XX show the operating condiions of the prop shaft, input shaft and carrier bearings, respectively. All operating conditions are defined at the mean cubic power of 5980 hp.

Table I-XVII. Planet bearing design parameters.

Bearing load from tangential gear forces — Ib	7,760
Gear centrifugal force — lb	2,782
Roller centrifugal force — lb	300
Bearing resultant load — Ib	4,508
Bearing radial rating — Ib	38,000
Life factor	30
B ₁₀ life — hr	83,700

Table I-XVIII. Prop shaft bearing design parameters.

Ball size

Radial load on front bearing — lb	6,090
Radial load on rear bearing — lb	3,990
Propeller thrust load — Ib	5,683
Helical gear thrust load — Ib	3,824
Front bearing resultant load — lb	6,090
Rear bearing resultant load — lb	5,555
Bearing radial rating — Ib	71,450
Life factor	30
Front bearing B ₁₀ life — hr	1,380,000
Rear bearing B ₁₀ life — hr	1,870,000

Table I-XIX. Input shaft bearing design parameters.

Thrust load — Ib	3,856
Reverse thrust — Ib	40
Bearing radial rating — Ib	16,800
Bearing thrust rating — Ib	53,600
Life factor	30
B ₁₀ life — hr	300,400
Rib stress — lb/in.2	45,100

Table I-XX. Carrier bearings design parameters.

Radial load on front bearing — Ib	101.5
Dynamic capacity of front bearing — Ib	26,870
Front bearing L ₁₀ life, hours	4.5 x 10 ₁₀
Radial load on rear bearing — Ib	70.2
Thermally induced thrust load	
on rear bearing — Ib	2,298
Resultant load on rear bearing — Ib	1,774
Dynamic capacity of rear bearing — Ib	15,210
Rear bearing L ₁₀ life — hours	237,000

Structure

Two major components in a planetary gear set structure are the external housing and the planet carrier. The external housing is made from cast aluminum, which provides better corrosion resistance than current magnesium housings. Creep resistance is not as critical for a planetary housing as for a parallel gear housing, because gear alignment is determined by the carrier. Housing movements determine spline alignment and bearing alignment both of which can be designed more tolerant than gear teeth.

The planet carrier is designed as a steel framework. Steel provides excellent stiffness and creep resistance for good alignment of the gear teeth. It also provides good fatigue strength and wear resistance for the integral shaft and spline portions. Weight is minimized by removal of unnecessary material.

Propfan Interfaces

Interface requirements between the gearbox and the propfan have been kept to a minimum. This simplicity improves the maintainability of both the propfan and the gearbox.

The propfan assembly is mounted to the gearbox by a curvic coupling that is directly connected to the gearbox outer output shaft. Flange details are listed in Table I-XXI.

The inner output shaft drives a quill shaft through an involute spline. This spline is helical, which creates an axial force that will force the shaft against the spherical seat. The details of this spline are listed in Table I-XXII.

Fresh oil is supplied to the propfan at the inside of the outer output shaft. Centrifugal action causes the oil to flow into the rear propfan spinner where it is scavenged by pumps. The heated, used oil is returned to the inside of the inner shaft. The gearbox returns this oil to the sump where it is cooled and filtered.

Control signals are transferred to the propfan by a capacitive coupling system. Provisions were made to attach the stationary component to the gearbox housing.

Weight, Cost, and Size Comparisons with Single Rotation Gearbox

Estimates of the gearbox weight and cost were made based on a detailed weight analysis of the individual compo-

Table I-XXI.
Propfan-gearbox curvic coupling dimensions.

Outside diameter — in.	13.75
Inside diameter — in.	10.25
Bolt circle diameter — in.	12.00
Number of bolts	24
Bolt size — in	9/16

Table I-XXII. Inner output shaft drive spline parameters.

Number of teeth	36
Diametral pitch	8/16
Helix angle — deg	1
Contact length — in.	2.50
Radius of crown — in.	156
Maximum contact stress — Ib/in 2	27 400

nent parts. The resulting weight estimate is 548 lb. The acquisition price is estimated to be \$149,500*. The maintenanc cost for the gearbox was estimated at \$1.01* per enging flight hour using the same procedures used for the single rotation gearbox discussed in Appendix F. A comparison of the counter rotation gearbox with the single rotation, 1990s gearbox is shown in Table I–XXIII.

COUNTER-ROTATION GEARBOX POWER LOSS

The CR gearbox design was analyzed for power loss t determine both gearbox performance and cooling requiments. The analysis follows that described in Ref 6 in whice the Allison T56–501 turboprop gearbox was analyzed for power loss and compared to measured test data. In the study, the predicted efficiency was found to be 0.3% higher than that measured. The calculated values listed in Tables I XXIV, I–XXV, I–XXVI and I–XXVII were decreased by 0.3% to be consistent with previously measured data.

Gear power loss was calculated by the method of Ar derson and Loewenthal described in Ref 7. It was modified thandle the helical gear geometry found in the CR gearbor. This method allows independent calculation of gear sliding rolling and windage losses. The friction coefficient developed in Ref 6 for a MIL-L-7808 lubricant was used her since it is expected to best approximate the friction characteristics of the advanced CR gearbox oils proposed for the gearbox. Losses were evaluated at both takeoff and cruis conditions as shown in Table I-XXIV.

Tapered roller bearing power loss was evaluated by the method of Witte described in Ref 8, the lightly loaded carries support bearings were analyzed by methods described Harris (Ref 9). The results are shown in Table I–XXV.

Oil pump losses were calculated using the followir equation.

Table I-XXIII.

Comparison of single-rotation and counter-rotation gearboxes.

Single rotation	Counte rotation
23.22	28.13
31.62	23.25
26.75	22.25
26.75	18.00
745	404
14.38	0
640	548
\$165,000	\$149,500
\$1.08	\$1.01
	23.22 31.62 26.75 26.75 745 14.38 640 \$165,000

^{*1984} year dollars

HP Loss = (Q)(H)/(33.000)(EFF)

nere:

HP loss = oil pump power loss, horsepower

Q = oil flow rate (lbs/min) H = oil pressure head (ft)

EFF = pump mechanical efficiency

The oil flow rates and oil pressure head were deterined as discussed in the lubrication section. Supply pump ficiency was assumed to be 35% while scavenge pump efciency was estimated to be 20% due to the highly aerated ate of the oil after passing through the rotating compoents. The oil pump specifications are shown in Table I–XXVI.

The results of the CR gearbox power loss analysis are nown in Figure 1–26 and Table I–XXVII at both cruise and keoff power levels. Efficiency indications of this gearbox arngement appear relatively high, 99.18% at cruise and 0.24% at full power. Improvements in sliding loss will probay result as tooth proportions are selected or minimum slidg velocities. This will in turn reduce the rather high sliding

Table I-XXIV.
CR gearbox gearing losses.

	Power level	
	Cruise — hp	Takeoff — hp
un/planet mesh		
Sliding loss	5.33	25.81
Rolling loss	1.03	1.02
anet/ring mesh		
Sliding loss	3.29	13.23
Rolling loss	1.08	1.07
indage		
Sun gear	0.48	0.50
Planet gears	0.40	0.42
Ring gear	0.06	0.06
Carrier	0.16	0.17
ccessory gears	1.10	1.16
tal gear loss	12.93	43.44

Table I-XXV.
CR gearbox bearing losses.

	Pow <u>er</u> level	
	Cruise — hp	Takeoff — hp
anet	8.69	11.53
in gear thrust	5.37	7.19
ор	4.31 ,	6.47
rrier-front	0.41	0.42
rrier-rear	0.17	0.18
tal bearing loss	18.95	25.79

Table I-XXVI.

Oil pump parameters and power loss.

	Flow rate — GPM	Pressure — Ib/in.² gage	Power loss — hp
Sun gear supply	7.5	80	1.6
Trans supply	8.1	30	0.6
Scavenge pumps	16.0	30	4.5

loss shown in Figure I–26. Rolling power loss is not significant due to the moderate film thickness values found for the heavily loaded teeth. The use of tapered roller bearings in many locations accounts for the high power loss of the bearings. These bearings are best suited for reacting the helical gear loads, however. Windage losses are a very small part of the total loss. Oil pump power loss is presently a small percentage of the total gearbox loss. These losses are not likely to fall any lower and might increase if the pump efficiency level of 35% cannot be reached.

COUNTER-ROTATION GEARBOX LUBRICATION SYSTEM

The CR gearbox lubrication system must provide an adequate supply of clean, cooled lubricant to both the gearbox and the prop pitch–change–mechanism. The system also must be designed to minimize parasitic losses such as oil churning, windage and oil pump power requirements. To accomplish these objectives, oil flow paths were selected to provide once through lubrication to all heat generating components. Extensive use was made of shaft rotation to centrifuge oil back to the housing sump and to eliminate entrained air at the same time. Oil pressure requirements were analyzed. These considerations led to a two pump constant flow/constant pressure lubrication supply system. The lubrication is shown schematically in Figure I–27.

Oil pump power requirements were minimized by supplying high pressure oil only to the sun/planet mesh. This is the only gearbox location requiring a high pressure jet of oil for adequate lubrication. The required pressure of the high pressure system was found to be 80 lb/in.² gage. All other lubrication lines required only 30 lb/in.² gage.

The two oil supply pressures will be provided by two independent oil pumps to avoid throttling losses. The prop

Table I-XXVII.
CR gearbox power loss breakdown.

	Power level	
	Cruise, hp	Full power, hp
Gears	12.93	43.44
Bearings	18.95	25.89
Oil pumps	6.61	6.91
Total loss	38.49	76.14

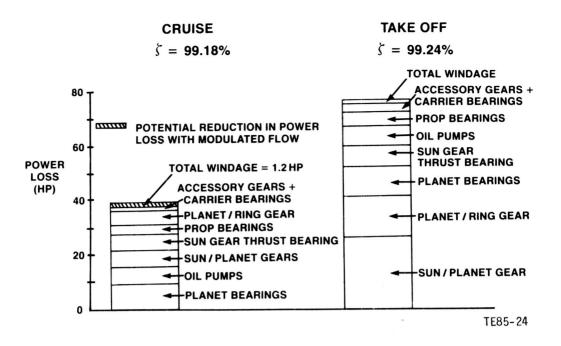


Figure I-26. Counter-rotation gearbox power loss breakdown.

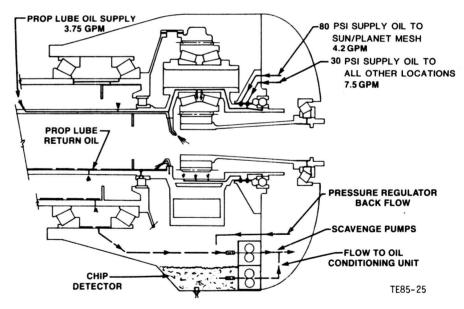


Figure I-27. Lubrication schematic diagram.

pitch change mechanism is supplied with oil at a rate of 3.75 GPM at 30 lb/in² gage which will be cooled and filtered by the gearbox lubrication system.

A fully modulated oil system was investigated but not implemented. Referring to Figure I–26, the only losses that would be affected by reducing the oil flow are the windage losses. Since the windage losses are such a small percentage of the total losses, there is little incentive to provide modulated oil flow. However, in a system where considerable oil

churning is present, a reduction in oil flow will reduce the gearbox loss. Churning losses are expected to be minimal in this gearbox.

The CR gearbox lubrication system will be independent of the engine oil supply system. This will allow the use of modern, high capacity gearbox oils such as Aeroshell 555 or Exxon Turbo Oil 25. These lubricants are particularly suited to aircraft gearbox systems and as such have demonstrated higher load capacity and higher allowable operating temper-

atures. Since this gearbox would include the latest technology available for aircraft transmission design, incorporation of an advanced lubricant would also be included.

Two scavenge pumps are used to remove oil from the gearbox: one scavenging the prop bearing area, the other the main gearbox sump. To scavenge oil at high altitudes these pumps are oversized. Scavenge pumps deliver oil to the oil conditioning exit shown in Figure I–28. Since this return oil contains any debris generated in the gearbox it is first directed through a lubrication (centrifuge device) equipped with a quantitative debris monitoring (QDM) sensor. The TEDECO QDM system will be used for monitoring debris in the lubrication system. This system captures, counts, and discriminates by size the ferrous particles generated in the CR gearbox. Differentiation between progressive and non-critical debris generation conditions avoid insignificant indications.

The oil is then directed to the oil tank where de-aeration takes place. A low pressure pump will drain oil from the tank and send it through an oil filter. Three micron filtration will be specified for this gearbox to help meet the 30,000 hour MT-BUR. Assuming that all bearings and gears have been designed for adequate fatigue life, the predominant failure mode will become surface originated failures. Fine filtration has been shown to be required in long life systems due to the inevitable generation of wear particles in mechanical systems (Ref. 10).

The oil will then either flow through the air/oil heat exchanger if it needs cooling or it will bypass the cooler completely. At this point, about one third of the oil is boosted to 80 b/in.² while the balance remains at 30 lb/in.². The boost pump used to create the higher pressure will be driven independently of the low pressure pump. If a low pressure pump

fails, the boost pump will supply oil to the sun gear mesh. The CR gearbox could then function for a limited amount of time after an oil pump failure.

Most of the oil supplied to the gearbox is centrifugally thrown off the rotating components after providing the required cooling. This will aid in reducing the possibility of oil churning. Components that could trap oil in a rotating annulus will have passages to allow the oil to exit. Oil being returned from the pitch change mechanism will flow into the inner prop drive shaft. Centrifugal pressure will force this oil to flow through the outer prop shaft and then to the drain port between the prop shaft bearings.

An oil cooler installation study was undertaken to address oil cooler size. Both air/oil and fuel/oil heat exchangers were considered. For this study it was assumed that all heat generated in the gearbox at takeoff conditions was to be removed by the cooling oil. Convective cooling was assumed to be zero.

Although the potential for rejecting the gearbox heat to the fuel system exists, it could not be fully explored in this study. Heat input of this magnitude must be considered in the initial design of the fuel control system.

An air/oil heat exchanger sized for the CR gearbox is shown in Figure I-29. The oil temperature difference of 90 °F is consistent with the 1990s advanced technology definition. A heat exchanger sized for a more typical oil temperature difference of 50 °F is only slightly larger — 15.50 x 15.08 x 3.84 in. at a weight of 22 lb. The heat exchanger was selected for a typical value of air pressure drop of 5 inches of water. The size of the unit must be balanced against airflow requirement. This core size is close to optimum for the requirements listed in Figure I–29. The size of the cooler and weight are very reasonable for a 10,000 hp drivetrain.

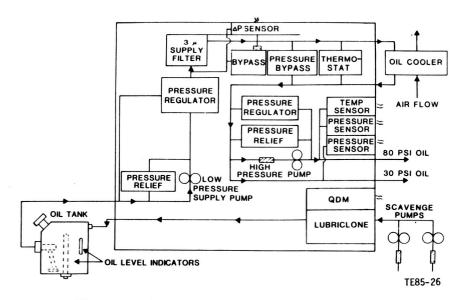


Figure I-28. Oil conditioning unit schematic diagram.

Installation of this oil cooler in the CR propfan nacelle might be similar to that shown in Figure I–30. A submerged ram–air inlet similar to that being proposed for the single rotation propfan test assessment (PTA) demonstrator is shown. This type of arrangement has been developed for turboprop aircraft by Lockheed. A thermostatically controlled flap on the duct exit is used to control oil temperature and eliminate drag losses when cooling is not required. During cruise conditions this flap is open very slightly causing most of the incoming air to bypass the inlet. Airflow can also be forced to flow through the oil cooler while on the ground prior to takeoff by setting the flap angle correctly. With the prop rotating

slowly a slight vacuum is created at the duct exit causing air to flow through the heat exchanger. This moderate amount of cooling is enough to allow control of the oil temperature on hot days prior to takeoff.

Calculation of the performance penalty associated with this type of inlet is difficult since the nacelle is not defined at this time. Work on this type of duct done by the National Advisory Committee on Aeronautics (NACA) in the past has shown that it can be designed to be very efficient. To determine an upper bound on performance penalty associated with gearbox oil cooling, an electric motor driven blower was sized for this cooler. Its installation is shown in Figure I–31.

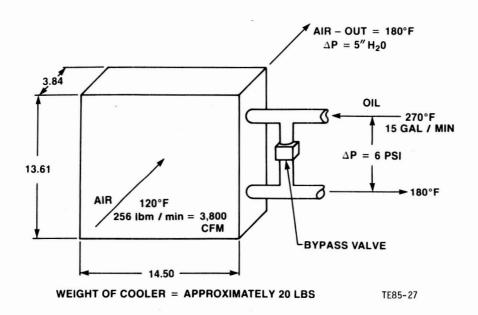


Figure I-29. Ram air oil cooler specifications.

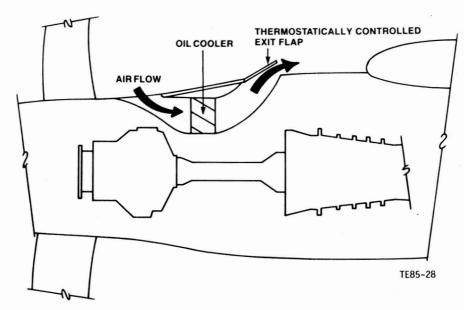


Figure I-30. Nacelle-mounted ram air cooler.

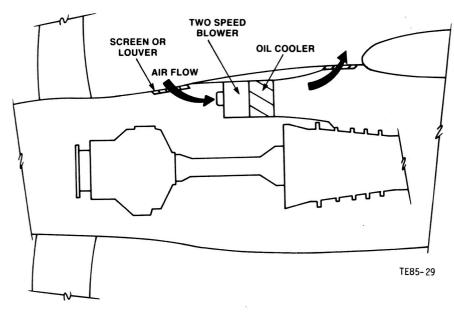


Figure I-31. Blower/air cooler arrangement.

An air inlet, per se, is not required but air must be allowed to enter and exit the nacelle freely through a screen or louvers. The blower shown is typical of those used in helicopter applications using three phase 400 hz power. The blower weighs 22 lb and requires 8 hp at full speed. This system then imposes an overall performance penalty of 0.08%. For flight conditions other than takeoff the blower can be switched to a lower speed to reduce the power requirement. A well designed inlet would reduce this power consumption even further.

In summary, the oil cooler required for the CR gearbox is neither large nor heavy. It should not be difficult to install the cooler in the nacelle, and the performance penalty associated with the oil cooler system is very small.

MODIFICATIONS FOR PUSHER CONFIGURATION

Changes to the gearbox for a pusher application are needed in three areas: bearings, structure, and lubrication. The gearing system does not have to be changed since the helical forces are in the proper direction without changing the hand of the helix.

Two bearing sets need to be changed for the pusher gearbox. The offset in the planet bearing centerline, allowing the equivalent radial load to be equal, needs to be at the op-

posite side from the tractor planet application. The planet could be designed with no offset for flexibility, but bearing life would be sacrificed. The input shaft bearing must support thrust forces in the opposite direction from the tractor design. The input shaft tapered roller bearing could be designed with the taper in the opposite direction. A crossed roller bearing could be designed as the input shaft bearing. This would give the flexibility of either application with the reduction of life not critical to the overall system life. The prop shaft bearings and the carrier bearings do not have to be changed.

The structure needs to be redesigned for a pusher application. The aircraft framework will not be able to reach through the engine exhaust to get to the mounts at the small end of the gearbox. A more likely structure will have three or more struts connecting the cover of the gearbox to the aircraft frame. The engine will then be mounted to the aircraft and not to the gearbox. The drive shaft to the gearbox from the engine will have to work through a flexible coupling to accommodate the increase in misalignment.

Lubricating jets for the sun gear in the planet carrier need to be adjusted. The sun gear is loaded on the opposite so the jets need to cool this side. The oil pump will rotate in the opposite direction and will need to accommodate this. All other lubrication uses centrifugal force so modifications are not needed.

REFERENCES

- D. P. Townsend, R. J. Parker, and E. V. Zaretsky, "Evaluation of CBS 600 Carburized Steel as a Gear Material," NASA TP 1390, 1979.
- E. N. Bamberger, T. A. Harris, W. M. Kacmarsky, C. A. Moyer, R. J. Parker, J. J. Sherlock, and E. V. Zaretsky, "Life Adjustment Factors for Ball and Roller Bearings. An Engineering Design Guide," ASME, 1971.
- D. G. Lewicki, J. D. Black, M. Savage, and J. J. Coy, "Fatigue Life Analysis of a Turboprop Reduction Gearbox," AIAA 84–1384, presented at the AIAA 20th Joint Propulsion Conference, Cincinnati, Ohio, 11–13 June 1984.
- B. J. Hamrock and D. Dowson, "Isothermal Elastohydrodynamic Lubrication of Point Contacts III — Fully Flooded Results," Journal of Lubrication Technology, April 1977, pp 264-276.
- H. S. Cheng, "Prediction of Film Thickness and Traction in Elastohydrodynmic Contacts," ASME Design Engi-

- neering Technology Conference, ASME, New York City, 1974, pp 285–293.
- N. E. Anderson, S. H. Loewenthal, and J. D. Black, "An Analytical Method to Predict Efficiency of Aircraft Gearboxes," NASA TM 83716; June 1984.
- N. E. Anderson and S. H. Loewenthal, "Spur Gear Efficiency at Part and Full Load," NASA TP 1622, 1980.
- 8. D. C. Witte, "Operating Torque of Tapered Roller Bearings," ASLE Paper 72LC-2C-1, 1972.
- 9. T. A. Harris, "Rolling Bearing Analysis," John Wiley and Sons, Inc. 1966, pp 446–450.
- S. H. Loewenthal, D. W. Mayer, and W. M. Needleman, "Effects of Ultra-Clean and Centrifugal Filtration on Rolling-Element Bearing Life," NASA TM 82660, 1982.

APPENDIX J

TASK XII. COUNTER-ROTATION PITCH CONTROL AND MECHANISM

TABLE OF CONTENTS

	rage
oduction	J-1
ceptual Design of the Counter-Rotation Pitch Change Control and Mechanism	J-2
Current Technology Overview	J-2
Trade Studies	J-3
Conceptual Design of Selected Concepts	J-7

LIST OF ILLUSTRATIONS

igure	litte	Page
J-1	Counter-rotating turboprop in-line gearbox configuration	J-2
J-2	Counter-rotating turboprop in-line gearbox configuration	J-3
J-3	Rotary hydraulic propfan power system from trade study	J-5
J-4	Rotary hydraulic control system concept	J-6
J - 5	Rotary hydraulic pitch control concept	J-8
J-6	Hydraulic system diagram (rotary)	J-9
J-7	Rotary/linear hydraulic pitch control concept	J-11
J-8	Hydraulic system diagram (rotary/linear)	J-12
J - 9	Linear hydraulic pitch control concept	J-13
J-10	Hydraulic system diagram (linear)	J-14
J-11	Advanced technology features requiring additional development	J-15
J-12	Modular design concept of propfan assembly	J-15

PRECEDING PAGE BLANK NOT FILMED

LIST OF TABLES

Table	Title	Pag
J-I	Power system concept ranking	J–
J-II	Blade angle feedback sensor ranking	J-
J-III	Single transfer ranking	J–
J-IV	Control system ranking	J–
	Pitch control concept ranking	
J-VI	Slew rates	J-1
J-VII	Blade angle setting	J-1
J-VIII	Unscheduled removals (all causes)	J-1
J-IX	Propfan reliability summary	J-1

INTRODUCTION

Task XII focused on the conceptual design of a counterotation (CR) pitch control and mechanism for the 10,000shp advanced propulsion system of Task III. This design is an
extension of work performed in Task III, which assumed a
state-of-the-art linear hydraulic piston type actuator, a beta
control valve, blade drive links, a mechanical in-place pitch
ock, an input shaft, and an oil transfer housing. The advanced system defined in Task XII provides for improved reliability and maintenance required for commercial airliners
and expected of propfan propulsion verification. The mission
s a 120-passenger advanced design airliner capable of
cruising at 0.72 Mach Number at a 32,000 ft altitude. The

pitch change mechanism is designed to the same propfan requirements as the CR gearbox described in Appendix I.

This pitch change system conceptual design was fully integrated with the advanced gearbox of Task XI so that maintenance of the pitch change control, pitch change mechanism, propfan, and gearbox can be accomplished in an economical and efficient manner. Sufficient details were defined to establish estimates of acquisition and maintenance costs and the anticipated reliability.

To fully realize the benefits projected for the advanced pitch control system requires implementation of the research and technology plan described in Appendix K.

CONCEPTUAL DESIGN OF THE COUNTER-ROTATION PITCH CHANGE CONTROL AND MECHANISM

A conceptual design study was conducted under Task XII to provide an advanced flight weight pitch change control and mechanism design that is compatible with the in-line gearbox designed in Task XI. Prior to the conceptual design, a Hamilton Standard funded conceptual trade study was conducted to select the concepts for further design effort under the APET contract. The selected concepts incorporated rotary and linear hydraulic actuators with hydraulic and electrical power generated within the propfan assembly. A digital electronic control and a rotary capacitor signal transfer assembly were also incorporated in the propfan. Modular design of all pitch control components was used to reduce maintenance cost.

The concept drawings, descriptions of operation, and estimates of acquisition cost, reliability (MTBUR) and maintenance cost of the propfan pitch control are presented in this report. Blade angles, twisting moments and slew rates are provided for key operating conditions. The qualitative changes to the pitch control system required by a pusher instead of a tractor propfan installation are also provided.

CURRENT TECHNOLOGY OVERVIEW

Blade pitch controls on new commuter turboprops ger erally incorporate a linear hydromechanical actuator with a metering valve and a mechanical pitch lock in the rotating hardware. Mechanical, hydraulic and electrical inputs mus be transmitted from the fixed nacelle-mounted component (i.e., the gearbox). Rotary mechanical inputs position the me tering valve and pitch lock and use either differential gearing or a bearing-mounted ball screw to transmit rotary motion across the rotating interface. High pressure oil is transmitted to the metering valve and actuator through a low clearance oil transfer bearing and transfer tubes. Electrical power for ice protection is transmitted to the turboprop through contact brushes running on a rotating slip ring assembly.

The turboprop assembly drawing shown in Figure J-defines a current pitch control concept for a counter-rotating propfan. Current technology for transmitting rotary me chanical and hydraulic pitch control inputs to a counter-rotating turboprop installed on an in-line planetary.

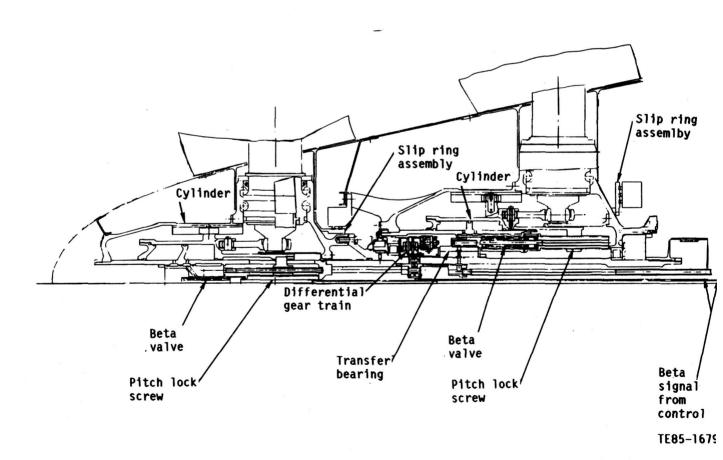


Figure J-1. Counter-rotating turboprop in-line gearbox configuration.

earbox are shown in the sectional drawing of Figure J–2. In his configuration, access to the axis of rotation from the rear of the gearbox is restricted by the drive shaft from the engine. Therefore, the mechanical signal must be transmitted from the rear face of the gearbox housing to the turboprop through ifferential gearing around the sun gear shaft, lay shafts through the planet cage, and additional gears to reach the exist of rotation. Similarly, high pressure pitch change oil must be transmitted through a large diameter (high leakage) than sfer bearing around the sun gear shaft and oil transfer ubes through the planet cage to the turboprop shaft.

The integration of non-modular pitch control inputs rithin the in-line gearbox introduces several complexities. In ddition to the complex gearing and large diameter transfer earing, there is a significant impact on the gearbox design. The overall effect is a reduction in reliability and an increase in maintenance costs. This configuration emphasizes the need to develop advanced pitch control systems that are reliable and easily maintained.

RADE STUDIES

Prior to the APET single rotation propfan (SR) pitch conol study, Hamilton Standard conducted company-funded itch control trade studies to select the advanced technology concepts that were subsequently used for the APET SR propfan and CR propfan studies. The primary criterion was that the pitch control system be adaptable to any gearbox configuration with minimal impact on the gearbox design. The pitch control was divided into two parts: a power system and a control system. A comprehensive matrix of the most viable concepts was prepared for each system and each matrix was evaluated separately as described for the single-rotation gearbox.

The power system matrix in Figure G–3 of Appendix G shows several concepts of pitch change mechanisms with prime movers and power supplies on either the stationary side (i.e., gearbox) or the rotating side (i.e., propfan) of the rotating interface. Several methods of power transfer across the rotating interface were considered. All components were comparatively evaluated using the following parameters listed in order of decreasing criticality: safety, reliability, maintainability, weight, performance (accuracy of blade angle control for Synchrophasing®), acquisition cost, impact on gearbox, mechanical risk, envelope and heat generation (efficiency). These evaluation parameters were assigned weighting factors and were used in conjunction with a forced decision rating technique.

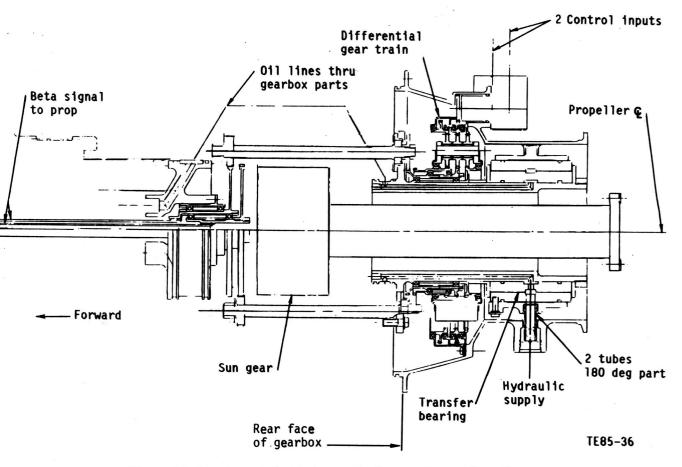


Figure J-2. Counter-rotating turboprop in-line gearbox configuration.

A first round of rating concepts of the same function. one to another, eliminated several concepts. This resulted in a reduced matrix of seven power systems represented by the shaded boxes in Figure G-4 of Appendix G. Pitch change mechanisms at the far left of the matrix were eliminated primarily because of weight penalties associated with the large bevel gears and cams required to actuate the propfan blades mounted in the large diameter hub. The ball screw and ball nut coupled with a spring no-back pitch lock in the left center of the matrix were eliminated because of unsatisfactory blade angle control. The backlash required to release and engage the pitch lock caused excessive hysteresis in the pitch control loop. Most of the power transfer components on the rotating interface were eliminated because of their low reliability when compared with systems incorporating dedicated propfan-mounted power supplies. In addition, slip rings incur high maintenance cost; transformers and generators driven at propfan speed are heavy; oil transfer bearings have low reliability and maintainability for the large diameters required by in-line gearbox installations; and the thrust bearing that transmits pitch change and pitch lock loads across the rotating interface rates low on reliability, maintainability and weight.

One of the final seven power system candidates incorporates a linear hydraulic piston that acts directly on a collector ring, links, and blade trunnions (crank arms) to change pitch. The remaining six systems incorporate a ball screw, which when rotated, translates a ball nut and links to change blade pitch. The ball screw can be driven by either a traction drive or motors (electric or hydraulic; rotating or stationary), which are powered by generators or pumps (rotating or stationary). Hydraulic pumps and motors are considered to be gear types operating at a system pressure of 6000 lb/in.². Electric generators and motors are considered to be the samarium—cobalt permanent magnet brushless type with appropriate electronic controls. The required motor size for maximum pitch rate is approximately 25 hp.

The magnetic coupling is an electric motor mounted on the rotating interface with the stator fixed to the gearbox and the rotor driving the ball screw through appropriate gearing. During fixed pitch operation, the rotor reacts blade torque and rotates at a reference speed dependent on propfan speed. Rotor speed is increased or decreased from the reference speed to change pitch toward high or low pitch. The traction drive is a toroidal variable ratio type with associated planetary gearing. This type of traction drive was selected rather than a constant ratio, multi-stage roller traction drive because it offered a mechanical method of providing bidirectional, variable speed pitch control.

The seven power system concepts were comparatively evaluated, one to another, and they are listed in Table J-I in order of ranking. The simplicity of the hydraulic piston concept resulted in high ratings for reliability, performance and cost, resulting in the highest total rating. Of the remaining

ball screw concepts, electric motor drives rated second to hydraulic motor drives based on reliability and weight. Differential gear concepts rated lower on reliability based on higher parts count. The toroidal traction drive was rated low on reliability, performance and technical risk. The hydraulic piston actuator (linear hydraulic) and the hydraulic motor driven ballscrew (rotary hydraulic) were considered the two final candidates for further study since they rated significantly higher than the other five concepts.

Both concepts are shown in the systems highlighted by the shaded boxes of the power matrices in Figure J-3 and Figure G-5 of Appendix G. Gearbox interface requirements for these self-contained hydraulic power systems are minimal, consisting only of a high-speed pump drive shaft from the sun gear and a nominal amount of cooling oil flow.

The control portion of the advanced pitch control trade studies will be described in the following paragraphs. Figure G-6 of Appendix G is a diagram representing a digital electronic aircraft propulsion control system in which a fullauthority digital electronic engine control (EEC) coordinates and commands engine fuel flow, compressor vane positions and propfan blade angle to control power and speed. The control is provided diagnostic feedback data from the engine and propfan. This system was reported in a NASA-sponsored study completed in 1978 (Report No. CR-135192), and is still considered desirable for advanced propfans. The control system matrix shown in Appendix G, Figure G-7 identifies different methods of transmitting a blade pitch command signal to the propfan power matrix from the EEC. Several methods of transmitting the digital signal across the rotating interface to a propfan mounted electronic controller are shown with several types of blade angle (B) feedback sensors. A stationary nacelle-mounted electronic controller was also considered in this analysis.

All control system components were comparatively evaluated using parameters and weighting factors similar to those employed in the power system study. These parameters are listed in order of decreasing criticality as follows: safety, reliability, maintainability, acquisition cost, accuracy (Synchrophasing control), weight, technical risk, adaptability (to single and counter-rotating propfans, in-line and offset gearbox configurations) and envelope. Five blade angle feed-

Table J-I.

Power system concept ranking.

Ranking	Power system concept
1	Hydraulic piston actuator
2	Ballscrew, hydraulic motor
3	Ballscrew, electric motor
4	Ballscrew, differential gears, hydraulic motor
5	Ballscrew, magnetic coupling
6	Ballscrew, differential gears, electric motor
7	Ballscrew, traction drive

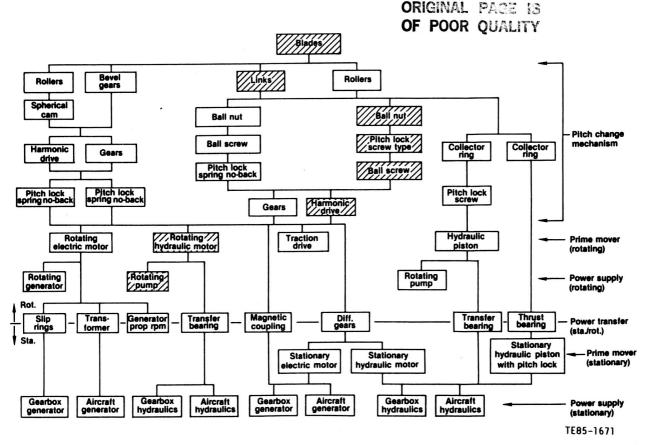


Figure J-3. Rotary hydraulic propfan power system from trade study.

back displacement sensors were considered: (1) linear variable differential transducer (LVDT), (2) rotary variable differential transducer (RVDT), (3) linear variable phase transducer (LVPT), (4) resolver and (5) optical encoders. The LVDT and LVPT measure linear displacement, RVDT and resolver measure rotary displacement and optical encoders can measure either linear or rotary displacements.

The rankings of the sensors determined by comparative evaluation are shown in Table J–II.

All sensors were found to provide sufficient accuracy, but each differed significantly in reliability, maintainability and cost. The first three rated sufficiently higher than the last two to qualify as candidates for selection. The LVDT and RVDT measure displacement as a function of output voltage amplitude and are widely used today. In contrast, the LVPT represents a relatively new technology. It measures displacement as a function of phase difference of two output voltages and unlike the LVDT, it does not require an analog/digital converter. Because of this latter feature, the LVPT rates slightly higher than the LVDT. The RVDT was selected for its adaptability to the rotary hydraulic power system previously selected for the APET study.

Five methods of transmitting digital control signals across the rotating interface were evaluated. These are: (1) radio, (2) capacitor, (3) optics, (4) transformer, and (5) acous-

Table J-II.

Blade angle feedback sensor ranking.

Ranking	Sensor	
1	LVPT	
2	LVDT	
3	RVDT	
4	Resolver	
5	Optical	

Table J-III.
Single transfer ranking.

Ranking	Single transfer method	
1	Capacitor	
2	Transformer	
3	Optics	
4	Radio	
5	Acoustics	

tics. Table J-III shows them listed in order of relative ranking following the evaluation.

Rating variations were based primarily on reliability, with particular emphasis on susceptibility to external interference. Optics rated lower than the capacitor and the transformer concept because it was considered more difficult to

protect optical components from contamination than to shield the capacitor and transformer from electromagnetic interference (EMI). Radio and acoustics were considered very difficult to protect from radio frequency (RF) and acoustic interference. The capacitor concept was selected based on high reliability and simplicity.

Three of the five control system concepts shown in Figure J–8 use a fractional horsepower, direct current (dc) electric servomotor to position a metering valve to provide high pressure oil to either a linear piston or a gear motor prime mover. The servomotor and its electronic controller are mounted in the rotating propfan in two of these concepts and on the stationary gearbox in the third concept. The remaining two concepts incorporate an electronic controller to directly control a large dc electric motor (approximately 25 hp) prime mover. One of these concepts has the controller and motor mounted in the rotating propfan and the other concept has the controller mounted on the gearbox to control the motor (magnetic coupling).

Comparative evaluation of the control systems resulted in the ranking list shown in Table J-IV.

The first two servomotor control systems are identical and share the same rating. They differ only in the prime movers being driven and their rating is significantly higher than ratings of the remaining three concepts. The third servomotor system was penalized on reliability and accuracy for transmitting the control input to the metering valve through differential gearing. Low ratings were assigned to the two large electric motor control concepts because the solid state components currently available for large motor and generator controls are less reliable and heavy. Considerable research and development effort is being expended to improve this technology for use in aerospace applications (i.e., the all electric aircraft). When electrical prime movers become competitive with hydraulic prime movers, if desired, they can be easily adapted to the rotary pitch change mechanism.

Table J-IV. Control system ranking.

Ranking	Control system concept
1	Electric servomotor, metering valve, hydraulic motor
2	Electric servomotor, metering valve, hydraulic piston
3	Electric servomotor, gears, metering valve
4	Electric motor (magnetic coupling)
5	Electric motor

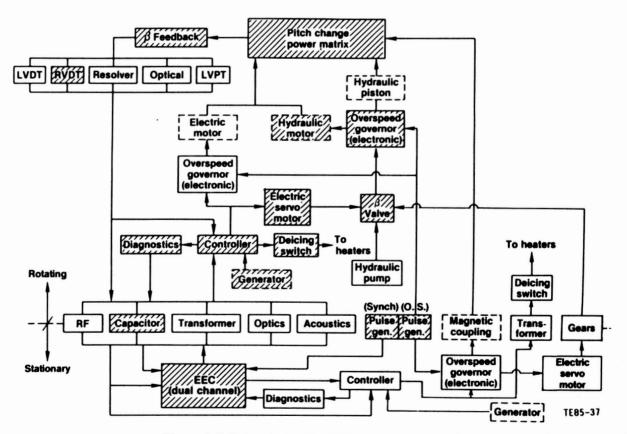


Figure J-4. Rotary hydraulic control system concept.

The pitch control system components selected for the otary and linear hydraulic power systems are highlighted by the shaded control matrix boxes in Figure J-4 and in Appenlix G, Figure G-8, respectively. Interface with the gearbox is minimal and consists of a support bracket for the stationary half of the capacitor signal transfer coupling and a high-peed generator drive shaft from the sun gear. This is the ame shaft that drives the pumps in the power system.

In summary, the trade studies showed that: (a) the linear ydraulic actuator rates slightly higher than the rotary hybraulic actuators but the latter is lighter and appears to be nore adaptable to counter-rotating propfans; both are viable oncepts for further study, (b) hydraulic systems are more reable and have a higher power density capability than electrial systems, (c) a power supply located on the rotating side of ne interface is more reliable than transmitting power across ne rotating interface from the stationary side, and (d) the caacitor control signal transfer across the rotating interface is imple and reliable.

The trade studies discussed so far are applicable to einer single-rotation propfan or counter-rotation propfan congurations. In addition, for the CR propfan, the trade study esults are applicable to either grounded or ungrounded lanetary gearbox systems. The results were used in both ne NASA APET single-rotation propfan pitch control studies nd the Hamilton Standard funded pre-APET CR propfan itch control conceptual design studies. Three CR propfan oncepts were studied for a pusher configuration in which ne blade angle of each rotor is controlled individually. These pree concepts are the rotary hydraulic, the rotary hydraulic with the CR propfan gearbox drive gearing located between ptors, and the linear hydraulic.

The primary difference between the two rotary conepts and the linear concept is the blade actuation method nd the method of pitch control power transfer from the aft otor to the forward rotor. For all three concepts, an electonic control module and hydraulic power module are loated on the aft rotor for ease of maintenance. Digital pitch ontrol signals are transmitted between the electronic enine control and the electronic control module by a capacitor ignal transfer module mounted on each rotor. Each rotor as a mechanical, in-place pitch lock. Gearbox interface reuirements are cooling flow and a high-speed drive shaft om the sun gear to drive the generator and pumps.

Both rotary hydraulic concepts incorporate a ball screw ctuator in each rotor to change blade pitch. Rotary power is ansmitted from a hydraulic power module mounted on the ft rotor to the forward rotor ball screw through differential earing. The linear hydraulic concept incorporates a linear iston actuator for each rotor, but both actuators are nounted on the aft rotor for ease of maintenance access. The of the actuators transmits pitch change power axially

across the rotating interface by the forward rotor blades through links and bearings. Evaluation of the three concepts, one to another, showed the rotary concepts to be superior to the linear concept. The large links and thrust bearings of the linear concept, used to transmit pitch change power to the forward rotor, resulted in lower reliability and higher weight than the rotary concepts. Of the two rotary concepts, the concept with gearbox gearing between rotors rated low on reliability, maintainability, and impact on the gearbox design.

Based on these pre-APET design studies, the rotary hydraulic concept and a new linear hydraulic concept were selected for further study within the CR propfan APET contract.

CONCEPTUAL DESIGN OF SELECTED CONCEPTS

The primary design objectives for the APET pitch control conceptual designs were to minimize impact on the gear-box and to maximize accessibility and maintainability. These objectives were attained by implementing a modular pitch control design, which is contained within the rotating propfan assembly. This simplifies the interface with the gearbox; improves gearbox reliability and maintenance cost; and reduces pitch change maintenance cost by providing accessible, easily maintainable modules.

This APET conceptual design study was conducted to refine the rotary and linear pitch control concepts selected from the trade studies. The study also evaluated the configurations to choose the best one for a counter-rotating propfan in a tractor installation. Evaluation of the rotary hydraulic concept was continued, and a new "non-modular" linear hydraulic concept was generated for comparison. The non-modular concept incorporates a power module and electronic control mounted in each hub to reduce parts count at the possible expense of maintainability.

A variation of the rotary concept called rotary/linear was also studied. This concept incorporates a linear actuator in the forward hub of the rotor system with the objective of reducing the total number of parts.

Description of Pitch Control Concepts

The counter rotating propfan is flange mounted to the gearbox output shaft through curvic face splines at the rear face of the aft hub. This flange reacts all CR propfan mounting loads and drives the aft rotor. The forward rotor is driven by the planet carrier of the gearbox output through a splined quill shaft.

Each blade is retained in the hub with a single row angular contact ball bearing. Additional support for static blade pitch operation is provided by an external blade clamp. Blade retention bearings are lubricated by a fixed amount of oil in the hub. A lip seal at the blade root prevents external leak-

age. A sectional assembly drawing of the CR propfan with rotary hydraulic pitch control (Concept 1) is shown in Figure J–5. Blade trunnion arms splined to the inboard end of the blades are used to rotate the blades about the pitch axis. Links with spherical rod–end bearings connect the trunnion arms to a ball screw nut assembly in each rotor that translates to change blade pitch. Each ball screw is straddle—mounted on hub mounted support bearings. Link forces impose torques on each ball nut, which are reacted by an integral lug riding in a slot in the forward and aft hub–mounted housings.

The ball screws are driven by a hydraulic power module that consists of drive gearing, hydraulic motors, 4-way metering valves (beta control), mechanical in place pitchlocks, pumps, oil sumps, pressure regulating and relief valves, and a generator. A bolted flange is used to mount the power module on the CR propfan forward hub-mounted housing. Blade pitch is changed toward high or low pitch by the ball screws that are rotated by drive gearing in response to pressurized oil applied to the high or low pitch side of hydraulic drive motors. An irreversible acme screw and nut acts as a pitch lock in each rotor. The pitch lock nuts are integral with the ball nuts. A small axial gap is maintained between the end of the pitch lock screw and the hub-mounted actuator bulkhead during operation. This prevents the blade pitch from decreasing by more than one degree toward low pitch if hydraulic power is inadvertently lost anywhere in the blade operating range.

The pitch lock screw is driven by a small bi-directional dc servomotor to control pitch upon command from the electronic control module. Each rotational position represents a discrete blade angle setting in the operating range. This position is measured by an RVDT that is geared to the servomotor

and fed back to both the electronic control module and th nacelle-mounted EEC.

Hydraulic System

Figure J–6 is a diagram showing the functional relation ship between the actuator, pitch lock, and the hydraulic con ponents for each rotor. The hydraulic system is designed to conserve power and reduce heat generation. Over 95% (CR propfan pitch control operating time is spent at power levels less than 20% of peak power. This is because comme cial aircraft require peak pitch rate power only for large blac angle excursions, i.e., reversing and feathering.

A small displacement main gear pump supplies hig pressure oil to each actuator motor via a beta metering valv for all low power pitch control requirements. Although th pump can provide the peak system pressure set by the hig pressure relief valve, the pump supply (discharge) pressur is regulated to a few hundred lb/in.2 above actuator operating pressure requirements. This is accomplished by the mai and standby regulating valve that regulates main pump sur ply pressure to the metering valve at a level slightly above th higher of the two high pitch pressures as indicated by th shuttle selector valve. This pressure regulation, coupled wi the small pump size, reduces pitch control power generatic to the low levels required for most of the flight spectrum with minimum heat generation. A standby gear pump with appro imately four times the capacity of the main pump circulate oil back to the pressurized sump at low pressure (low powe most of the time. When the beta metering valves are pos tioned for high flow (pitch rate), the regulating valve ar standby check valve combine both the standby pump flo and the main pump flow, at high pressure, to provide the r

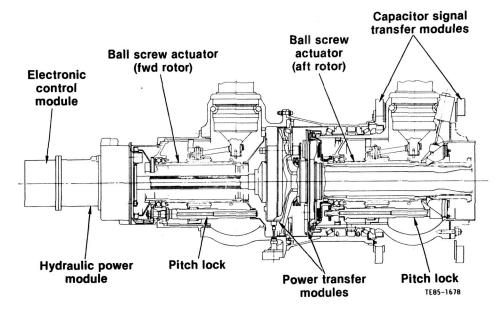


Figure J-5. Rotary hydraulic pitch control concept.

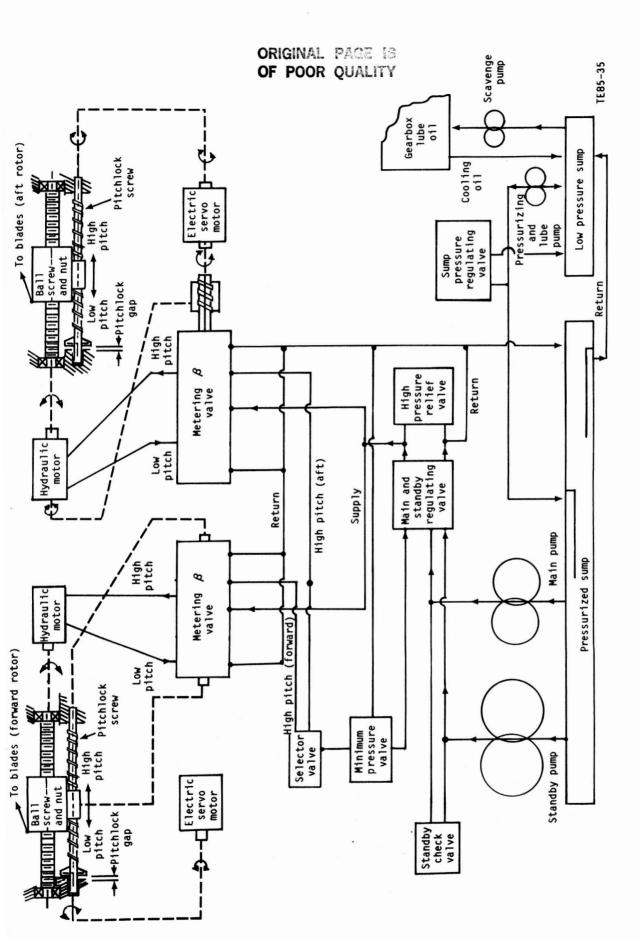


Figure J-6. Hydraulic system diagram (rotary).

quired high power. This is a transient condition and heat generation is minimal.

A pitch control system pressure versus weight trade study showed that 6000 lb/in.2 is the optimum pressure for minimum weight. However, 4750 lb/in.2 was selected because it results in higher reliability and lower cost for a weight penalty less than 2% of pitch control weight. The pressurized sump is charged to 75 lb/in.2 minimum by the lubrication pump located between rotors. This pressure insures that the main and standby high speed pumps are adequately supplied with oil to prevent cavitation. The lubrication pump also circulates cooling oil from the gearbox lube system through the pressurized sump to mix directly with pitch control oil and return filtered to the gearbox cooler. The power module pumps and forward generator are driven by the differential rotation of the two rotors through a differential planetary gear system and concentric geared transfer shafts.

The generator is a light-weight, samarium-cobalt, permanent magnet, externally-commutated alternate current (ac) type. Alternate current output is rectified to dc by the electronic control module. Dual generator windings provide separate voltage supplies for pitch control and blade deicing. An overrunning clutch is provided at the generator drive shaft to permit the generator to be powered as a motor for static ground operation of the pitch control. Auxiliary ground cart power supplied to the generator with the engine inoperative drives the pumps to develop pressurized oil for pitch change. A separate generator for de-icing of the aft rotor blades is mounted on the aft hub near the flange mounting face and driven by the relative rotation of the two rotors through a bevel gear set.

Electronic Control System

The electronic control module incorporates the printed circuit boards and solid state components required to (a) provide control of the dc servomotor for each rotor under pitch control command from the nacelle-mounted full authority digital EEC and from separate overspeed pitch control circuitry in the module, (b) transmit blade angle feedback and other diagnostic signals from each rotor to the EEC, and (c) provide power switching for blade de-icing. Rotary capacitor signal transfer modules located at the rear end of each hub, transmit serial digital pitch control signals bi-directionally between the EEC and the rotating electronic control module. Each transfer module contains two electrical paths. Each path consists of two parallel annular metal disks, one on each side of the rotating interface, separated by an air gap.

Under normal operating conditions, the electronic control module provides only blade pitch control as commanded by the EEC. All intelligence for governing speed, synchrophasing, feathering, reversing and ground handling is located in the dual-channel EEC. This permits the more complex electronic control circuitry to be located in the sta-

tionary nacelle where it is more accessible for maintenance and for modification of control parameters. In the event of e ther an erroneous signal or loss of signal from the EEC, the electronic control module has a solid–state speed governowith separate power supply, circuitry and speed sensor that will govern speed at a set percentage of normal speed. The flight may then continue with only the loss of synchrophasinand reversing capability. Provision is made to conduct a preflight check of this back–up control circuit.

Blade pitch angle change originates with a requirement and a command signal from the EEC to change pitch a dis crete amount toward either high or low pitch. The signal transmitted across the capacitor signal transfer modules 1 the electronic control module, which powers two dc serve motors to rotate the pitch lock screws through gearing an translate the metering valve spools. Translation of the aft re tor valve is obtained by rotating a valve-mounted screv while the forward rotor valve is translated by a linkage syster coupled to the forward pitch lock screw. Concentric geare tubes and a differential provide the drive coupling to the a rotor ball screw and pitch lock screw. Pressurized oil is the metered to the system hydraulic motors that drive the ba screw nut assemblies to the commanded blade angle pos tion and null the metering valves. The in-place pitch lock ga between the screw and ground toward low pitch is continously maintained within one degree of blade angle (i.e., fu metering valve authority is sustained within the pitch loc gap). Blade angle position in each rotor is continuously me sured by RVDT's and fed back to the control to terminate th signal when the commanded angles are reached.

Maintainability Features

The modular component design of the rotary hydraul pitch control system satisfies the primary design objective of minimum impact on the gearbox and maximum accessib ity and maintainability for any gearbox configuration. After r moval of the CR propfan spinner, the electronic contr module can be easily removed by removing bolts from the mounting flange and then pulling the module forward coguide pins to release the plug-in wiring connectors. Remov of the electro-mechanical module mounting bolts permit the dc servomotors, RVDT's, and associated reduction geaing to be removed as a unit. The hydraulic power module cat be removed by removing mounting flange bolts. The forward and aft generators, lube pump, and scavenge pump cat each be removed and replaced without disturbing other conponents.

Access is gained to the blade links, ball screw, and pitc lock of the forward rotor for inspection, maintenance, or replacement by removing the cylindrical support housing boll from the hub at the mounting flange and sliding the housir forward. Blades in the forward rotor can also be removed an replaced, if required, as follows:

- disconnect the blade link at the trunnion arm
- disengage the de-icing brush assembly from the blade slip rings
- remove the external split clamp and lip seal from the hub
- move the blade into the hub a small distance and remove the retention bearing balls, self-contained in a flexible plastic retainer
- remove the blade from the hub

The capacitor signal transfer modules are fabricated in egments that are easily removed for replacement or repair. emaining CR propfan components incorporate modular deign to facilitate shop maintenance. Replacement of the aft otor blades requires removal of the aft alternator drive gearing to gain access to the blade links. This requires removal of ne CRP assembly from the aircraft. A simpler method of aft otor blade replacement is being pursued in separate design tudies at Hamilton Standard.

Alternate Concepts

A sectional assembly of the CR propfan concept with roIry/linear pitch control (Concept 2) is shown in Figure J-7.
Igure J-8 is a diagram showing the functional relationship stween the actuator, pitch lock, and hydraulic components or each rotor. This concept is essentially the same as Consept 1 except that a linear hydraulic actuator replaces the all screw actuator in the forward rotor. The actuator piston stationary and is straddle mounted on support rings attached to the hub. The blade links are attached to the actuator cylinder, which translates to change blade pitch. Torque estraint of the cylinder is accomplished by an integral cylinrical bushing riding on a shaft fixed to the piston support ngs. The pitch lock nut is integral with the actuator cylinder

and the screw is supported on bearings in the piston support rings. Blade pitch angle control signals power the dc servomotor to drive the pitch lock screw through gearing. Linkage attached to the pitch lock screw causes translation of the metering valve spool. High or low pitch pressure is directed to the appropriate side of the piston. As the cylinder translates, the pitch lock nut returns the metering valve to null position through the pitch lock screw and linkage.

A sectional assembly of the CR propfan concept with linear pitch control (Concept 3) is shown in Figure J-9. Figure J-10 is a diagram showing the functional relationship between the actuator, pitch lock, and hydraulic components for each rotor. This concept incorporates two linear hydraulic actuators, as described in Concept 2, to change blade pitch of both rotors. Both pistons are stationary and are straddle mounted on support rings attached to the hubs. Blade links in each rotor are attached to the actuator cylinder and change blade angle as the cylinder translates. Torque restraint of the actuator cylinders is accomplished by integral lugs riding in slots in the forward and aft housings. The pitch lock nuts for the pitch lock screws are integral with the actuator cylinders and the screws are bearing-supported on the piston support rings. Blade pitch angle control signals power the dc servomotors through gearing to drive the pitch lock screws. Linkage attached to the pitch lock screws causes translation of the metering valve spool sending high or low pitch pressure to the appropriate side of the piston. As the actuator cylinder translates, the pitch lock nut returns the metering valve to null position through the pitch lock screw and linkage. Each rotor actuator is powered by an individual hydraulic power module incorporating a dc servomotor, drive gearing, a 4way metering valve (beta control), main and standby pumps. a pressurized sump, pressure regulating and relief valves,

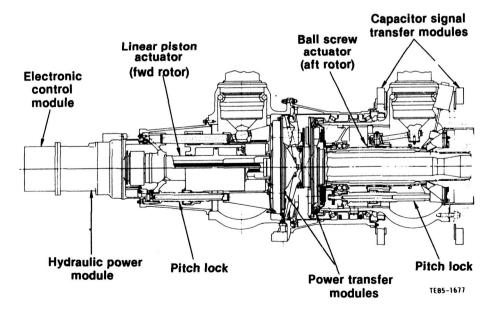


Figure J-7. Rotary/linear hydraulic pitch control concept.

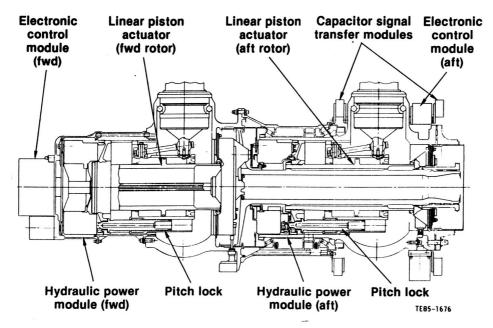


Figure J-9. Linear hydraulic pitch control concept.

nd a generator. The power module for the forward rotor is olted to the forward hub-mounted housing, and the aft rotor ower module is bolted to the aft hub-mounted housing. Indidual electronic control modules provide pitch control for ach rotor. The aft module is mounted in an annular segment ear the CR propfan assembly mounting flange, and the forward module is mounted at the forward end on the axis of rotion. Servicing the forward rotor actuator and removing lades is essentially the same as that described for Concept. Servicing the aft rotor actuator, the hydraulic power modle, and the removal of blades requires the removal of the CR ropfan assembly from the aircraft.

The three concepts were rated to the same evaluation arameters used in the trade studies and the results are sted in Table J–V in order of ranking.

Rating scores for the three concepts were close but the near concept rated slightly higher than the rotary concepts ased on cost and technical risk. The rotary and rotary/linear oncepts rated the same, but the rotary is favored because if the commonality of the fore and aft actuators. Common ctuators reduce development cost and logistic cost of relacement parts.

The rotary concept shown in Figure J–5 was selected inead of the linear concept on the basis of the following addional considerations:

- Location of the electronic control and hydraulic power module on the forward end of the propfan facilitates providing power for static check-out and mounting instrumentation for diagnostics.
- The ball screw actuator is more adaptable to utilization of propfan rotational energy to mechanically feather the blades if normal power is lost.

 Lower system pressure can be used with the rotary concept, with minimal weight penalty, since it is significantly less weight sensitive to pressure level than the linear piston concept.

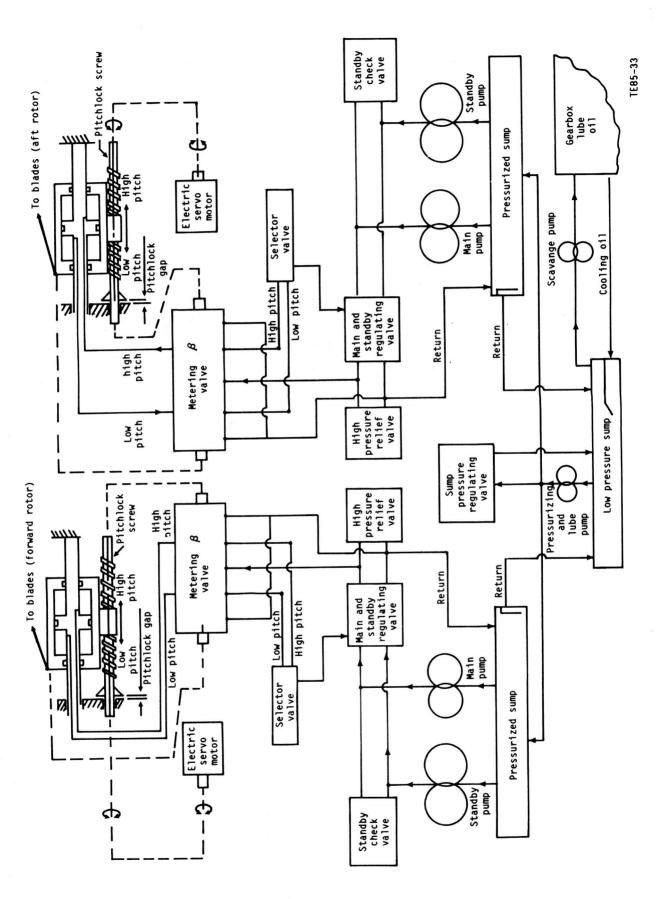
Technology development for the three components shown in Figure J–11 is required prior to inclusion of this hardware in an advanced propfan application. An efficient shielding system against EMI must be developed for the rotary capacitor signal transfer module. Electronic control components must be mounted and packaged in the module to withstand the G-field environment of the rotating propfan (approximately 40 G's per in. of radius from the axis of rotation). Hydraulic gear pumps and gear motors must be developed for the high speed, high pressure application of the power module. A research and technology plan has been prepared and is included in Appendix K of this report defining the programs required for technology development. Figure J-11 also shows a typical propfan spinner contour.

Line and shop maintenance costs are reduced substantially by the modular pitch control design concept shown in Figure J-12. All electrical, electronic and hydraulic components can be replaced in modules on the aircraft. The remaining modular components facilitate shop maintenance actions.

Table J-V.

Pitch control concept ranking.

Ranking	Pitch control concept
1	Linear
2	Rotary
3	Rotary/Linear



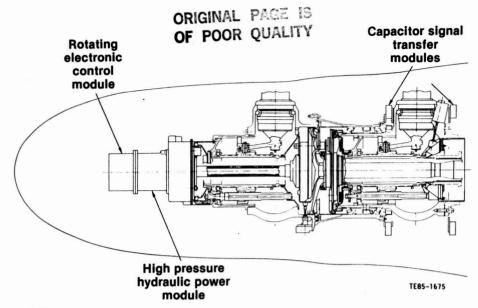


Figure J-11. Advanced technology features requiring additional development.

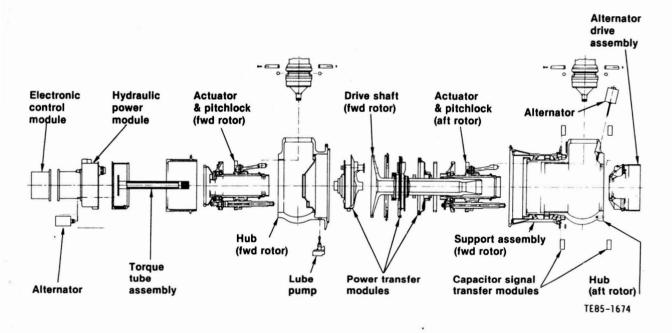


Figure J-12. Modular design concept of propfan assembly.

Pitch Control Parameters

The primary propfan design parameters used in the conceptual design of the advanced technology pitch control were blade pitch slew rates, blade angles and blade twisting moments. These are presented in the following sections.

Slew Rates

Blade pitch slew rate requirements for various propfan operating conditions are shown in Table J-VI. Normal slew

Table J-VI. Slew rates.

Condition	Blade pitch rate — deg/sec
Normal control	0–3
Synchrophasing	0–1
Feathering	15
Reversing	15
Ground operation	
(engine inoperative)	0–3

rate requirements for most of the fight spectrum are low. Blade pitch angle is held essentially constant at each flight condition with small excursions of less than ± 0.1 deg during Synchrophasing. Synchrophasing is a fine-tuning control of blade pitch through very small angles that do not require high slew rates.

The maximum slew rate is normally set by the aircraft requirements based on the time to reach the full reverse angle on landing. The rates shown are based on the capability to fully reverse from flight idle in three seconds. These rates are judged to be satisfactory for advanced turboprop propulsion systems. However, different rate requirements can be easily satisfied with minor changes to the pitch control.

Blade Pitch Angle Settings

The blade angle settings for each rotor are given in Table J-VII for various operating conditions. Angles are specified at the blade 3/4 radius. Allison indicates that the engine can start with the blades at any angle including feather. The minimum propfan torque blade angle is therefore somewhat academic for this propulsion system. Emergency blade angles are set by the mechanical in-place pitch lock, which follows approximately one degree below any commanded blade angle.

Blade Twisting Moment

The pitch control system must be capable of rotating the blades about the pitch axis, counteracting the total blade twisting moment. The total moment is comprised of the following individual twisting moments:

- centrifugal, acting toward flat pitch
- aerodynamic, acting toward either high or low pitch depending on the flight condition
- friction, acting to impede motion toward either high or low pitch

Centrifugal twisting moment results from centrifugal forces on the blade mass as a function of distance from the pitch axis and makes up most of the total moment. Highly swept propfan blades have significantly higher twisting moments than more conventional blades with less sweep because of the increase in overhang from the pitch axis.

The maximum total blade twisting moment that the pitch control must overcome to move 12 blades toward high pitch is 280,000 lb/in. The maximum total twisting moment required to hold the blades in position is slightly less than this value due to exclusion of the friction moment. It is this reduced moment that the pitch control or the pitch lock must react to hold the blades at a fixed blade angle setting.

Weight

Results of a weight analysis conducted on the advanced pitch control conceptual design showed the weight to be the same as the weight of the baseline pitch control concept,

shown in Figures J-1 and J-2, which originated in NASA re port CR 168258, "Technology and Benefits of Aircraf Counter-Rotation Propellers," December 1982. Total propfar weight is the same as the baseline weight provided in Figure 79 of the reference report. This represents an improvemen since the advanced concept has the additional advantage o modularity for improved maintainability at no increase it weight.

CR Propfan Pusher Installation

The advanced pitch control concept is easily adapted to either pusher or tractor propfan installations. Position of the ball screw actuators changes from forward of the blades fo a tractor to aft of the blades for a pusher. This changes the load direction in the blade links and requires the pitch loc gap to be relocated from one end of the lock screw to the other end. The pusher installation also requires engine-supplied cooling air inside the propfan spinner to maintain the thermal environment for the electronic control module within acceptable limits.

Reliability

A component failure rate and unscheduled removal rate analysis was performed for all the pitch control modules. These rates were then added to the respective rates of the remaining propfan hardware to arrive at the total propfan system rates.

Failure rate is defined as any event chargeable to the hardware. Removal rates include additional non-chargeable events such as maintenance damage, unsubstantiated removals (no failures), and accident and foreign object damage (FOD), where applicable, in addition to the chargeable removal rates. The mean time between unscheduled removal (MTBUR) for all causes is the inverse of the total removarate. The MTBUR of 2600 hours for the advanced technolog propfan system is derived in Table J-VIII. It is based on propfan assembly removals as well as removals of replaceable components such as the electronic control, hydraulic power module, electric motor module and spinner.

Table J-VII.
Blade angle setting.

Beta 3/4—deg

Condition	Fwd Rotor	Aft Roto
Feather	+ 85	+ 85
Flight idle	+ 40	+ 38
Cruise (0.8 Mn)	+ 56	+ 52
Maximum reverse	~15	-15
Minimum propfan torque (static conditions)	~ 1	- 1
Emergencies	1 below beta setting when condition occurs	

This MTBUR represents an improvement of 73% over e 1500 hr MTBUR for the baseline propfan system defined NASA report CR 168258, Figures 76, 77 and 81, pages 55, 266 and 270, respectively.

The predicted MTBUR (chargeable events) of 13,800 hr r the advanced technology propfan system is based on ally those failures that require removal of the entire propfan seembly. This represents a significant improvement over e 4900 hr for a propfan using the current technology sysm defined by the pitch control concept in NASA report CR 58258. The increase in MTBUR is a result of the high reliatity of the individual components in the advanced pitch concept system.

Table J-IX is a summary of the propfan reliability for both urrent and advanced technology pitch control concepts.

Propfan Failure Mode Considerations

The CR propfan pitch change mechanism and control gic have been subjected to an evaluation to assure the degn philosophy provides for safe operation. This section prodes a summary of this evaluation with regard to both the opfan and its resulting impact on the selected gearbox.

The fundamental premise of the propfan safety philosony is that "fail fixed is fail safe", and that uncontrollable derease pitch is unacceptable. Uncontrollable decrease in tch is prevented by an in-place pitch lock for protection gainst mechanical and hydraulic failures. Redundant overneed limiting provides protection against control failures toard decreased pitch. Additional safety features include fuel

Table J-VIII.
Unscheduled removals (all causes).

Component	Removal Rate (Events 1000 flight hr)
Spinner	0.0086
Cover and fairings	0.0110
Blades	0.0688
Disks and fairings	0.0058
Aft power transfer module	0.0165
orward power transfer module	0.0070
Aft actuator module	0.0118
orward actuator module	0.0110
Hydraulic power module	0.0664
lectric drive module	0.0280
lectronic control module	0.0836
Aft de-icing electronic control	0.0297
ube pump module	0.0169
Iternator drive assembly	0.0037
Aft alternator	0.0034
orward alternator	0.0033
ft signal transfer assembly	0.0002
orward signal transfer assembly	0.0002
Other	0.0054
Total:	0.3813

MTBUR = (1/0.3813)(1000) = 2600 hours

limiting capability in the engine fuel control to prevent overspeed, and fuel cutback as a function of measured torque to prevent transmittal of excessive torque. Also, although fixed pitch operation on the pitch lock is considered flight safe, the pilot has the option to feather the blades with a separate analog emergency feather signal, which bypasses the normal digital control.

Safety features are also incorporated in the full authority digital electronic engine control (EEC), which coordinates and commands engine fuel flow, compressor vane positions and propfan blade angle to control power and speed. The control is provided diagnostic feedback data from the engine and propfan. If loss of the EEC is experienced, the propfan reverts to 100% rpm speed control with the use of the electronic control that is mounted on the propfan.

Both grounded and ungrounded gearboxes were considered relative to the specified safety philosophy. For a grounded gearbox installation, the blade pitch angle controls the torque in each rotor drive path. For an ungrounded gearbox installation, the blade pitch angle controls the speed of each rotor drive path. The results of trade studies presented in this report are applicable to both systems. However, the CR propfan pitch control concepts in this report are based on an ungrounded differential planetary gearbox system.

A preliminary FMEA indicates that the propfan safety philosophy also protects the gearbox. To summarize the key results of the FMEA, three failure modes will be discussed, 1) failure of the forward rotor blade angle toward feather with power on, 2) feathering of the forward rotor during in flight shutdown with the aft rotor pitch locked, and 3) feathering of the aft rotor during in flight shutdown with the forward rotor pitch locked.

For condition 1, the forward rotor will decrease its speed while the aft rotor will maintain its speed through the governing system, and the engine speed will decrease with the torque limiter regulating its output. For condition 2, the feathered rotor will rotate in the same direction as the aft rotor at a low speed, the pitch locked rotor will rotate at less than 100% speed, and the engine will rotate at less than 50% speed. For condition 3, the feathered rotor will also rotate in the same direction as the aft rotor at a low speed, the

Table J-IX.

Propfan reliability summary.

	Current Technology	Advanced Technology
 MTBUR, propfan assembly (chargeable), hrs MTBUR, propfan assembly and 	4,900	13,800
components (all causes), hrs	1,500	2,600

pitch locked rotor will also rotate at less than 100% speed, and the engine will also rotate at less than 50% speed.

Similar ungrounded gearboxes have been successfully used on two Russian applications, the Tupolev TU-95 "Bear" and the Antonov AN-22 "Cock." This experience provides evidence to confirm the results of analytical studies regarding the safety of the ungrounded gearbox.

Maintenance Cost

Maintenance costs for the propfan with the advanced technology pitch change system were estimated using an on-condition philosophy established for the propfan. This philosophy, which is in line with present day turboprop field service experience, involves repair or replacement of only the faulty module as determined by built-in health monitoring diagnostics.

The maintenance cost was developed for the 6x6 bladed, 10.78 ft diameter propfan by considering all the elements of maintenance, namely:

- 1. scheduled inspections
- 2. unscheduled line repairs
- 3. unscheduled removals

Scheduled inspections consist of four basic checks: a walk around check, which is performed routinely and as a minimum every 10 flight hr; a line check, which is performed approximately every 35 hr, a base check, which is performed approximately every 1000 hr (can be made to coincide with periodic check of the engine or aircraft) in which the spinner is removed; and a major check, which is performed approximately every 18 months (about 4,500 operating hr) to coincide with a major shop aircraft check. Unscheduled maintenance includes blade line repairs and unscheduled removals of major components such as the spinner, disc and aft fairing, pitch change modules, blades, and forward cover and fairing. A significant factor in the maintenance cost of propfan hardware is the design philosophy used at Hamilton Standard. This philosophy includes designing both the propfan blade and hub for infinite life. Consequently, these items will only require replacement in the event of an accident or significant FOD. Blades are repairable for all FOD except cases where spar damage is evident. Therefore, there will be no life limit on major parts, and accordingly low maintenance costs associated with scrap. Another design characteristic is the absence of major components that will be subjected to replacement due to wearing out. Periodic replacement of the few secondary parts subject to wear and replacement are not a significant contributor to the maintenance cost.

Maintenance cost estimates for the unscheduled removals of the propfan system were obtained by adding removals of all the advanced technology pitch change module to maintenance costs of the spinner, blades, disc and fairing Costs for unscheduled removals reflect both line manpower and shop costs to repair the faulty component.

The maintenance cost projections for the advanced tu boprop propulsion system were generated by multiplying lin and shop labor cost estimates (converted to dollars usin 1984 fully burdened labor rates) and material charges permaintenance action, by the corresponding rate of maintenance action or repair. The line and shop labor cost estimates are based on industrial engineering evaluation of the design, in conjuction with historical data for similiar hardware.

Parts cost per event were developed using estimate acquisition costs and historical data relating per repair matrial costs to acquisition costs on a percentage basis. Th propfan acquisition costs were developed by the Cost Eng neering Group based on analysis of the hardware as define on the concept drawings and the developed parts list. Th analyses use standard techniques for estimating productic hardware costs including comparisons with costs for similar parts currently in production. The maintenance manhou per 1,000 flight hours include both scheduled inspectior and all unscheduled maintenance. The parts cost assume 1984 economy and includes all unscheduled maintenance Based on the maintenance philosophy established by Ham ton Standard for the propfan system, all unscheduled action have been accounted for. This includes maintenance actior where hardware is removed as well as actions where repa is accomplished on the aircraft.

The total maintenance cost for the propfan with an a vanced technology pitch control represents a 19% decreas from the baseline propfan relative maintenance cost referenced in NASA report CR 168258, Figure 82. Baseline cost were escalated for the 1984 economy and adjusted to the 10.78 ft diameter. The lower maintenance cost of the a vanced system is primarily the result of a reduction in the frequency of maintenance actions and the increase modularity.

Acquistion Cost

The acquisition cost for a propfan with an advance technology pitch control concept is approximately equal the baseline current technology concept. Acquisition co estimates were developed as described in the section c maintenance cost.

APPENDIX K

TASK XIII. RESEARCH AND TECHNOLOGY PLAN FOR TASKS XI AND XII

TABLE OF CONTENTS

Title Land Control of the Control of	Page
Introduction	K-1
Counter-Rotation Gearbox Technology Plan	K-2
Counter-Rotation Pitch Control and Mechanism Technology Plan	K-6

LIST OF ILLUSTRATIONS

ure	I ITI O	Page
1	Counter- rotation gearbox technology plan schedule	K-5
2	Counter-rotation pitch control and mechanism technology estimated program schedule for capacitor signal	
	transfer, high pressure hydraulics, and rotating electronics	K-7

PRECEDING PAGE BLANK NOT FILMED

INTRODUCTION

The counter-rotation gearbox and pitch change system designs have incorporated advanced technology features hat are not yet demonstrated or verified for the conditions encountered in a propfan propulsion system. Since the first production of these systems is intended to be in the early

1990s, advanced technology issues would need to be verified during the late 1980s before finalizing production designs. The objective of Appendix K is to present the specific advanced technologies applied in the designs.

COUNTER-ROTATION GEARBOX TECHNOLOGY PLAN

The preliminary analysis of the counter rotating (CR) gearbox has identified areas of research that could have impact on the gearbox design. Two technology items, tapered roller planet bearings and steep—angle single row tapered roller thrust bearings with bidirectional load capability, are required to achieve the level of performance predicted for the CR gearbox. The technologies listed below would enhance the design but are not required for the gearbox defined as a result of Task XI.

- 1. Double helical gearing
- 2. Single row spherical planet bearings
- 3. Fluid film planet bearings
- 4. Lubrication system methods to allow 30 min of gearbox operation without oil
- 5. Stainless steel housing
- Long life flexible splines for the gearbox/prop interface

All areas of research detailed in Appendix H are applicable to the CR gearbox as well.

REQUIRED DESIGN TECHNOLOGIES

Tapered Roller Planet Bearings

Background

The tapered roller bearing was selected for the planet bearing in this study because of its high capacity and ability to react to the overturning moment created by the helical gears. Although tapered roller bearings have been operated at the speeds required in this design, a development effort would be required to ensure satisfactory operation in a planet bearing environment. The planet bearing requires opposite rotation of the inner and outer races in a high "g" field created by rotation of the planet carrier. There is no experimental data available for this application.

Recommended Program

A subcontract would be arranged with a bearing manufacturer who would perform analyses according to specifications provided by Allison. In–house computer studies would augment work being done at the bearing supplier. At the completion of the design, fabrication of the planet bearings would begin. Testing of the bearings would best be accomplished in the CR gearbox since at present there is no test rig available to test this bearing under the gearbox loads. If time and funds are available, a planet bearing test rig would be constructed to simulate planet bearing operation. Parametric tests would determine operating temperatures, heat generation, and integrity of design.

Steep Angle, Single Row Tapered Roller Thrust Bearings With Bidirectional Load Capability

Background

Tapered roller bearings can carry large thrust loads ye require a minimum amount of space. In situations where th thrust load can reverse direction, two tapered roller bearing are required. The CR gearbox input shaft bearing must carr a significant thrust load, normally, in one direction only. Ur der some conditions, the thrust can reverse direction but th magnitude of the reversed load is low. Preliminary design of this bearing indicates that it is possible to use only one to pered roller bearing with an additional thrust rib to handle th reverse thrust loading. It has not been proved, however, that this bearing will function in practice since under maximur thrust in the normal direction, the roller retaining rib must or erate at maximum allowable bending stress levels. The cor cept of using a cup rib to absorb the light reversed thrust i also unproven. Cylindrical roller bearings are currently bein designed to carry moderate thrust loads; the same techno ogy should apply to this bearing.

Recommended Program

To verify the bearing performance, it would be subjected to conditions that simulate its actual operating environment. A similar test will soon be conducted at Timken for an Allison engine application. Since Timken can readily perform this type of test, a subcontract would be arranged so that the CR gearbox sun gear thrust bearing design would be optimized to both Allison's and Timken's satisfaction and then fabricated and tested at Timken. The tests would determine operating temperatures, power loss and integrity of the design.

DESIGN ENHANCEMENTS (NOT REQUIRED FOR INITIAL PRODUCTION)

Double Helical Gearing

Background

Double helical gears provide very smooth power transfer at high power levels. Internal work at Allison in the 1960 demonstrated these advantages for high power T56 turborop gearboxes in the M–18 and A–18 programs. Since helical gear thrust loads are balanced in the structure of eact gear, there are no significant bearing thrust reactions. This implifies the design of the planet and sun gear bearings. This high torque capacity of double helical gears allows drivetral growth potential without increasing the gearbox size. The low vibration levels inherent in this type of gearing meet the 30,000 hr MTBUR. Fasteners and mechanical connection

points will be able to perform at these low vibration levels.

The fabrication of double helical gears allows little space for a grinding wheel to pass because the two rows of helical gears are located adjacent to each other. Three techniques to overcome this were: (1) use of small diameter grinding wheels, (2) use of Nitralloy steel which minimizes tooth distortion during heat treatment so that grinding is not necessary, and (3) electron beam welding of two single helical gears.

Recommended Program

A complete double helical planetary gear set would be designed for installation in the CR gearbox. This design would be compatible with the CR gearbox designed for single helical gears so that the two gearsets can be easily interchanged for direct comparison.

Finite element methods would be used to optimize the gear teeth and supporting structure. Planet bearing selection would be dependent upon the results of this analysis.

Static and dynamic stress analysis of these gears would determine actual operating levels and the degree of load sharing both between the two rows of helical gears and between the planets. Vibration and noise levels would be monitored for comparison to existing data. Efficiency tests would determine performance of the gears. At the conclusion of these parametric tests, a series of endurance tests would be run at full power to uncover any long term operating difficulties

Single Row Spherical Planet Bearings

Background

The single row spherical bearing was determined to be a strong candidate for the high contact ratio spur gear planet bearing. Since there is no overturning moment in a spur gear, the planet bearing requirements are less restrictive than those for its helical gear counterpart. The broad roller/row contact surface reduces operating stresses and extends fatigue life. The spherical surface allows the planet to align itself to the sun or ring gear mesh. There is only one planet bearing per planet gear, which reduces the part count, extends the system fatigue life, and reduces power loss.

In the past, single row spherical bearings have been used for heavily loaded, slow-rotating machinery. More recently these bearings have been used for planet bearings in the Blackhawk helicopter transmission. The advantages of this type of bearing are recognized in the aircraft industry. Their application to the CR gearbox, however, requires a significant increase in operating speed. There is no known data available to determine their use in a high power, high speed planetary gear set.

Recommended Program

The research program proposed would begin with a computer analysis of the CR gearbox planet bearing arrange-

ment. As the design becomes finalized, bearings would be procured. An assessment would be made of existing bearing test equipment to determine if it can be adapted to simulate the gearbox planet gear environment. If necessary, a new rig would be designed and fabricated. Results of parametric testing would be compared to earlier predicted performances. If necessary, the computer models would be reviewed to determine if changes were required. This program would provide needed experimental data and computer code verification to assess the value of single row spherical roller bearings in a high speed planet bearing system.

Fluid Film Planet Bearings

Background

The fluid film bearing has several advantages for a propfan gearbox planet bearing. The fluid film bearing has a high load capacity yet requires a minimum amount of space. Cost should be low due to the uncomplicated design, and life can be long if the start/stop problems can be solved. The Rolls Royce Tyne gearbox has proven that fluid film bearings can work in a turboprop planetary gearset. Fluid film bearings have been used in experimental Alison gearboxes as planet bearings in the past, but their performance was poor. As such it is expected that a special development program would be required to attain a satisfactory fluid film planet bearing for a counter-rotation propfan gearbox.

Proposed Program

Analysis techniques for this type of bearing are not available at Allison. To design a test fluid film bearing, a subcontract would be arranged with a consulting firm such as Mechanical Technology Inc. (Latham, New York). This design would probably result in new analysis techniques since the requirement for operation of the bearing in a high 'g' field is not common. Test bearings would be manufactured at Allison for subsequent testing. A special test rig would be fabricated to perform initial testing on this bearing to check the speed and load characteristics. After successful rig testing, the bearing would be installed in the CR gearbox to determine its performance in the actual operating environment.

Lubrication System Methods To Allow Thirty Minutes Of Gearbox Operation Without Oil

Background

The CR gearbox design would not include special equipment to handle an oil-off situation. If this condition were to occur, the drivetrain would have to be shut down within minutes to avoid damage to the bearings and gears. Methods have been developed to allow at least thirty minutes of operating time after loss of the lubricating oil for helicopter transmissions where this time is very critical, especially in combat situations. The same techniques could be applied to the CR gearbox to provide additional safety for the aircraft and its occupants.

Recommended Program

A design study would be required to determine if any of the known oil–off survival techniques might be applied to the CR gearbox or if new methods can be developed. The weight, reliability and/or performance penalty must be assessed to determine if these systems are acceptable for flight hardware. When the best concepts have been identified, hardware would be designed for retrofit to the CR gearbox. During the back–to–back gearbox test schedule, this hardware would be installed for oil–off testing. Instrumentation would be installed to track key operating temperature and vibration level so that the test hardware would not be damaged during the test. If any of these systems perform well without detracting from the overall gearbox design, it would be implemented as a standard part of the design.

Stainless Steel Housing

Background

Magnesium housings have been the standard of the aircraft industry for many years due to magnesium's high strength, light weight properties. In designing a transmission housing for long life, magnesium has some disadvantages. Creep or stretch of the magnesium, due to the long term application of high loads, distorts the housing causing misalignment in gear meshes and bearings. This can lead to premature failure of these components.

Another consideration is the difference in the thermal expansion rate of magnesium and steel. Relative movement between the bearing and housing results in fretting and wear. Magnesium's disadvantages have been minimized in the past, but they may become serious problems in long life situations.

Two other problems typically found in the design of magnesium transmission housings are corrosion and lack of adequate strength at high operating temperatures. Corrosion occurs in the early stages and in the latter stages weakening of the structure occurs. The military services would like to correct the corrosion problems. In designing gearboxes for higher operating temperatures, there is very little margin available with current magnesium alloys. Material properties are seriously affected at temperatures above 300 °F.

Work on helicopter transmission housings completed by others has shown that flight gearboxes can be fabricated of stainless steel. All of the above stated problems can be eliminated by using stainless steel — material creep is non-existent, thermal expansion coefficients are identical between bearings, gears and housing, stainless steel does not corrode, and material strength at elevated operating temperatures is good. The primary difficulty involved in designing a stainless steel housing is minimizing gearbox weight since steel is heavier than magnesium. Through the use of computerized structural analysis, load carrying members can be configured for high strength to weight ratios. The other prob-

lem associated with this type of housing is the method of fabrication. Although some development is required, the fabrication technique would differ little from current magnesium castings techniques.

Recommended Program

A detailed finite element analysis of the CR gearbox must be performed using stainless steel material properties. The structural design would be significantly different than the current magnesium housing design since steel is much heavier than magnesium. To minimize weight, extensive use would have to be made of thin, lightweight but structurally strong members. Fabrication techniques would have to be carefully analyzed to insure that the design can be fabricated and that the latest fabrication techniques are made known to the designer. A stainless steel housing would then be fabricated and subjected to static tests to insure its integrity. Finally, the housing would be tested in the back—to—back test rig parametric and endurance tests.

Long Life Flexible Splines For Gearbox/Prop Interface

Background

Splines combine high torque capacity and low mechanical complexity that connect drive shaft components to gether. Flexible splines can tolerate the misalignment that occurs between different areas of the gearbox. The analytical techniques available for designing flexible splines are basic. As a result there is no guarantee that a given design will function properly. Techniques that address questions such as allowable relative velocities, lubrication, and spline materials are required to provide the designer with enough information to develop a reliable design.

Recommended Program

A thorough literature search would bring together information from several areas of technology to design a flexible spline. Work already has been done in the areas of wear, fretting, boundary lubrication and spline tooth analysis. This study would view many concepts together to formulate a design methodology and point out areas of weakness. If the deficient areas of technology can be filled by programs consistent with Allison's mission, they would be undertaken.

Counter-rotation Gearbox Technology Plan Schedule

A schedule for the counter-rotation gearbox technology program is shown in Figure K-1. The first two items, tapered roller planet bearings and the steep angle, single row tapered roller thrust bearing with bidirectional load capability are required technology items to achieve the performance level

redicted for the counter-rotation gearbox. These two techologies could be completed within a two year timespan. The remaining six technologies listed would enhance the design but are not required for the gearbox defined in Task XI.

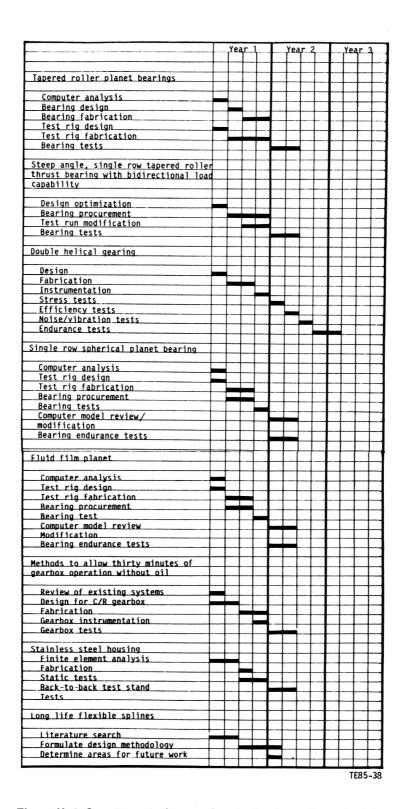


Figure K-1. Counter-rotation gearbox technology plan schedule.

COUNTER-ROTATION PITCH CONTROL AND MECHANISM TECHNOLOGY PLAN

The conceptual design of a pitch change mechanism developed under the counter-rotation APET Add-On contract identified advanced technology features that will require technology programs to establish their acceptability for future production development programs. These technology features are a capacitor signal transfer, a high pressure rotating hydraulic power module, and a rotating electronic control module.

BACKGROUND

Current turboprops transmit an electrical signal across a rotating interface. This is accomplished through the use of brushes and slip rings, which have inherent problems, the most notable being carbon buildup due to brush wear and susceptibility to contamination from oil. These problems result in high maintenance requirements.

Current turboprop systems use low pressure hydraulics with the hydraulic power components mounted on the stationary side. The oil required for changing pitch is supplied to the rotating components through a transfer bearing. Experience has demonstrated that large diameter transfer bearings, which are common with many current systems, are a high maintenance item. Also, independent studies by Hamilton Standard indicate that system weight can be reduced through the use of high pressure hydraulics.

Current turboprop systems use hydro-mechanical pitch change controls, which are mounted on the stationary side of the system. Mechanical signal transfer is required from the control to the pitch change actuator across the rotating interface. This task is particularly difficult for in-line gearbox configurations and results in pitch change hardware being located within the gearbox. This has a significant impact on gearbox reliability and maintenance cost.

PROPOSED PLAN

The proposed technology plan will address the following three features:

- capacitor signal
- high pressure rotating hydraulic power module (gear pump and motor)
- rotating electronic control

CAPACITOR SIGNAL TRANSFER

There are two major areas of concern with regard to the capacitor signal transfer concept. First is the susceptibility to electromagnetic interference (EMI) and vulnerability to lightning strike interference. Second, the concern is to ensure that the capacitor does not emit electromagnetic interference.

The program will include the design, fabrication an testing of a shielded capacitor system. This system, whic will be adaptable to an existing propeller barrel, will include breadboard transmitter/receiver and will be subjected to a EMI survey test for susceptibility and emission. If necessary additional shielding systems will be concepted, fabricate and tested.

Lightning transient tests will be conducted to determin if the capacitor ring can withstand high voltage transient without damage. This program will result in a control signitransfer technique that is adaptable to both current and future turboprop systems and eliminate the need for brushe and slip rings.

HIGH PRESSURE HYDRAULIC POWER MODULE

A system has been devised for changing pitch on futur turboprops with high pressure hydraulic supply components For in-line gearbox systems, the components would b mounted on the rotating portion of the system. This elim nates the need for a transfer bearing and permits removal (hydraulic pitch change hardware from the gearbox. For of set gearbox configurations, the option exists to mount the h draulic supply components on the stationary side of th system. A concept has been developed whereby this can t achieved with a reliable, small diameter transfer bearing ar without impacting the gearbox. The use of high pressure h draulics result in reduced size and weight of these comp nents for optimized installation and maintenance. Th objective of the pitch change technology program for in-lir gearbox configurations is to establish an acceptable gepump and gear motor that will operate at 4750 lb/in.2 in a r tating environment, with an operating life design goal 30.000 hr.

The recommended approach is to design and build bo a gear pump and gear motor sized for the requirements of potential propfan system. Testing to determine torque cha acteristics, leakage, endurance and susceptibility to cavit tion will be conducted. Gear motor testing will also include measurement of break out Δ P and assessment of low speecharacteristics due to the requirements for low friction.

This program will establish the feasibility of a 4750 l in.² gear pump and gear motor, and will define hardwa which is suitable for development on advanced pitch chanç systems.

ROTATING ELECTRONICS

The objective of this technology program will be to determine both the operational characteristics and the survivability

ne electronic controller (the interfacing electronics package for ignal conditioning, feedback signals, and control of the electron-hydraulic servomotor), when mounted and operating in a roating field. Concerns have been expressed regarding the ability of the electronic circuits to operate and survive in a high level g" field.

It is first necessary to establish the environmental reuirements. Concepts for the structural packaging of the lectronics for survival in this environment will be developed nd a breadboard differential input digital data transmitter/ receiver circuit will be constructed for dynamic test evaluation. These tests will include both whirl tests and vibration tests over the total frequency spectrum anticipated for propfan mounted hardware. This program will establish the feasibility of a rotating electronic control and will define hardware that is suitable for development for advanced pitch change systems.

A schedule for the counter-rotation pitch control and mechanism technology program is shown in Figure K-2.

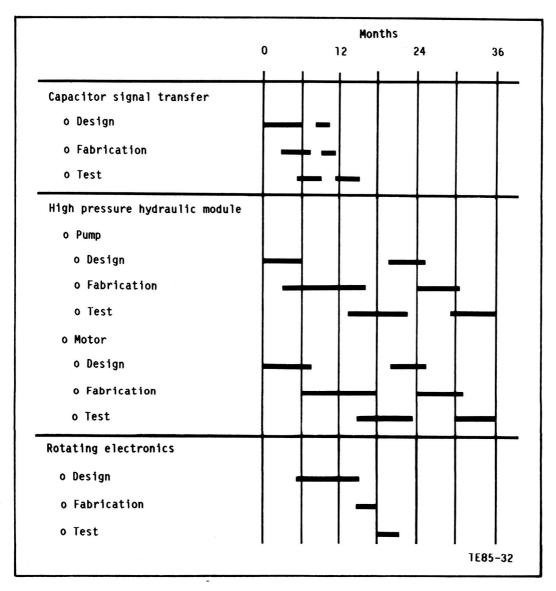


Figure K-2. Counter-rotation pitch control and mechanism technology estimated program schedule for capacitor signal transfer, high pressure hydraulics, and rotating electronics.

APPENDIX L

LIST OF ABBREVIATIONS

	area	PL	payload, power loading
Α	μ in. arithmetic	PMG	permanent magnet generator
/A	axial/axial	PS	power section
/C	axial/centrifugal	QDM	quantitative debris monitoring
GMA	American Gear Manufacturers Association	R	radius
MADS	aircraft mounted accessories drive system	R _C	compressor pressure ratio
OT	burner outlet temperature	R _C RIT	rotor inlet temperature
AB	Civil Aeronautics Board	RVDT	rotary variable differential transducer
fm	cubic feet per minute	R1	first rotor
MP R	cubic mean power	SE	specific endurance
, ,	counter-rotation centerline	shp	shaft horsepower
,	diameter	SL	sea level
С	direct current	SLS	sea level static
oc	direct operating cost	SRP	single rotation propfan
s	directionally solidified	SR	specific range
EC	electronic engine control	SS	single spool
EE	energy efficient engine	S1	first stator
FH	engine flight hour	T.	turbine, temperature
MI	electro magnetic interference		10 100
ммн	engine maintenance man-hour	TOCW	takeoff power
S	extension shaft	TOGW	takeoff gross weight
/A	fuel-to-air ratio	TSFC	thrust specific fuel consumption
ADEC	full authority digital electronic control	T/W	thrust-to-weight ratio
AR	Federal Aviation Regulation	VIM/VAR	
N	thrust	W	flow
ΩO	foreign object damage	W/S	wing loading parameter
В	gearbox	1P	loads that occur 1 time per revolution
pm	gallons per minute	γ	ratio of specific heats
Р	high pressure	ΔP	pressure change
р	horsepower	d	pressure/pressure standard
iCR	high contact ratio	٤	$(0.740/\gamma)(\gamma + 1/2)^{\gamma/(\gamma - 1)}$
G۷	inlet guide vane	η	efficiency
	ratio between radial rating to thrust rating of taper	θ	temperature/temperature standard
	roller bearing	ζ	correction factor
ias	knots indicated air speed	μ	micron
	length	•	
p/in.2	pounds per square inch		
p/in. ²	pounds per square inch gage pound/mass	SUBSCR	RIPTS
om /D	lift-to-drag ratio	а	air
GC		C	compressor
P .	Lockheed Georgia Company	coa	overall compressor pressure ratio
VDT	low pressure	E	
	linear variable differential transducer	f	engine
VPT	linear variable phase transducer		fuel
MMC	metal matrix composite	h	hub
N _N	Mach number		mechanical
MTBR	mean time between removals		nacelle
MTBUR	mean time between unscheduled removals		turbine
h	speed		tip
ımi	nautical miles	t-t	total to total
DEI	one engine inoperative	t-x	total to axial
οGV	outlet guide vane	w	wetted

APPENDIX M DISTRIBUTION LIST

NASA Lewis Research Center 21000 Brookpark Road Cleveland, OH 44135

creverand,	UH 44135	
		No. of Copies
Attn:	Report Control Office, MS 60-1	1
,,,,,,,,,,,,,,,,,,,,,,,,,,,,,,,,,,,,,,,	Library, MS 60-3	2
	L. J. Bober, MS 86-7	1
	L. C. Franciscus MS 6-12	i
	E. J. Graber, MS 86-7	1
	J. F. Groeneweg, MS 86-7	1
	G. A. Kraft, MS 86-7	25
	E. T. Meleason, MS 86-7	1
	J. E. Rohde, MS 86-7	1
	D. A. Sagerser, MS 86-7	1
	G. K. Sievers, MS 86-7	1
	W. C. Strack, MS 6-12	1
	J. A. Ziemianski, MS 86-7	1
	tific and Technical Information Facility	
P. 0. Box		
Baltimore	Washington International Airport, MD 21240	
Attn:	Accessioning Department	20
ALCII.	Accessioning Department	20
NASA Headqu	uarters	
	DC 20546	
nasii iiig voii	, 50 20010	
Attn:	RJ/W. S. Aiken, Jr.	1
	RP/J. R. Facey	1
NASA Ames A	Research Center	
Moffett Fie	eld, CA 94035	
		*
Attn:	D. P. Bencze, MS 227-6	1
	R. C. Smith, MS 227-6	1
NASA Dryder	Flight Research Center	
P. 0. Box 2		
Edwards, CA	A 93523	
A++	D. C. Daman, MC D. FD	,
Attn:	R. S. Baron, MS D-FP]

NASA Langley Research Center Hampton, VA 23665			
Attn:	C. Driver, MS 249A	1	
	R. W. Koenig, MS 249	1	
	Research Information Center, MS 151A	1	
	Aero Propulsion Lab terson AFB, OH 45433		
Attn:	H. F. Jones AFWAL/POSL	3	
Naval Air Systems Command Jefferson Plaza #1 Arlington, VA 20360			
Attn:	G. Derderian, AIR 310-E	3	
	J. Klapper, AIR 532C-1	1	
Naval Air Propulsion Center P. O. Box 7176 Trenton, NJ 08628			
0.4.4	D. 1 Manajana M.S. DE 22	2	
Attn:	P. J. Mangione, M.S. PE-32		
Allison Gas Turbine Operations General Motors Corporation P.O. Box 894 Indianapolis, IN 46206-0894			
Attn:	R. D. Anderson, MS T-18	1	
	A. S. Novick, MS T-18	6	
	D. A. Wagner, MS T-18		
Beech Aircraft Corporation Wichita, KS 67201			
Attn:	R.W. Awker	2	
Boeing Commercial Airplane Company P.O. Box 3707 Seattle, WA 98124			

Attn: G. P. Evelyn, MS 72-27

Boeing Military Airplane Company P. O. Box ?730 Wichita, KS 67277-7730				
Attn:	D. Axelson, MS K77-24 C. T. Havey, MS 75-76	2		
P. 0. Box	Cessna Aircraft Company P. O. Box 154 Wichita, KS 67201			
Attn:	Dave Ellis, Dept. 178	2		
Douglas Ain 3855 Lakewo Long Beach	ood Blvd.			
Attn:	R. F. Chapier, MS 3641 S. S. Harutunian, MS 3641 E. S. Johnson, MS 3641 F. C. Newton, MS 3584	1 1 1		
	Corporation National Plaza 45402			
Attn:	A. E. Hause	1		
General Electric Company Aircraft Engine Business Group 1000 Western Avenue Lynn, MA 01905				
Attn:	R. J. Willis, Jr., M.S. WL 345	2		
General Ele Aircraft En One Neumann Cincinnati,	n Way	,		
Attn:	J. E. Johnson, M.S. H6, Bldg. 305	8		

Grumman Aerospace Corporation B-thpage, NY 11714 Attn: N. F. Dannenhoffer, M.S. C32-05 1 C. Lehman, M.S. C42-05 J. Karanik, M.S. C32-05 Hamilton Standard Div., UTC Windsor Locks, CT 06096 J. A. Baum, M.S. 1-2-11 Attn: S. H. Cohen, M.S. 1-2-11 B. S. Gatzen, M.S. 1-2-11 2 M. G. Mayo, M.S. 1A-3-2 2 Hartzell Propeller Products P. O. Box 1458 1800 Covington Avenue Pigua, OH 45356 Attn: A. R. Disbrow 7 Lockheed-California Company P. O. Box 551 Burbank, CA 91503 Attn: A. R. Yackle, Bldg. 90-1, Dept. 69-05 2 Lockheed-Georgia Company 86 South Cobb Drive Marietta, GA 30063 W. E. Arndt, M.S. D/72-17, Zone 418 Attn: 4 D. M. Winkeljohn, M.S. D/72-79, Zone 419 Pratt & Whitney Aircraft United Technologies Corporation Commercial Products Division 400 Main Street East Hartford, CT 06108 J. Godston, M.S. 118-26 Attn: 1

6

A. McKibben, M.S. 163-12 C. Reynolds, M.S. 118-26 N. Sandt, M.S. 118-27 Pratt & Whitney Aircraft United Technologies Corporation Military Products Division P. O. Box 2691 West Palm Beach, FL 33402

West Palm Beach, FL 33402			
Attn: L. Coons, M.S. 711-69 W. King, M.S. 702-05 H. D. Snyder, M.S. 711-67 S. Spoleer, M.S. 702-50 H. D. Stetson, M.S. 713-09			
Sikorsky Aircraft Transmission Engineering North Main Street Stratford, CN 06601			
Attn: R. Stone, M.S. S-318A 3			
Williams International 2280 West Maple Road P. O. Box 200 Walled Lake, MI 48088			
Attn: Edward Lays, M.S. 4-9			
Air Canada Dorval Base H4Y-1CZ Quebec, Canada			
Attn: Goeff Haigh - Zip 14 1 B. H. Jones - Zip 66 1			
Air Transport Association 1709 New York Avenue, NW Washington, DC 20006			
Attn: D. J. Collier 1			
Delta Air Lines Inc. Hartsfield Atlanta International Airport Atlanta, GA 30320			

J.T. Davis, Engineering Department

Attn:

2

Federal Express P. O.Box 727-4021 Memphis, TN 38194		
Attn: B. M. Dotson, M.S. 4021	1	
Ozark Air Lines Inc. P. O. Box 10007 Lambert St. Louis Airport St. Louis, MO 63145		
Attn: Phil Rogers - Engineering Dept.		
Trans World Airlines Inc. 605 Third Avenue New York, NY 10016		
Attn: Engineering Dept.	2	
United Air Lines P. O. Box 66100 Chicago, IL 60666		
Attn: Engineering Dept.	2	
United Air Lines San Francisco International Airport San Francisco, CA 94128		

2

Engineering Dept.

Attn:

LIMITED DISTRIBUTION

This document shall remain under distribution limitation until July 1987.

	la a	3. Recipient's Catalog No.	
1. Report No.	2. Government Accession No.	3. Recipient's Catalog No.	
NASA CR-168115		5. Report Date	
4. Title and Subtitle ADVANCED PROPFAN ENGINE TECHNOLOGY (APET) AND SINGLE AND COUNTER-ROTATION GEARBOX/PITCH CHANGE MECHANISM		July 1985 6. Performing Organization Code	
		O. De describe Organization Report No.	
7. Author(s) R. D. Anderson (Allison Gas Turbine Operations)		8. Performing Organization Report No. EDR 11283	
		10. Work Unit No.	
9. Performing Organization Name and Address			
Allison Gas Turbine Divi		11. Contract or Grant No.	
General Motors Corporati	on	NAS3-23046	
P. O. Box 894, Indianapolis, IN 46206-	0894	13. Type of Report and Period Covered	
12. Sponsoring Agency Name and Address National Aeronautics and		Contractor Report	
Lewis Research Center	Space Administration	14. Sponsoring Agency Code	
21000 Brookpark Road Cleveland, OH 44135			
15. Supplementary Notes			
Contract Project Manager: Gerald A. Kraft, Advanced Turboprop Project Office, NASA Lewis Research Center, Cleveland, OH 44135			
Advanced engine studies for single-rotation propfan-powered regional transport aircraft were performed to identify key technology development issues and programs. The need for improved thrust specific fuel consumption to reduce fuel burned and aircraft direct operating cost is the dominant factor. Typical cycle trends for minimizing fuel consumption are reviewed, and two 10,000 shp class engine configurations for propfan propulsion systems for the 1990's are presented. Recommended engine configurations are both three-spool designs with dual-spool compressors and free power turbines. Cycle pressure ratio of 32.5:1 and turbine temperatures up to 2500°F provide fuel efficient operation at the 32,000 ft., 0.72 Mach number cruise condition of the study. Higher pressure ratios and corresponding higher turbine temperatures are desirable for larger power class			
engines. In the performance of this study, the benefits of these new propulsion system concepts were evaluated using an advanced airframe, and results were compared for single-rotation propfan and turbofan advanced technology propulsion systems. The propfan system was shown to have a 9.7% direct operating cost advantage and to burn 18.6% less fuel than the turbofan system on a typical 300 nmi intercity flight. Similar advantages were shown for a 1000 nmi mission.			
As this study progressed, additional efforts were added for the preliminary design of single and counter-rotation gearboxes and the conceptual design of compatible, advanced pitch change systems. A dual, off-set compound idler gearbox was designed for single-rotation propfans and an inline differential planetary gearbox was designed for the counter-rotation propfans. In addition, the single-rotation gearbox was compared to a similar design with current technology to establish the benefits of the advanced gearbox technology.			
The conceptual design of the advanced pitch change mechanism identified a high pressure hydraulic system that was superior to the other contenders and completely external to the gearboxes. The designs were very modular which resulted in low maintenance costs. 17. Key Words (Suggested by Author(s)) [18. Distribution Statement			
Turboprop engine, Turboprop, Propfan, Pitch change mechanism, Gearbox, Engine/ aircraft evaluation, Propfan engine technology plan			
19. Security Classif. (of this report)	D. Security Classif. (of this page)	21. No. of pages 22. Price*	
Unclassified	Unclassified		